Synthesis, Characterization and Redox Properties of Expanded Isophlorinoids Containing Six, Seven, Eight, Nine and Ten Heterocyclic Units

A thesis
Submitted in partial fulfilment of the requirements
Of the degree of
Doctor of Philosophy

By

Prachi Gupta

20163429

INDIAN INSTITUTE OF SCIENCE EDUCATION AND RESEARCH PUNE
(2022)

Dedicated to

My Beloved Family, Friends &

Teachers

CERTIFICATE

Certified that the work incorporated in the thesis entitled "*Synthesis, Characterization and Redox Properties of Expanded Isophlorinoids Containing Six, Seven, Eight, Nine and Ten Heterocyclic Units* "
Submitted by Prachi Gupta was carried out by the candidate, under my supervision. The work presented here or any part of it has not been included in any other thesis submitted previously for the award of any degree or diploma from any other University or institution.

V.G.

Prof. V. G. Anand
Date: 04/02/2022

Declaration

I declare that this written submission represents my ideas in my own words and where others' ideas have been included, I have adequately cited and referenced the original sources. I also declare that I have adhered to all principles of academic honesty and integrity and have not misrepresented or fabricated or falsified any idea/data/fact/source in my submission. I understand that violation of the above will be cause for disciplinary action by the Institute and can also evoke penal action from the sources which have thus not been properly cited or from whom proper permission has not been taken when needed.

Prachi Gupta
Roll No. 20163429
Date: 04/02/2022

Acknowledgements

Accomplishment of this doctoral thesis was possible with the support and understanding of several people throughout my Ph.D. journey. I would like to acknowledge each individual and express my heartfelt gratitude to them.

I would like to thank my Ph.D. thesis supervisor Prof. V. G. Anand for his constant support, motivation, constant encouragement and active guidance. Sir's suggestions and ideas were of valuable importance. Sir guided me throughout the journey and kept me motivated from the very beginning till the end. Every time I was stuck with a problem during my synthesis, he provided me with a solution. I would like to thank sir for patiently correcting my mistakes and helping me enhance my writing and presentation skills as well. Thankyou sir for believing in me and for all your encouragement and guidance. It was a pleasure to work in Sir's research group.

No words are adequate to thank my loving mother, Mrs. Mani Gupta and my father, Mr. Sudhir Gupta, for their unconditional love for me, motivating me and having a strong believe in me. I wish to express my extreme gratefulness to my loving sister Ms. Pooja for cheering my life up. I am also lucky to have a great husband Dr. Moreshwar Chaudhari

who supported me all along as a great friend and wish to thank him for always helping me unconditionally. I would also like to thank my cousins Aditi, Pranav, Bharat, Sunaina and Tanisha who came all the way to Pune whenever I needed them. I would also like to thank my grandparents and relatives who were there by my side.

I am thankful to our former director, Prof. K. N. Ganesh, and current director Prof. Jayant Udgaonkar for providing excellent research platform, financial support, and facilities at the Indian Institute of Science Education and Research (IISER), Pune, India. I also would like to extend my gratitude to my thesis Research Advisory Committee members, Dr. Muhammed Musthafa and Dr. Asha S.K. for their valuable inputs during my RAC meetings. I want to thank former Chair chemistry Prof. M. Jayakannan and current Chair Prof. H. N. Gopi for their support and various departmental activities, including Chemsymphoria. I am also thankful to all the chemistry faculty members at IISER-Pune for their support.

I also thank all administrative staff (Mahesh, Yathish, Ganesh, Mayuresh, Megha, Sanjay, Tushar, Sayalee, Hemlata) and instrument operators (Archana, Swati, Sandip, Sandeep, Nitin, Ravindar, Chinmay, Dipali).

I am really lucky to have wonderful lab mates. It's my pleasure to thank all the lovable lab members Dr. Kiran Reddy, Dr. Santosh C. Gadekar, Dr. Neelam Shivran, Dr. Rashmi Nayak, Dr. Jyotsna Arora, Dr. Brijesh Chandra, Dr. Sujit P. Chavan, Dr. Sunita Gadakh, Dr. Rakesh Gaur, Dr. Madan Ambhore, Ashok kumar B., Udaya H. S., Markose Joshi, Pragati Shukla, Ramesh Hiremath and Vishnu Mishra. Friendly discussions in the lab helped me gain a lot of knowledge. Without them working would have become boring in the lab. I am thankful for every one of my research group for their timely help. I owe my gratitude to Dr. T. Y. Gopalakrishna for his valuable help.

I am obliged to my loving batch-mates of 2016 batch, Prerona, Debashish, Pankaj, Yogesh, Laxman, Iranna, Zahid, Vikas and IISER friends Anandita, Mishika, Shikha, Neetu, Ravi and my non-IISER friends Anchal, Sidharth, Shikhar, Chayan, Aarushi, Kaushal, Saumya, Shweta, Mimma for their ardent and assiduous support, care and attention.

Finally, I am thankful to DST-Inspire for Research Fellowship (JRF and SRF).

Above all, I am grateful to the almighty god for granting me the wisdom, health and strength to undertake this research task and enabling me to its completion. I would also like to acknowledge all the

teachers who imparted wisdom and knowledge from my childhood. Due acknowledgement to those whose names were unintentionally missed out, despite their unconditional help throughout my life.

Prachi Gupta

Contents

Synopsis

The present thesis entitled "*Synthesis, Characterization and Redox Properties of Expanded Isophlorinoids Containing Six, Seven, Eight, Nine and Ten Heterocyclic Units"*, describes the efficacious efforts at the synthesis of range of expanded porphyrins consisting heterocyclic units ranging from six to ten. It further deals with the aromatic and antiaromatic properties associated with these conjugated macrocycles. The flexibility of each system changes by varying the number of heterocyclic units and bridging carbons present in the core of the macrocycle. The first chapter provides a detailed review about antiaromatic porphyrinoids. Different expanded porphyrins display diverse aromatic- antiaromatic-nonaromatic properties based on their π electron count and the planarity of the macrocycle. It is interesting to study and explore more of such expanded porphyrins for their attractive redox properties.

The second chapter deals with the study of expanded porphyrins a step further and describes the synthesis of completely core modified antiaromatic 32π heptaphyrins for the very first time. To achieve the synthesis of target 32π heptaphyrin, a novel asymmetric tristhiophene oligomeric unit was designed and synthesized. The asymmetric tristhiophene was then condensed with thiophene/furan diol in a 2:1 ratio followed by oxidation using dichlorodicyanoquinone to obtain the desired 32π heptaphyrin as major product. Even though three different products can be expected from this reaction, it was observed that the two asymmetric tristhiophene units underwent α–α coupling at their head-to-head position resulting in a symmetric heptaphyrin with C_2 axis of symmetry in both of the cases. Both the heptaphyrins displayed antiaromatic properties, which were indicated by paratropic ring current effect observed in their proton NMR spectra.

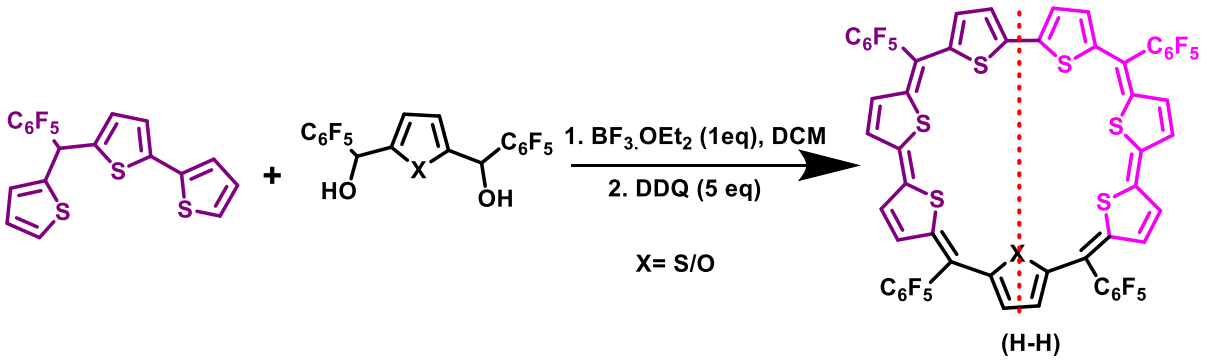

Further, the synthesized heptaphyrins were explored for their redox properties, wherein the 32π heptaphyrins underwent reversible two electron oxidation both electrochemically and, chemically with Meerwein's salt. The obtained dications in both cases were stable under ambient conditions and were marked by a red shift of more than 116 nm in their electronic absorption spectrum. The dications displayed aromatic properties and it was justified by the diatropic ring current effect observed in their proton NMR spectra. The heptaphyrin containing two furan units displayed two ring inversions which was revealed by its proton NMR. The geometry of the molecule retained even up on undergoing two electron oxidation, where the two thiophene ring flipping could be seen in the case of dication as well which was confirmed by both the proton NMR and the single crystal X-ray analysis. These studies were further supported by quantum chemical calculations.

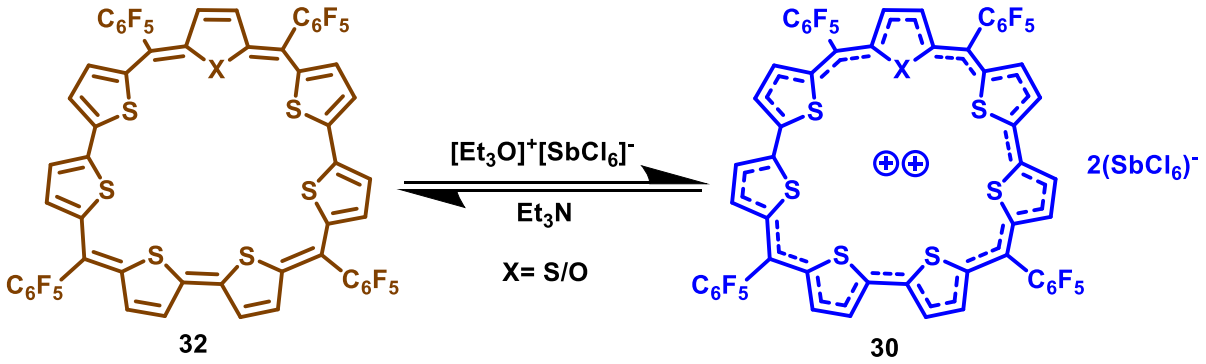

Third chapter of the thesis is focused on the study of various octaphyrins. Particularly, it describes the synthesis and redox properties of 40π and 36π octaphyrins. 40π octaphyrin with eight bridging positions was flexible and attained a figure-of-eight geometry. The macrocycle

being nonplanar was non antiaromatic and did not display significant ring current effect in its proton NMR spectrum.

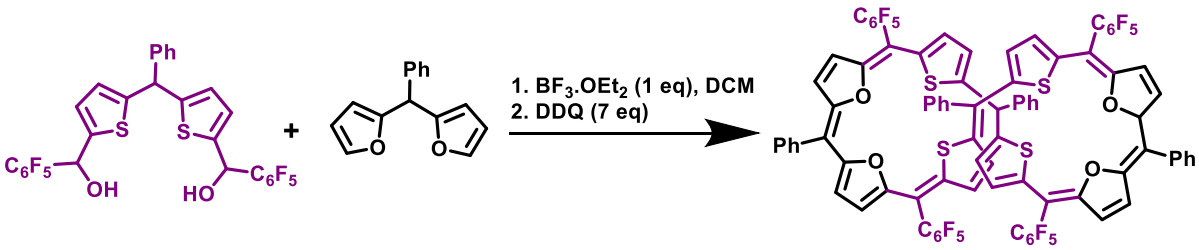

However, the octaphyrin displayed chemical redox where a stable 38π dication could be obtained on addition of Meerwein salt to the octaphyrin. The dication also retained the same figure-of-eight geometry confirmed by their single crystal X-ray structure.

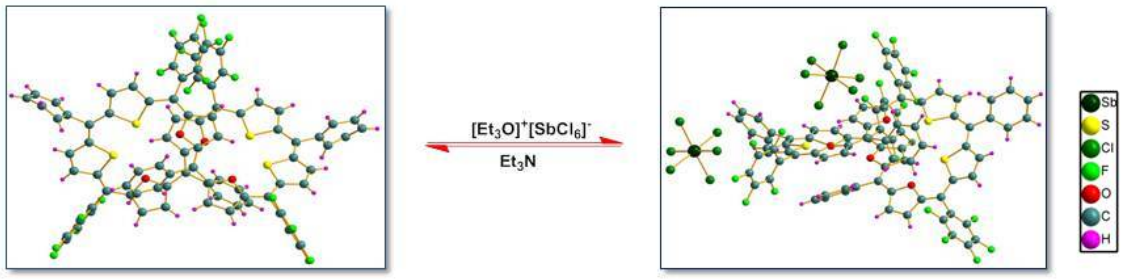

Further on the verge of synthesis of a neutral 38π octaphyrin, a novel product was observed by condensation of two diol units together possibly by elimination of H_2O_2 to yield a 38π neutral octaphyrin.

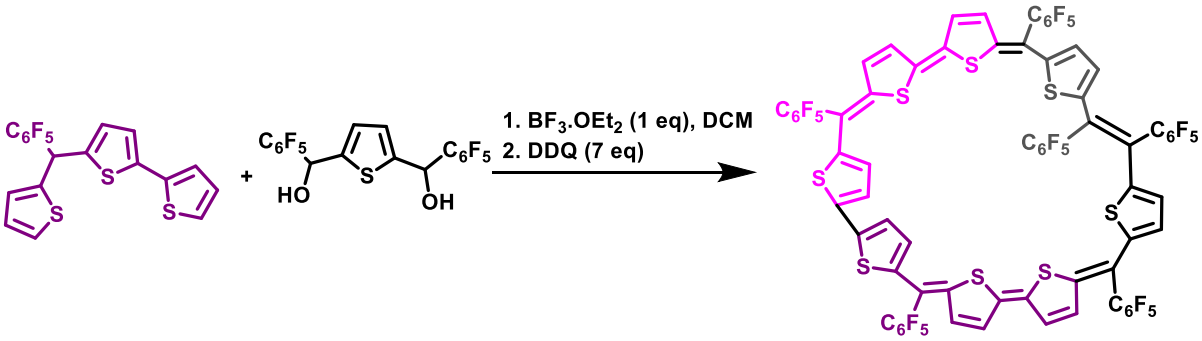

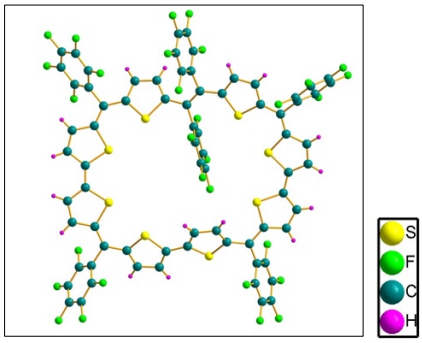

To explore similar chemistry further, an analogous synthesis of 38π octaphyrin with two furan units was attempted. The reaction revealed the formation of two different isomers of 38π octaphyrins from the same reaction mixture. This was the first time where two different isomers of an expanded porphyrin had been obtained from the same reaction. However, the molecular structure for both the octaphyrins could not be confirmed by single crystal X-ray diffraction.

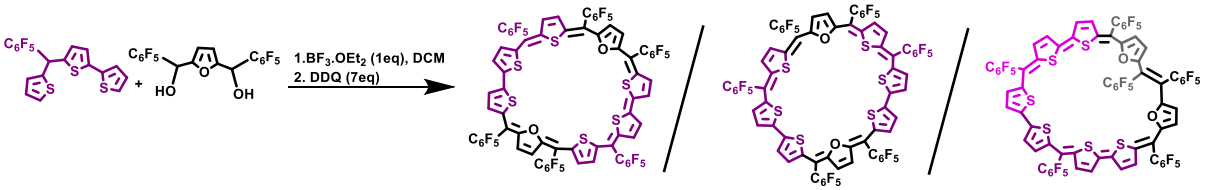

In the curiosity to deduce the structure of these octaphyrins, the pentafluoro substituents on four of the bridging carbons were replaced by mesityl group. Though the structure for this 38π octaphyrin was confirmed by single crystal X-ray analysis, formation of only one isomer was observed, which could be related to only one of the isomers of 38π isophlorin with all the pentafluoro substituents.

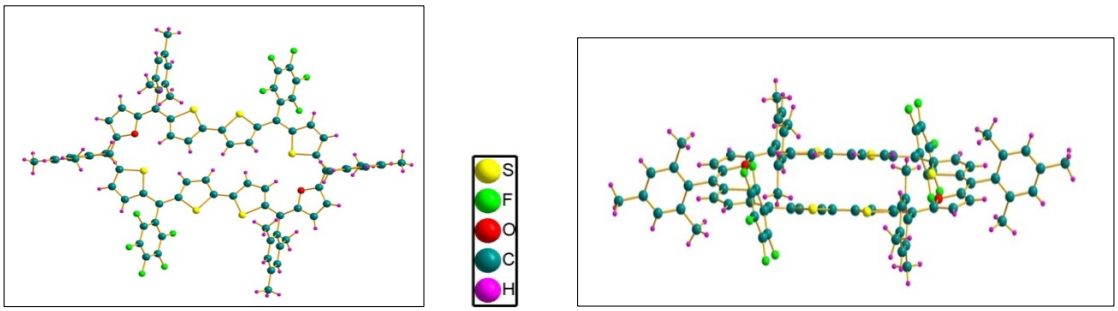

In the fourth chapter, synthesis of expanded porphyrins with ten heterocyclic units and isolation of 46π decaphyrins has been described in detail. The completely core modified

46π decaphyrins synthesis was attempted by [2+2] MacDonald condensation of 5,5''-((perfluorophenyl)methylene)di-2,2'-bithiophene with the corresponding diol. The isolated decaphyrins were characterized using spectroscopic techniques and quantum mechanical calculations were performed on energy optimised structures. The decaphyrins did not display any significant ring current effects and hence were perceived to be nonaromatic in nature.

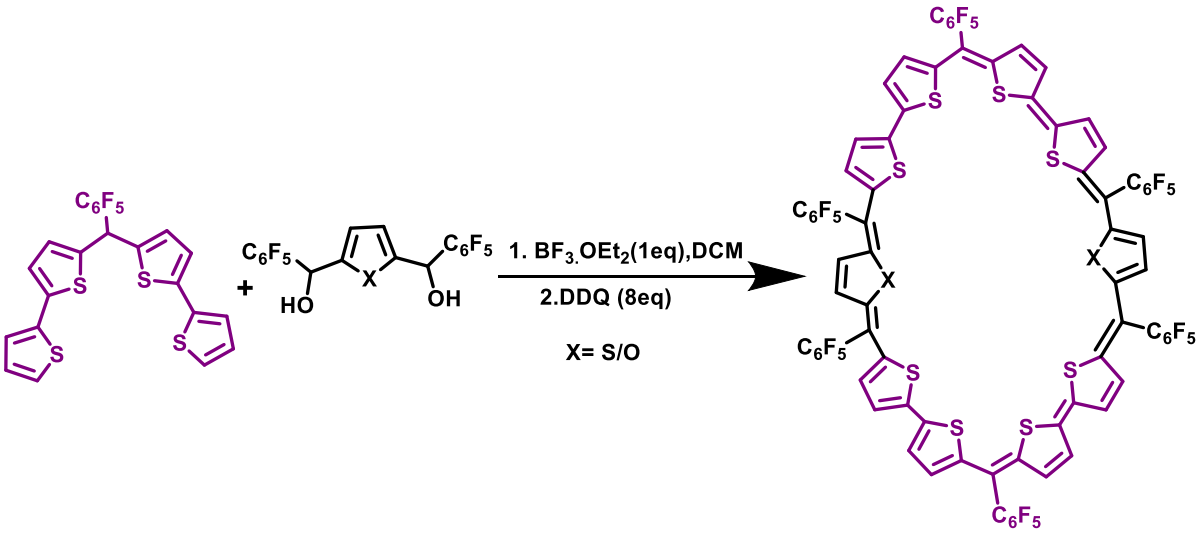

Finally, the fifth chapter of this thesis describes the introduction of an ethylene bridge in *Z* conformer within the macrocyclic core. The synthesis was attempted by condensing (*Z*)-1,2-diphenyl-1,2-di(thiophen-2-yl)ethene with corresponding diol under acidic conditions followed by oxidation. The reaction resulted in the formation of 32π six membered and 48π nine membered expanded porphyrnoids.

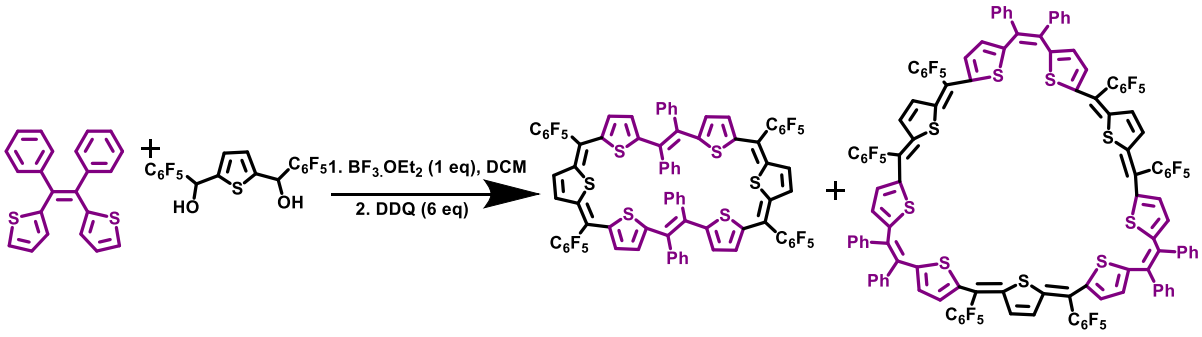

Despite the selective use of oligomeric unit containing ethylene unit in *Z* conformer only the 32π hexaphyrin with ethylene unit in *E* conformer was identified from the reaction mixture.

This led to conclude that the stability of *E* conformer was higher than the *Z* conformer in this macrocycle. The 48π nonaphyrin was well characterized by spectroscopic techniques but its absolute structure could not be determined from X-ray diffraction analysis.

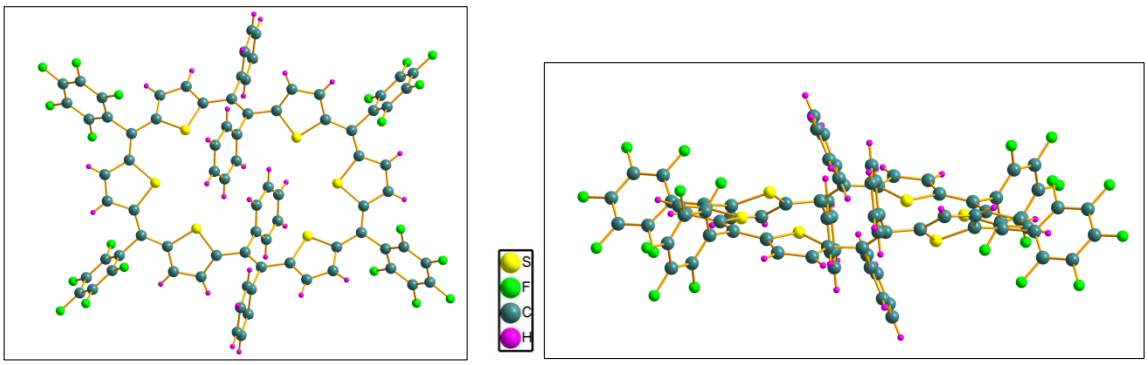

List of publications

1. Gupta, P.; Panchal, S.; Anand, V. G. Two-electron Oxidation of a Twisted Non Anti-aromatic 40π Expanded Isophlorin. *J. Chem. Sci*. **2016**, *128*, 1703-1707.

2. Gupta, P.; Anand, V. G. Symmetric 32π (1.0.1.0.1.0.1) Core-Modified Heptaphyrins from Asymmetric Building Block *Org. Lett.* **2021**, *23*, 3481-3485.

3. Synthesis and Study of 38π Novel Isomeric Octaphyrins (MANUSCRIPT UNDER PREPRATION)

I.1 Introduction

Macrocycles with four pyrrole rings connected with methine bridges at their alpha position with 18π electrons in the conjugation pathway are termed as porphyrins (Figure I.1; **I.1**). These stable aromatic molecules have been imbibed in nature since time immemorial. Having a strong affinity to ligate metals, nature has deployed porphyrins for various metal assisted electron transfer processes.[1] It is also crucial and a major component of Hemoglobin which transports oxygen in blood. Nature has also systematically arranged porphyrins not only for oxygen transport, but also for photosynthesis and methanogenesis, and hence earned the sobriquet as ''pigments of life''.[2] Apart from being found in nature, porphyrin plays an important role in applications such as organic electronics and in medicine. Due to its attractive photo-physical properties, derivatives of porphyrin have been used as photo sensitizers in photodynamic therapy.[3] Further, metallo-porphyrins are utilized as oxidation catalysts[4] and have been industrially employed for cancer therapeutics,[5] non-linear optical devices,[6] mediator for artificial photosynthesis[7] and many more.[8] The extensive scope of application of porphyrins have always encouraged scientists to study porphyrins in much detail.

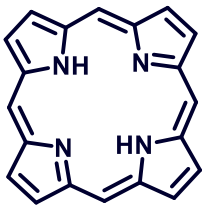

I.1

Figure I.1*: Skeleton of a non-substituted porphyrin*

The simplest synthetic route for porphyrin is to react pyrrole with the desired aldehyde under acidic conditions followed by air-oxidation to yield the desired porphyrin.[9] Though the method is simple, but can result in multiple macrocycles bearing different number of heterocyclic units. These larger analogues of porphyrin with more than four heterocyclic units are termed as expanded porphyrins.

Extending the π conjugation of porphyrins, opens the door for a whole range of novel conjugated macrocyles and are hence being studied extensively.[10] These macrocycles termed as pentaphyrin, hexaphyrin, heptaphyrin and octaphyrin depending on number of heterocyclic units varying from five to eight respectively.[10] However, macrocycles with more than eight heterocycles are also known to be present in the core of the macrocycle. In these expanded isophlorins, heterocylic units can be linked together with a varying number of *meso* positions. For example, a pentaphyrin with four *meso* positions is termed as sapphyrin.[11] Similarly, hexaphyrins with five and four *meso* positions have also been identified with reduced number of π electrons along the conjugated pathway.[12] Pentaphyrins and hexaphyrins have been studied widely in comparison to their higher analogues like heptaphyrins and octaphyrins. Surprisingly, only a few analogues of heptaphyrins have been synthesized till date.

I.2 Heptaphyrins

Heptaphyrins are a class of macrocycles with seven heterocylic units arranged in a cyclic conjugated fashion. Similar to pentaphyrin and hexaphyrin, heptaphyrin can also be formed with a varying number of *meso* carbons ranging from zero to seven. The first heptaphyrin (Figure I.2; **I.2**) synthesized by Sessler and coworkers was reported in 1999 with only two *meso* positions.[13]

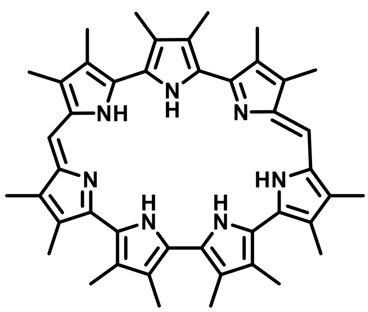

I.2

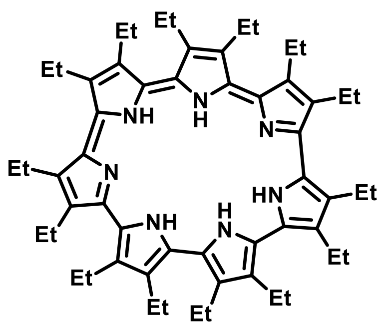

I.3

Figure I.2: *Heptaphyrins with two and zero bridging units*

The 28π Heptaphyrin (1.0.0.0.1.0.0) bearing only two *meso* carbons, attained a planar geometry and hence was antiaromatic in nature. The 26π heptaphyrin with zero *meso*

positions[14] (Figure I.2; **I.3**) attained a near planar configuration and displayed aromatic behavior. Later a thiophene analogue (Scheme I.1; **I.6**) with one of the centre pyrrole unit of tripyrrolic unit being replaced by thiophene was synthesised by Anguera and co-workers by condensing two oligomer units **I.4** with **I.5** under acidic conditions.[15]

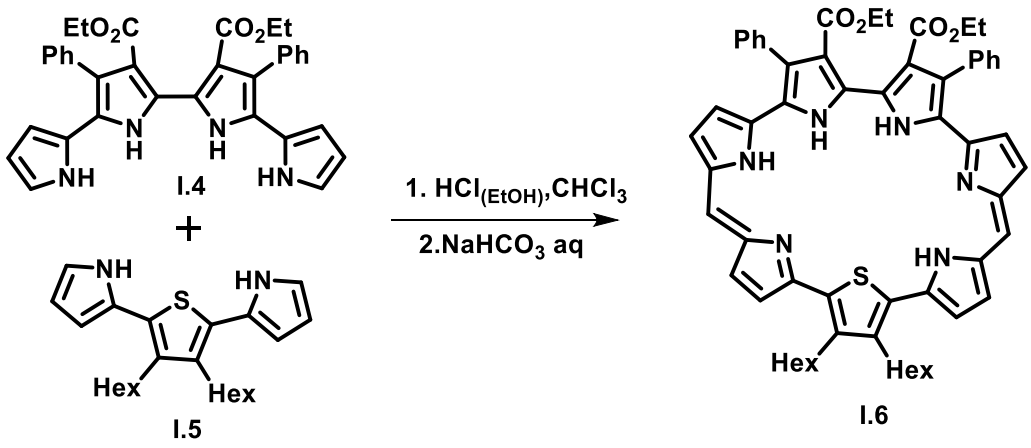

Scheme I.1*: Synthesis of heptaphyrin* ***I.6*** *with one thiophene and two meso position*

Further, a range of 30π heptaphyrins were reported by Chandrashekar and co-workers.[16-18] These heptaphyrins (Figure I.2; **I.7** to **I.11**) varied in number of pyrrole units and the bridging carbon atoms (Figure I.3). In most of the cases, crystal structure revealed that while the pyrrole rings were intact, one or two of the thiophene rings had been inverted. The proton NMR for 30π heptaphyrins revealed the aromatic nature for these macrocycles. It was observed that increasing the number of *meso* carbons from four to five enhanced the flexibility and hence it attained a figure of eight conformation, again with two inversions of thiophene rings.

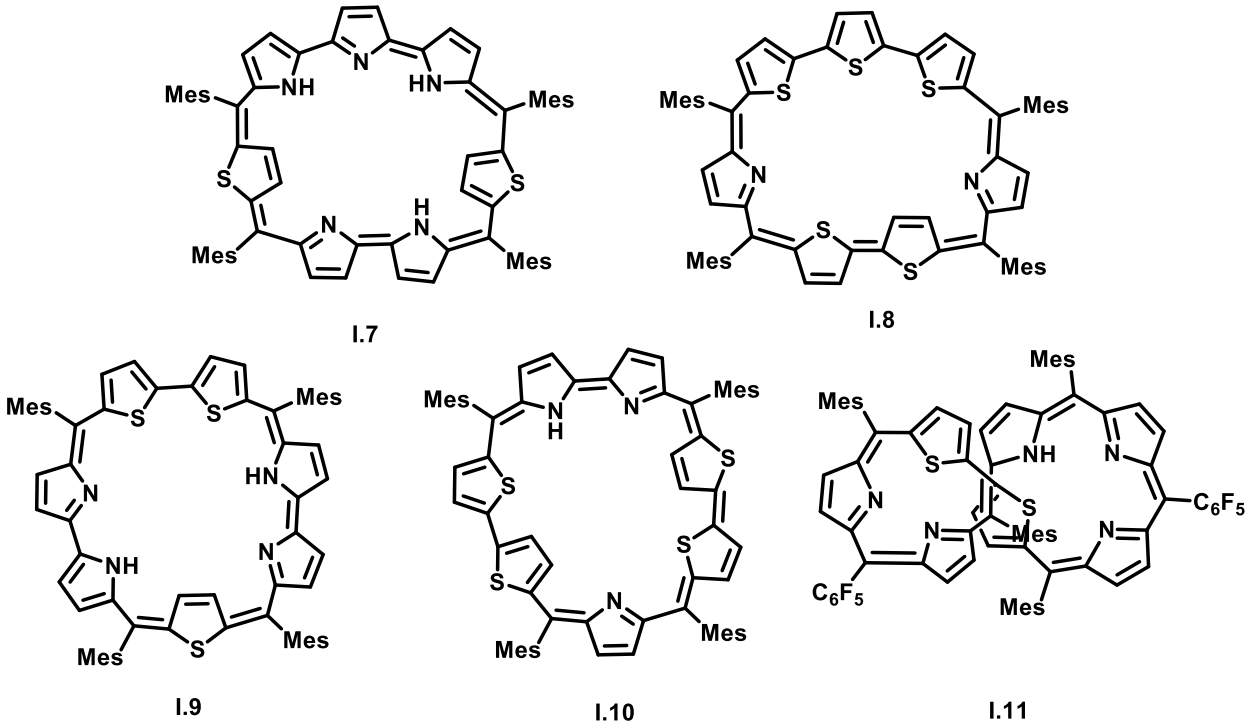

***Figure I.3**: 30π Heptaphyrins with varying number of pyrrole units*

Two other heptaphyrins, (Figure I.4; **I.12-1.13**) with five *meso* carbons and all the pyrrole rings in the core of macrocycle[19] displayed different conformational arrangement in solution and solid states. Based on proton NMR spectroscopy, it was suggested that despite bearing a flat conformation, it also included the inversion of a β-substituted pyrrole ring along with one of the phenyl ring being directed towards the center of the heptaphyrin. While, in the solid state its molecular structure revealed a figure of eight conformation.

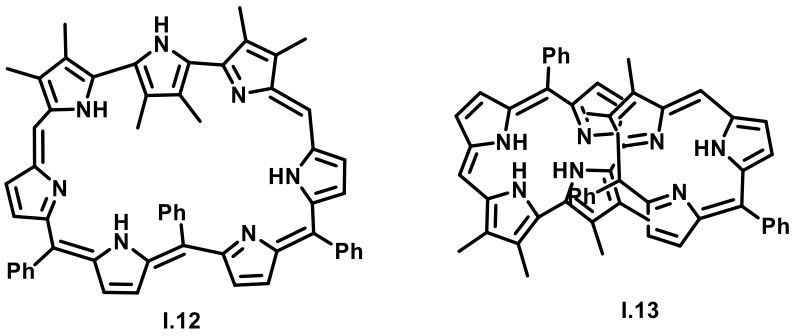

***Figure I.4**: Heptaphyrins with different conformation in solution and solid state*

Replacing a bithiophene with a dithienothiophene resulted in a (1.1.1.1.1.1.0) 32π heptaphyrin[20] with Möbius aromaticity (Figure I.5; **I.14**). Protonation of the macrocycle,

enhanced the diatropic property of the hetpaphyrin as evident from its proton NMR spectrum and further supported by a significant increase in the magnitude of negative Nucleus Independent Chemical Shift (NICS) value.[21] Interestingly, replacing one of the pyrrole rings by a selenophene unit resulted in planar geometry[22], indicating the importance of pyrrole ring for the Möbius aromaticity in the molecule (Figure I.5; **I.15**).

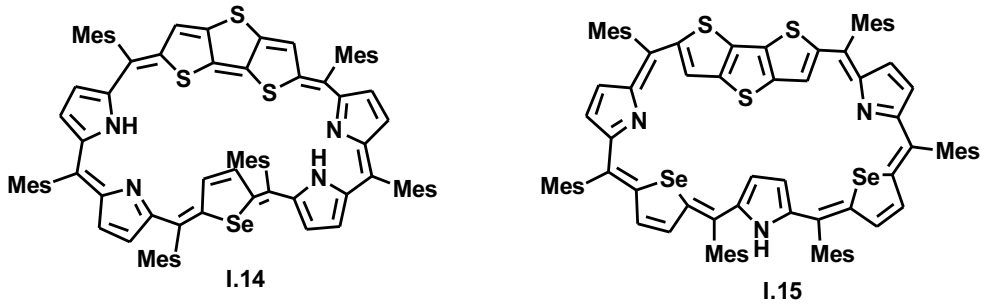

Figure I.5*: Importance of pyrrole ring to attain Möbius aromaticity*

The 32π heptaphyrin(1.1.1.1.1.0.0) (Figure I.6; **1.16**), with five *meso* carbons (Figure I.6) also displayed conformational flexibility and hence making it non aromatic in nature.[23] The macrocycle could easily be oxidized to 30π electron system (Figure I.6; **I.17**), which attained a near planar geometry and displayed aromatic behavior.

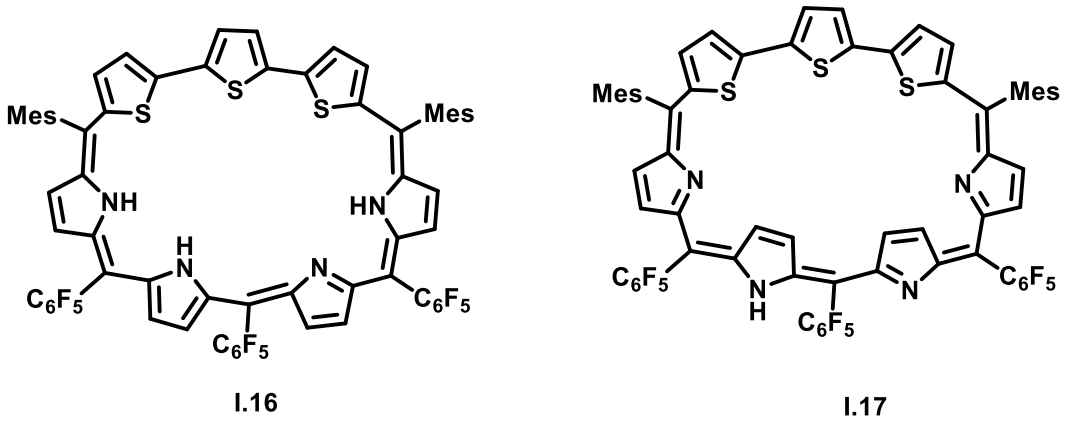

Figure I.6*: 32π and 30π heptaphyrin*

Another set of 30π heptaphyrins[24-25] with four and six *meso* carbons were reported by Osuka and coworkers. A 30π heptaphyrin with four *meso* carbon bridges (Figure I.7; **I.18**) was found to be planar with one inverted pyrrole ring and displayed aromatic characteristics. This

macrocycle also displayed solvatochromism, wherein the color of heptaphyrin solution in MeOH, MeCN, CH_2Cl_2, or $CHCl_3$ was blue in color and suggested two pyrrole ring inversions (Figure I.7; **I.19**) while in acetone it displayed red-purple color having only one ring inversion (Figure I.7; **I.18**). Another heptaphyrin with six *meso* carbons (Figure I.7; **I.20**), as expected was flexible in nature and attained a figure of eight conformation. Upon deprotonation, its crystal structure revealed the inversion of three pyrrole rings in the heptaphyrin (Figure I.7; **I.21**).

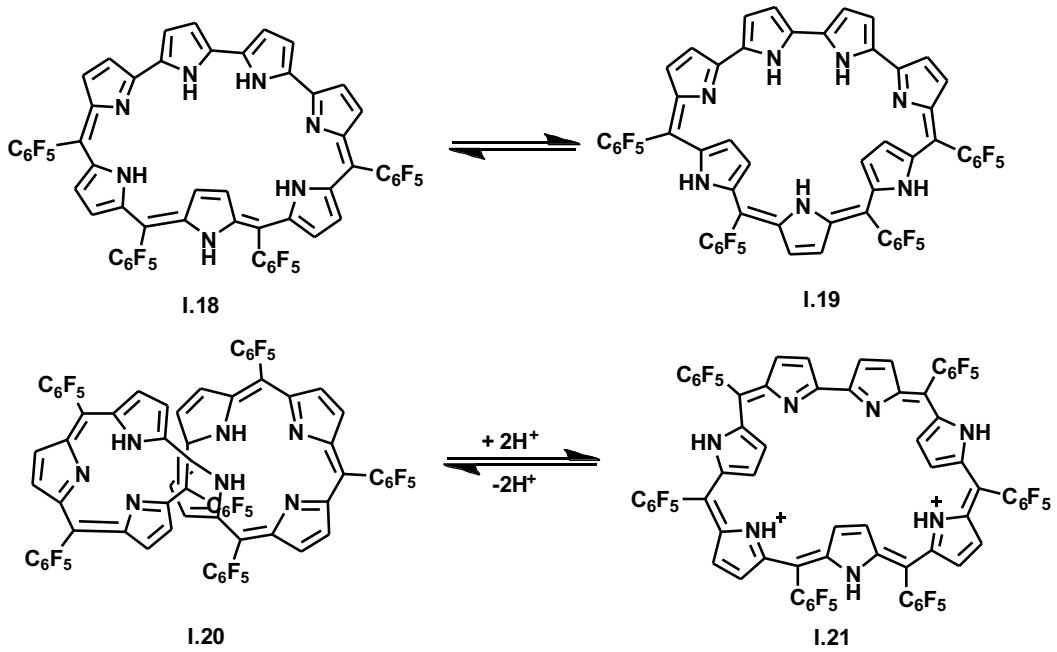

Figure I.7*: Rearrangement controlled by solvent (top) and protonation (bottom) in heptaphyrin*

Other heptaphyrins with seven *meso* carbons and bearing only pyrrole rings in the core of the macrocycle but with different *meso* substituents were synthesized.[26-27] As expected all the heptaphyrins deviated from the planar conformation. The macrocycle with seven *meso* pentafluoro units of the heptaphyrin was elucidated as a distorted figure of eight conformation and displayed weak paratropic ring current effect (Figure I.8; **I.22**). Due to the twisted topology, close proximity of a pyrrole ring with the *meso* pentafluoro group lead to a C-N bond formation with simultaneous elimination of hydrogen fluoride.

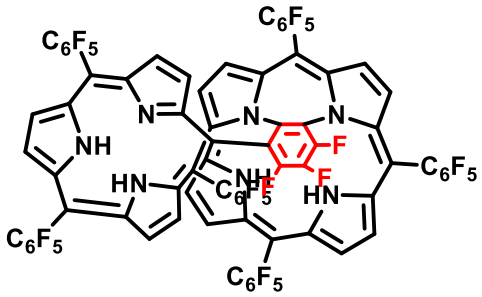

I.22

***Figure I.8**: C-N Bond formation in heptaphyrin having seven pentafluoro groups*

Overall, hetaphyrins bear a rich structural diversity and can be tuned to exist as either 4nπ or (4n+2)π systems. The role of heterocycles and number of *meso* carbon atoms were found to be crucial to synthesize a variety of hetpaphyrin analogues varying between 28π and 32π-electrons. Similar to the heptaphyrins, their immediate higher analogue i.e., octaphyrins are also known to have a much broader spectrum of macrocycles with a varying degree of aromaticity.

I.3 Octaphyrins

Octaphyrins are a class of expanded porphyrins with eight heterocyclic units in the core of the macrocycle.[10] They can be linked together with varying number of *meso* positions or even without any *meso* position in the macrocycle. The 30π octaphyrin(0.0.0.0.0.0.0.0)cyclo[8]pyrrole (Figure I.9; **I.23**) was reported by Sessler and coworkers in 2002.[28] The macrocyclic rigidity was relatively higher due to lack of *meso* carbons and hence attained a planar conformation making it a fully conjugated molecule. Inclusion of two *meso* positions enhanced the flexibility of 32π octaphyrin (1.0.0.0.1.0.0.0), (Figure I.9; **I.24**), and was found to be devoid of a planar topology.[29]

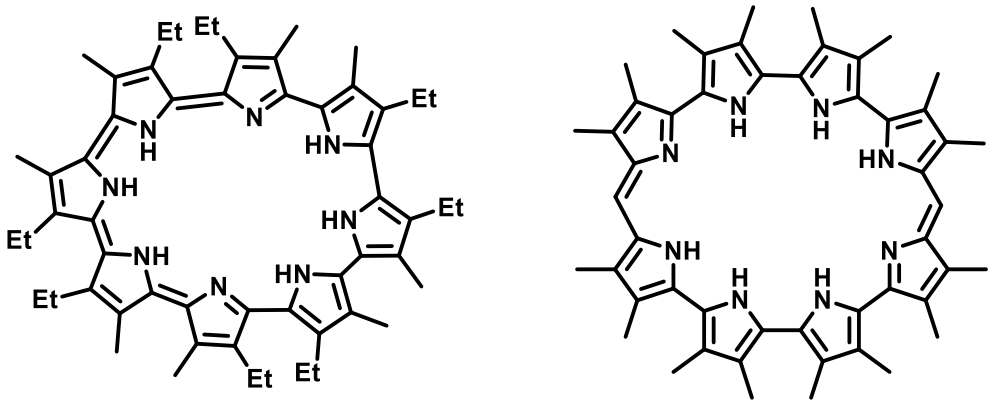

I.23 I.24

Figure I.9*: Octaphyrins with zero and two bridging units*

However, a 32π octaphyrin(1.0.1.0.1.0.1.0)[30] with four *meso* positions attained a figure of eight conformation. This structure is stabilized by multiple non-covalent interactions such as π···π and C−H···π interactions, and also by N−H···N hydrogen bonds.[31, 32] Alternatively, on replacing the two bipyrrole units with a bithiophene or a bifuran or a biselenophene unit, also resulted in a planar conformation.[33] Hence modifying the core of the macrocycle by replacing pyrrole with other heterocycles, resulted in significant alteration to the structural and electronic properties of the macrocycle. Replacing four of the pyrroles with other heterocycles with similar structural and electronic properties can modify the conjugation pathway of the octaphyrin making them 34π planar aromatic octaphyrin. The crystal structure revealed the inversion of two of the heterocylic rings in the macrocycle (Figure I.10; **I.25**). It was observed that the substituent on the *meso* positions also play a crucial role in the geometry of macrocycle. Replacing the *meso*-mesityl group by *m*-xylyl substituent[34] resulted in inversion of pyrrole rings (Figure I.10; **I.26**), instead of the thiophene rings as observed in the previous case. Another 34π octaphyrin containing biselenophene units also displayed a planar geometry with two inverted biselenophene units (Figure I.10; **I.27**).[35]

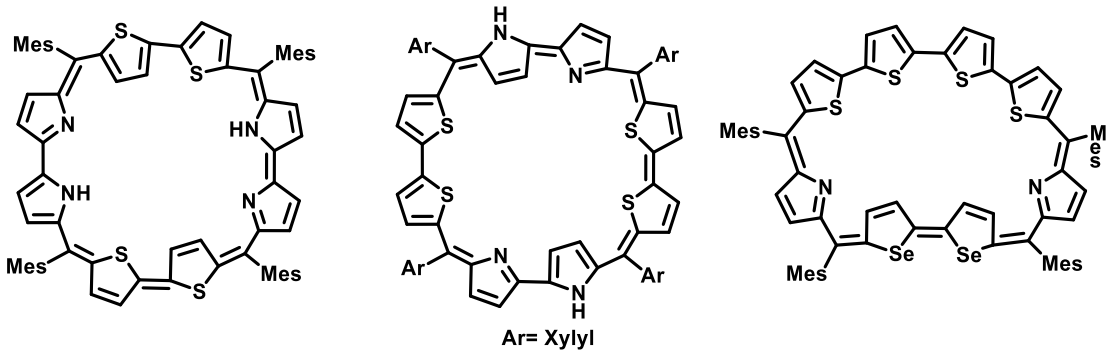

I.25 I.26 I.27

***Figure I.10**: Ring inversions in Octaphyrins with four bridging units*

A 36π octaphyrin with eight *meso* linkages (Figure I.11; **I.28**) was found to adopt a figure of eight conformation in the neutral form, but on protonation it attained a near planar conformation.[36] A complete core modification by replacing all the pyrrole units with furan units and eight *meso* positions resulted in near planar 40π octaphyrin (Figure I.11; **I.29**).[37] The crystal structure revealed a planar topology and alternate furan rings were inverted.

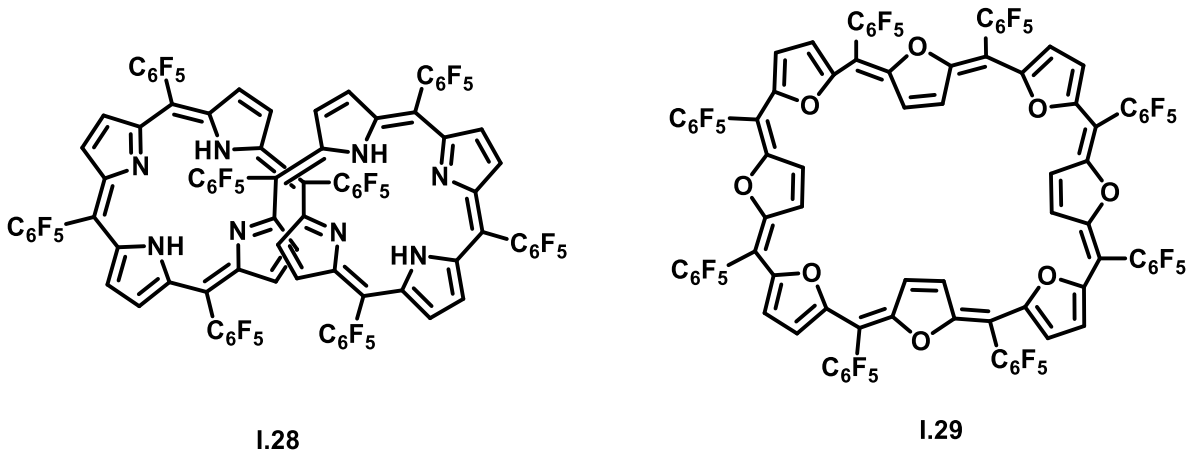

I.28 **I.29**

***Figure I.11**: 36π and 40π Octaphyrin*

I.4 Concept of aromaticity

A study of examples reported in literature, reveals that the aromaticity of a given macrocycle was conditional to pyrrole's capability to undergo amine-imine interconversion in that particular system. To control the aromaticity of the macrocycle, core modifications by replacing pyrrole with other heterocycles have been studied widely as already discussed with

some of the examples above. To obtain deeper insights about the properties of these macrocycles, it is pertinent to correlate the concept of aromaticity in the cyclic conjugates systems.

According to Hückel's theory completely conjugated and planar molecules with 4n+2π systems are classified as aromatic molecules.[38] These molecules were stable in nature due to their large HOMO-LUMO gap, and benzene being the simplest example of the same (**Figure I.12**). On the contrary, it is conceived that 4nπ systems are unstable in nature and in principle adopt an open shell configuration leading to a triplet ground state (**Figure I.12**).[39] However, the Jahn Teller distortion in these molecules can make them lose their degeneracy, thus creating a small HOMO-LUMO gap, and making them relatively stable in nature. Breslow coined the term "antiaromatic" for such planar, conjugated 4nπ systems.[40] These molecules display paratropic ring current effects in contrast to the diatropic ring current effect studied in the case of aromatic molecules. These ring current effects were mainly evaluated using chemical shift values from proton NMR spectroscopy. In aromatic molecules with effective diatropic ring current effect, the protons on the periphery of the ring were highly deshielded and their chemical shift values shifted downfield while the inner protons resonated upfield in the NMR spectrum. In contrast, the antiaromatic macrocycles displaying paratropic ring current effect induced the peripheral protons to resonate upfield and inner protons resonate downfield. Quantum chemical calculations such as the Nucleus Independent Chemical Shift (NICS) value[21] developed by Schleyer and coworkers and Anisotropy of the Induced Current Density (ACID)[41] developed by Herges and coworkers support these studies.

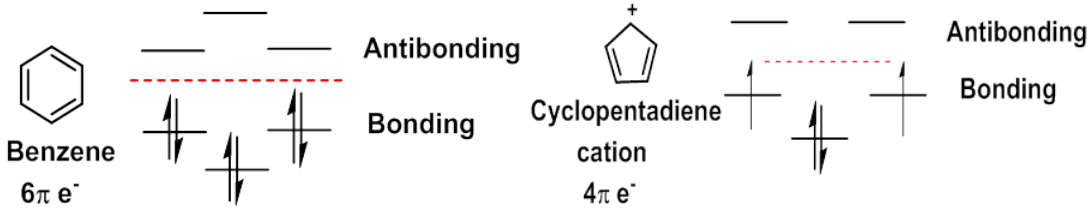

***Figure I.12**: Bonding and antibonding orbitals for an aromatic and antiaromatic system*

Indeed there are a few examples of macrocycles which deviate from planarity and yet display diatropic ring current effect. Apart from Hückels aromatic molecules, there are a whole range of different macrocycles displaying Möbius aromaticity. In 1964, based on Hückel's molecular orbital theory, Heilbronner proposed that a closed shell 4nπ system can be obtained "without loss in π-electron energy by twisting the system into a Möbius strip conformation".[42] This theory was proposed for annulenes with more than twenty carbon atoms. However, such large annulenes are difficult to synthesize and so such systems were hardly available for further studies. However, later Osuka, Kim and collaborators[43] reported Möbius aromatic molecules, in the form of metallated expanded porphyrins. A non-planar 36π octaphyrin[44], originally reported in 2001, upon complexing with palladium yielded two different bispalladium(II) complexes with different geometries. Having the same π electron count, one of the macrocycles with figure of eight conformations, having C_2 axis of symmetry displayed paratropic ring current effect and was anti aromatic in nature, while the other attained a Möbius topology and displayed diatropic ring current effect suggestive of its aromatic nature. Later a range of metallated and non metallated expanded porphyrnoids were also found to display Möbius aromaticity.[45]

I.5 Isophlorins

However, Hückel type 4nπ systems are interesting molecules and have attracted a lot of researchers towards its study. Woodward during the synthesis of chlorophyll hypothesized one such 20π system.[46] He termed it as "Isophlorin" supposedly an unstable intermediate which is readily oxidized by two-electrons to yield the 18π porphyrin. It was suggested that pyrrole and aldehyde under acidic conditions condense into an unconjugated cyclic tetrapyrrolic system (Scheme I.2; **I.30**).[47] Further **I.30** is oxidized to porphyrin **I.1** (as mentioned on first page) in two sequential steps. It was anticipated that **I.30** undergoes a four-electron oxidation to form

an unstable intermediate termed as isophlorin (Scheme I.2; **I.31**) which subsequently undergoes two-electron oxidation to yield the stable 18π porphyrin (Scheme I.2; **I.1**).

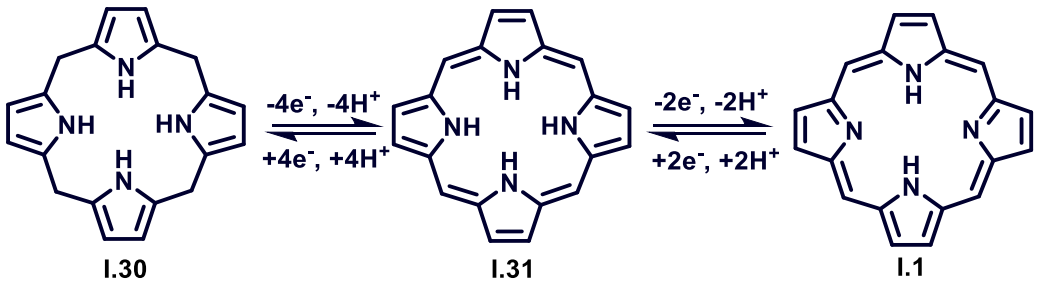

Scheme I.2*: Synthesis of porphyrin **I.1** from porphyrinogen **I.30** via hypothetical isophlorin **I.31***

It is interesting to note that both **I.31** and **I.1** differ only by two electrons, but the conjugated pathway is completely different in both the macrocycles. In the case of isophlorin, the π electrons flow through the carbon atoms on the periphery of the ring, while in porphyrins, two of the pyrrolic nitrogen also takes part in the conjugation. The difference in π electron count makes the 20π isophlorin antiaromatic while the 18π porphyrin adopts aromaticity. The ability of isophlorin to undergo oxidation readily makes it a challenge to isolate this 4nπ macrocycle under ambient conditions. In many attempts to accomplish the synthesis of a stable isophlorin, variety of modifications have been explored such as metallation, core modification and expansion in the π conjugation pathway.

The first successfully synthesized 20π isophlorin (Scheme I.3; **I.33**) by Vogel and coworkers[48] involved controlled reduction of an 18π dication (Scheme I.3; **I.32**) where the H atoms of the pyrrole nitrogen were substituted by the methyl group. Owing to the steric hindrance of the methy groups in the core of the macrocycle, **I.33** adopted a non planar topology. Hence it displayed non aromatic characteristics.

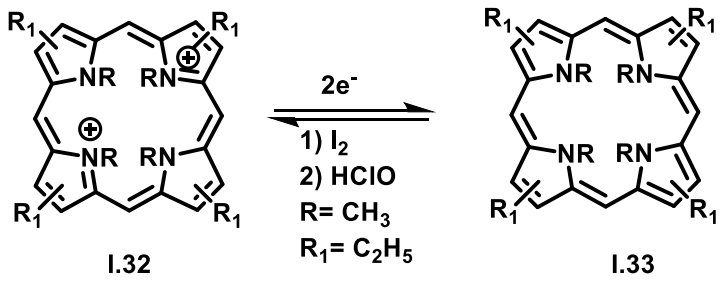

Scheme I.3*: Redox chemistry of N-tetramethylisophlorin* ***I.33*** *to its dication*

Later many attempts were made by the same group to synthesize pyrrole free isophlorins, wherein the pyrrole was replaced by furan subunits. Despite so many attempts, isophlorins could not be stabilized under ambient conditions and hindered its study further. Chen and co-workers[49] were successful in isolating a tetrapyrrole isophlorin under harsh conditions where a β tetrafluoromethyl substituted porphyrin Cu(II) complex was reduced by two electrons to demetallated isophlorin. The green copper complex solution of **I.34** (Scheme I.4) in DMSO was simultaneously reduced and demetallated with Zn powder at room temperature. This was marked by a quick color change from green to reddish brown solution under inert conditions. This was well characterized via crystal structure and revealed saddle shaped geometry. The loss of planarity was attributed to the steric hindrance of four hydrogens present in the cavity of isophlorin **I.35** (Scheme I.4) in comparison to only two hydrogens present in porphyrins. The non-planarity of the molecule made it to deviate from both aromatic as well as antiaromatic properties. To further confirm the presence of four NH in the molecule it was treated with methyl iodide, and it was revealed by crystal structure that all the four nitrogens of the pyrrole ring were derivatized with methyl group to give **I.36** (Scheme I.4). The macrocycle **I.36** also displayed a similar nonplanar geometry in its crystal structure. It was hypothesized that the presence of electron withdrawing group on pyrrole rings provided relative stability to 20π isophlorin under inert conditions.

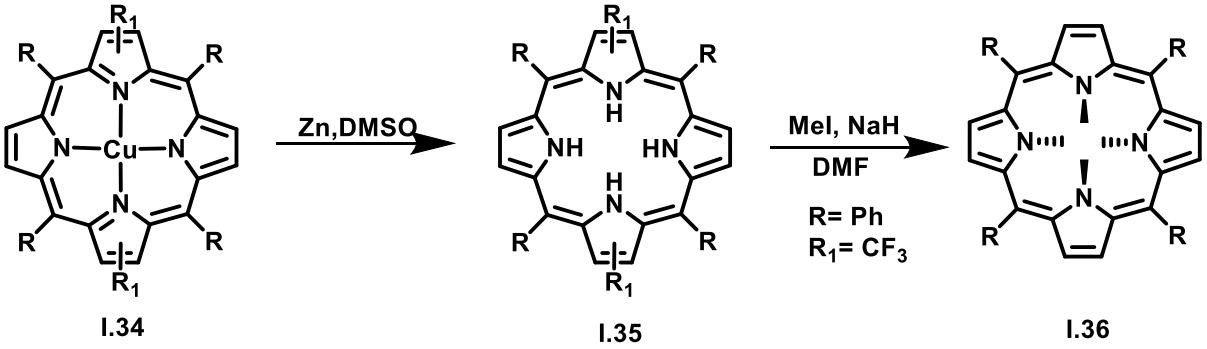

Scheme I.4*: Synthesis of isophlorin* ***I.35*** *from copper complex via simultaneous reduction and demetallation of* ***I.34***

Since presence of four hydrogens was the reason for the loss of planarity of isophlorin **I.36**, attempts were made for its thiophene and furan derivatives. But unfortunately both the molecules were stable only in its oxidized aromatic dication form.

In 2008[50], an attempt was made towards the synthesis of stable planar isophlorin **I.37** (Scheme I.5) by substituting the electron withdrawing group at the *meso* positions of the macrocycle.

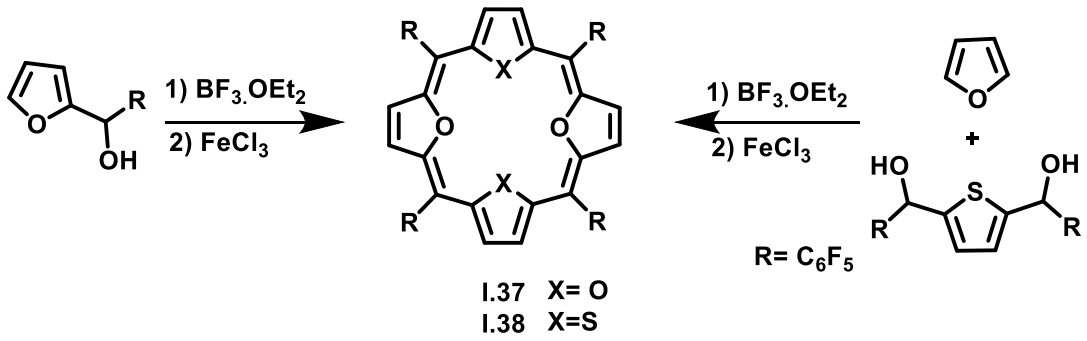

Scheme I.5*: Synthesis of stable furan and thiophene derivative of meso substituted 20π isophlorin*

Pentafluorophenyl furfural was self-condensed under acidic conditions followed by $FeCl_3$ oxidation to yield the 20π isophlorin **I.37**. The molecule displayed only a singlet in its proton NMR resonating at δ 2.49 ppm, suggesting strong paratropic ring current effects for the macrocycle. The crystal structure revealed that the molecule was completely planar, which was quite evident from the paratropic ring current effect observed in the molecule. A thiophene derivative for the same conjugation system was synthesized by modifying the scheme, where thiophene diol was condensed with furan under acidic conditions followed by oxidation to yield

I.38 (Scheme I.5). This molecule also revealed a planar structure and the two distinct protons resonated at δ 3.37 and δ 3.33 ppm suggesting the presence of significant paratropic ring current effects.

Later Shinmyozu and coworkers[51] prepared a tetrathia isophlorin **I.40** (Scheme I.6) with 18π electrons. The macrocycle adopted a non-planar topology and displayed singlet at δ 6.19 ppm in its proton NMR suggesting poor paratropic ring current effect.

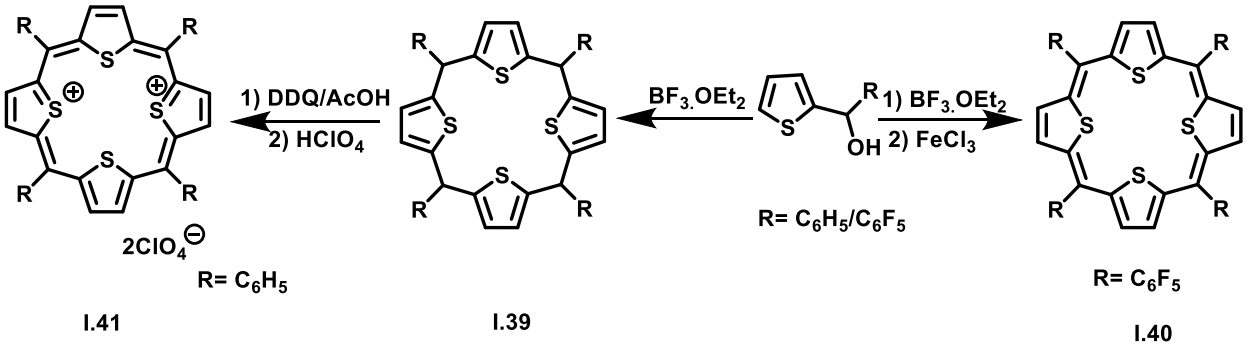

Scheme I.6: *Synthetic route for 20π Stable tetrathiaisophlorin*

The drive to synthesize a stable pyrrole derivative of isophlorin was achieved by modifying the core of the 18π porphyrin **I.1** (as mentioned on first page). **I.1** being aromatic in nature did not alter its aromatic properties on replacing one or two pyrrole rings with thiophene/furan (Figure I.13; **I.42** and **I.43**), but when three or four pyrrole rings were replaced by other similar heterocycles, the conjugation pathway changed drastically to transform into 20π antiaromatic system (Figure I.13; **1.44**).[52]

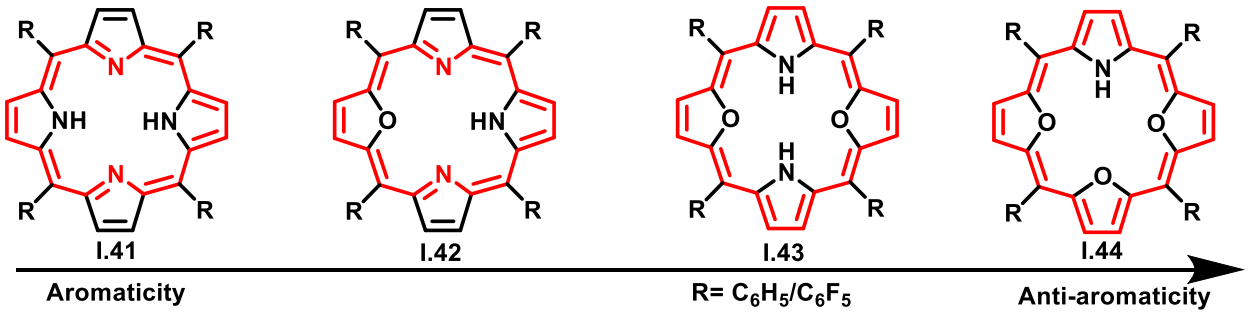

Figure I.13: *Reversal of behavior from aromatic to anti aromatic on replacement of pyrrole rings with furan*

To study 4nπ systems better, the core modification was extended to expanded porphynoid systems also.

The conjugation pathway in isophlorins is always through the carbons, unlike porphyrnoids where the conjugation flows through nitrogen of the pyrrole ring. Hence replacing all the nitrogen by other chalcogens favor synthesis of 4nπ isophlorins, provided the system is capable of complete conjugation.

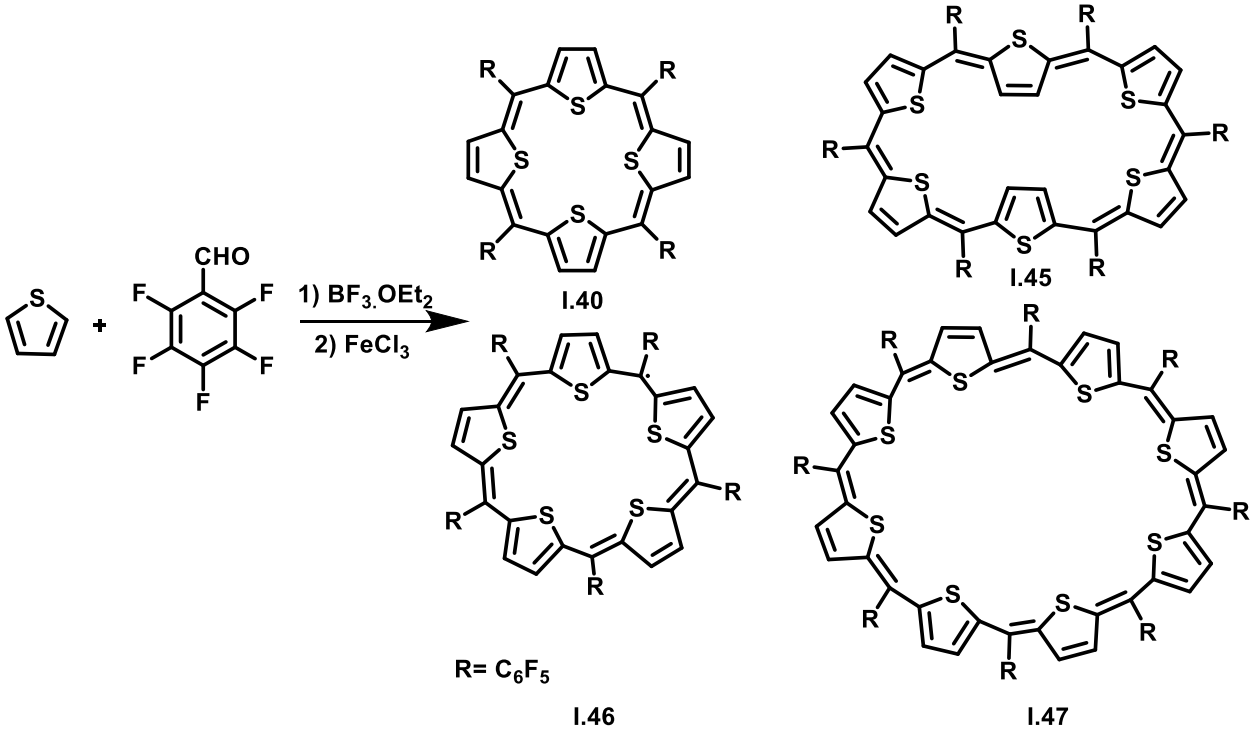

Scheme I.7: *One-pot cyclisation reaction resulting in multiple expanded isophlorins*

One pot condensation of thiophene with pentafluorobenzaldehyde using $BF_3.OEt_2$, followed by $FeCl_3$ oxidation gave multiple macrocycles varying from four membered to eight membered (Scheme I.7; **I.40**, **1.45-I.47**). **I.46** (Scheme I.7) having five thiophene units was unexpectedly found to be fully conjugated stable, neutral and an air stable 25π radical.[53] This radical was capable of undergoing both one-electron oxidation and reduction under suitable conditions to yield the stable antiaromatic 24π cation and aromatic 26π anion respectively.

The six membered macrocycle **I.45** (Scheme I.7) formed along with other macrocycles in this reaction was characterized as a fully conjugated 30π aromatic isophlorin.[53] The molecule was

planar and the two of the thiophene rings had inverted evident from its crystal structure and proton NMR. The molecule displayed diatropic ring current effect where the inverted ring protons resonated at δ -0.46 ppm and the other two thiophene ring protons resonated at δ 9.18 and 9.09 ppm. To exclusively synthesize the six membered aromatic isophlorins, the synthetic scheme was modified and thiophene diol was condensed with thiophene. In a comparative study similar protocol was followed and thiophene diol was condensed with furan and selenophene to yield the 30π isophlorin (Scheme I.8). However the crystal structure revealed a difference in topology, wherein the macrocycle with selenophene and all thiophenes in the core (Scheme I.8; **I.48**) displayed a rectangular topology with two ring inversions, whereas the one with alternate furan rings (Scheme I.8; **I.49**) displayed a triangular topology with no ring inversion.[54]

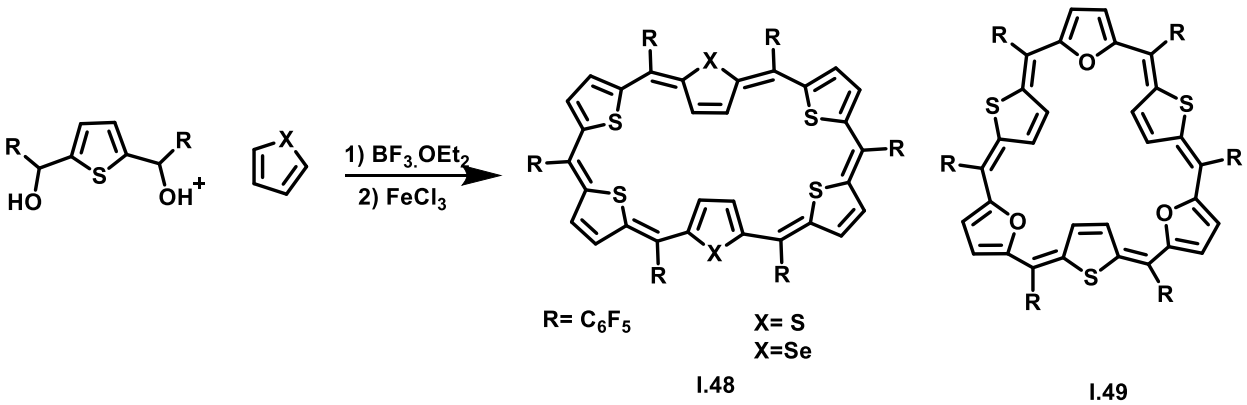

Scheme I.8*: Acid-catalyzed condensation of thiophene diol with thiophene/ furan/ selenophene to yield 30π isophlorins*

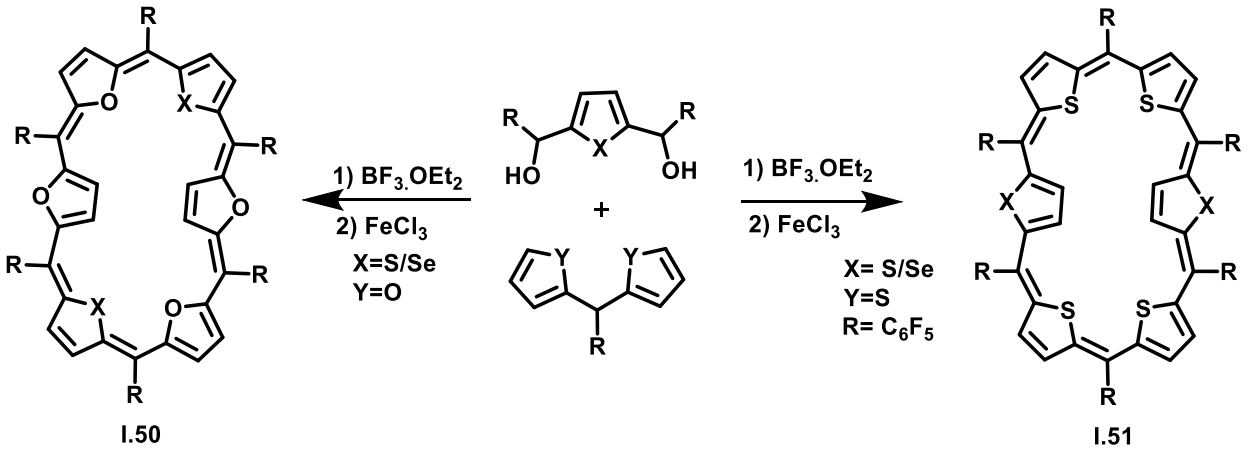

Scheme I.9*: Alternate synthetic route to yield 30π isophlorins*

Another set of 30π isophlorins were synthesized via acid condensation of dithienyl/difuranyl methane with thiophene or selenophene diol (Scheme I.9).[54] In all the above described protocols, the topology of hexaphyrin remained planar with two ring inversions.

One pot condensation of furan with pentafluorobenzaldehyde resulted in only two products which were identified as 30π hexaphyrin **I.52** (Scheme I.10) and 40π octaphyrin **I.53** (Scheme I.10). The six membered 30π hexafuran was aromatic and displayed diatropic ring current effect in contrast to the 40π octaphyrin which was antiaromatic and displayed paratropic ring current effect.[37]

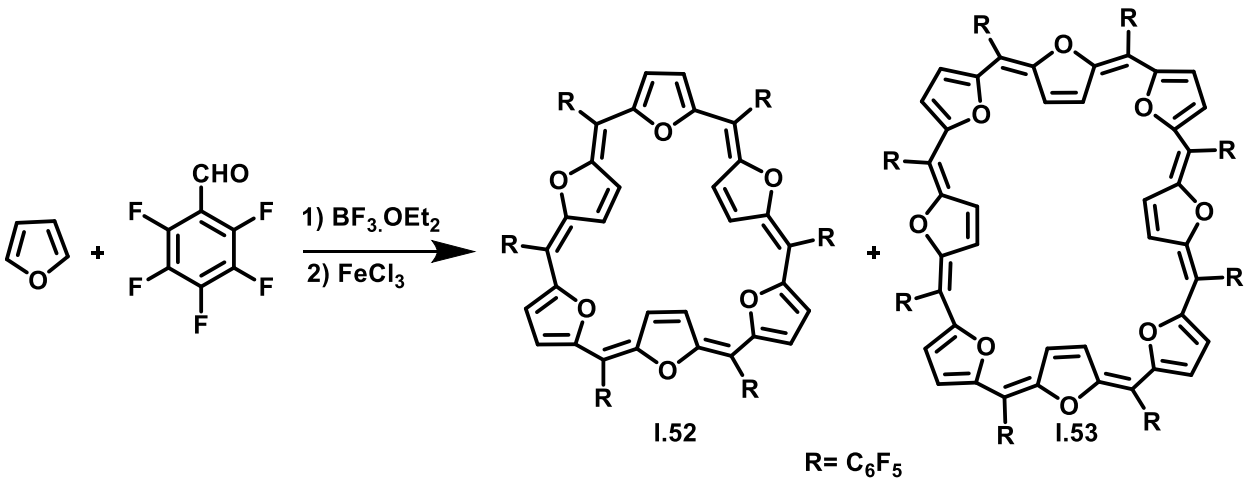

Scheme I.10*: Acid catalysed condensation of furan with pentafluorobenzaldehyde to yield 30π and 40π isophlorins*

Later another 30π system (Scheme I.11; **I.54**) was explored wherein the two thiophene rings of **I.48** (Scheme I.8) were replaced with benzene units.[55]

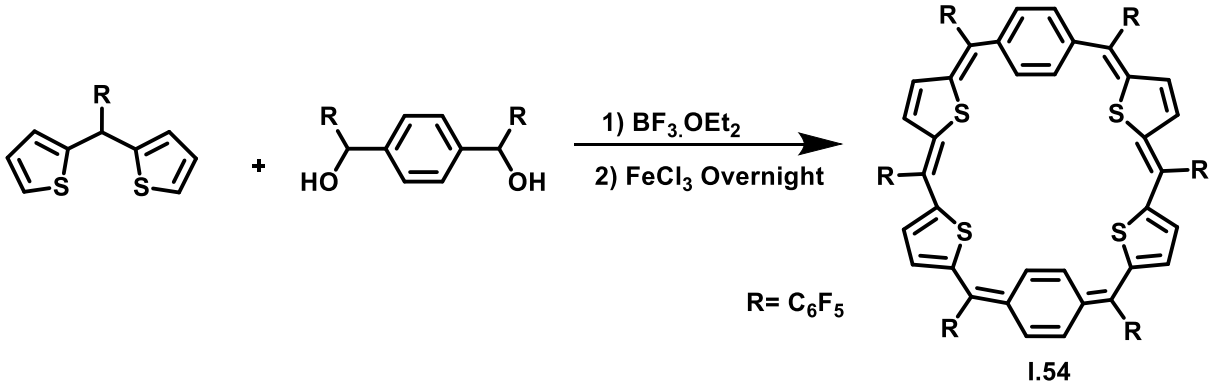

Scheme I.11*: Introduction of benzene units in the core of the isophlorins*

The π conjugation of these expanded isophlorins was further extended by including ethylene bridges in the conjugated system. The isophlorin **I.55** (Scheme I.12) was synthesized by condensing (E)-1,2-Dithienylethylene with thiophene diol using $BF_3.OEt_2$ followed by $FeCl_3$ oxidation. The paratropic ring current was evident from its low temperature proton NMR spectrum, where the inner protons of the ethylene bridge resonated at δ 12.83 ppm while the outer protons resonated at δ 5.37 ppm.[56]

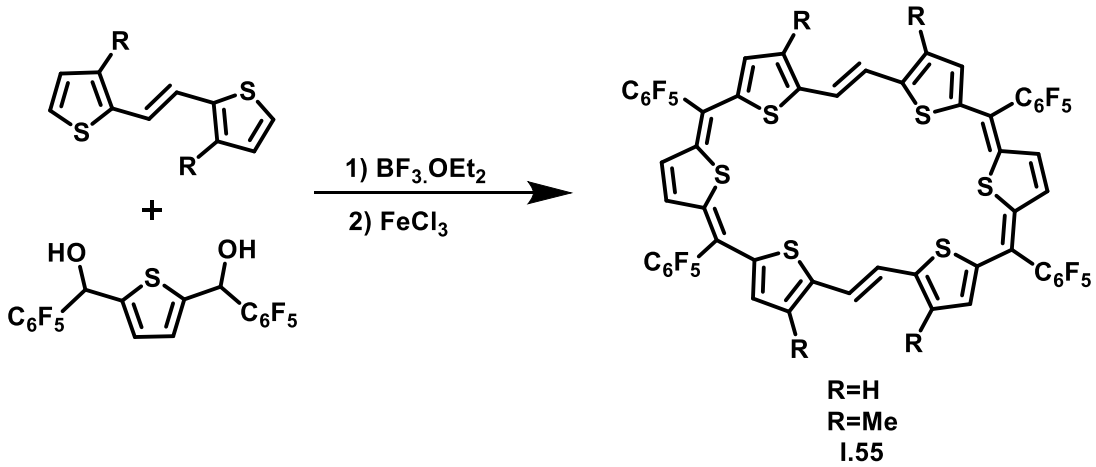

Scheme I.12*: Acid catalyzed condensation of thiophene diol with (E)-1,2-Dithienylethylene to yield ethylene bridged 32π isophlorin*

Later a similar protocol was employed where bisfuran ethylene was condensed with thiophene diol, furandiol and selenophene diol, in each case forming 32π expanded isophlorin.[57] X-ray studies revealed that while **I.56** and **I.57** (Scheme I.13) were planar, **I.58** (Scheme I.13) had attained a figure of eight conformation. However, on oxidation with trifluoroacetic acid the molecule attained a planar topology with two trifluoroacetate as the counter anions in the crystal lattice. All the above three 32π isophlorins underwent reversible two-electron oxidation using trifluoroacetic acid as well as Meerweins salt.

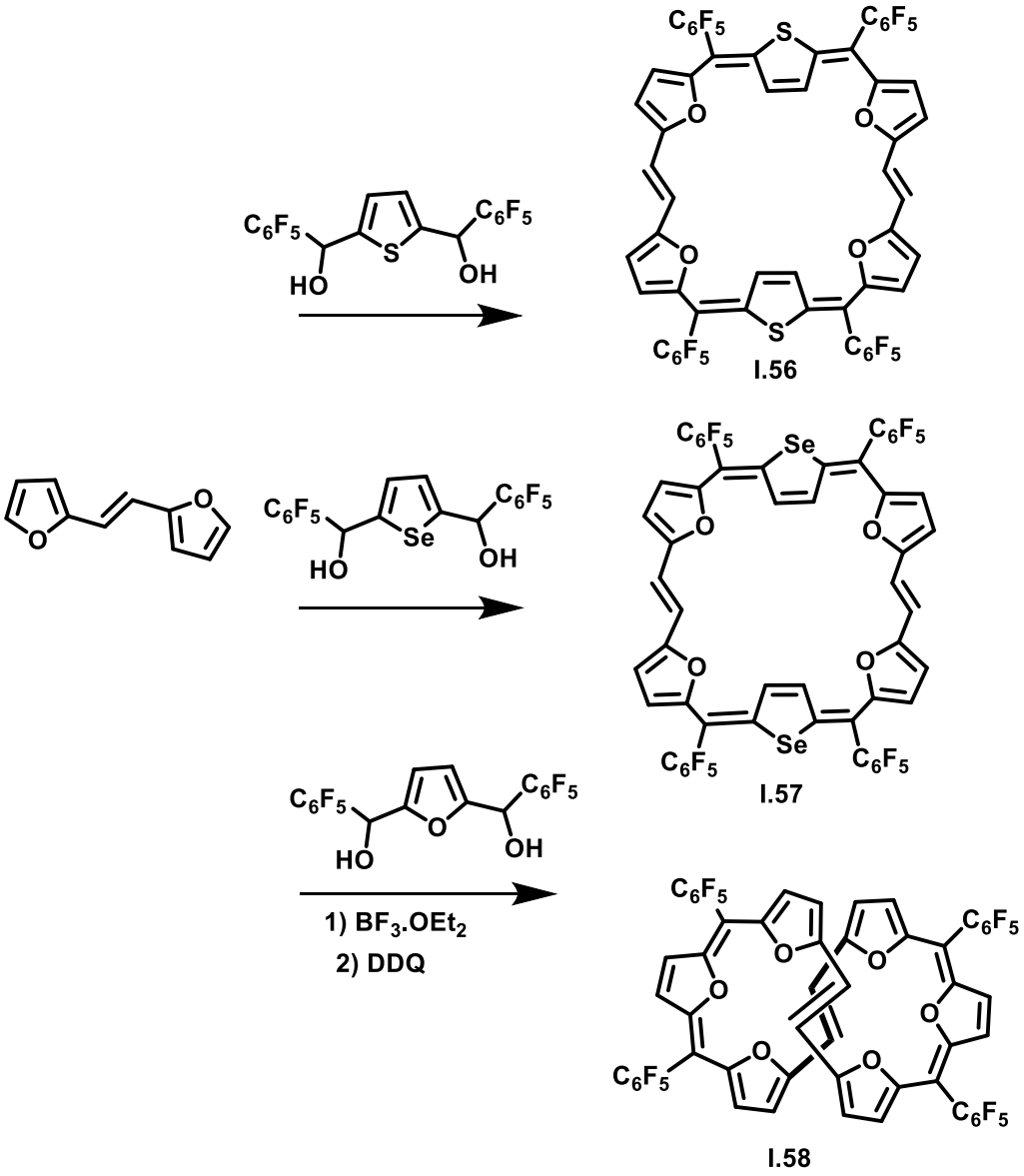

Scheme I.13*: Synthesis of various derivatives of ethylene bridged 32π isophlorin*

Ethylene bridges with *cis* configuration was also synthesized by McMurry coupling of different dialdehydes (Scheme I.14). A 22π expanded isophlorin (Scheme I.14; **I.59**) was prepared using McMurry coupling of dithienyl dialdehyde.[58]

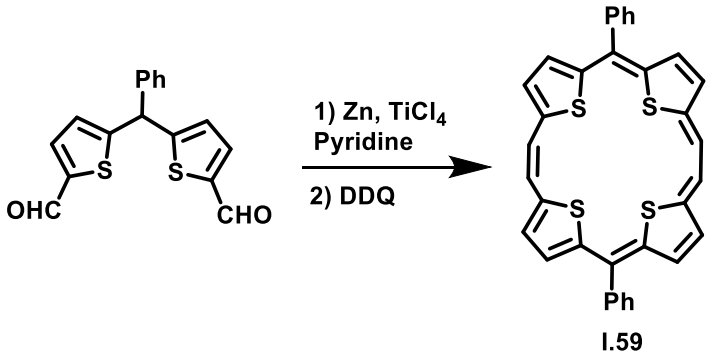

Scheme I.14*: Synthesis of ethylene bridged 22π isophlorin*

Some other ethylene bridged isophlorins (**I.60** to **I.63**) that were synthesized are shown in Scheme **I.15**. However, many of these macrocycles did not display significant ring current effects as expected of either 4nπ or (4n+2)π systems.[59]

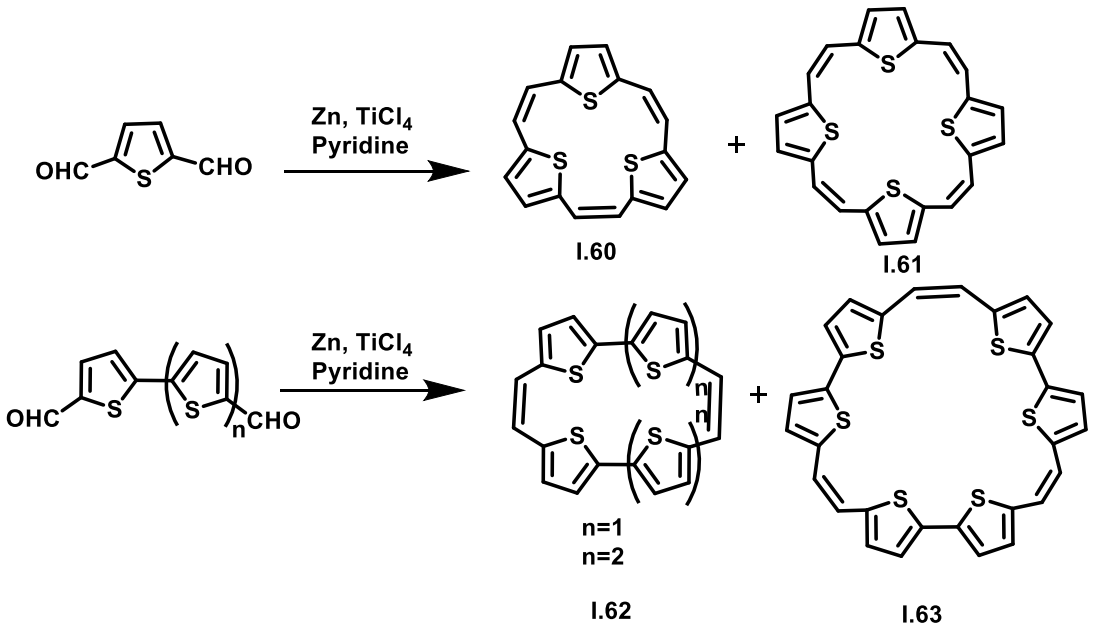

Scheme I.15*: McMurry coupling for the introduction of ethylene bridge in the isophlorin core*

I.6 Aim of the thesis

Aromatic molecules as stated by Hückel are planar, conjugated, (4n+2)π electronic systems.[37] Benzene is the simplest known example for the same. On the other hand, 4nπ systems are anti-aromatic and not so stable. Isophlorinoids are typical examples for stable anti-aromatic systems. Such 4nπ conjugated macrocycles could be stabilized by changing the core of a porphyrin by substituting pyrrole with other heterocyclic units such as furan or thiophene. Signature paratropic ring current effects from NMR spectroscopy are crucial to evaluate the extent of planarity and antiaromaticity of these macrocycles. Such molecules are vulnerable to redox reactions similar to metal ions. However, large expanded porphyrins adopt figure-of-eight topology owing to their structural flexibility.

This thesis aims towards the synthesis, characterization and redox study of novel core modified expanded isophlorinoids with six, seven, eight, nine and ten heterocyclic units. Synthesis of only a few heptaphyrins consisting of two or more pyrrole rings in the core of the macrocycle has been established till date. The pyrrole's innate nature to undergo imine-amine inter-conversion leads to the stabilization of aromatic heptaphyrins in most of the known macrocycles. Based on the complexity involved in the synthesis of heptaphyrins due to the presence of odd number of repeating units, a main aim of this thesis will be to develop a novel asymmetric tristhiophene precursor which could be further utilized towards the synthesis of completely core modified planar antiaromatic 32π heptaphyrin containing four bridging carbons. The 32π heptaphyrin being antiaromaic in nature would be further explored for its redox properties. Then, its utility will be explored to synthesize higher members of the family. Core modified octaphyrins containing either thiophene or furan units[36] and having eight bridging units are known to be planar with alternate ring inversions. Hence asymmetrical precursor will be apt to explore the mixed octaphyrins having both thiophene and furan units in the core of the macrocycle and study the redox behavior of the obtained 40π octaphyrin.

Further, the studies will be oriented towards macrocycles with decreased number of bridging carbons. The novel asymmetric tristhiophene would be further utilized to synthesis 38π octaphyrin with six bridging units. It is expected that this methodology will lead isomeric octaphyrins from the same reaction and then each octaphyrin can be individually studied. A similar protocol would be utilized to decrease the bridging carbons and synthesis higher analogues of these macrocycles such as 46π decaphyrins. Further, this study would explore macrocycles with higher number of bridging units than the heterocyclic units present in the core of the macrocycle. Most of the expanded porphyrins containing ethylene bridges are synthesized using McMurry coupling, which leads to the stabilization of ethylene bridge in the *E* conformer. Further, this methodology will be explored for the synthesis of hexaphyrin and nonaphyrin containing ethylene bridged *Z* conformer. This is expected to be successful by modifying the synthetic strategy and utilizing a precursor containing ethylene bridge in *Z* conformer. Further, adequate quantum calculations would be performed on these synthesized macrocycles in support of these studies.

I.7 References

(1) Johnson, D. G.; Niemczyk, M. P.; Minsek, D. W.; Wiederrecht, G. P.; Svec, W. A.; Gaines, G. L.; Wasielewski, M. R. *J. Am. Chem. Soc.* **1993**, *115*, 5692-5701.

(2) (a) Battersby, A. R. *Nat. Prod. Rep*. **2000**, *17*, 507-526; (b) L. R. Milgrom, The Colours of Life: An Introduction to the Chemistry of Porphyrins and Related Compounds, Oxford University Press, New York, **1997**.

(3) (a) Moan, J.; Berg. K. *Photochem. Photobiol.* **1991**, *53*, 549–553. (b) Davia, K.; King. D.; Hong, Y.; Swavey, S. *Inorg. Chem. Commun.* **2008**, *11*, 584-586. (c) Ko, Y. J.; Yun, K. J.; Kang, J. P.; Lee, K. T.; Park, S. B.; Shin, J. H. *Bioorg. Med. Chem. Lett.* **2007**, *17*, 2789-2794.

(4) Montanari, F.; Casella, L. *Metalloporphyrins Catalyzed Oxidations*; Kluwer: Dordrecht, **1994.**

(5) Sokolov, V. S.; Batishchev, O. V.; Akimov, S. A.; Galimzyanov, T. R.; Konstantinova, A. N.; Malingriaux, E.; Gorbunova, Y. G.; Knyazev, D. G.; Pohl, P. *Sci. Rep.* **2018**, *8*, 1-11. (b) Zhao, J.; Liu, C. S.; Yuan, Y.; Tao, X. Y.; Shan, X. Q.; Sheng, Y.; Wu. F. *Biomaterials,* **2007**, *28*, 1414-1422.

(6) (a) Norwood, R. A.; Sounik, J. R. *Appl. Phys. Lett.* **1992**, *60*, 295-297. (b) Keinan, S.; Therien, M. J.; Beratan, D. N.; Yang, W. *Phys. Chem. A* **2008**, *112*, 12203-12207.

(7) Harriman, A. *J. Photochem. Photobiol., A*, **1990**, *51*, 9-19.

(8) Senge, M. O.; Sergeeva, N. N.; Hale, K. J. *Chem. Soc. Rev*. **2021**, *50*, 4730-4789.

(9) Wallace, D. M.; Leung, S. H.; Senge, M. O.; Smith, K. M. *J. Org. Chem.* **1993**, *58*, 7245-7257.

(10) Sessler, J. L.; Seidel, D. *Angew. Chem. Int. Ed.* **2003**, *42*, 5134-5175.

(11) Sessler, J. L.; Cyr, M. J.; Lynch, V.; McGhee, E.; Ibers, J. A. *J. Am. Chem. Soc.* **1990**, *112*, 7, 2810-2813.

(12) Szyszko, B.; Białek, M. J.; Pacholska-Dudziak, E.; Latos-Grażyński, L. *Chem. Rev.* **2017**, *117*, 4, 2839-2909.

(13) Sessler, J. L.; Seidel, D.; Lynch, V. *J. Am. Chem. Soc*. **1999**, *121*, 11257-11258.

(14) Köhler, T.; Seidel, D.; Lynch, V.; Arp, F. O.; Ou, Z.; Kadish, K. M.; Sessler, J. L. *J. Am. Chem. Soc.* **2003**, *125*, 6872-6873.

(15) Anguera, G.; Kauffmann, B.; Borrell, J. I.; Borrós, S.; Sánchez-García, D. *Org. Lett*. **2015**, *17*, 2194-2197.

(16) Anand, V. R. G.; Pushpan, S. K.; Srinivasan, A.; Narayanan, S. J.; Sridevi, B.; Chandrashekar, T. K.; Roy, R.; Joshi, B. S. *Org. Lett*. **2000**, *2*, 3829-3832.

(17) Anand, V. G.; Pushpan, S. K.; Venkatraman, S.; Narayanan, S. J.; Dey, A.; Chandrashekar, T. K.; Roy, R.; Joshi, B. S.; Deepa, S.; Sastry, G. N. *J. Org. Chem.* **2002**, *67*, 6309-6319.

(18) Rath, H.; Sankar, J.; PrabhuRaja, V.; Chandrashekar, T. K.; Joshi, B. S. *Org. Lett*. **2005**, *7*, 5445-5448.

(19) Bucher, C.; Seidel, D.; Lynch, V.; Sessler, J. L. *Chem. Commun.* **2002**, 328-329.

(20) Ghosh, A.; Chaudhary, A.; Srinivasan, A.; Suresh, C. H.; Chandrashekar, T. K. *Chem. Eur. J.* **2016**, *22*, 3942-3946.

(21) Schleyer, P. v. R.; Maerker, C.; Dransfeld, A.; Jiao, H.; Hommes, N. J. R. v. E. *J. Am. Chem. Soc.* **1996**, *118*, 6317-6318.

(22) Karthik, G.; Srinivasan, A.; Suresh, C. H.; Chandrashekar, T. K. *Chem. Commun*. **2014**, *50*, 12127-12130.

(23) Gokulnath, S.; Prabhuraja, V.; Chandrashekar, T. K. *Org. Lett*. **2007**, *9*, 3355-3357.

(24) Hiroto, S.; Shinokubo, H.; Osuka, A. *J. Am. Chem. Soc*. **2006**, *128*, 6568-6569.

(25) Shin, J. Y.; Lim, J. M.; Yoon, Z. S.; Kim, K. S.; Yoon, M.-C.; Hiroto, S.; Shinokubo, H.; Shimizu, S.; Osuka, A.; Kim, D. *J. Phys. Chem. B* **2009**, *113*, 5794-5802.

(26) Shin, J. Y.; Furuta, H.; Yoza, K.; Igarashi, S.; Osuka, A. *J. Am. Chem. Soc.* **2001**, *123*, 7190-7191.

(27) Saito, S.; Osuka, A. *Chem. Eur. J.* **2006**, *12*, 9095-9102.

(28) Seidel, D.; Lynch, V.; Sessler, J. L. *Angew. Chem. Int. Ed.* **2002**, *41*, 1422-1425.

(29) Sessler, J. L.; Seidel, D. *J. Am. Chem. Soc.* **1999**, *121*, 11257-11258.

(30) Bröring, M.; Jendrny, J.; Zander, L.; Schmickler, H.; Lex, J.; Wu, Y. D.; Nendel, M.; Chen, J.; Plattner, D. A.; Houk, K. N.; Vogel, E. *Angew. Chem., Int. Ed. Engl*. **1995**, *34*, 2515-251.

(31) Woller, T.; Contreras-Garcia, J.; Geerlings, P.; De Proft, F.; Alonso, M. *Phys. Chem. Chem. Phys.* **2016**, *18*, 11885-11900.

(32) Mori, M.; Okawa, T.; Iizuna, N.; Nakayama, K.; Lintuluoto, J. M.; Setsune, J. I. *J. Org. Chem*. **2009**, *74*, 3579-3582.

(33) Anand, V. G.; Pushpan, S. K.; Venkatraman, S.; Dey, A.; Chandrashekar, T. K.; Joshi, B. S.; Roy, R.; Teng, W.; Senge, K. R. *J. Am. Chem. Soc.* **2001**, *123*, 8620-8621.

(34) Anand, V. G.; Venkatraman, S.; Rath, H.; Chandrashekar, T. K.; Teng, W. J.; Ruhlandt-Senge, K. *Chem. Eur. J.* **2003**, *9*, 2282-2290.

(35) Kumar, R.; Misra, R.; Chandrashekar, T. K.; Suresh, E. *Chem. Commun.* **2007**, 43-45.

(36) Taniguchi, R.; Shimizu, S.; Suzuki, M.; Shin, J. Y.; Furuta, H.; Osuka, A. *Tetrahedron Lett*. **2003**, *44*, 2505-2507.

(37) Reddy, J. S.; Mandal, S.; Anand, V. G. *Org. Lett*. **2006**, *8*, 5541-5543.

(38) Garratt, V. P. J. *Aromaticity*; Wiley-Interscience: New York, **1986**.

(39) Breslow, R.; Jaun, B.; Kluttz, R. Q.; Xia, C. Z. *Tetrahedron* **1982**, *38*, 863-867.

(40) Breslow, R. *Acc. Chem. Res.* **1973**, *6*, 393-398.

(41) Geuenich, D.; Hess, K.; Kohler, F.; Herges, R. *Chem. Rev.* **2005**, *105*, 3758-3772.

(42) Heilbronner, E. *Tetrahedron Lett.* **1964,** *5*, 1923-1928.

(43) Tanaka, Y.; Saito, S.; Mori, S.; Aratani, N.; Shinokubo, H.; Shibata, N.; Higuchi, Y.; Yoon, Z. S.; Kim, K. S.; Noh, S. B.; Park, J. K.; Kim, D.; Osuka, A. *Angew. Chem., Int. Ed.* **2008**, *47*, 681-684.

(44) Shin, J.-Y.; Furuta. H.; Yoza, K.; Igarashi, S.; Osuka, *J. Am. Chem. Soc.* **2001**, 123, 7190-7191.

(45) Yoon, Z., Osuka, A.; Kim, D. *Nature Chem* **2009**, *1*, 113-122.

(46) Woodward, R. B. *Angew. Chem*. **1960**, *72*, 651-662.

(47) Ghosh, A. *Angew. Chem., Int. Ed.* **2004**, *43*, 1918-1931.

(48) Vogel, E. *Pure Appl. Chem.* **1993**, *65*, 143-152.

(49) Liu, C.; Shen, D.-M.; Chen, Q.-Y. *J. Am. Chem. Soc.* **2007**, *129*, 5814-5815.

(50) Reddy, J. S.; Anand, V. G. *J. Am. Chem. Soc.* **2008**, *130*, 3718-3719.

(51) Kon-no, M.; Mack, J.; Kobayashi, N.; Suenaga, M.; Yoza, K.; Shinmyozu, T. *Chem. Eur. J.* **2012**, *18*, 13361-13371.

(52) Reddy, B. K.; Basavarajappa, A.; Ambhore, M. D.; Anand, V. G. *Chem. Rev*. **2017**, *117*, 3420-3443.

(53) Gopalakrishna, T. Y.; Reddy, J. S.; Anand, V. G. *Angew. Chem., Int. Ed.* **2014**, *53*, 10984-10987.

(54) Reddy, J. S.; Anand, V. G. *J. Am. Chem. Soc*. **2009**, *131*, 15433-15439.

(55) Reddy, J. S.; Anand, V. G. *Chem. Commun*. **2008**, 1326-1328.

(56) Gopalakrishna, T. Y.; Reddy, J. S.; Anand, V. G. *Angew. Chem., Int. Ed.* **2013**, *52*, 1763-1767.

(57) Gopalakrishna, T. Y.; Anand, V. G. *Angew. Chem., Int. Ed*. **2014**, *53*, 6678-6682.

(58) Singh, K.; Sharma, A.; Zhang, J.; Xu, W.; Zhu, D. *Chem. Commun*. **2011**, *47*, 905-907.

(59) Hu, Z. Y.; Atwood, J. L.; Cava, M. P. *J. Org. Chem*. **1994**, *59*, 8071-8075.

Chapter 2

Synthesis, Characterization and Redox Properties of 32π Heptaphyrins

II.1 Introduction

Heptaphyrins are expanded porphyrnoids with seven heterocycles in the core of the macrocycle. Bearing odd number of heterocycles, their synthesis is complex in comparison to octaphyrins and hexaphyrins and hence are under explored macrocycles. The earliest known heptaphyrin **II.1** (Figure II.1) was reported by Sessler[1] where oligo pyrroles were oxidatively coupled under acidic conditions to yield [3+2+2] cyclisation product. A heptaphyrin thus obtained containing two bridging carbons was identified as a planar 28π nonaromatic macrocycle.

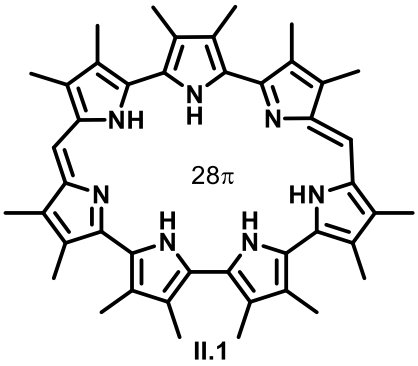

Figure II.1*: First reported heptaphyrin*

Later another 30π heptaphyrin[2] was synthesized by the same group with five bridging carbons. Further, a few more heptaphyrins[3] with varying number of *meso* carbons have been synthesized. In a few examples, two or more pyrrole rings were replaced by other heterocycles to yield other heptaphyrin derivatives. Presence of pyrrole rings in these heptaphyrins enables a global π conjugation in the macrocycle due to the innate ability of pyrrole to undergo reversible amine-immine interconversion. Heptaphyrins (Scheme II.I; **II.2**)[4] containing five *meso* positions and four pyrrole rings were found to be redox active and interconvertible between 32π and 30π heptaphyrin, **II.3**.

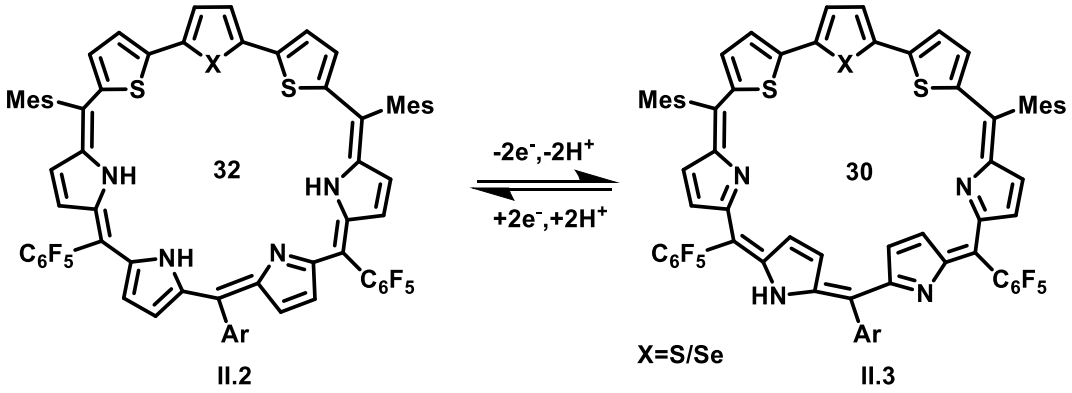

Scheme II.1*: Redox interconversion between 32π heptaphyrin to 30π heptaphyrin*

All the known heptaphyrins in literature contained atleast two or more pyrrole rings in the core of macrocycle. To overcome the amine-imine interconversion, an attempt was made to synthesize pyrrole free core modified heptaphyrins.

II.2 Synthesis of 32π expanded heptaphyrin

As the macrocycle has seven heterocycles, it is essential to design at least one precursor to have an odd number of heterocyclic units. Adoption of this synthetic strategy required the synthesis of a novel and asymmetrical tri-thiophene oligomer **II.6** as described in Scheme II.2. At first, the monobromo derivative of dithienyl thiophene **II.5** was synthesized by condensing thiophene monol **II.4** with 2-Bromothiophene, further Kumada coupling of **II.5** with 2-bromothriophene yielded the novel asymmetric tristhiophene **II.6** in 35% yields. Further, the synthesis of 32π heptaphyrin (Scheme II.3; **II.8-II.9**) was attempted by condensing two equivalents of asymmetric tristhiophene (Scheme II.2; **II.6**) with one equivalent of furan[5] or thiophene diol[6] (Scheme II.2; **II.7**) with catalytic amount of $BF_3.OEt_2$. The reaction mixture was stirred under dark and inert conditions for two hours followed by oxidation using DDQ. The reaction mixture was passed through a pad of basic alumina and further purified on alumina column with DCM and hexane as eluent.

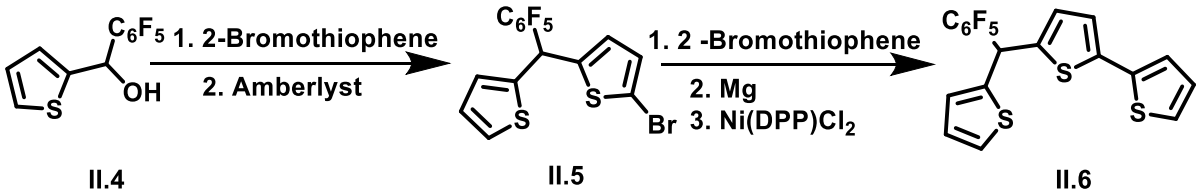

***Scheme II.2**: Synthesis of novel asymmetric tristhiophene*

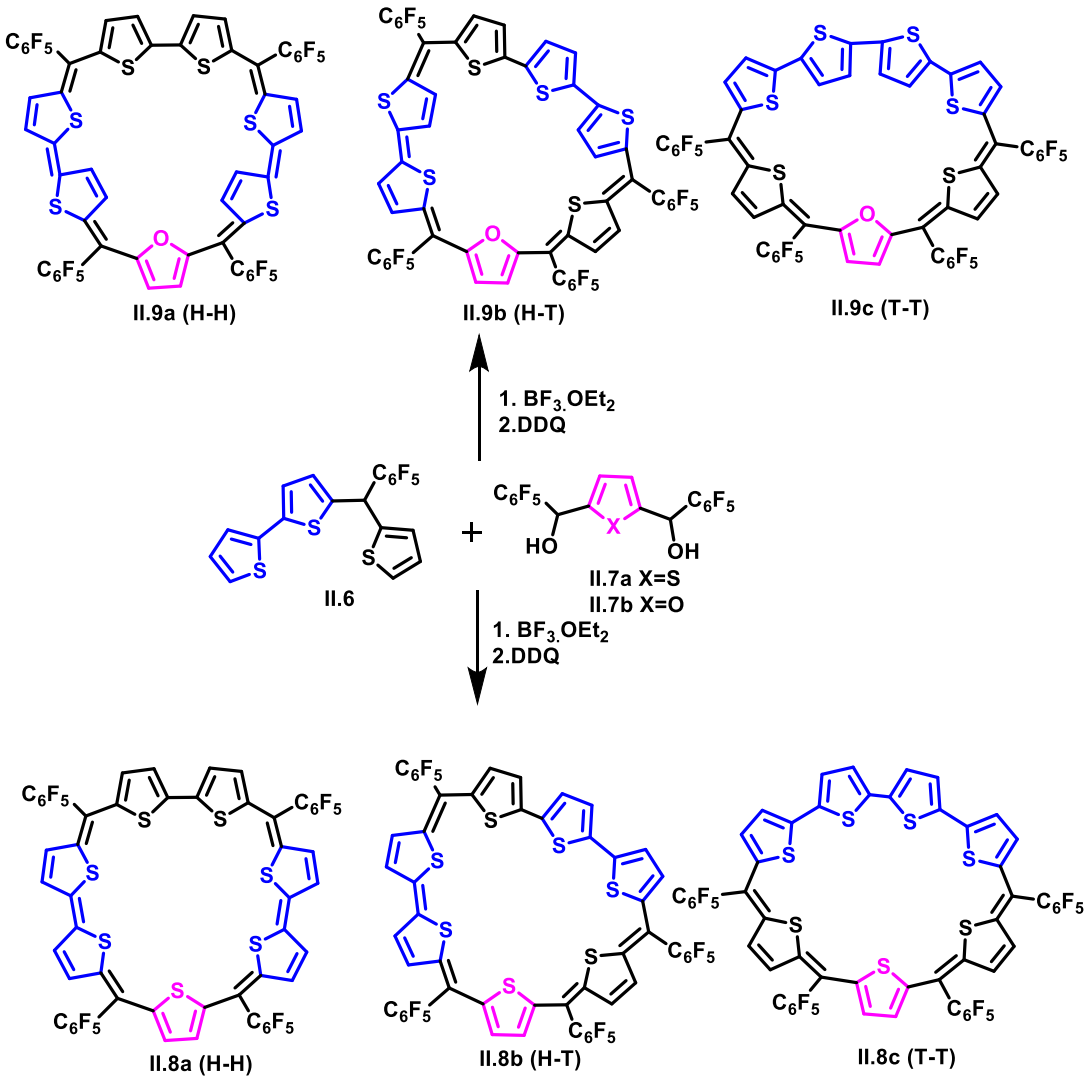

***Scheme II.3**: Synthesis of core modified 32π heptaphyrin*

The reaction mixture in both the cases was analyzed through MALDI TOF/TOF spectrometry (Figure II.2-II.3). The spectra confirmed the formation of a seven membered macrocycle as the major product in the reaction, in both the cases, along with some higher member macrocycles in very poor yields. As shown in the synthetic scheme, there are three different possibilities for

the formation of seven membered macrocycle. In this strategy, a 2:1 condensation of tris-thiophene with the alcohol results in the generation of a seven membered oligomer. However, based on the oligomer formed through this condensation, three different coupling either head-to-head (H-H) or head to tail (H-T) or tail to tail (T-T) can be envisaged for the terminal thiophenes. However, all the three structural isomers correspond to 32π electrons. Even though the MALDI TOF/TOF mass spectrum confirmed the formation of the product, but it could not distinguish the major or minor isomer.

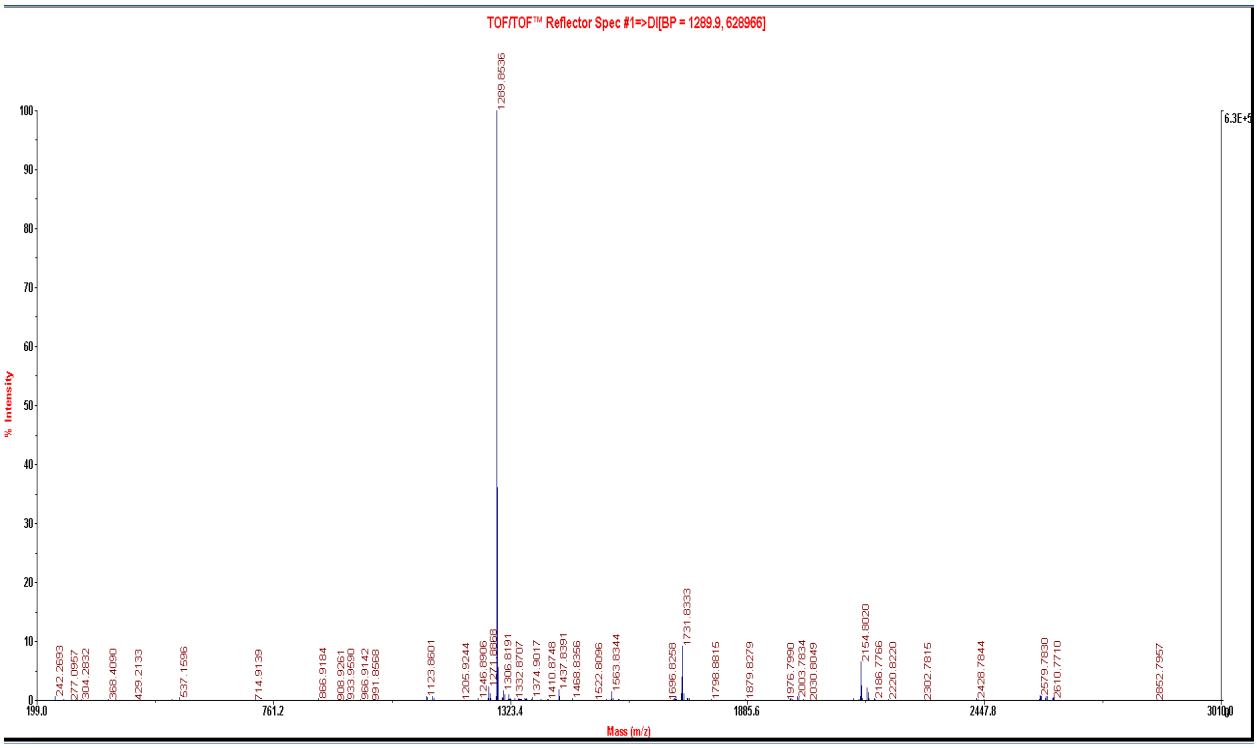

Figure II.2**: MALDI-TOF/TOF spectrum of the reaction mixture for condensation of asymmetric tristhiophene **(II.6)** with thiophene diol **(II.7a)

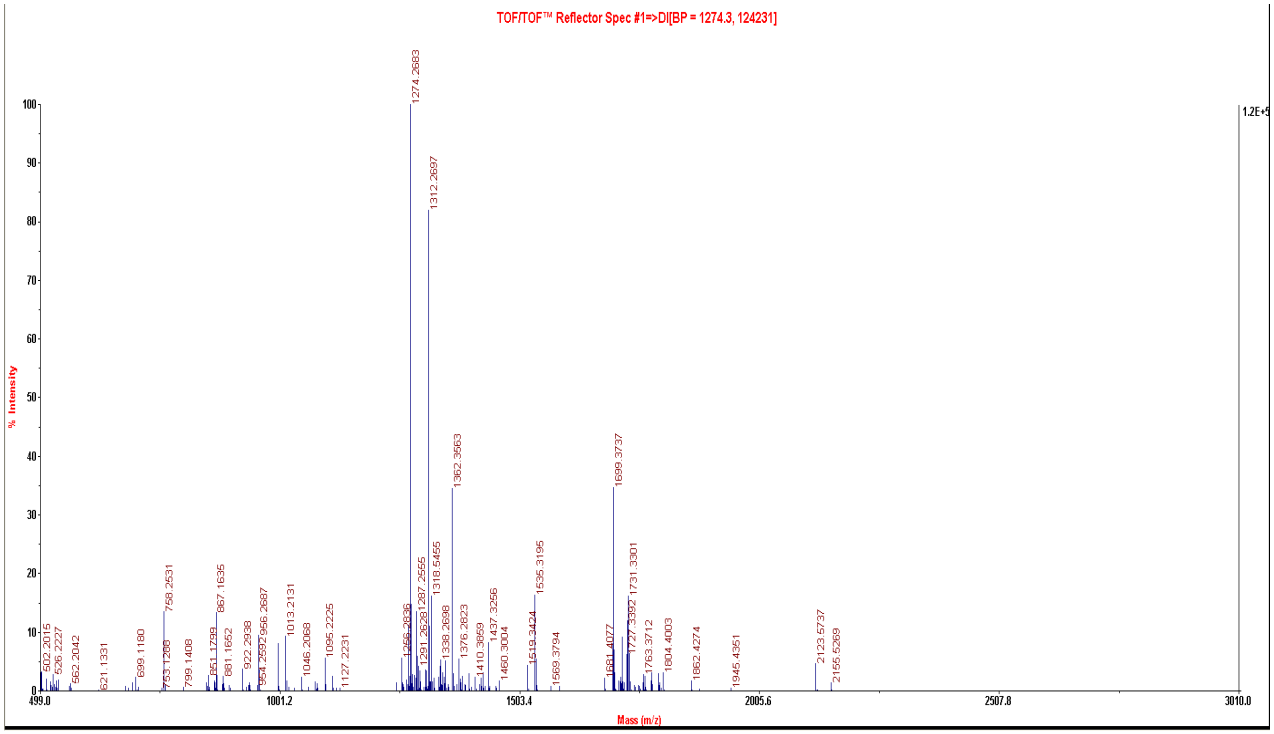

Figure II.3*: MALDI TOF/TOF spectrum of the reaction mixture of condensation of asymmetric tristhiophene* ***(II.6)*** *with furan diol* ***(II.7b)***

II.3 Isolation and characterization of 32π heptaphyrins

II.3.1 Characterization of heptaphyrin having all thiophene units (II.8)

After the reaction mixture was filtered through basic alumina and concentrated under reduced pressure, it was subjected to purification via column chromatography. The heptaphyrin **II.8** was purified over basic alumina column using DCM/hexane as the eluent. After repeated column chromatography, a heptaphyrin could be completely purified and isolated as a brown colored band which displayed an intense absorption at 500 nm (262000 ε, $Lmol^{-1}cm^{-1}$) along with a band at 468 nm (133000) in its electronic absorption spectrum (Figure II.5). It displayed a molecular ion peak at 1289.8815 in the HR-MS spectrum, corresponding to $C_{56}H_{14}F_{20}S_7$ with calculated M^+ value to be 1289.8821(Figure II.4). This confirmed the α-α coupling of the terminal thiophenes, resulting in the cyclization of the oligomer.

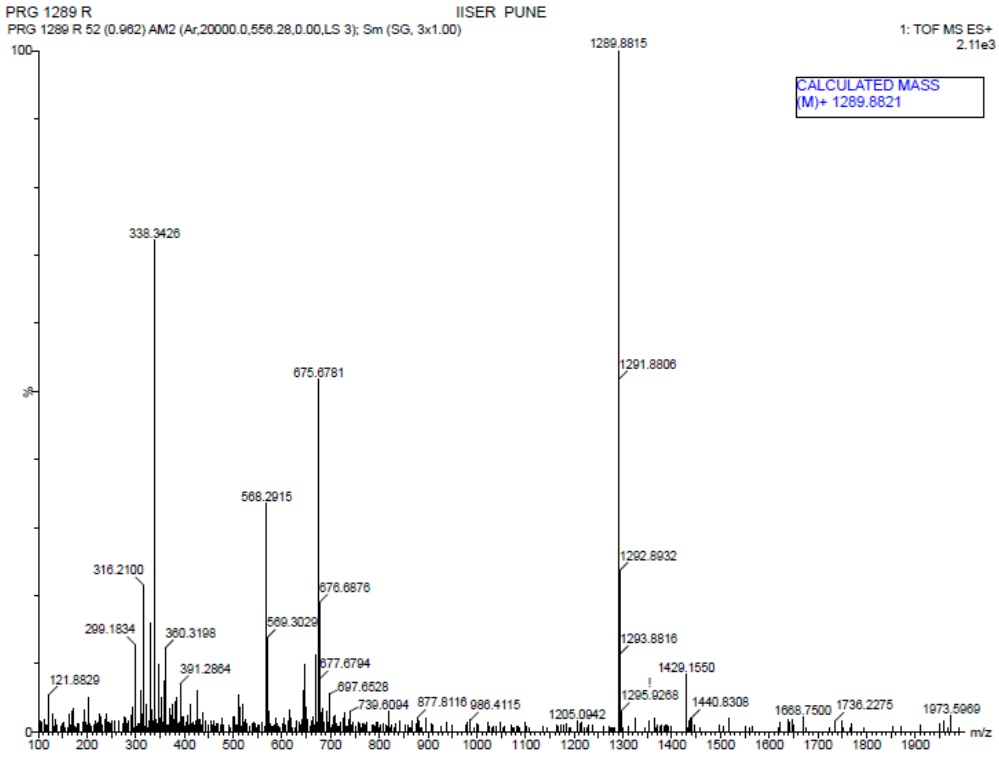

Figure II.4**: HR-MS spectrum of **II.8

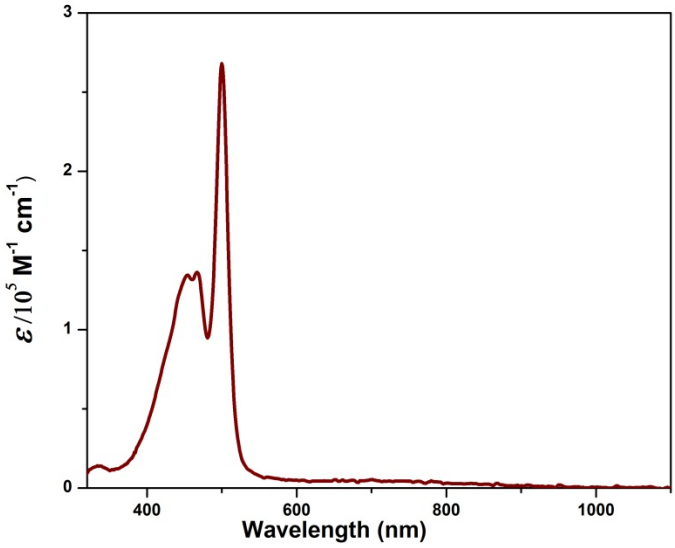

***Figure II.5**: Electronic absorption spectrum of **II.8** in DCM at ~10^{-5}M concentration*

Since the electronic absorption spectrum of the isolated macrocycle revealed a characteristic absorption of an expanded porphyrinoid, it also suggested the formation of a single species instead of three different isomers. In the proton NMR spectrum at room temperature, it displayed well resolved six doublets and one singlet resonating between δ 5.07 and 5.97 ppm.

Each signal corresponded to an equal number of protons (Figure II.6). All the six doublets had a coupling constant of 4 Hz. Seven signals corresponding to a total of fourteen protons suggested the formation of a symmetric macrocycle with a C_2 axis of symmetry. Hence, this spectrum revealed the exclusive formation of a single symmetrical isomer and negates the formation of **II.8b**. Therefore, the NMR spectrum suggested the formation of either **II.8a** or **II.8c** as the only 32π macrocycle from the reaction mixture. The observed upfield chemical shift for the signals suggested the paratropic ring current nature for 32π heptaphyrin. Further, a well resolved spectrum at room temperature also confirmed the lack of solution state dynamics or of any fluxional behavior. The ^{1}H-^{1}H COSY spectrum recorded at room temperature displayed three correlations for the six doublets (Figure II.7). Further the ^{13}C NMR (Figure II.8) and ^{19}F NMR (Figure II.9) were also recorded at room temperature which justified the structure of the heptaphyrin **II.8a**.

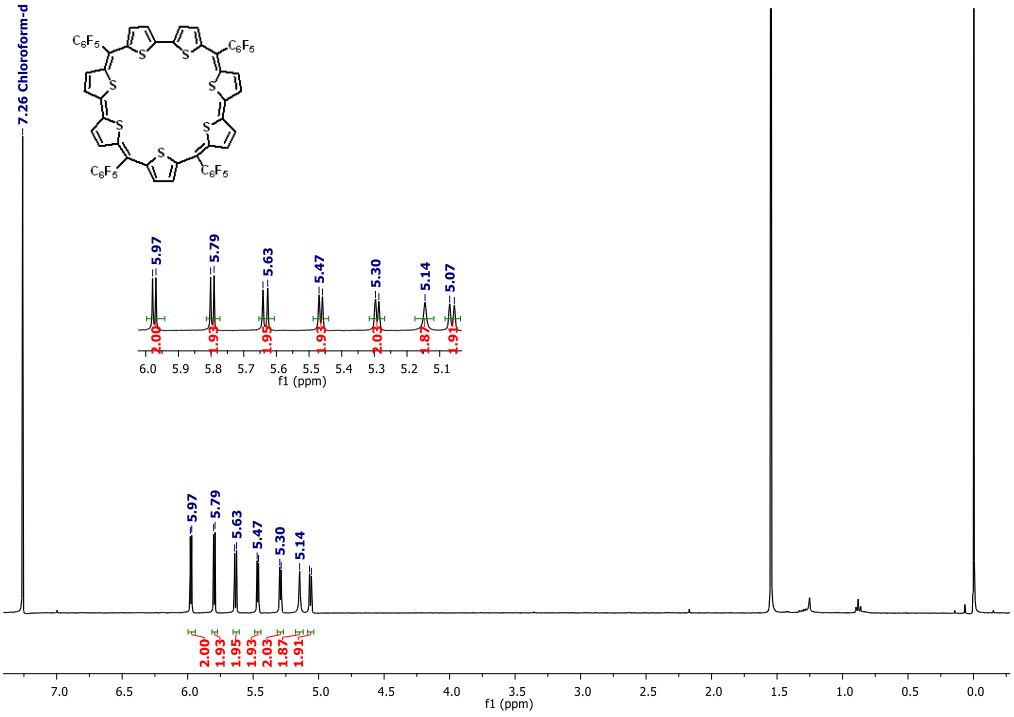

***Figure II.6**: ^{1}H NMR spectrum of **II.8** recorded in $CDCl_3$ at room temperature*

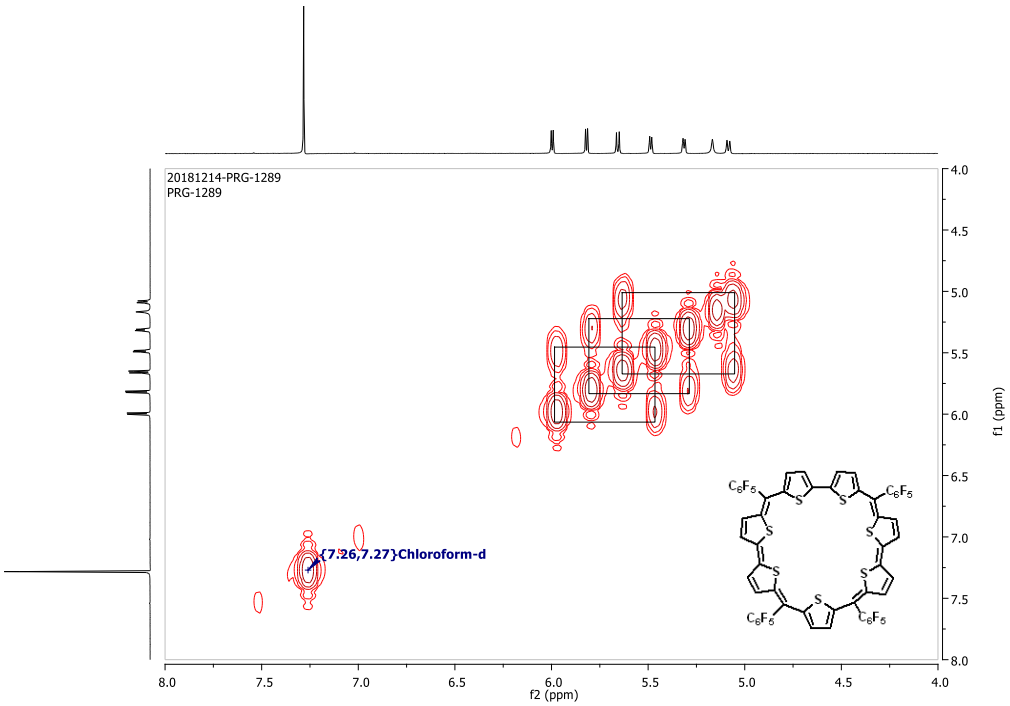

***Figure II.7**: ^{1}H-^{1}H COSY NMR spectrum of **II.8** recorded in $CDCl_3$ at room temperature*

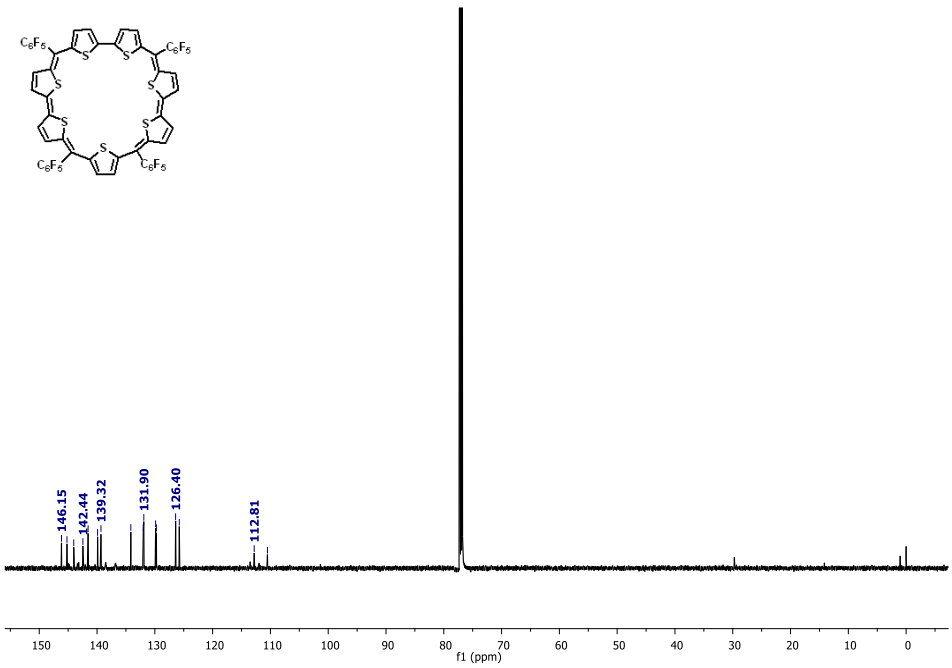

***Figure II.8**: ^{13}C NMR spectrum of **II.8** recorded in $CDCl_3$ at room temperature*

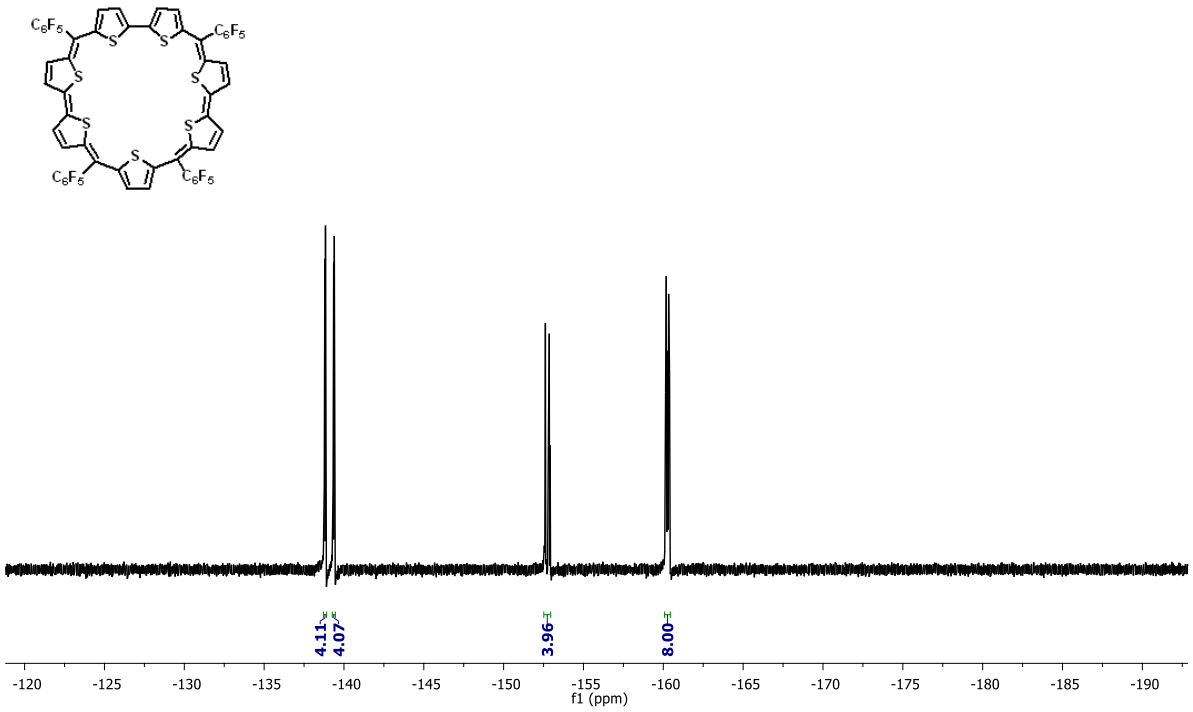

***Figure II.9**: ^{19}F NMR spectrum of **II.8** recorded in $CDCl_3$ at room temperature*

The proton NMR displayed paratropic ring current effect and suggested the formation of a near planar symmetric heptaphyrin. To get better insights of the molecular structure, attempts were made to grow good quality crystals of **II.8**. Single crystal X-ray diffraction analysis revealed a near planar structure with a slight bent conformation (Figure II.10). This topology was in complete agreement with the antiaromatic character of the 32π heptaphyrin. Moreover, it also confirmed the exclusive formation of isomer **II.8a** for the heptaphyrin.

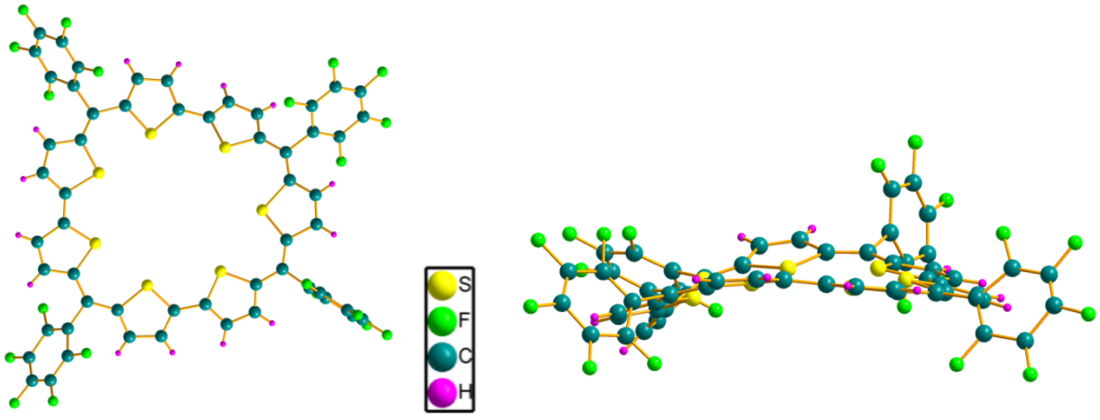

Figure II.10**: Single Crystal X-ray structure [top view(left) and lateral view (right)] of **II.8a

II.3.2 Characterization of heptaphyrin having one furan unit (II.9)

Similar to the hepta-thiophene derivative, heptaphyrin **II.9** containing one furan ring was isolated from basic alumina column chromatography with DCM/hexane as the eluent. Even from this reaction, isolation of only a single brown color band suggested the formation of a unique structural isomer. The isolated macrocycle displayed a sharp intense band at 498 nm (88900) along with another band at 440 nm (77900) (Figure II.12). It displayed a molecular ion peak at 1273.9043 in its HR-MS for $C_{56}H_{14}F_{20}OS_6$ with a calculated M^+ value of 1273.9050 (Figure II.11).

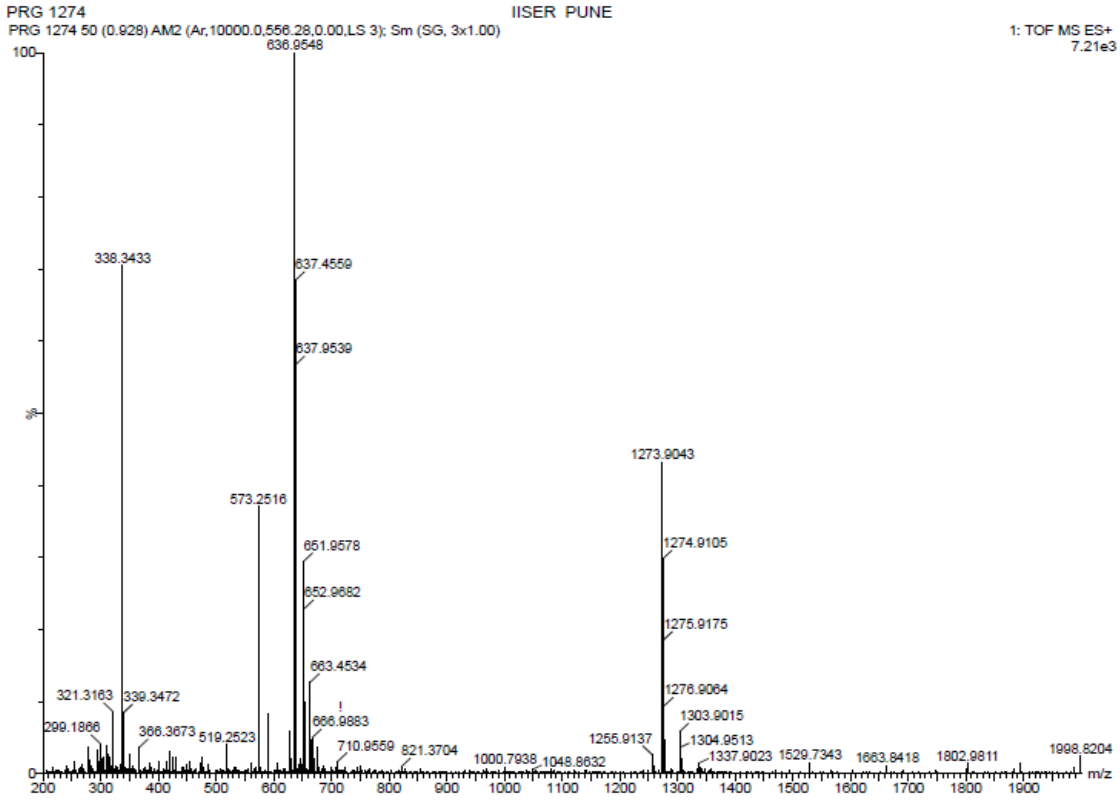

Figure II.11**: HR-MS spectrum of **II.9

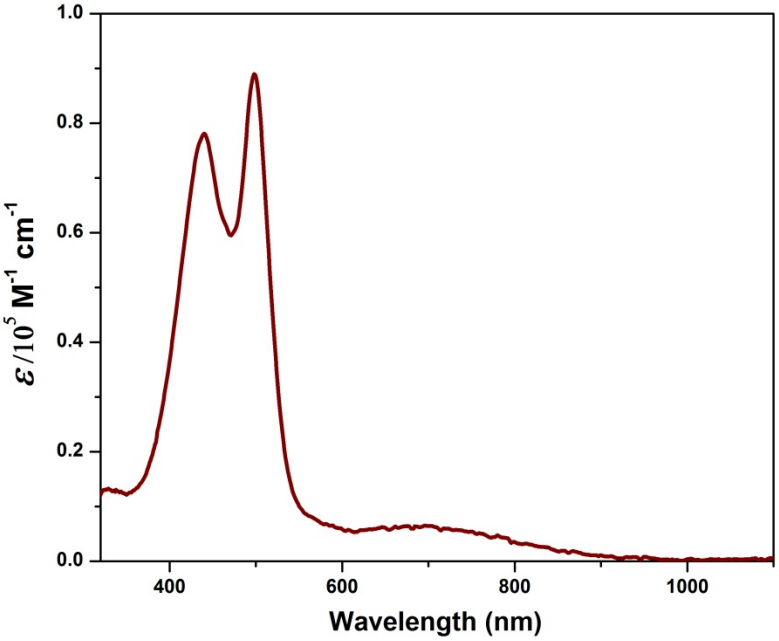

***Figure II.12**: Electronic absorption spectrum of **II.9** in dichloromethane at ~10^{-5}M concentration*

Even though this macrocycle also displayed the same number of signals as of **II.8a,** the proton NMR for this heptaphyrin displayed six signals where two signals were suspected to be merged to appear as a triplet at room temperature. Apart from this triplet, the spectrum comprised of four doublets and a singlet. Surprisingly, two of these doublets were downfield shifted in comparison to other four signals and resonated between δ 9.43 to 10.01 ppm, while the upfield signals resonated between δ 5.69 to 6.22 ppm (Figure II.13). The coupling constant for each of the doublets was found to be 4 Hz, and the coupling constant for triplet-like signal was also found to be 4 Hz. The ^{1}H-^{1}H COSY spectrum displayed clear three correlations for the doublets (Figure II.14). The triplet-like signal at δ 6.2 ppm displayed two correlations confirming the overlap of two doublets. Even though, the proton NMR spectrum confirmed the formation of a unique 32π isomer, it could not conclusively reveal the actual isomer found in the solution. Further the ^{13}C NMR (Figure II.15) and ^{19}F NMR (Figure II.16) were also recorded at room temperature which justified the structure of the heptaphyrin **II.9**.

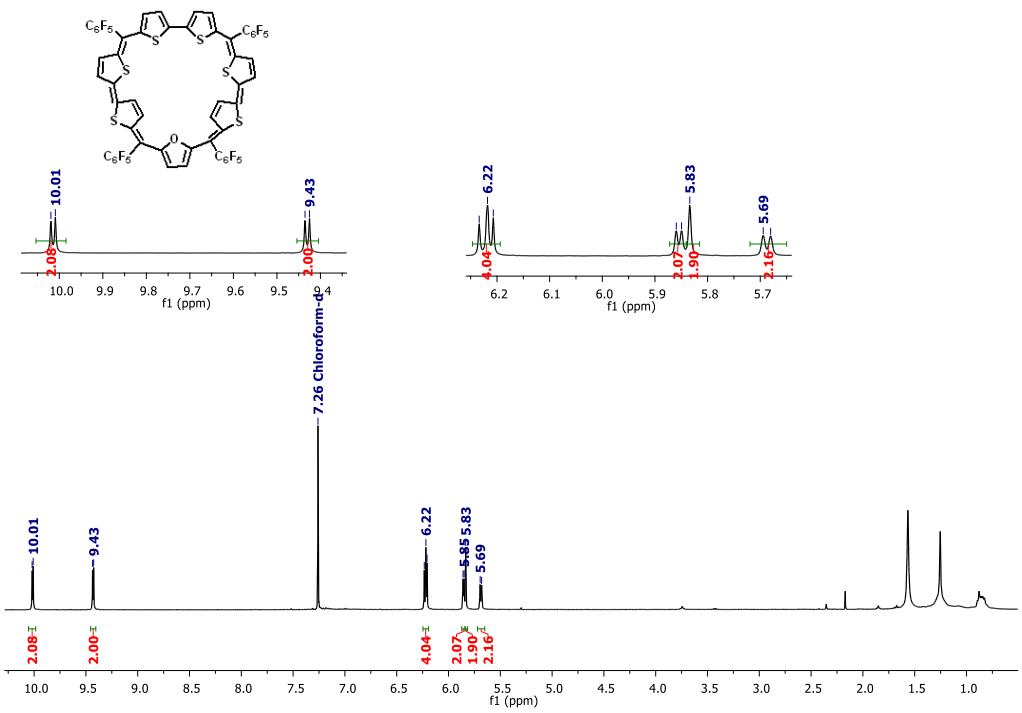

***Figure II.13**: [1]H NMR spectrum of **II.9** in $CDCl_3$ at room temperature*

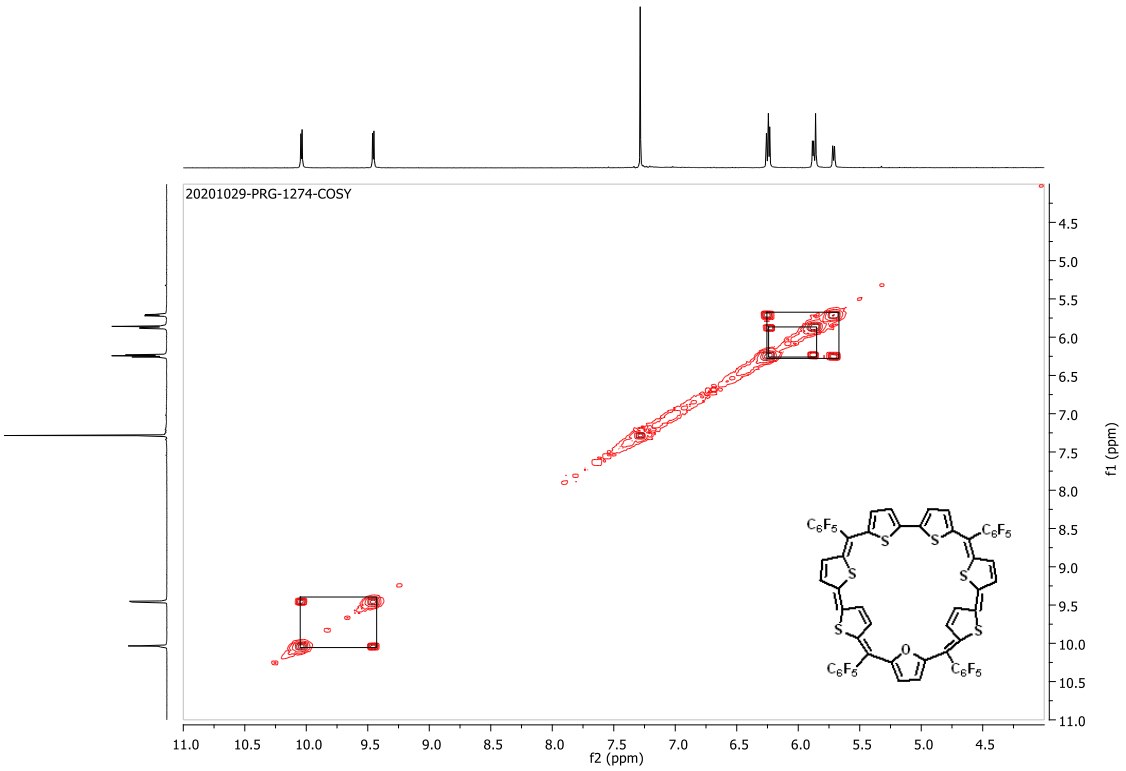

***Figure II.14**: [1]H-[1]H COSY NMR spectrum of **II.9** in $CDCl_3$ at room temperature*

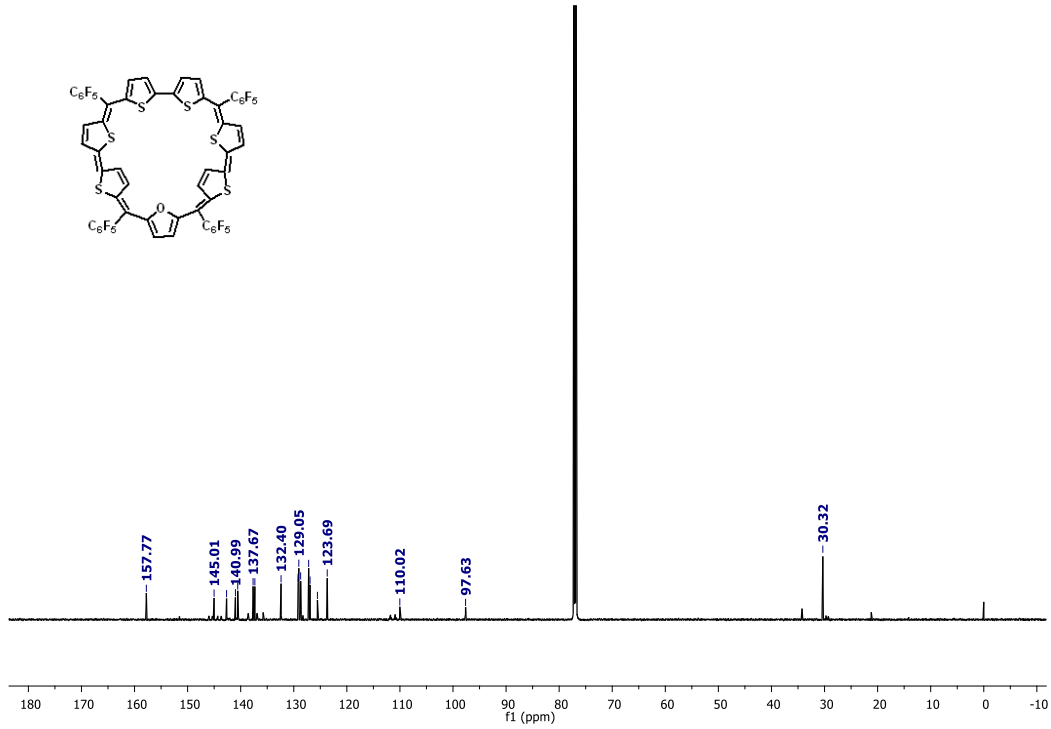

***Figure II.15**: ^{13}C NMR spectrum of **II.9** in $CDCl_3$ at room temperature*

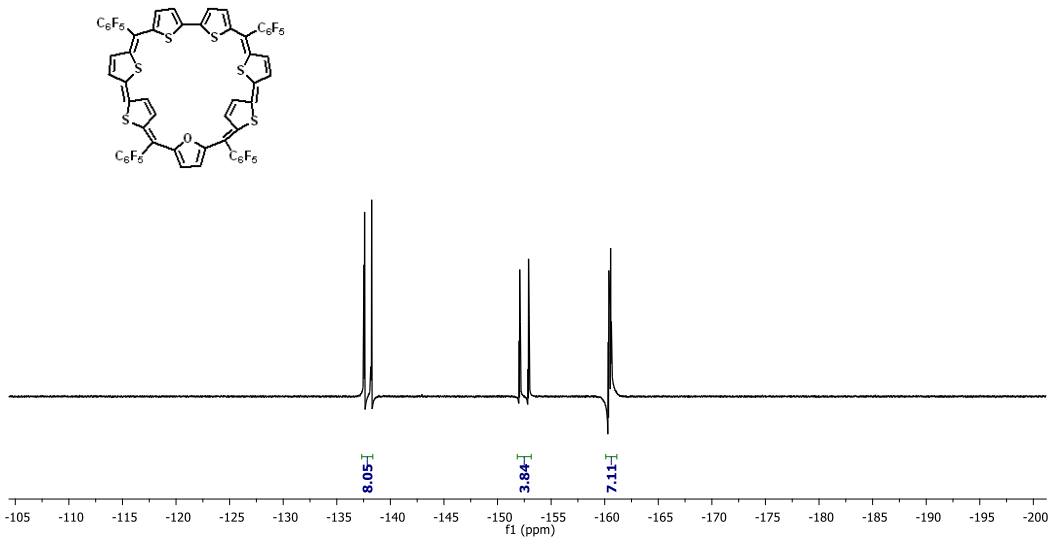

***Figure II.16**: ^{19}F NMR of **II.9** in CD_3CN at room temperature*

II.4 Redox properties of 4nπ heptaphyrins

The macrocycle **II.8a** was characterized as 4nπ antiaromatic system with 32π electrons. Cyclic voltammetry studies revealed two reversible oxidation peaks at +0.47 and +0.56 V (Figure II.17) respectively suggesting the tendency of **II.8a** to be oxidized to a dicationic species.

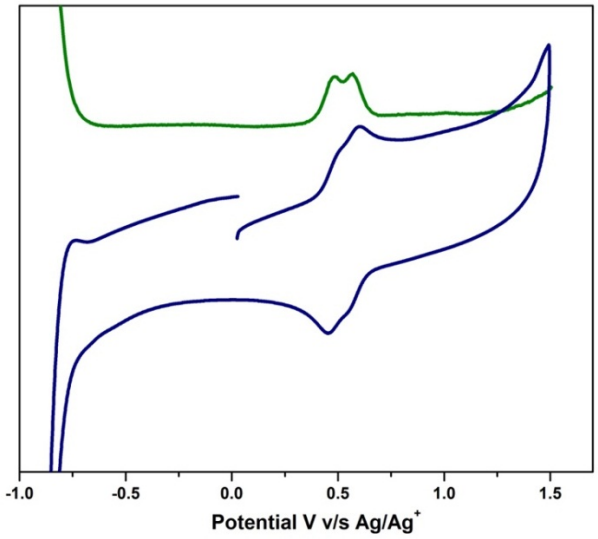

Figure II.17*: Cyclic Voltammetry (blue) and Differential Pulse Voltammetry (green) of ~10^{-5}M solution of II.8a recorded in dry dichloromethane at 50 mV scan rate with 0.1M tetrabutylammonium perchlorate as the supporting electrolyte*

Similarly, cyclic voltammetric studies of **II.9** also revealed two reversible oxidation peaks at +0.53 V and +0.61 V respectively (Figure II.17). In both the cases no reduction potentials were observed in their respective cyclic voltammogram.

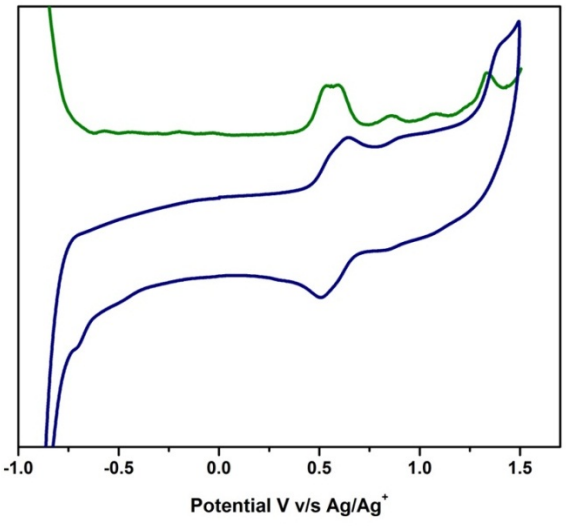

Figure II.18*: Cyclic Voltammetry (blue) and Differential Pulse Voltammetry (green) of 10^{-5}M solution of* ***II.9*** *recorded in dry dichloromethane at 50 mV scan rate with 0.1M tetrabutylammonium perchlorate as the supporting electrolyte*

II.5 Reversible redox chemistry

In both the cases 32π heptaphyrins were subjected to two-electron oxidation using oxidizing agent such as Meerwein's salt[7] or triflic acid. The addition of either Meerwein's salt or triflic acid to a solution of **II.8a** in dichloromethane was marked by a sudden color change from brown to blue (Scheme II.3). The blue colored solution was cooled to 253 K to obtain the recrystallized product. The blue solid was washed multiple times with hexane and in the electronic absorption spectrum it displayed a red shift (616 nm ε, $Lmol^{-1}cm^{-1}$) relative to the free base **II.8a** (498 nm). Intense peaks were observed at 616 nm (417000) along with a peak at 988 nm (35300) (Figure II.19).

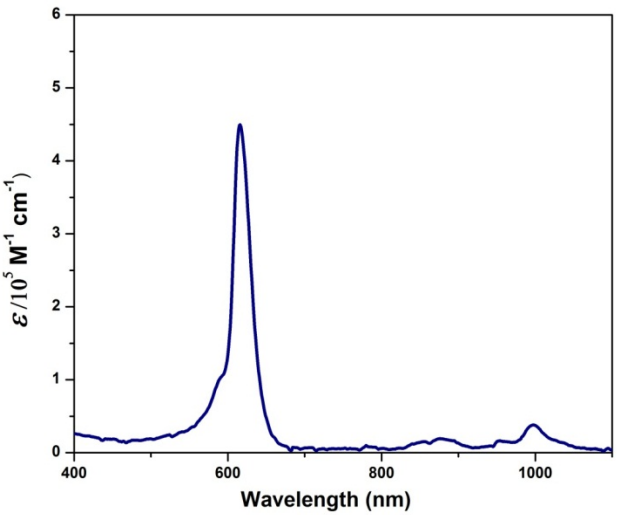

Figure II.19*: Electronic absorption spectrum of purified* ***II.8a***$^{2+}$ *in dichloromethane at ~*10^{-5}*M concentration*

The oxidized product in both cases was well characterized via HR-MS, proton NMR and crystal structure.

The HR-MS for oxidized species of **II.8a** displayed m*/2* peak at 644.9431 confirming the formation of dicationic species **[II.8a]**$^{2+}$(Figure II.20).

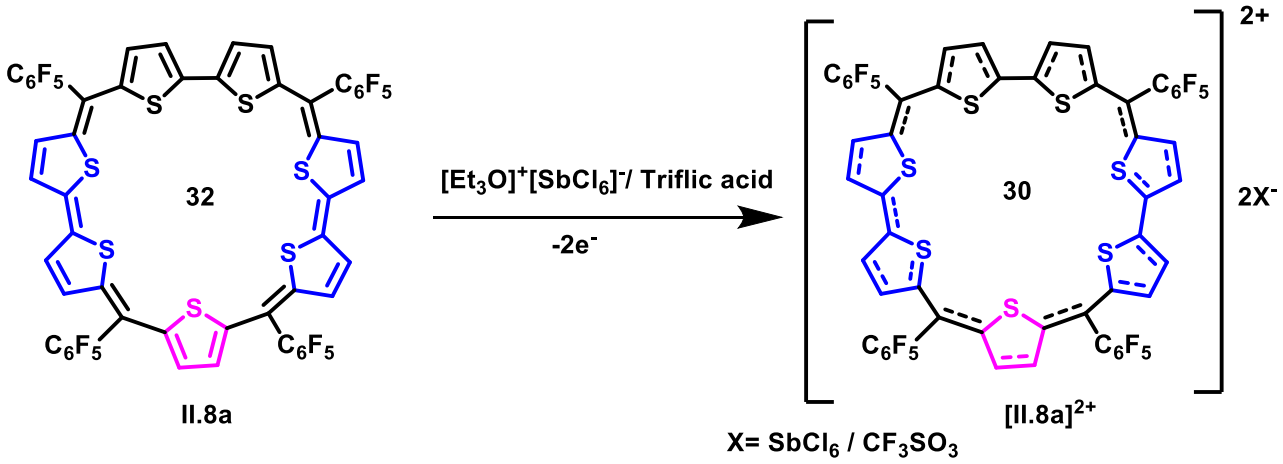

***Scheme II.3**: Chemical oxidation of 32π heptaphyrin **II.8a** to 30π heptaphyrin **II.8a**$^{2+}$*

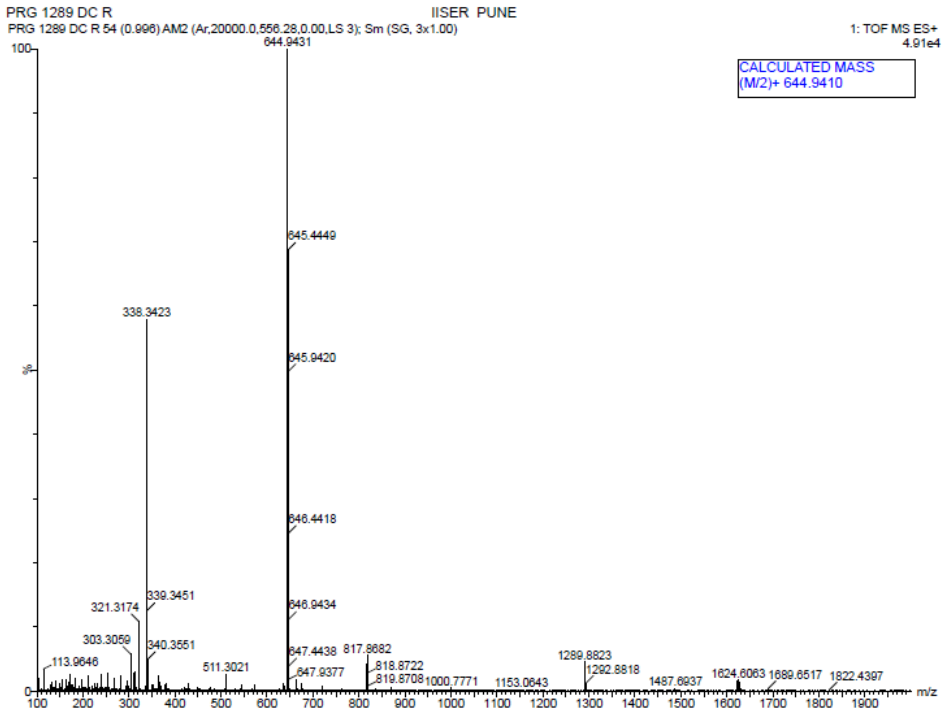

***Figure II.20**: HR-MS of **II.8a**$^{2+}$*

The proton NMR of **II.8a**$^{2+}$ also displayed seven signals at room temperature, which were relatively shifted downfield in comparison to the freebase. The signals were observed in the region between δ 12.50 and 14.16 ppm (Figure II.21). The dication displayed six clear doublets with a coupling constant of 4 Hz. The ^{1}H-^{1}H COSY spectrum also displayed three correlations for the six doublets (Figure II.22). Such down field shifts are attributed the ring oxidation induced aromaticity in the dicationic species and is a unique feature of 4nπ porphyrinoids.

Further the ^{19}F NMR (Figure II.23) was also recorded at room temperature which justified the total number of fluorine atoms in the dication **II.8a**$^{2+}$.

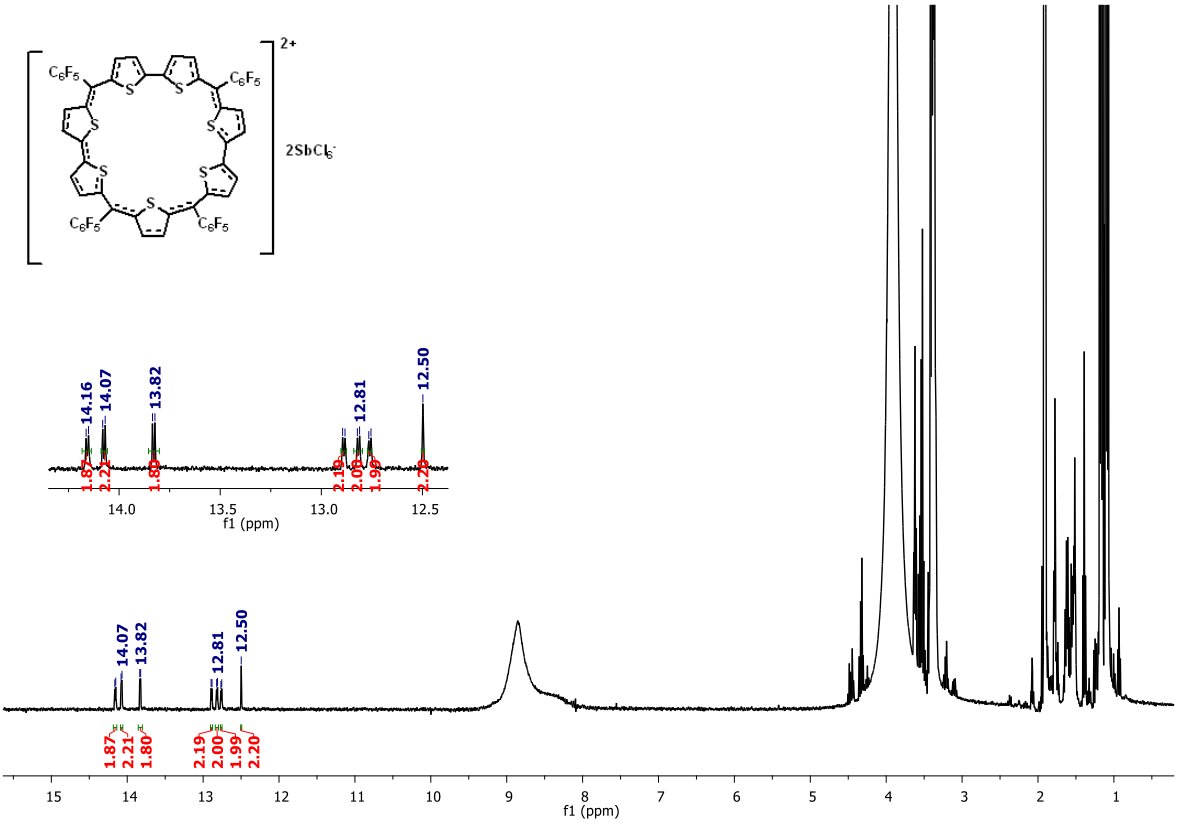

Figure II.21: *^1H NMR spectrum of **II.8a**$^{2+}$ in $CDCl_3$ at room temperature*

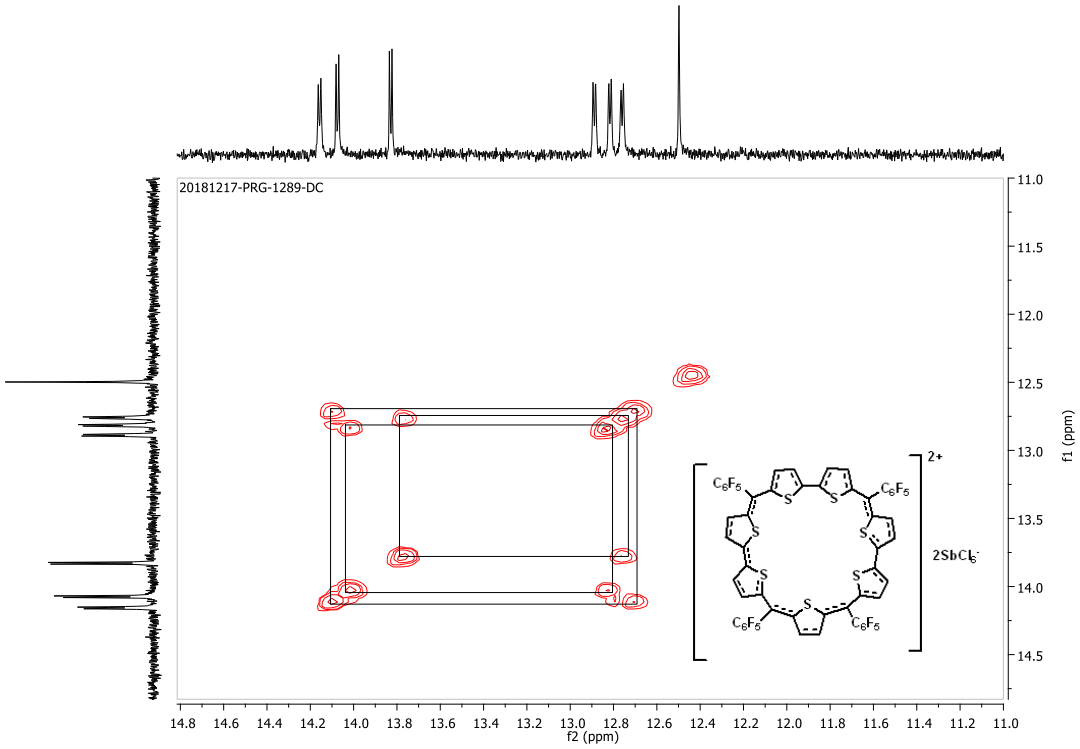

***Figure II.22**: ^{1}H-^{1}H COSY NMR of **II.8a^{2+}.2[SbCl$_6$]$^-$** at room temperature*

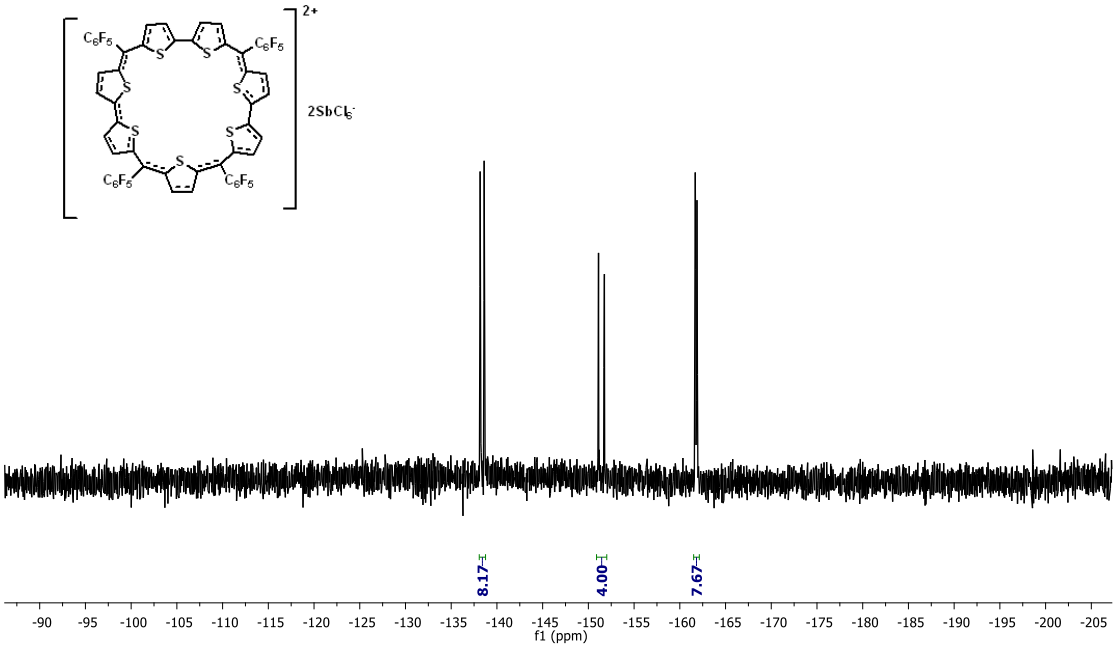

***Figure II.23**: ^{19}F NMR of **II.8a^{2+}.2[SbCl$_6$]$^-$** in CD_3CN at room temperature*

Attempts were made to grow good quality crystals of the dicationic species. Unfortunately, the molecule did not crystallize in the presence of Meerwein's salt, but diffractable crystals were obtained with triflic acid. Single crystal X-ray diffraction analysis revealed the molecule to

sustain its near planar geometry, and two counter triflate anions were present along with the heptaphyrin, confirming the formation of dication (Figure II.24).

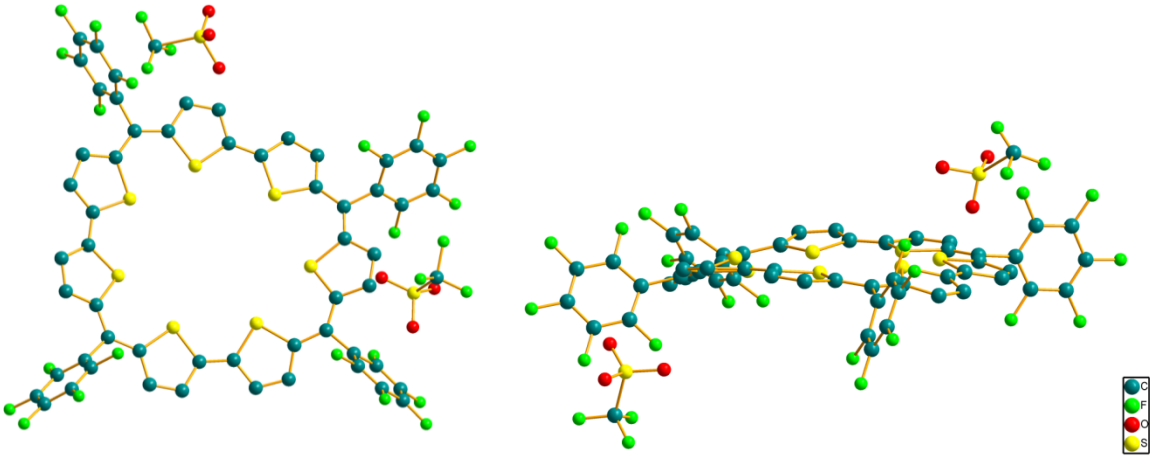

***Figure II.24**: Single Crystal X-ray structure [top view(left) and lateral view (right)] of **II.8a**$^{2+}$**.2[CF$_3$SO$_3$]**$^-$*

A similar two-electron oxidation was observed for **II.9** where in addition of either Meerwein's salt or triflic acid to a solution of **II.9** in dichloromethane resulted in a change from brown to blue color (Scheme II.4). Upon cooling the solution to 253 K, the oxidized product recrystallized and was washed multiple times with hexane. The blue colored solution displayed an intense band at 633 nm (414000 ε, Lmol^{-1}cm^{-1}) along with peaks at 874 nm (22500), 914 nm (23300) and 1041 nm (59600) in its electronic absorption spectrum (Figure II.25). It exhibited significant red shift by more than 116 nm suggesting the ring oxidation of the macrocycle.

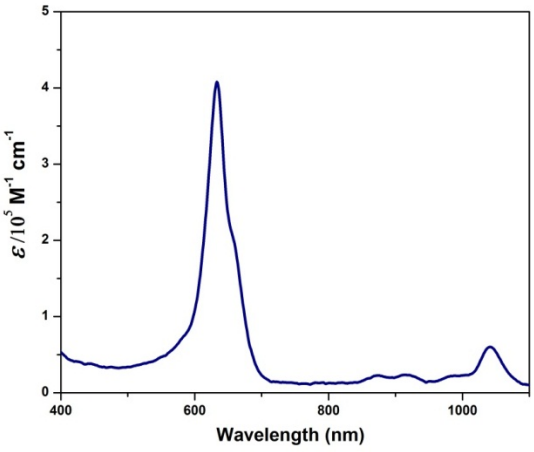

***Figure II.25**: Electronic absorption spectrum of **II.9a**$^{2+}$ in dichloromethane at ~10^{-5}M concentration*

The blue colored solution displayed *m/2* peak at 636.9501 confirming the formation of dication **II.9**$^{2+}$ (Figure II.26).

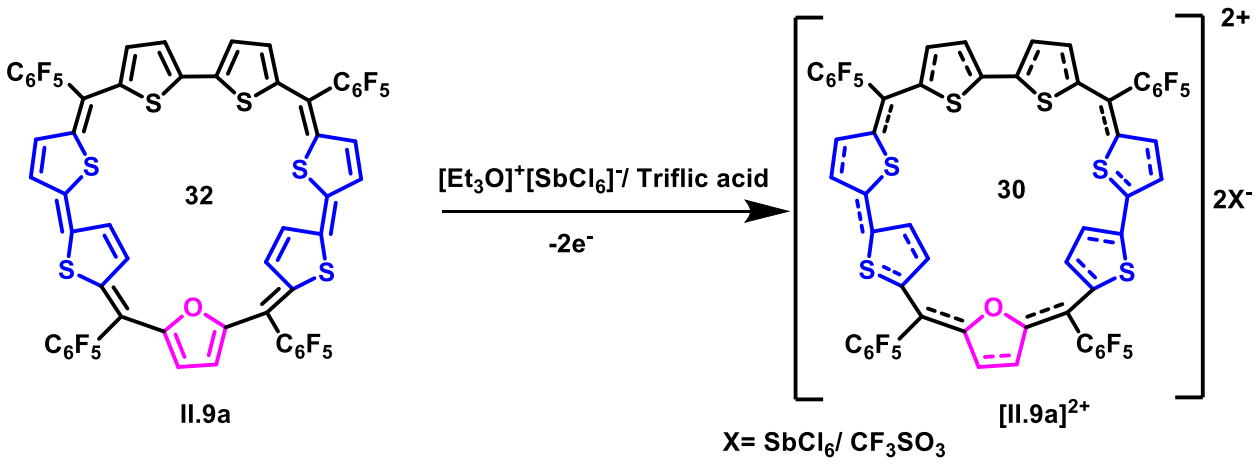

Scheme II.4*: Chemical oxidation of 32π heptaphyrin* ***II.9a*** *to 30π heptaphyrin dication* ***II.9a***$^{2+}$

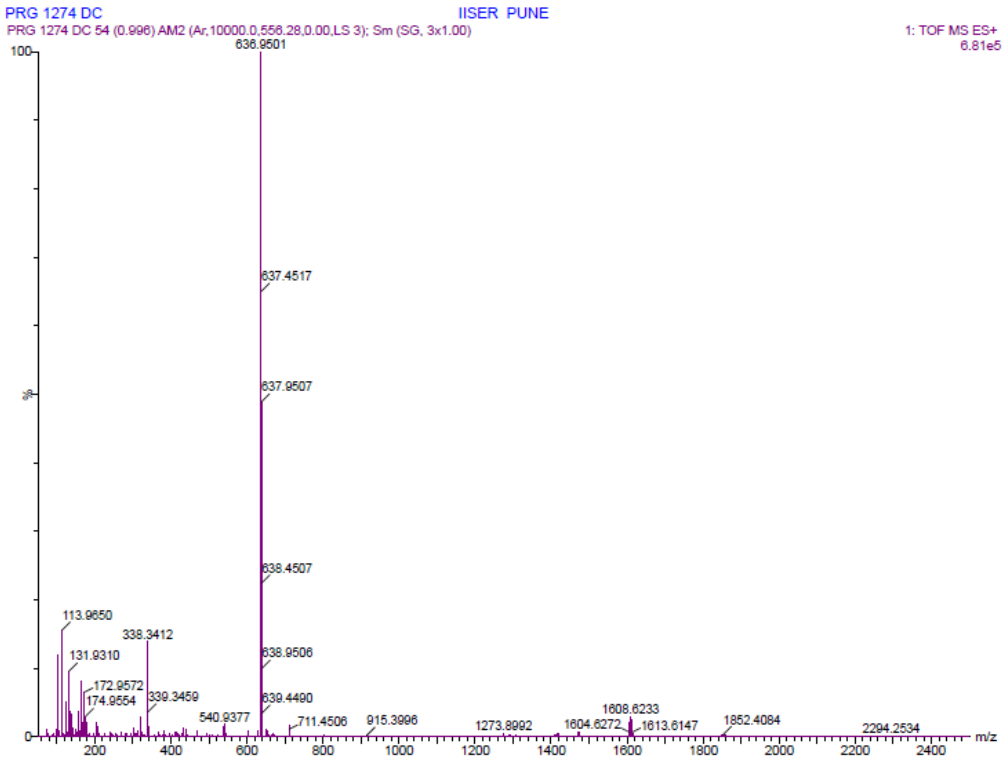

Figure II.26*: HR-MS spectrum of* ***II.9a***$^{2+}$***.2[SbCl6]***$^{-}$

Unlike **II.8a**, the oxidized macrocycle **II.9** did not display a clear proton NMR, suggestive of solution state dynamics at room temperature. However, a well resolved spectrum was observed upon lowering the temperature to 243 K. Six doublets with coupling constant of 4 Hz and one

singlet was observed with a wide span of chemical shift values. Two of the doublets were highly upfield shifted and resonated between δ -5.17 and -4.21 ppm, while rest of the signals were downfield shifted and resonated between δ 11.10 and 12.49 ppm (Figure II.27). A large Δδ value of more than 16.5 explicitly suggested strong diatropic ring current effect for the aromatic dicationic species. Further, the two signals observed with upfield chemical shift values, suggested the possibility of two ring inversions in the macrocycle. Hence the protons of the inverted rings experienced diatropic ring current effects and resonate upfield.

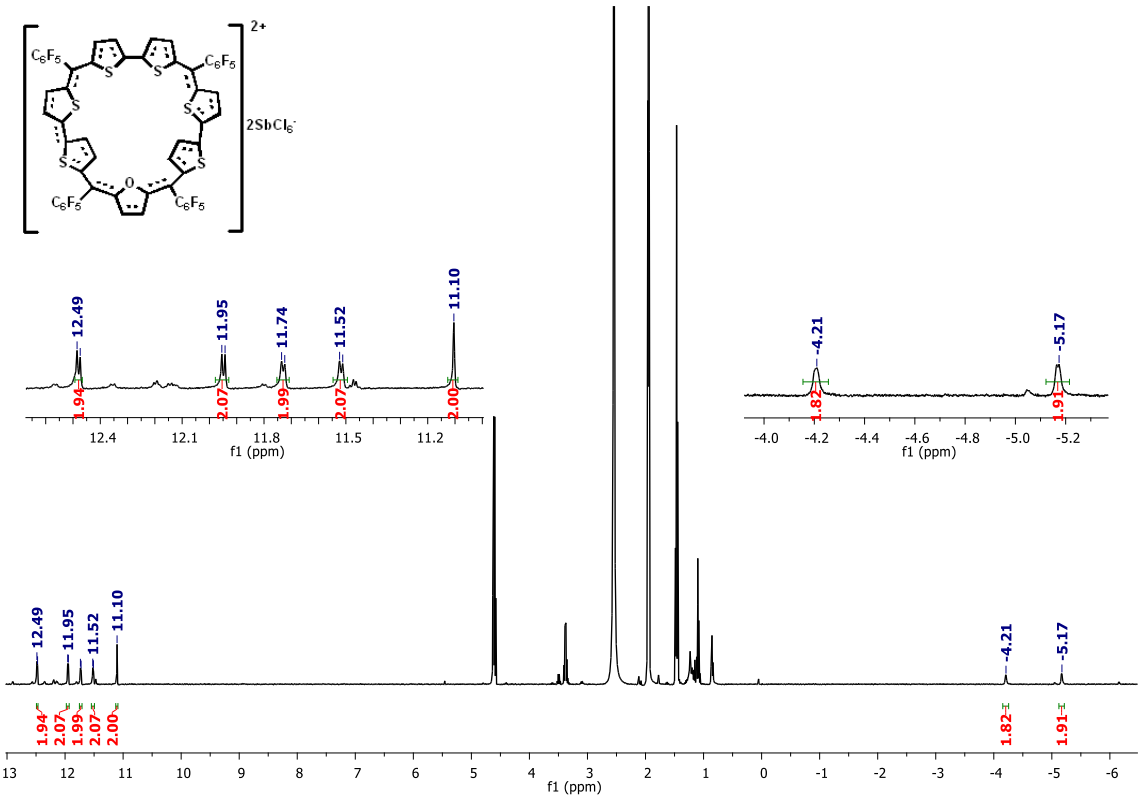

***Figure II.27**: [1]H NMR spectrum of **II.9a**$^{2+}$**.2[SbCl$_6$]**$^-$ in CD$_3$CN at 243 K*

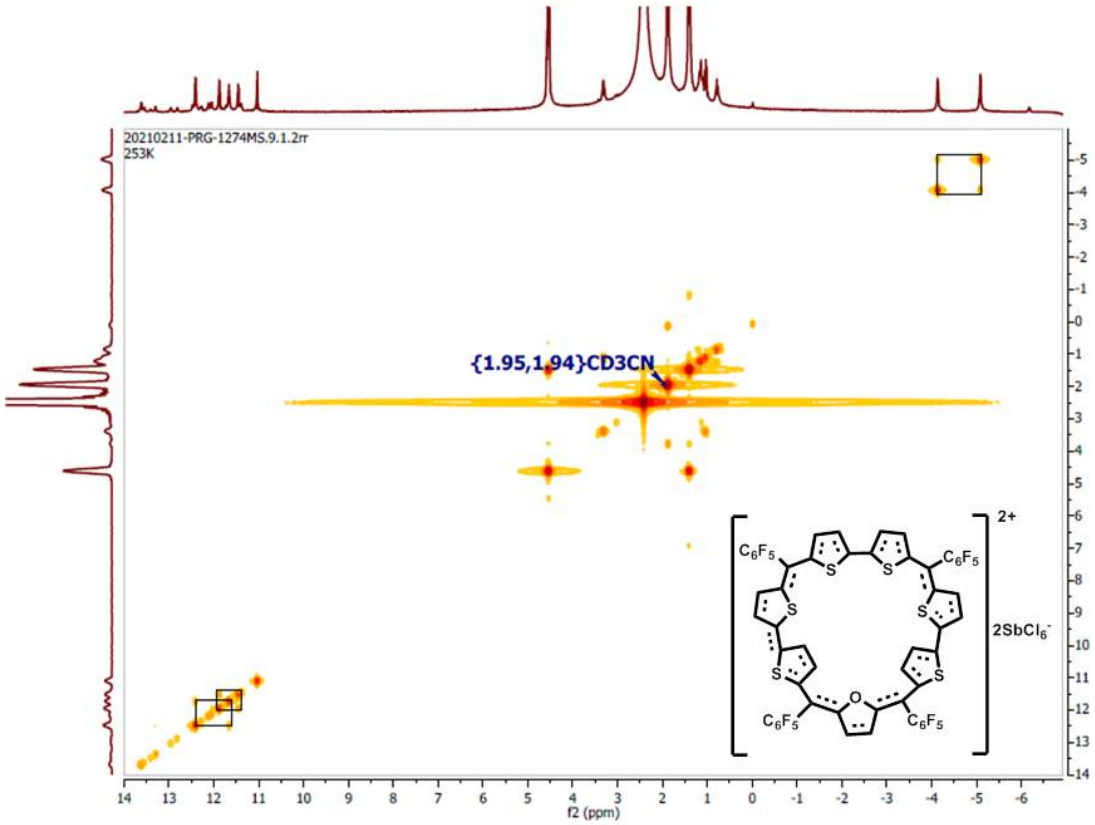

***Figure II.28**: ^{1}H-^{1}H COSY NMR of **II.9a**$^{2+}$**.2[SbCl$_6$]$^-$** in CD_3CN at 253 K.*

The structure of the 30π dication, **[II.9]**$^{2+}$ was confirmed by single crystal X-ray studies. It revealed a near planar conformation and a structure very similar to **II.8a** and hence could be confirmed as the isomer **II.9a**. However, two of the thiophene rings adjacent to the furan rings were inverted (Figure II.29). This observation matches with that revealed by proton NMR studies. The inverted ring protons of thiophene in the freebase are down field shifted due to the paratropic ring current effect of 32π electrons. Upon two-electron ring oxidation the same protons experience diatropic ring current due to the 30π electrons and are hence up field shifted by more than 16 ppm. Two-electron oxidation of the macrocycle was justified by two the presence of two counter anions in the crystal lattice.

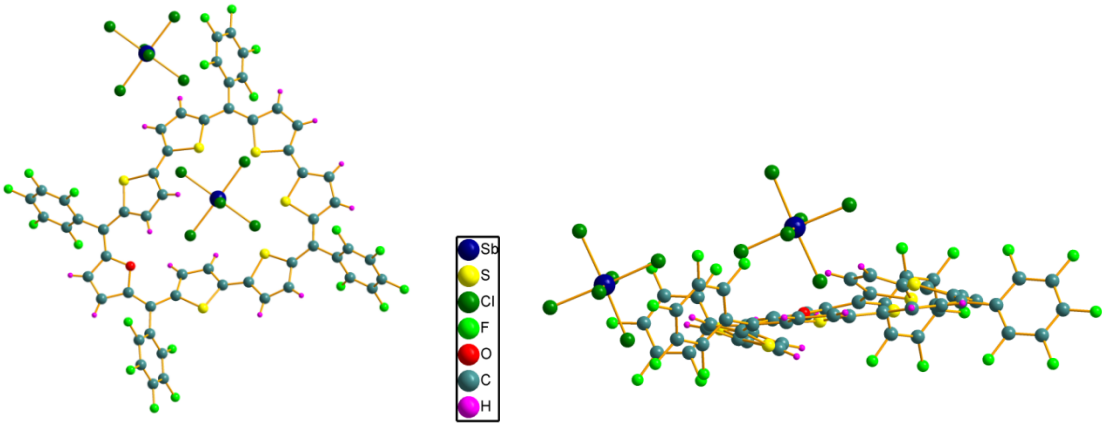

***Figure II.29**: Single Crystal X-ray structure [top view(left) and lateral view (right)] of **II.9a**$^{2+}$**.2[SbCl$_6$]**$^-$*

II.6 Chemical reversibility

As supported by cyclic voltammetry studies, the reversibility of chemical oxidation was studied by electronic absorption spectroscopy for both the macrocycles **II.8a** and **II.9a** and their respective dications.

Addition of triethyl ammine to the blue colored solution of **II.8a**$^{2+}$ induced a subtle change to brown color in dichloromethane. Absorption of this brown colored solution was found similar to the freebase 32π macrocycle and hence confirmed the reversible chemically oxidation of the 32π heptaphyrin (Scheme II.5).

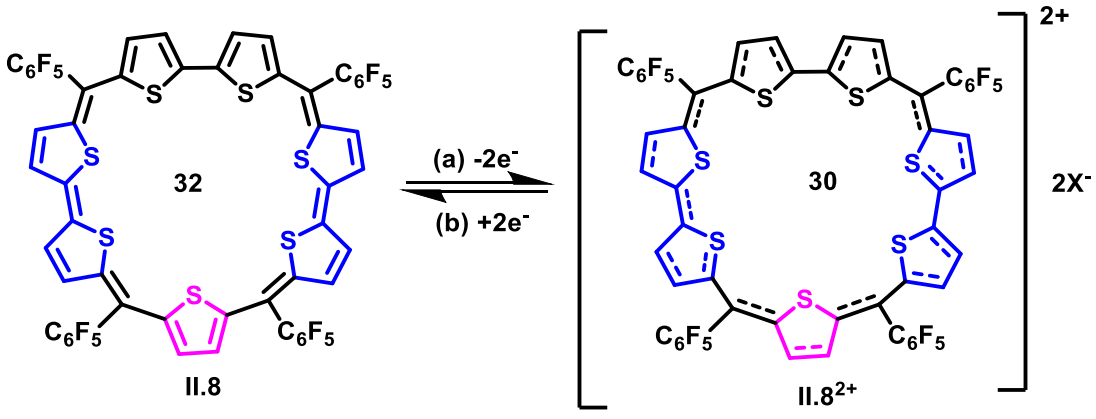

***Scheme II.5**: Reversible chemical oxidation of 32π heptaphyrin **II.8** to 30π heptaphyrin dication **II.8**$^{2+}$*

Similarly, the blue colored oxidized species **II.9a**$^{2+}$ also displayed chemically reversible oxidation upon the addition of triethyl ammine. It reduced the oxidized product to a brown colored freebase **II.9a** as confirmed by electronic absorption spectrum (Scheme II.6).

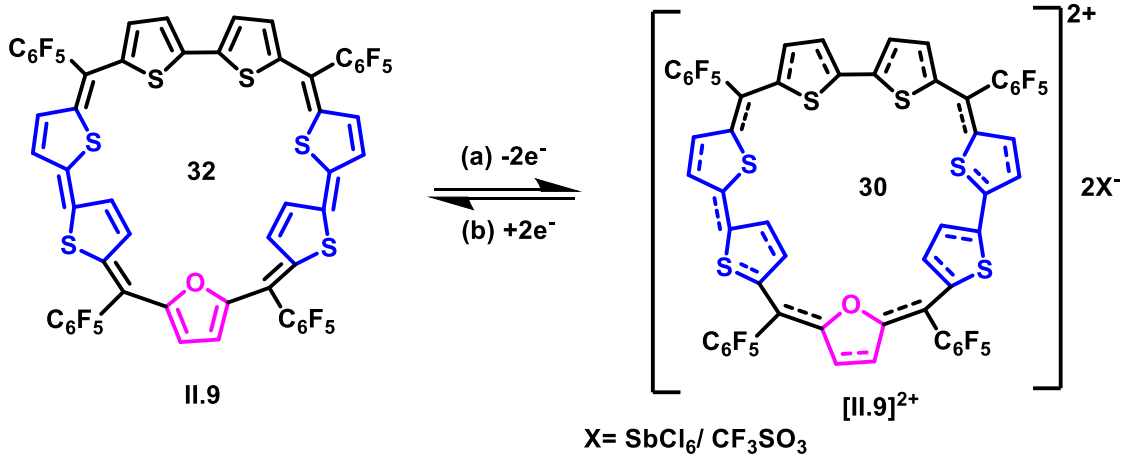

***Scheme II.6**: Interconversion of 32π heptaphyrin **II.9** to 30π heptaphyrin dication **II.9**$^{2+}$*

II.7 Quantum chemical calculations

In support of aromaticity and antiaromaticity in both heptaphyrins and their respective dications, quantum mechanical calculations were employed using Gaussian09 rev D programme.[8] The obtained crystal structures were optimized using Density Functional Theory (DFT) with Beckes's three-parameter hybrid exchange function and the lee-Yang-Parr correlation function (B3LYP)[9] and 6-31G(d,p)basis set for all the atoms in the macrocycle. Then, the negative of the calculated magnetic shielding at the center of the ring, first introduced by Schleyer, commonly referred as "Nucleus Independent Chemical Shift" (NICS)[10] value was calculated. NICS value provides a numerical estimate while studying the aromaticity and antiaromaticity of cyclic conjugated molecules. Aromatic molecules tend to show negative NICS value whereas antiaromatic molecules display positive NICS value.

Molecule	NICS(0)	AICD	λ_{max} (nm)	Hückel Aromaticity
II.8a	+9.90	Anti-clockwise	500	Antiaromatic
II.8a^{2+}	-13.03	Clockwise	616	Aromatic
II.9a	+8.21	Anti-clockwise	498	Antiaromatic
II.9a^{2+}	-12.26	Clockwise	633	Aromatic

Table II.1*: Quantum Chemical Calculations for Heptaphyrins*

The NICS value was obtained using gauge independent atomic orbital (GIAO) method. The NICS(0) was calculated by denoting the global ring centre at the non-weighed mean center of the macrocycle. A large positive NICS(0) value of δ +9.90 ppm for **II.8a** and +8.21 ppm for **II.9a** is in agreement with the presence of paratropic ring current effect observed in proton NMR spectrum for the 32π heptaphyrins. The negative NICS value of -13.03 ppm for **II.8a**$^{2+}$ and -12.26 ppm for **II.9a**$^{2+}$ further justified the diatropic ring current effect observed in their respective proton NMR spectrum (Table II.1).

Another computational method used to support these studies is Anisotropy of Induced-Current Density (AICD).[11] It visualizes the ring currents present due to the delocalization of π electrons. These plots help in viewing the magnitude and direction of the induced ring current when an external magnetic field is applied orthogonal to the plane of the molecule. Continuous set of gauge transformation (CGST) method is employed on the macrocycle which is then visualized using POV-ray 3.7 software. The clockwise direction of arrow suggests the aromatic nature of the molecule, while the anticlockwise direction of arrow suggests the anti-aromatic nature of the macrocycle.

Both the free base heptaphyrins **II.8a** and **II.9a** show anti-clockwise direction of arrows in their AICD plot suggesting the antiaromatic nature of the molecule, while both the dication **II.8a**$^{2+}$

and **II.9a**$^{2+}$ displayed clockwise direction of arrow in their plot suggesting aromatic nature of the dication (Figure II.30-II.31).

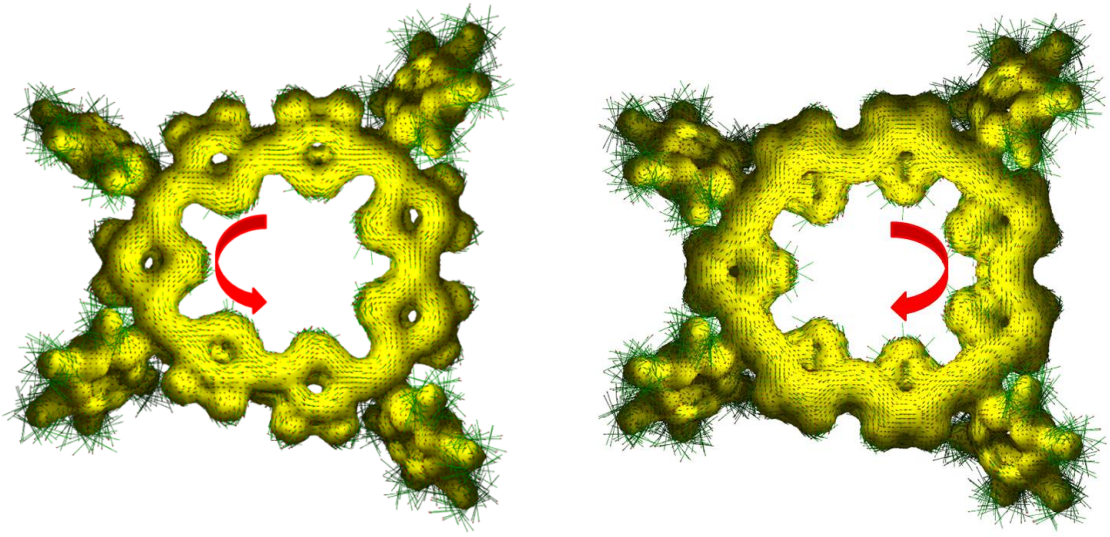

Figure II.30*: AICD plot for* ***II.8a*** *and* ***II.8a***$^{2+}$

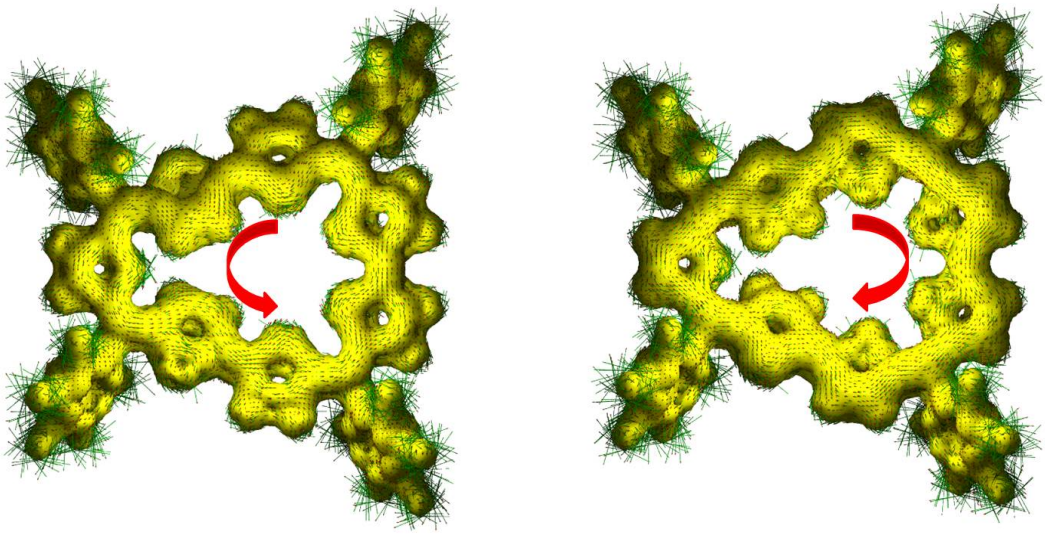

Figure II.31*: AICD plot for* ***II.9a*** *and* ***II.9a***$^{2+}$

Further, steady-state absorption spectra were studied using Time dependent TD-DFT calculations. The absorption spectra for **II.8a** and **II.8a**$^{2+}$ matched with the calculated TD-DFT values (Figure II.32).

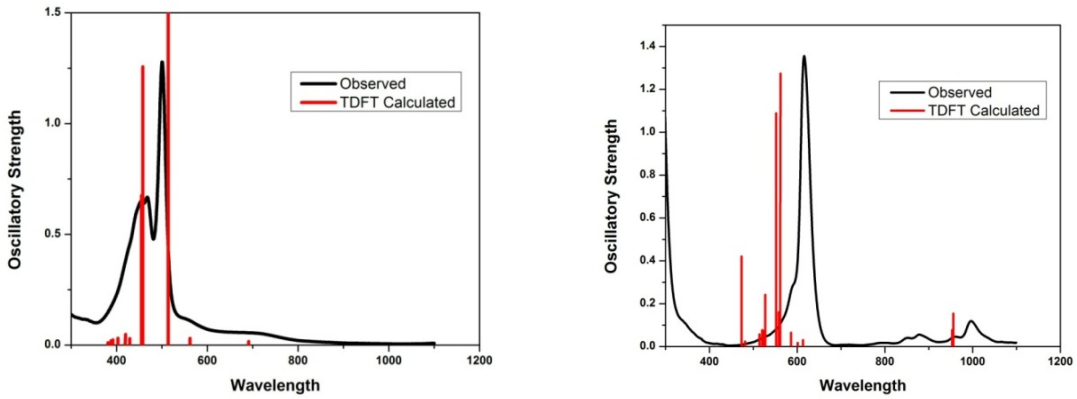

***Figure II.32**: Time dependent functional theory (TD-DFT) calculation overlaid on experimental UV-VIS absorption spectra of **II.8a** (left) and **II.8a**$^{2+}$ (right).*

Similarly the TD-DFT spectra of **II.9a** and **II.9a**$^{2+}$also matched with the observed absorption spectra (Figure II.33).

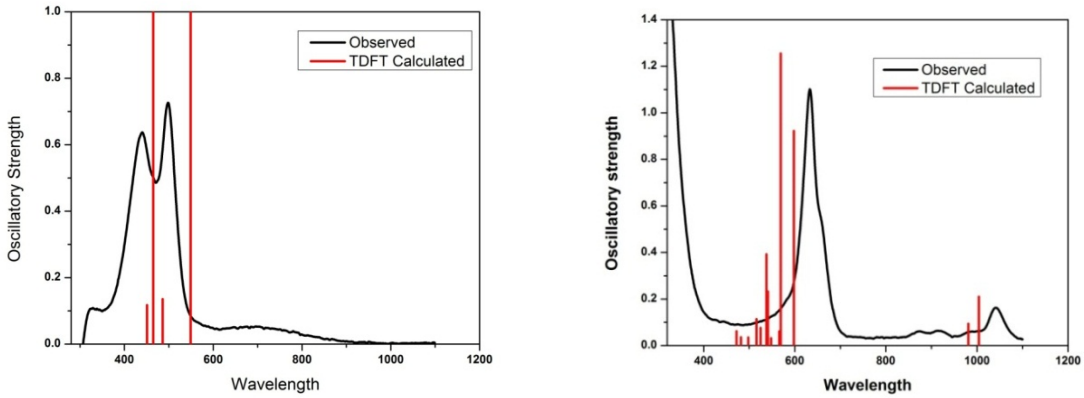

***Figure II.33**: Time dependent functional theory (TD-DFT) calculation overlaid on experimental UV-VIS absorption spectra of **II.9a** (left) and **II.9a**$^{2+}$ (right).*

II.8 Conclusions

The synthesis of first completely core modified 32π (1.0.1.0.1.0.1) heptaphyrin was obtained by condensing a novel asymmetric tristhiophene with either thiophene/furan diol under acidic conditions using $BF_3.OEt_2$ followed by DDQ oxidation. In both the cases, heptaphyrin was the major macrocycle being formed and displayed brownish color in solutions. Despite the possibility of three different heptaphyrins being formed, in both the cases only head to tail cyclisation product was obtained. Both the heptaphyrins **II.8a** and **II.9a** were slightly bent in

geometry. They displayed paratropic ring current effects as observed from their proton NMR spectrum as well as supported by quantum calculations such as negative NICS value and anticlockwise direction of arrow in the AICD plot. Both the 32π heptaphyrins undergo reversible two-electron oxidation both chemically and electrochemically. Chemically 32π heptaphyrin oxidized to 30π dication by addition of either Meerwein's salt or triflic acid as the oxidizing agent. The 30π dication could be reduced by two electrons to the antiaromatic 32π freebase by addition of a base such as triethyl ammine. These results were also supported by cyclic voltammetry studies. The 30π dication was well characterized using spectroscopic techniques such as proton NMR as well as HR-MS and electronic absorption spectrum. The proton NMR suggested the diatropic ring current present in the oxidized 30π dication, which was well supported by NICS and AICD plots. In case of **II.8a** no ring inversion was observed, while the crystal structure and proton NMR for **II.9a** as well as **II.9a**$^{2+}$ displayed two ring inversions where the thiophene rings next to furan ring had been inverted.

II.9 Experimental section

Asymmetric tristhiophene (**II.6**) and corresponding diol (**II.7**) were dissolved in two is to one ratio in 150 mL of dry dichloromethane and degassed with nitrogen for five minutes. Then the round bottom flask containing the solution was covered with aluminum foil to maintain dark conditions. To this mixture, one equivalent of $BF_3.OEt_2$ was added and stirred the solution for two hours maintaining the dark and inert conditions. After two hours the reaction mixture was subjected to five equivalents of dichlorodicyanoquinone (DDQ) and stirred for four hours. Finally the reaction mixture was passed through basic alumina column and purified using alumina column. The dication was synthesized by two electron oxidation by addition of either Meerwein's salt $[Et_3O]^+[SbCl_6]^-$ or triflic acid to the solution of heptaphyrin in Dichloromethane. The solution was cooled to 253K to obtain recrystallized product which was washed with hexane multiple times.

Synthetic procedure of asymmetric tristhiophene (II.6)

Step 1: Synthesis of 2-bromo-5-((perfluorophenyl)(thiophen-2-yl)methyl) thiophene (II.5):

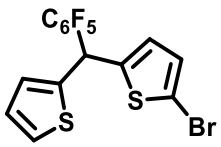

Thiophene monol **II.3** (17.84 mmol, 5 g) was added to a stirred solution of 2-bromothiophene (392 mmol, 38 mL) in a round bottom flask, under nitrogen atmosphere and dark conditions.1g of amberlyst-15 was added to the reaction mixture and stirred for five hours. The reaction was quenched with water and filtered over glass funnel and finally extracted using diethyl ether. The compound was purified using silica gel glass column using hexane as eluent. The compound **II.5** was isolated as yellowish oily liquid in 90% yields. The novel monomer was fully characterized using the HR-MS and spectroscopic techniques. The melting point of the compound was found to be 48.2 -51.3˚C.

HR-MS (ESI) m/z: $[M+H]^+$ Calcd. for $C_{15}H_6BrF_5S_2$ 424.9087; Found 425.2169.

^1H NMR (400 MHz, $CDCl_3$) δ: 7.28 (dd, *J* = 5.1, 1.3 Hz, 1H), 7.02 (d, *J* = 3.4 Hz, 1H), 6.99 (dd, *J* = 5.0, 3.6 Hz, 1H), 6.93 (d, *J* = 3.9 Hz, 1H), 6.78-6.69 (m, 1H), 6.17 (s, 1H).

Step 2: Synthesis of 5-((perfluorophenyl)(thiophen-2-yl)methyl)-2,2'-bithiophene (II.6):

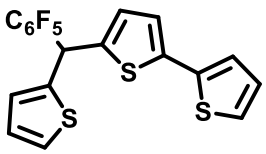

To a stirred solution of above compound **II.5** (8.76 mmol, 3.73 g) in 20 mL of dry diethyl ether at 0˚C, 0.01 equivalent of $Ni(dpp)_2Cl_2$ catalyst was added under argon atmosphere. To this solution, freshly prepared Grignard reagent ($C_{15}H_6F_5S_2MgBr$) was added slowly maintaining the temperature at 0˚C. The solution was slowly brought to room temperature and further refluxed for 40 hours to obtain the desired product. The reaction was cooled to room

temperature and as being exothermic in nature, was carefully quenched using ice cold ammonium chloride solution. The compound **II.6** was extracted using diethyl ether and purified using silica gel mesh 100-200 glass column using hexane as eluent. The compound was purified in 35% yields and was yellowish oily liquid which solidified on cooling. The molecule was fully characterized using the HR-MS and ^{1}H NMR spectroscopic techniques. The melting point of the compound was found to be 51.7-53.8˚C.

HR-MS (ESI) m/z: $[M]^+$ Calcd. for $C_{19}H_9F_5S_3$ 427.9787; Found 427.9780.

^{1}H NMR (400 MHz, $CDCl_3$) δ: 7.27 (dd, *J* = 5.4, 1.5 Hz, 1H), 7.20 (dd, *J* = 5.1, 1.1 Hz, 1H), 7.11 (dd, *J* = 3.6, 1.1 Hz, 1H), 6.97-7.02 (m, *J* = 8.5, 5.4, 3.6 Hz, 4H), 6.85 (d, *J* = 3.6 Hz, 1H), 6.19 (s, 1H).

Synthetic procedure of II.8a

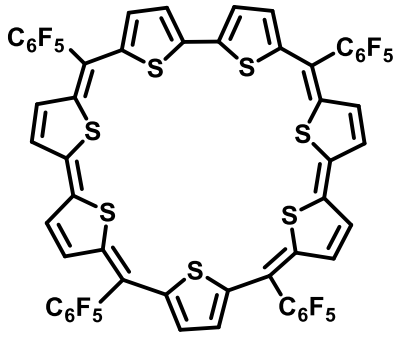

A clean dried 250 mL round bottom flask was charged with compound **II.6** (220 mg, 513.48 μmol). To this compound **II.7a**[6] (114.05 mg, 256.74 μmol) was added and 140 mL of dry dichloromethane was added. The solution was nicely stirred and maintained under dark and inert condition. To this reaction mixture, $BF_3.OEt_2$ (513.48 μmol, 0.06 mL) was added slowly and stirred further for two hours. Subsequently after two hours, dichlorodicyanoquinone (250 mg, 1.54 mmol) was added to the reaction mixture and stirred further for four hours. The reaction mixture was filtered through basic alumina column and purified on a neutral alumina glass column. The major fraction obtained was a seven membered, 32π heptaphyrin isolated in

11% yields. The molecule was completely characterized using the HRMS and spectroscopic techniques.

HR-MS (ESI) m/z: $[M]^+$Calcd. for $C_{56}H_{14}F_{20}S_7$ 1289.8821; Found 1289.8815.

UV-Vis (CH_2Cl_2): λ_{max} nm (ε, $Lmol^{-1}cm^{-1}$): 500 nm (262000), 468 nm (133000).

^1H NMR (400 MHz, $CDCl_3$) δ: 5.97 (d, *J* = 4.2 Hz, 2H), 5.80 (d, *J* = 4.2 Hz, 2H), 5.63 (d, *J* = 5.8 Hz, 2H), 5.46 (d, *J* = 4.2 Hz, 2H), 5.29 (d, *J* = 4.2 Hz, 2H), 5.14 (s, 2H), 5.06 (d, *J* = 5.7 Hz, 2H).

Selected Crystal data: triclinic, space group *P -1*, *a* = 8.084 (4), *b* = 18.585 (8), *c* = 19.669 (9) Å, α = 90.273 (16), β = 93.457 (17), γ = 90.810 (16), *V*= 2949 (2) $Å^3$, T= 120 K, D_{cal} = 1.454 gcm^{-3}, R_1 = 0.0896, wR_2 = 0.2505, GOF = 1.026

Synthetic procedure of $II.8a^+.2[SbCl_6]^-$

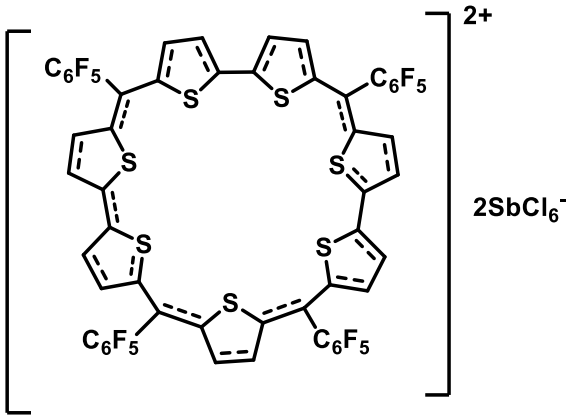

Dication of **II.8a** was generated by dissolving 5 mg of **II.8a** in 10 mL of dry DCM and adding excess of Meerwein's salt to the solution. The mixture was stirred at -20°C for 20 minutes and then kept for crystallization at -20°C. Dark blue colored crystals of $[\mathbf{II.8a}]^{2+}$ were formed, which were the filtered and washed with *n*-hexane.

Synthetic procedure of $[II.8a]^{2+}.2[CF_3SO_3]^-$

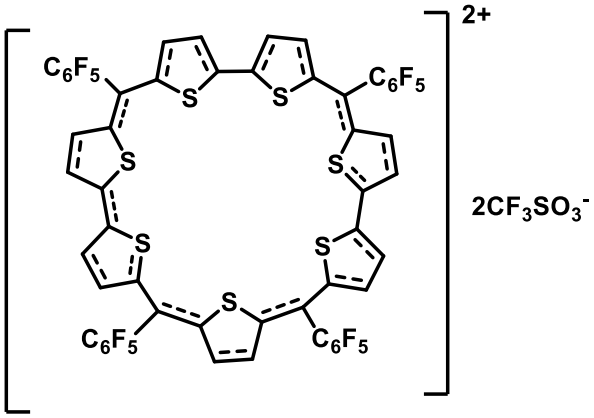

Crystals of $\mathbf{II.8a^{2+}}$ with triflate ions were obtained upon addition of triflic acid in molar excess to a solution of **II.8a** dissolved in 5 mL of distilled DCM. Its electronic absorption and ^{1}H NMR spectrum were identical with $\mathbf{[II.8a]^{2+}.2[SbCl_6]^-}$.

The molecules were characterized using the HR-MS and other spectroscopic techniques.

HR-MS (ESI) m/z: $[M]^{2+}$Calcd. for $C_{56}H_{14}F_{20}S_7$ 644.9410; Found 644.9431.

UV-Vis (CH_2Cl_2): λ_{max} nm (ε, $Lmol^{-1}cm^{-1}$): 616 (417000), 988 (35300).

^{1}H NMR (400 MHz, CD_3CN) δ: 14.16 (d, J = 4.7 Hz, 2H), 14.07 (d, J = 4.9 Hz, 2H), 13.83 (d, J = 4.8 Hz, 2H), 12.89 (d, J = 4.8 Hz, 2H), 12.82 (d, J = 4.4 Hz, 2H), 12.76 (d, J = 4.3 Hz, 2H), 12.50 (s, 2H).

Selected Crystal data: triclinic, space group $P\text{-}1$, a =12.210 (3), b = 16.427 (4), c = 18.223 (4) Å, α = 96.418 (6), β = 95.129 (7), γ = 102.509 (6), V = 3521.5 (14) Å^3, T= 120 K, D_{cal} = 1.475 gcm^{-3}, R_1 = 0.0945, wR_2 = 0.3319, GOF = 1.066

Synthetic procedure of II.9a

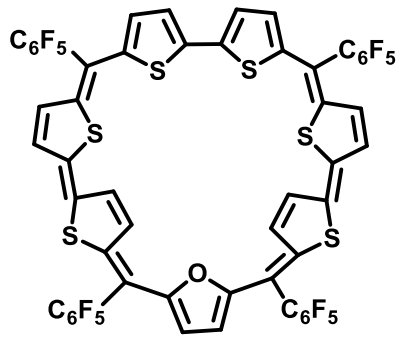

In a clean and dried 250 mL round bottom flask, **II.6** (220 mg, 513.48 μmol) and **II.7b**[5] (118.16 mg, 256.74 μmol) were dissolved in 140 mL of dry dichloromethane. The solution was stirred under dark and inert atmosphere. To this solution $BF_3.OEt_2$ (256.74 μmol, 0.03 mL) was added slowly and stirred under dark and inert conditions for two hours. Later, the reaction was oxidized using dichlorodicyanoquinone (250 mg,1.54 mmol) and stirred further for additional four hours. The reaction mixture was filtered through basic alumina column and purified on a neutral alumina glass column. **II.9a** was isolated as a brown colored band in 9% yields. The molecule was characterized using HR-MS and other spectroscopic techniques.

HR-MS (ESI) m/z: $[M]^+$Calcd. for $C_{56}H_{14}F_{20}OS_6$ 1273.9050; Found 1273.9043.

UV-Vis (CH_2Cl_2): λ_{max} nm (ε, $Lmol^{-1}cm^{-1}$): 440 nm (77900), 498 nm (88900).

^1H NMR (400 MHz, $CDCl_3$) δ: 10.02 (d, *J* = 4.1 Hz, 2H), 9.44 (d, *J* = 4.1 Hz, 2H), 6.34-6.06 (m, 4H), 5.86 (d, *J* = 3.9 Hz, 2H), 5.84 (s, 2H), 5.69 (d, *J* = 5.5 Hz, 2H).

Synthetic procedure of $[II.9a]^{2+}.2[SbCl_6]^-$

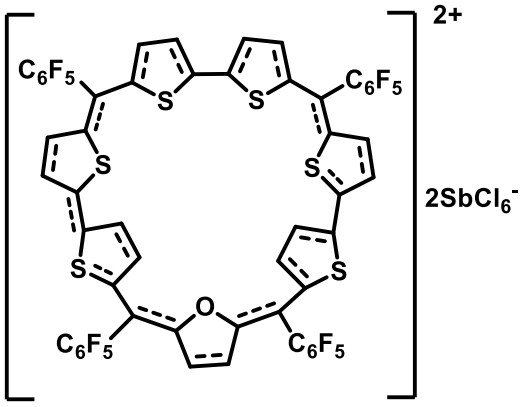

Dication of **II.9a** was generated by dissolving 5 mg of **II.9a** in 10 mL of dry DCM and adding excess Meerwein's salt to the solution. The mixture was stirred at -20° C for 20 minutes and then crystallized at -20° C. Dark blue colored crystals of $[\mathbf{II.9a}]^{2+}.\mathbf{2[SbCl_6]}^-$ were formed, which were washed with n-hexane and further crystallized with DCM/n-hexane system.

The molecule was fully characterized using the HR-MS and other spectroscopic techniques.

HR-MS (ESI) m/z: $[M]^{2+}$ Calcd. for $C_{56}H_{14}F_{20}OS_6$ 636.9521; Found 636.9501.

UV-Vis (CH_2Cl_2): λ_{max} nm (ε, $Lmol^{-1}cm^{-1}$): 633 nm (414000), 874 nm (22500), 914 nm (23300), 1041 nm (59600).

^1H NMR (400 MHz, CD_3CN) δ: 12.48 (d, *J* = 4.6 Hz, 2H), 11.95 (d, *J* = 4.8 Hz, 2H), 11.73 (d, *J* = 4.6 Hz, 2H), 11.52 (d, *J* = 4.6 Hz, 2H), 11.10 (s, 2H), -4.21 (s, 2H), -5.17 (s, 2H).

Selected Crystal data: triclinic, space group *P -1*, *a* =11.8368 (14), *b* = 18.534 (2), *c* = 18.945 (2) Å, α = 105.089 (4), β = 96.584 (4), γ = 104.816 (4), *V*= 3805.7 (7) $Å^3$, T= 120 K, D_{cal} = 1.770 gcm^{-3}, R_1 = 0.0533, wR_2 = 0.1861, GOF = 0.710

Crystal Parameters	II.8a	II.8a^{2+}	II.9a^{2+}
Crystal System	Triclinic	Triclinic	Triclinic
Space group	P-1	P-1	P-1
a (Å)	8.084 Å	12.210Å	11.8368 Å
b (Å)	18.585 Å	16.427Å	18.534 Å
c (Å)	19.669 Å	18.223Å	18.945 Å
α	90.273	96.418	105.089
β	93.457	95.129	96.584
γ	90.810	102.509	104.816
Volume (Å^3)	2949 Å^3	3521.5 Å^3	3805.7 Å^3
T	120 K	120 K	120 K
Z	2	2	1
Density calculated (gcm^{-3})	1.454 gcm^{-3}	1.475 gcm^{-3}	1.770 gcm^{-3}
F(000)	1284.0	1551.1	3132
Absorption coefficient	3.376 mm^{-1}	0.388 mm^{-1}	0.726 mm^{-1}
Reflections reported	4625	18079	18958
Theta (max)	46.183	29.068	28.379
Goodness-of-fit on F^2	1.026	1.066	0.710
R_1	0.0896	0.0945	0.0533
wR_2	0.2505	0.3319	0.1861

***Table II.2**: Selected crystal data for **II.8a**, **II.8a**$^{2+}$ and **II.9a**$^{2+}$*

II.10 References

(1) Sessler, J. L.; Seidel, D. *J. Am. Chem. Soc.* **1999**, *121*, 11257-11258.

(2) Bucher, C.; Seidel, D.; Lynch, V.; Sessler, J. L. *Chem. Comm.* **2002**, 328-29.

(3) Anand, V. R. G.; Pushpan, S. K.; Srinivasan, A.; Narayanan, S. J.; Sridevi, B.; Chandrashehar, T. K. *Org. Lett.* **2000**, *2*, 3829-3832.

(4) Gokulnath, S.; Prabhuraja, V.; Chandrashekar, T. K. *Org. Lett*. **2007**, *9*, 3355-3357.

(5) Gopalakrishna, T. Y.; Anand, V. G. *Angew. Chem., Int. Ed.* **2014**, *53*, 6678-6682.

(6) Reddy, J. S.; Anand, V. G. *J. Am. Chem. Soc.* **2008**, *130*, 3718-3719.

(7) Rathore, R.; Kumar, A. S.; Lindeman, S. V.; Kochi, J. K. *J. Org. Chem.* **1998**, *63*, 5847-5856.

(8) Gaussian 09; Revision A.2; Frisch, M. J.; Trucks, G. W.; Schlegel, H. B.; Scuseria, G. E.; Robb, M. A.; Cheeseman, J. R.; Scalmani, G.; Barone, V.; Mennucci, B.; Petersson, G. A.; Nakatsuji, H.; Caricato, M.; Li, X.; Hratchian, H. P.; Izmaylov, A. F.; Bloino, J.; Zheng, G.; Sonnenberg, J. L.; Hada, M.; Ehara, M.; Toyota, K.; Fukuda, R.; Hasegawa, J.; Ishida, M.; Nakajima, T.; Honda, Y.; Kitao, O.; Nakai, H.; Vreven, T.; Montgomery, J., J. A.; Peralta, J. E.; Ogliaro, F.; Bearpark, M.; Heyd, J. J.; Brothers, E.; Kudin, K. N.; Staroverov, V. N.; Kobayashi, R.; Normand, J.; Raghavachari, K.; Rendell, A.; Burant, J. C.; Iyengar, S. S.; Tomasi, J.; Cossi, M.; Rega, N.; Millam, N. J.; Klene, M.; Knox, J. E.; Cross, J. B.; Bakken, V.; Adamo, C.; Jaramillo, J.; Gomperts, R.; Stratmann, R. E.; Yazyev, O.; Austin, A. J.; Cammi, R.; Pomelli, C.; Ochterski, J. W.; Martin, R. L.; Morokuma, K.; Zakrzewski, V. G.; Voth, G. A.; Salvador, P.; Dannenberg, J. J.; Dapprich, S.; Daniels, A. D.; Farkas, Ö.; Foresman, J. B.; Ortiz, J. V.; Cioslowski, J.; Fox, D. J.; *Gaussian, Inc., Wallingford CT*, **2009**.

(9) (a) Becke, A. D. *J. Chem. Phys.***1993,** *98*, 5648-5652. (b) Lee, C.; Yang, W.; Parr, R. G. *Phys. Rev. B* **1988,** *37*, 785-789. (c) Yanai, T.; Tew, D. P.; Handy, N. C. *Chem. Phys. Lett.* **2004,** *393*, 51-57. (d) Ditchfield, R.; Hehre, W. J.; Pople, J. A. *J. Chem. Phys.* **1971,** *54*, 724-

728. (e) Hehre, W. J.; Lathan, W. A. *J. Chem. Phys.***1972,** *56*, 5255-5257. (f) Hariharan, P. C.; Pople, J. A. *Theor chim acta.* **1973,** *28*, 213-222.

(10) Schleyer, P. V. R.; Maerker, C.; Dransfeld, A.; Jiao, H.; Van Eikema Hommes, N. J. R. *J. Am. Chem. Soc.***1996**, *118*, 6317-6318.

(11) Geuenich, D.; Hess, K.; Köhler, F.; Herges, R. *Chem. Rev.* **2005**, *105*, 3758-3772.

Chapter 3

Synthesis Characterization and Redox Properties of 38π and 40π Octaphyrins

Section IIIA

IIIA.1 Introduction

Octaphyrins are expanded porphyrnoids with eight heterocycle units in the core of a macrocycle.[1] These units can be connected to each other in a cyclic fashion with or without bridging carbon atoms. 30π octaphyrin(0.0.0.0.0.0.0.0)-cyclo[8]pyrrole[2] (Figure IIIA.1; **IIIA.1**), is the simplest of the octaphyrins without bridging carbons. Due to a rigid framework, it acquires a planar configuration and exhibits aromatic characteristics.

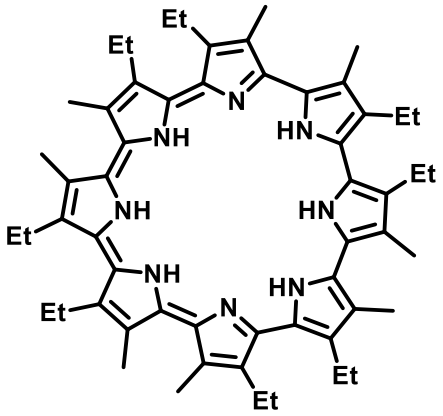

Figure IIIA.1: *Octaphyrin with no bridging carbons*

Vogel and co-workers reported the example of octaphyrins with eight pyrrole units connected in a cyclic fashion with six or four bridging carbons.[3] Interestingly, these macrocycles adopted a figure-of-eight configuration and hence classified as non-aromatic species. Later, Osuka and co-workers reported a true octaphyrin with eight pyrroles and eight *meso* carbons which also adopted a figure-of-eight configuration.[4] Increasing the number of *meso* position leads to a fluxional behavior in the molecule, and the porphyrnoid generally deviates from planarity. However, 40π isophlorin having eight *meso* positions with eight furans in the core attained a near planar configuration (Figure IIIA.2; **IIIA.2**).[5] The molecule displayed paratropic ring

current affect and did not display any fluxonial behavior. Proton NMR analysis and molecular structure determined from single crystal X-ray diffraction revealed that the alternate furan rings were inverted; this helped in reducing the bulk strain of the molecule and hence barred it from twisting. A similar planar structure has been observed when all furans in **IIIA.2** were replaced by thiophene units.

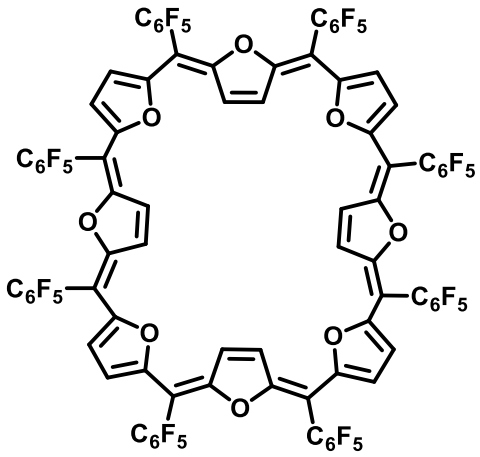

IIIA.2

Figure IIIA.2: *A planar 40π octaphyrin with eight meso positions*

However, Latos and co-workers reported an octaphyrin with four thiophene and pyrrole units which was analyzed as a figure-of-eight configuration in the solution state.[6] Octaphyrins reported by both Latos and Osuka also exhibited proton-coupled-electron-transfer (PCET) redox process to interchange between 36π and 38π electrons.[4,6] Since both octa-thiophene and octa-furan exhibited planar structures, it was of interest to explore a 40π macrocycle with combination of four furans and thiophenes.

IIIA.2 Synthesis of 40π expanded isophlorin

Using a standard protocol[7], attempts were made to synthesize a 40π isophlorin by condensing dithienyl diol (**IIIA.3**)[8] with difuryl methane (**IIIA.4**)[9] in an equimolar ratio using boron trifluoride etherate followed by dichlorodicyanoquinone (DDQ) oxidation (Scheme IIIA.1).

The reaction was quenched with triethylamine. MALDI TOF/TOF analysis of the reaction mixture revealed the formation of a four membered 20π isophlorin (**IIIA.5**) in very less yield while a six membered macrocycle (**IIIA.6**) and the eight membered macrocycle (**IIIA.7**) were formed in the major yields.

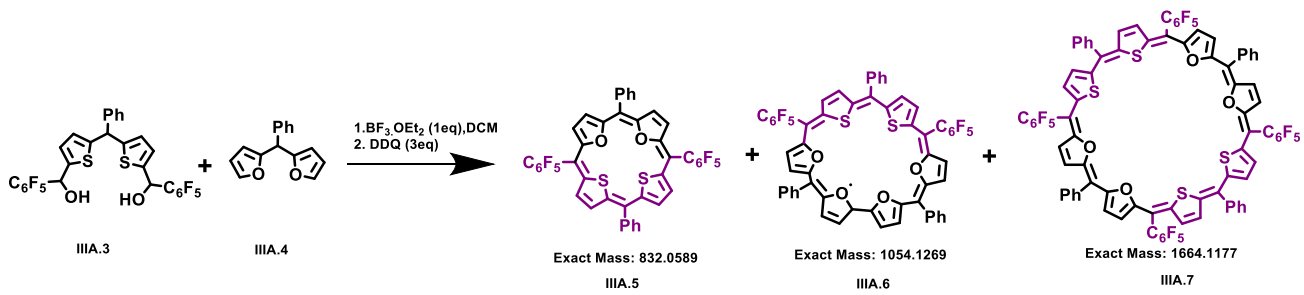

Scheme IIIA.1: *Synthesis of expanded isophlorins*

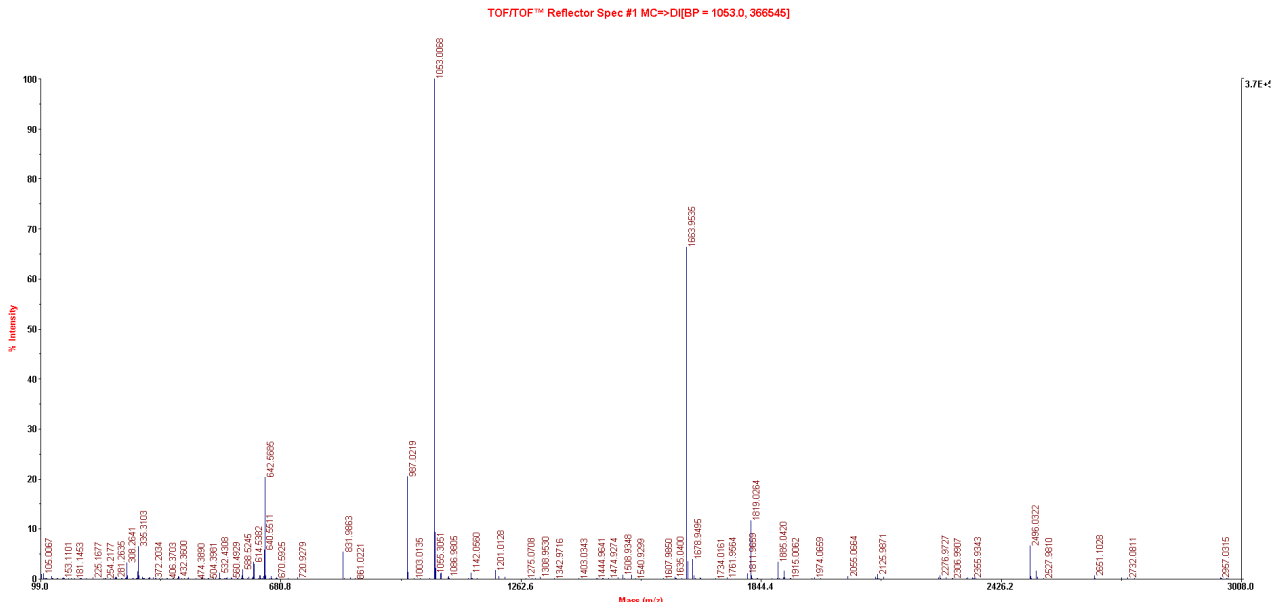

Figure IIIA.3: *MALDI TOF/TOF mass spectrum of the reaction mixture*

IIIA.3 Isolation and characterization of 40π octaphyrin

Attempts were made to isolate each of the above macrocycles from the reaction mixture. Unfortunately, due to very poor yields, the four membered 20π isophlorin, **IIIA.5**, could not be isolated in quantifiable yields for characterization. It came to light that the six membered

macrocycle was unstable over column and only a minute fraction could be isolated which was insufficient for complete characterization. The 40π expanded isophlorin eluted as an intense blue band with CH_2Cl_2/hexane in silica gel column. It displayed a sharp intense band at 587 nm (9.3×10^4 ε, $Lmol^{-1}cm^{-1}$) along with another band at 406 nm (1.3×10^5) (Figure IIIA.5). It displayed $(M+H)^+$ peak at 1665.1107 corresponding to calculated value for $C_{88}H_{36}F_{20}O_4S_4$ 1665.1255 (Figure IIIA.4).

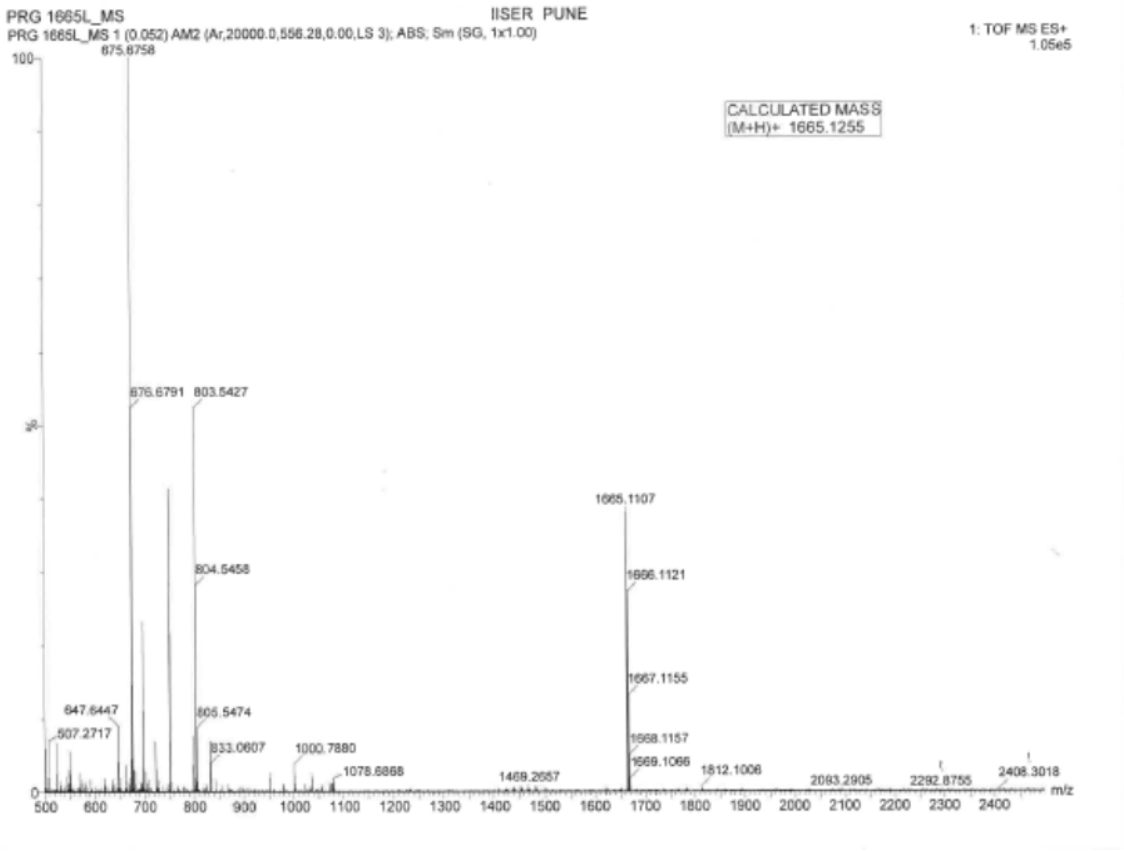

Figure IIIA.4: *HR-MS spectrum of* ***IIIA.7***

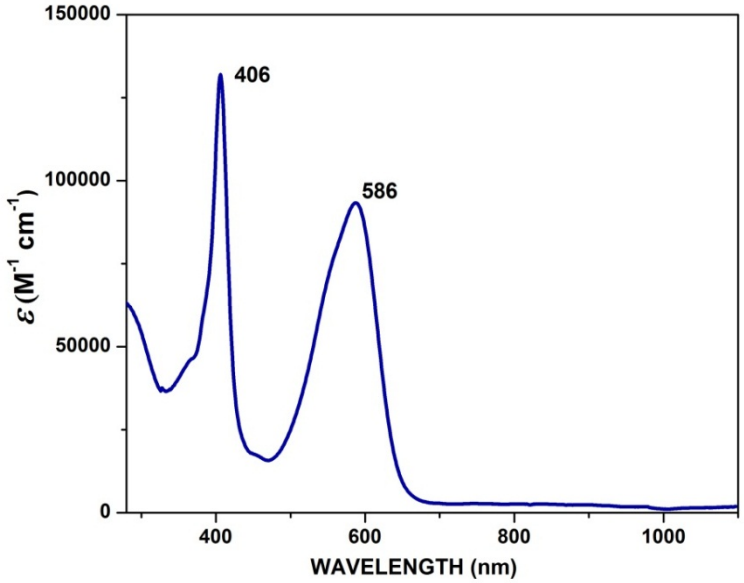

Figure IIIA.5: *Electronic absorption spectrum of* ***IIIA.7*** *in dichloromethane at ~10^{-5}M concentration*

Room temperature ^{1}H NMR spectrum of **IIIA.7** did not yield a well resolved spectrum suggestive of solution state dynamics. However, upon lowering the temperature to 223 K (Figure IIIA.6 and IIIA.7), the signals were well resolved and resonated between δ 6.11 and 8.98 ppm corresponding to a total of thirty-two protons. Even though the macrocycle accounted for 40π electrons, it did not display any significant ring current effect suggesting a non-planar configuration in the solution state. The ^{1}H-^{1}H COSY spectrum (Figure IIIA.8) of octaphyrin **IIIa.7** displayed clear five correlations between the protons in support of the coupling for β protons of the heterocyclic rings, thiophene and furan.

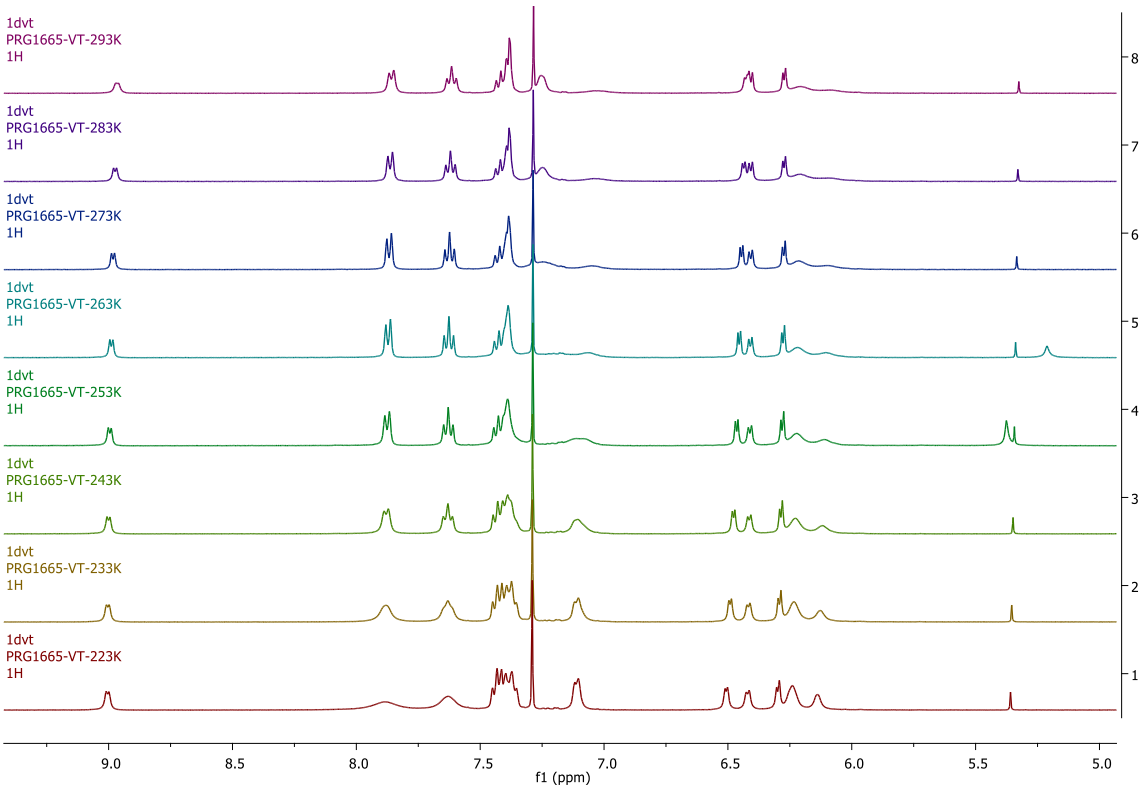

Figure IIIA.6: *Variable temperature proton NMR spectra of* ***IIIA.7*** *in* $CDCl_3$ *from 223 K to 293 K*

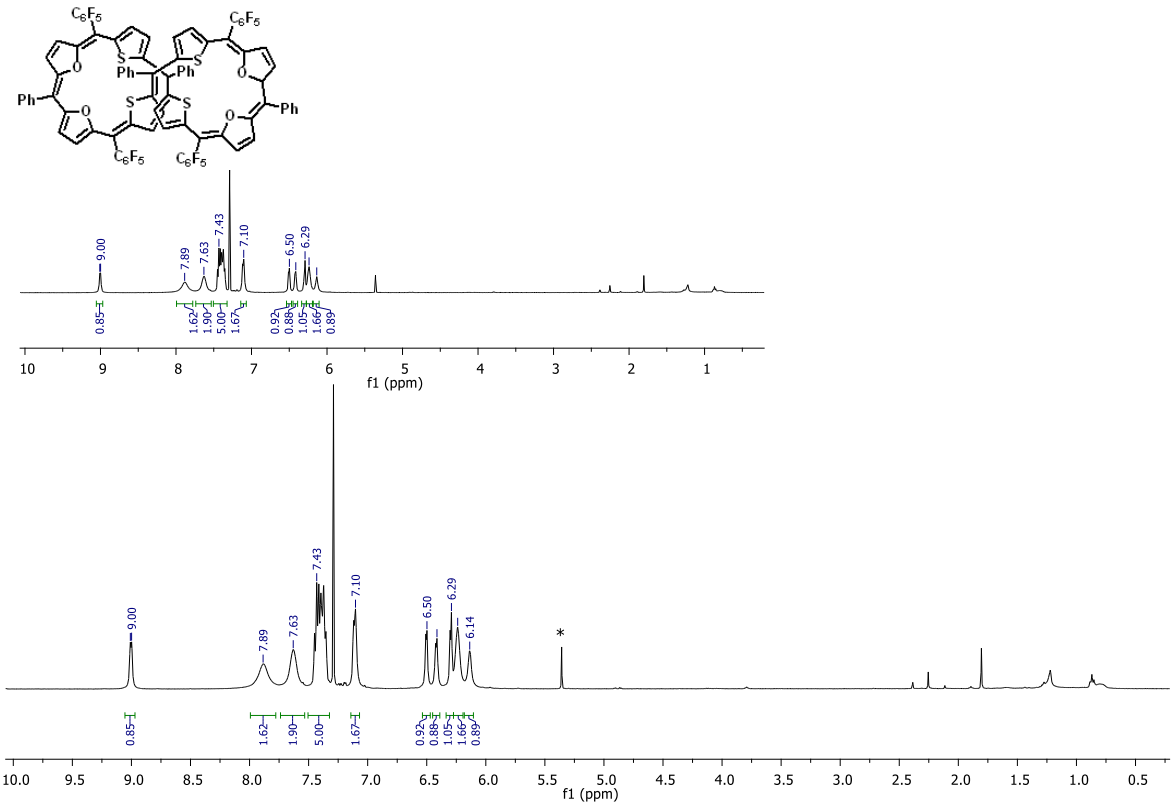

Figure IIIA.7: *^{1}H NMR spectrum of* ***IIIA.7*** *in* $CDCl_3$ *at 223 K*

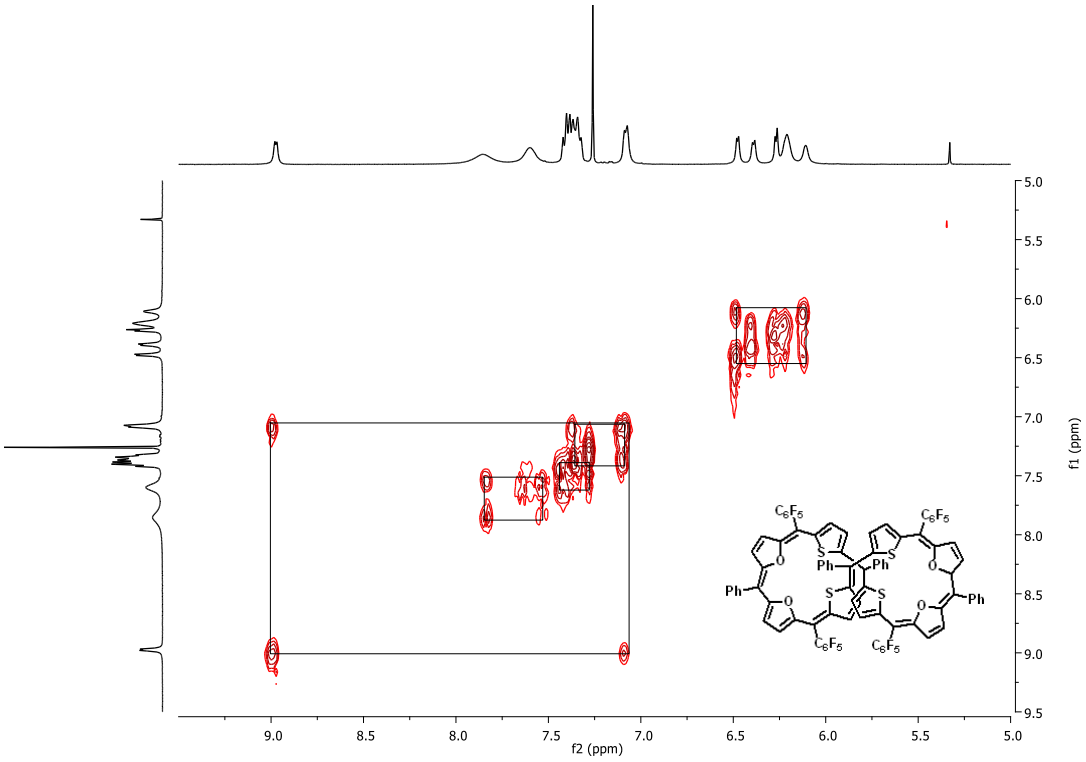

Figure IIIA.8: *^{1}H-^{1}H COSY NMR spectrum of* ***IIIA.7*** *in $CDCl_3$ at 223 K*

Lack of significant ring current effect in its ^{1}H NMR spectrum suggested the possible loss of macrocyclic planarity. To confirm the structure of the molecule, good quality crystals were grown by vapor diffusion of hexane into a solution of **IIIA.7** in chloroform. Single crystal X-ray diffraction analysis revealed an unexpected figure-of-eight configuration justifying the loss of ring current effects in its ^{1}H NMR spectrum.

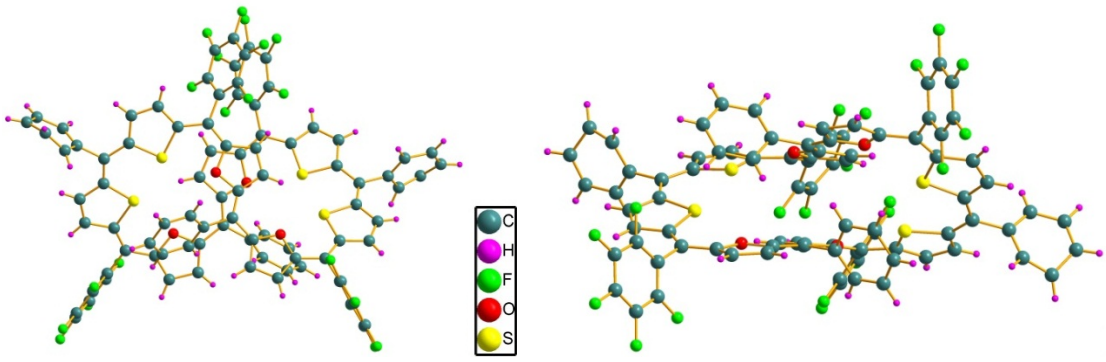

Figure IIIA.9: *Single Crystal X-ray structure [top view(left) and lateral view (right)] of* ***IIIA.7***

IIIA.4 Two Electron Oxidation

Being a 4nπ non-antiaromatic system, octaphyrin **IIIA.7** was subjected to two-electron oxidation to evaluate the formation of its corresponding 38π dicationic species (Scheme-IIIA.2). Addition of Meerwein's salt[10] to a solution of **IIIA.7** in dichloromethane was marked by an observable color change from blue to green. In comparison to its freebase absorption, the green color solution displayed an intense absorption band at 793 nm (121000 ε, $Lmol^{-1}cm^{-1}$) with a red shift of more than 200 nm. In addition to this intense absorption, three other bands at 434 (49500), 1107 (10130), 1253 (5130) (Figure IIIA.10) were also observed in the spectrum.

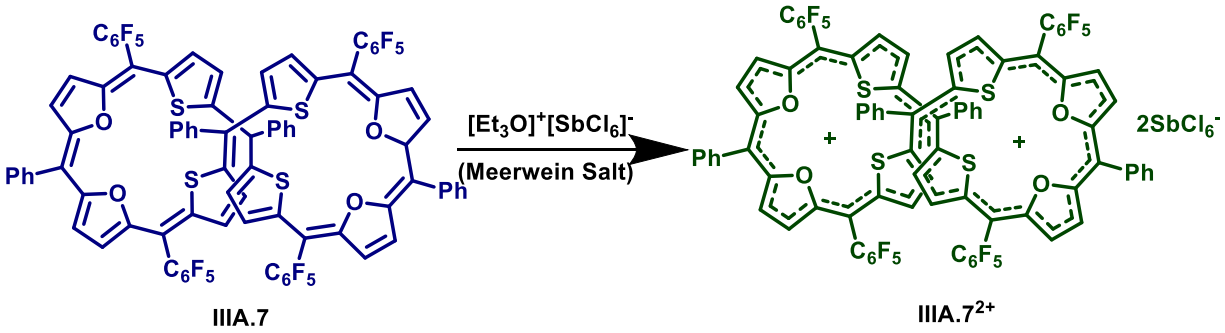

Scheme IIIA.2: *Chemical two-electron oxidation of* ***IIIA.7***

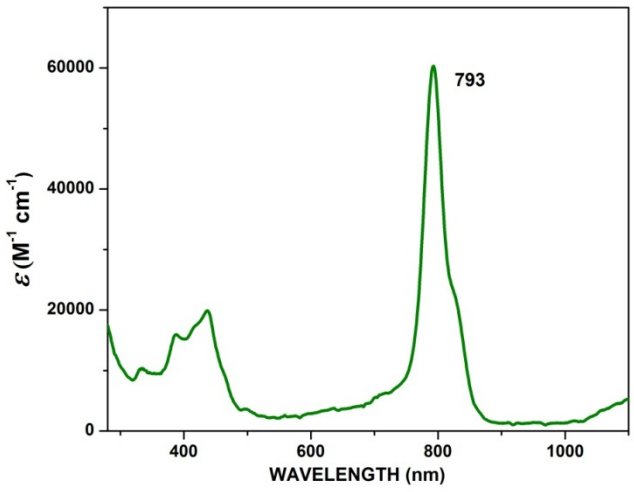

Figure IIIA.10: *Electronic absorption spectrum of* ***[IIIA.7]***^{2} *dichloromethane at ~*10^{-5}*M concentration*

HR-MS of the oxidized macrocycle displayed *m/2* peak at 832.0589 in support of the formation of dication (Figure IIIA.11). Further, the dicationic macrocycle unlike the parent freebase displayed a well-resolved proton NMR spectrum at room temperature (Figure IIIA.12). All the signals for this dicationic species molecule resonated between δ 5.82 to 8.52 ppm in acetonitrile-d_3. Yet, it did not display any significant ring current effect suggesting the figure-of-eight configuration being intact. There were three correlations observed in its ^{1}H-^{1}H COSY spectrum (Figure IIIA.13) recorded at room temperature.

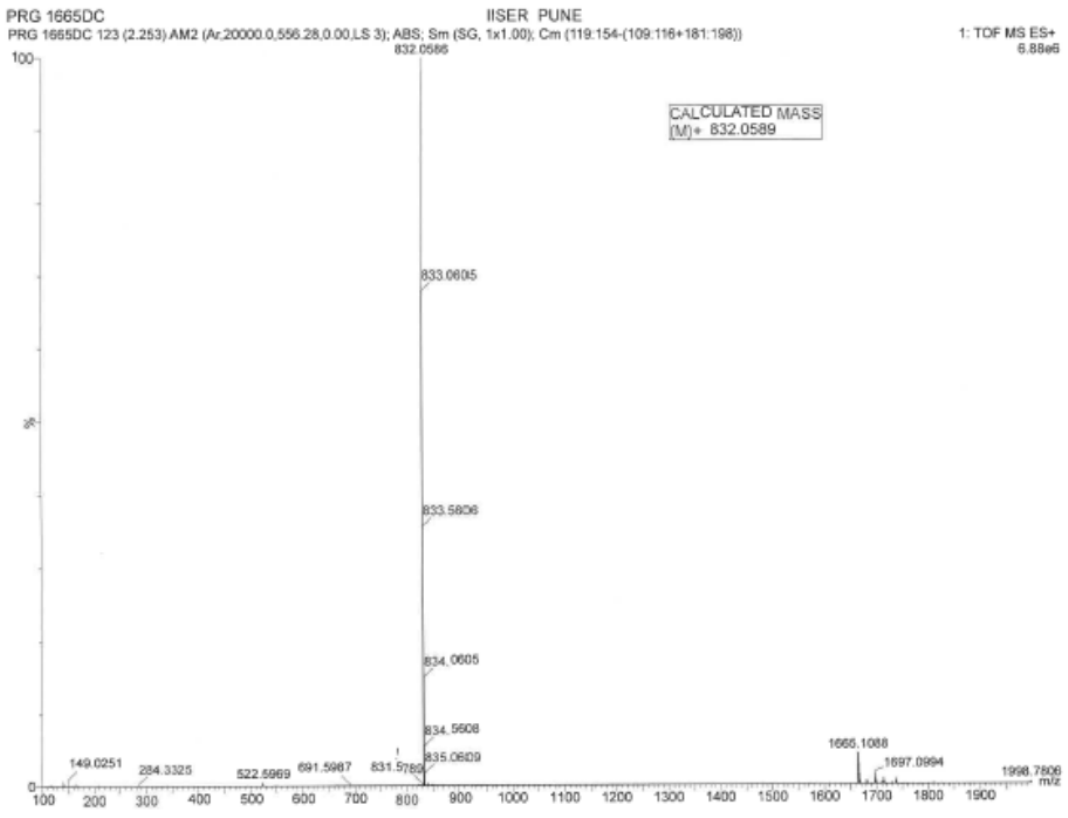

Figure IIIA.11: *HR-MS spectrum of* ***IIIA.7***$^{2+}$

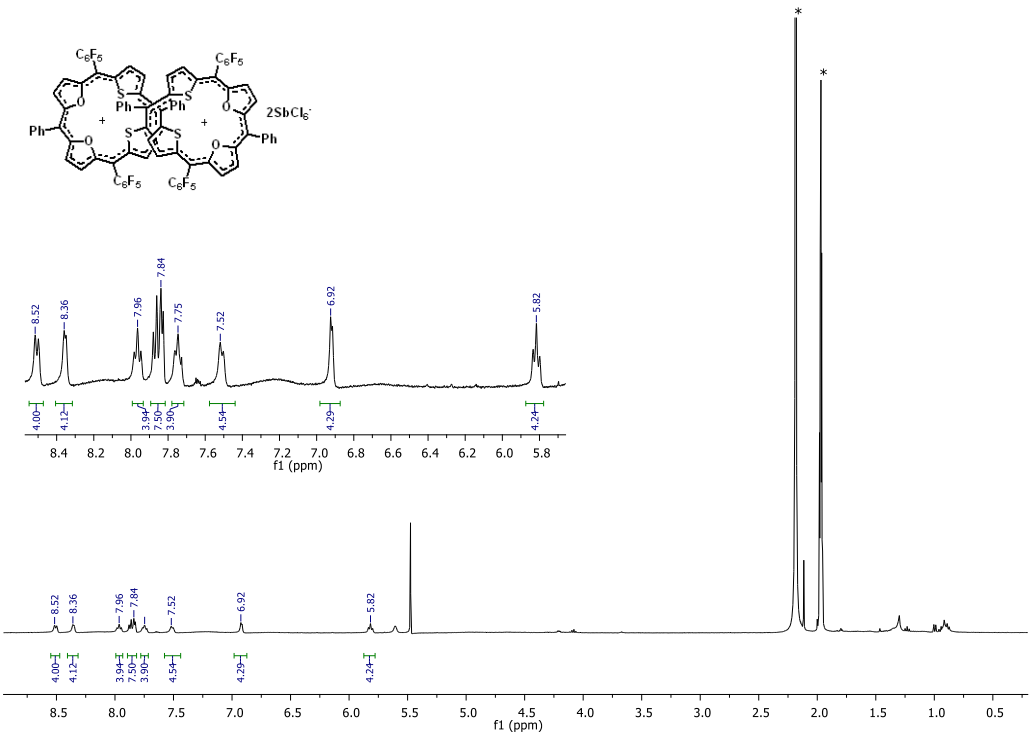

Figure IIIA.12: *^{1}H NMR spectrum of* ***IIIA.7^{2+}*** *in acetonitrile-d_3 at 293 K*

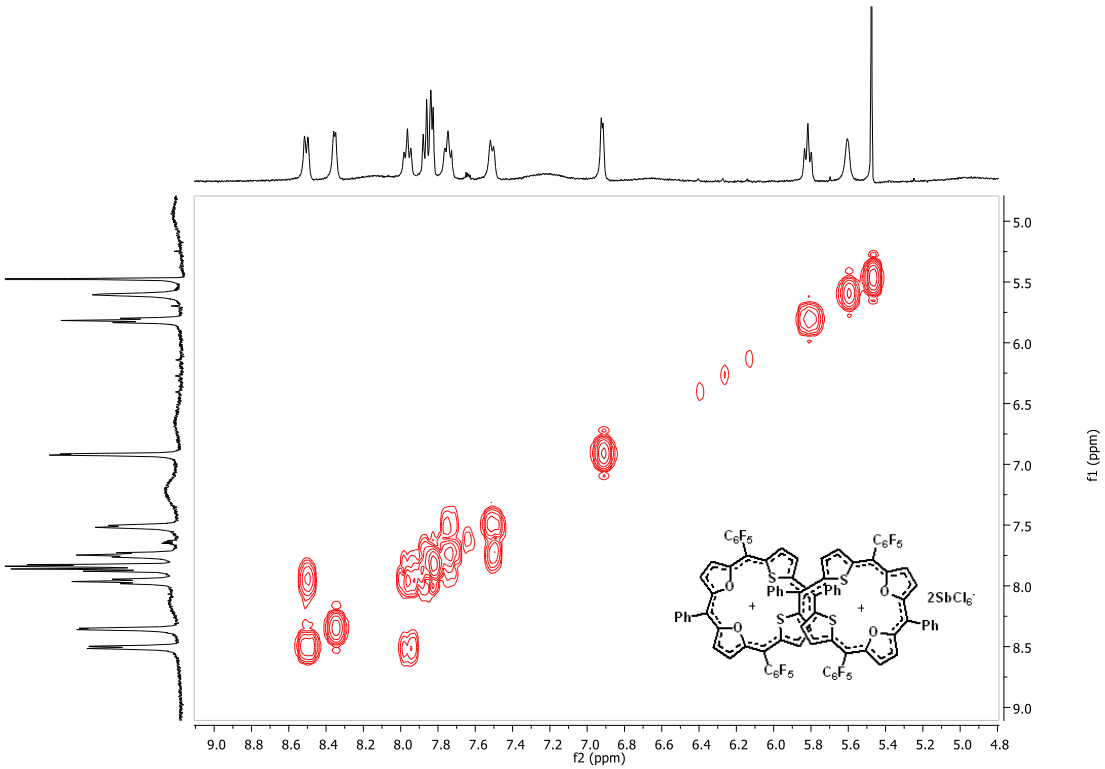

Figure IIIA.13: *^{1}H-^{1}H COSY spectrum of* ***IIIA.7^{2+}*** *recorded in acetonitrile-d_3 at 293 K*

To deduce the molecular structure, the green colored solution was cooled to 233 K and allowed to crystallize in acetonitrile/ hexane by slow diffusion method. Its single crystal X-ray structure revealed that two counter $[SbCl_6]^-$ anions were associated with the macrocycle (Figure IIIA.14) in the packing diagram. More importantly, the dicationic macrocycle **IIIA.7**$^{2+}$ retained its figure of eight configuration and hence justified the lack of any ring current affect for the 38π system in its ^{1}H NMR spectrum.

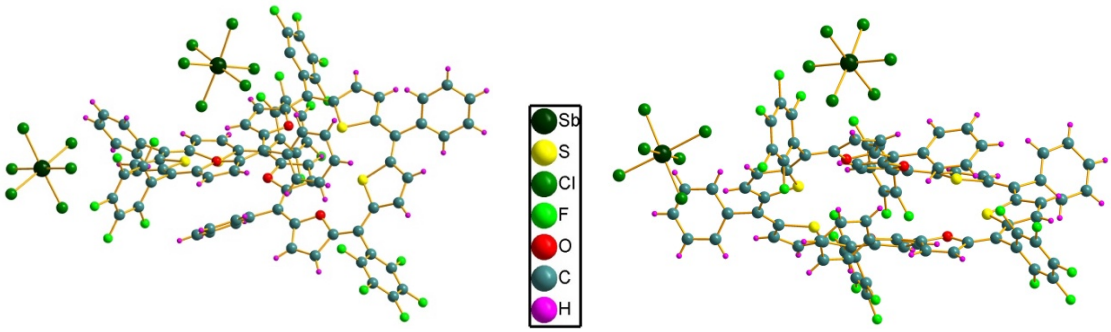

Figure IIIA.14: *Single Crystal X-ray structure [top view(left) and lateral view (right)] of* ***IIIA.7***$^{2+}$

IIIA.5 Quantum Chemical Calculations

To measure the antiaromaticity and aromaticity in 40π octaphyrin and its 38π dication respectively, quantum chemical calculations were employed using Gaussian09 rev D program. The obtained crystal structures were optimized using Density Functional Theory (DFT) with Beckes's three-parameter hybrid exchange function and the lee-Yang-Parr correlation function (B3LYP)[11] and 6-31G(d,p) basis set for all the atoms in the molecule. Then the "Nucleus Independent Chemical Shift" (NICS)[12] value was calculated and tabulated below (Table IIIA.1).

Molecule	NICS(0)	AICD	λ_{max} (nm)	Hückel Aromaticity
IIIA.7	+3.51	Anti-clockwise	587	Antiaromatic
IIIA.7^{2+}	-7.75	Clockwise	793	Aromatic

Table IIIA.1: *Quantum chemical calculations of* ***IIIA.7*** *and* ***IIIA.7^{2+}***

The NICS value was estimated using gauge independent atomic orbital (GIAO)[13] method. NICS(0)[12] was calculated by denoting the global ring centre at the non-weighed mean center of the macrocycle. A low positive NICS(0) value of δ +3.51 ppm for **IIIA.7** is in agreement with weak paratropic ring current effect as observed in the proton NMR spectrum of the 40π octaphyrin. Even though a negative NICS(0) value of δ -7.75 ppm for **IIIA.7^{2+}** was suggestive of moderate aromatic character, yet the non-planar topology justifies the very weak diatropic ring current effect observed in its proton NMR spectrum.

IIIA.6 Conclusion

Section-A of chapter 3 describes the successful synthesis of a 40π Octaphyrin **IIIA.7** containing four thiophene and furan units respectively. Comprehensive characterization both in solution and solid states revealed a non-planar 40π octaphyrin macrocycle. However, it undergoes chemical two-electron oxidation with appropriate reagents. The isolated 38π dication was also characterized as a non-planar macrocycle and hence adopted non-aromatic character. Absence of (anti)aromatic character for both macrocycles was strikingly evident from lack of significant ring current effect in their respective ^{1}H NMR spectrum. These findings were further justified by quantum chemical and NICS calculations.

IIIA.7 Experimental section

All solvents and reagents used were of commercials grade and were utilized as such unless mentioned otherwise. Inert reactions were performed using freshly dried solvents. Dichloromethane was dried by refluxing and distillation over P_2O_5. Tetrahydrofuran was dried by refluxing and distilling over Sodium metal. Purification of compounds was done using glass column chromatography packed with silica gel (230-400) mesh or basic alumina. ^{1}H NMR was recorded on a JEOL 400 MHz or Bruker 500 MHz spectrometer. Absorption spectra were recorded on a Perkin-Elmer λ-950 ultraviolet−visible (UV−vis) spectro-photometer. WATERS G2 Synapt Mass Spectrometer was used to record High Resolution Mass spectrum. BRUKER KAPPA APEX II CCD Duo diffractometer (operated at 1500 W power: 50 kV, 30 mA) was used for Single-crystal diffraction analysis data collected at 100K using graphite-mono chromated Mo Kα radiation (λ = 0.71073 Å).

Synthetic Procedure of ((phenylmethylene)bis(thiophene-5,2-diyl))bis((perfluorophenyl)methanol) IIIA.3[8]

IIIA.3 was synthesized in three steps.

Step 1: Synthetic procedure of 2,2'-(phenylmethylene)dithiophene

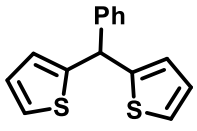

To a clean dried round bottom flask 33mL of thiophene (424 mmol) was taken. To this benzaldehyde (1.44 mL, 14.13 mmol) was added and the solution was stirred at room temperature under dark and inert atmosphere. $BF_3.OEt_2$ (1.74 mL, 14.13 mmol) was added to the above reaction mixture and further stirred for one hour. The reaction was quenched with

water after one hour and extracted from ethyl acetate. It was purified in silica gel column to give desired compound (2,2'-(phenylmethylene)dithiophene) in 85% yield.

^{1}H NMR (400 MHz, $CDCl_3$) δ: 7.43 -7.24 (m, 7H), 6.35 (dd, *J* = 3.2, 1.9 Hz, 2H), 6.11-6.02 (m, 2H), 5.49 (s, 1H).

Step 2: Synthetic procedure of 5,5'-(phenylmethylene)bis(thiophene-2-carbaldehyde)

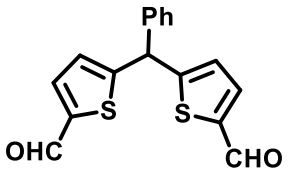

In a round bottom flask, 2,2'-(phenylmethylene)dithiophene (3g, 11.70 mmol) was taken. To this 100 mL of dry diethy ether was added under nitrogen atmosphere. The reaction mixture was stirred and then 1.6 M *n*BuLi (29.98 mL, 47.98 mmol) was added under nitrogen atmosphere. After 15 minutes DMF (8.84 mL, 113.50 mmol) dissolved in 30mL of dry diethyl ether was added slowly and further stirred for two hours. The reaction mixture was washed with water, diluted hydrochloric acid and sodium bicarbonate solution and extracted from ethyl acetate. The solid residue of was purified by column chromatography to give desired product (5,5'-(phenylmethylene)bis(thiophene-2-carbaldehyde)) in 81% yield.

^{1}H NMR (400 MHz, $CDCl_3$) δ: 9.85 (s, 2H), 7.65 (t, *J* = 4 Hz, 2H), 7.39 -7.26 (m, 5H), 6.98 (dd, *J* = 3.8, 0.9 Hz, 2H), 5.89 (s, 1H).

Step 3: Synthetic procedure of ((phenylmethylene)bis(thiophene-5,2-diyl))bis((perfluorophenyl)methanol) **IIIA.3**

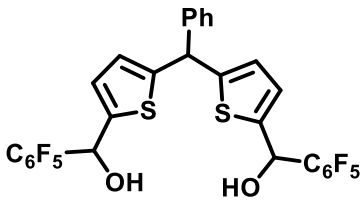

To a stirred solution of 5,5'-(phenylmethylene)bis(thiophene-2-carbaldehyde) (500 mg, 1.60 mmol) in 15 mL dry THF, freshly prepared grignard reagent (C_6F_5MgBr, 3.52 mmol) in 15 mL of dry THF was added. The reaction mixture was stirred for two hours and then quenched with saturated ammonium chloride solution. The compound **IIIA.3** was extracted with ethyl acetate and dried over sodium sulphate. The molecule **IIIA.3** (((phenylmethylene)bis(thiophene-5,2-diyl))bis((perfluorophenyl)methanol)) being unstable was instantly used for cyclisation reaction.

Synthetic Procedure of 2,2'-(phenylmethylene)difuran IIIA.4[9]

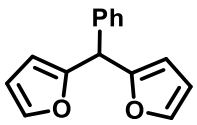

To 20 mL of furan 2.8 mL (28.27 mmol) of benzaldehyde was added and stirred under dark and inert conditions. To the above reaction mixture 1.2 g of Amberlyst-16 was added and further stirred under dark and inert conditions for four hours. The reaction mixture was filtered and extracted with ethyl acetate to give desired compound **IIIA.4** in 85% yields.

^{1}H NMR (400 MHz, $CDCl_3$) δ: 7.43-7.24 (m, 7H), 6.35 (dd, *J* = 3.2, 1.9 Hz, 2H), 6.11-6.02 (m, 2H), 5.49 (s, 1H).

Synthetic Procedure of IIIA.7

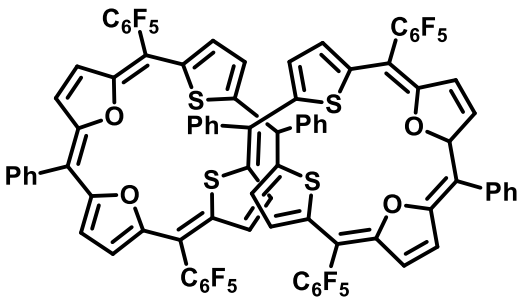

A cleaned dry round bottom flask was charged with an equimolar concentration of difurylmethane[9] (172 mg, 770 µmol), **IIIA.4**, and diol of dithienylmethane[8] (500 mg, 770 µmol), **IIIA.3**, in 200 mL of dry dichloromethane. The reaction mixture was degassed and stirred for 10 minutes. Then under dark and inert conditions it was subjected to 0.09 mL of $BF_3.OEt_2$ (770 µmol) and stirred further for 1.5 hours. Then three equivalents of dichlorodicyanoquinone (DDQ) (375 mg, 2.31 mmol) were added and stirring was continued for another one and half hours. The reaction mixture was then quenched using catalytic amount of triethyl ammine and then passing through basic alumina column. The reaction mixture was concentrated and further blue colored band of **IIIA.7** was purified on silica gel column using dichloromethane/ hexane as eluent. **IIIA.7** was crystallized using slow diffusion method with dichloromethane/hexane solvent system.

^{1}H NMR (400 MHz, $CDCl_3$) δ: 9.00 (d, *J* = 4.3 Hz, 2H), 7.89 (s, 4H), 7.59 (d, *J* = 32.6 Hz, 4H), 7.40 (dt, *J* = 17.0, 7.5 Hz, 10H), 7.11 (d, *J* = 6.0 Hz, 4H), 6.50 (d, *J* = 3.9 Hz, 2H), 6.42 (d, *J* = 4.6 Hz, 2H), 6.30 (d, *J* = 4.4 Hz, 2H), 6.24 (s, 4H), 6.14 (s, 2H).

UV/Vis ($CHCl_3$): λ_{max} nm (ε)L mol^{-1} cm^{-1} = 587 nm (9.3×10^4), 406 nm (1.3×10^5), 279 nm (6.3×10^5).

HR-MS: ($M+H^+$) =1665.1255 (Calcd. for $C_{88}H_{36}F_{20}O_4S_4$); Observed: 1665.1107

Selected Crystal data: Orthorhombic, space group I b a 2, a = 13.0601, b = 20.885, c = 28.618Å, α = 90, β = 90, γ = 90, V= 7805.9 $Å^3$, T= 100 K, D_{cal} = 1.444 gcm^{-3}, R_1 = 0.0957, wR_2 = 0.2857, GOF = 1.048

Synthetic Procedure of IIIA.7^{2+}

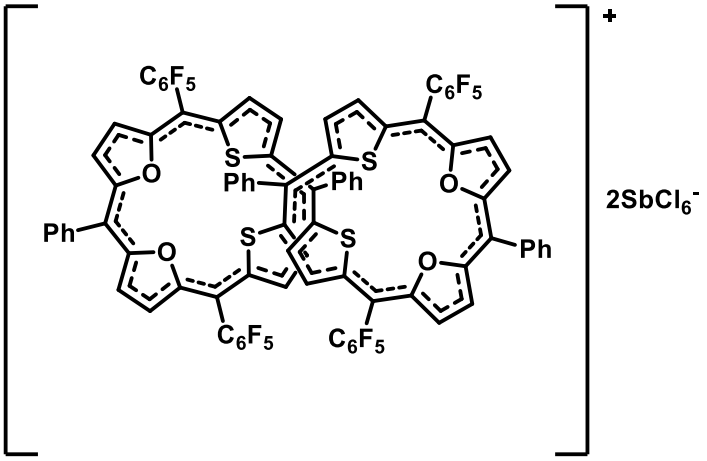

The solution of **IIIA.7** was dissolved in dichloromethane and excess of Meerwein's salt[9] was added to it and stirred at 253 K for 20 minutes. Then it was allowed to recrystallize at 253 K. The green colored crystals were washed with hexane and kept for crystallization using DCM/Hexane.

^{1}H NMR (400 MHz, CD_3CN) δ: 8.51 (d, *J* = 7.0 Hz, 4H), 8.36 (s, 4H), 7.96 (t, *J* = 7.1 Hz, 4H), 7.85 (dd, *J* = 15.2, 6.2 Hz, 8H), 7.75 (t, *J* = 7.2 Hz, 4H), 7.51 (d, *J* = 6.8 Hz, 4H), 6.92 (s, 4H), 5.82 (s, 4H)**.**

UV/Vis ($CHCl_3$): λ_{max} nm (ε)L mol^{-1} cm^{-1} = 1253 nm (5.13×10^3), 1107 nm (1.013×10^4), 793 nm (1.21×10^5), 434 nm (4.95×10^4).

HR-MS: *m*/*z* = 832.0589 Calcd. for $[C_{88}H_{36}F_{20}O_4S_4]^{2+}$; Observed: 832.0586

Selected Crystal data: triclinic, space group P-1, a = 18.012, b = 18.338, c = 19.375 Å, α = 92.256, β = 99.338, γ = 111.588, V= 5837.6 Å^3, T= 100 K, D_{cal} = 1.328 gcm^{-3}, R_1 = 0.0741, wR_2 = 0.2496, GOF = 0.707

Crystal Parameters	IIIA.7	IIIA.7^{2+}
Crystal System	Orthorhombic	Triclinic
Space group	I b a 2	P-1
a (Å)	13.0601Å	18.012 Å
b (Å)	20.885Å	18.338 Å
c (Å)	28.618 Å	19.375 Å
α	90	92.256
β	90	99.338
γ	90	111.588
Volume (Å^3)	7805.9 Å^3	5837.6 Å^3
T	100 K	100 K
Z	4	2
Density calculated (gcm^{-3})	1.444 gcm^{-3}	1.328 gcm^{-3}
F(000)	3424.0	2292.0
Absorption coefficient	0.225 mm^{-1}	0.880 mm^{-1}
Reflections reported	9498	29467
Theta (max)	28.418	28.450
Goodness-of-fit on F^2	1.048	0.707
R_1	0.0957	0.0741
wR_2	0.2857	0.2496

Table IIIA.2*: Selected crystal data for* ***IIIA.7*** *and* ***IIIA.7^{2+}***

Section 3B

IIIB.1 Introduction

In the above section, an approach towards the synthesis of a 40π octaphyrin and its subsequent oxidation to 38π dication has been described. This section describes an approach to synthesize an aromatic 38π octaphyrin by decreasing the number of bridging positions to six sp^2 carbons.

Prior to this approach, it has been observed that octaphyrins with pyrrole units in the core of the macrocycle, usually stabilize the 36π macrocycle (Figure IIIB.1; **IIIB.1**) which resisted further oxidation (Figure IIIB.1; **IIIB.2**).[14]

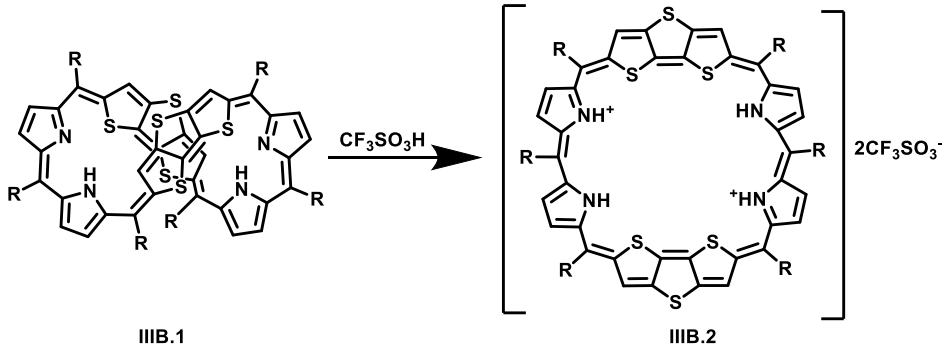

Figure IIIB.1: *36π Octaphyrin with six bridging units*

Therefore, a possible option available to synthesize 38π octaphyrin is by employing only six bridging carbons and replacing pyrrole by thiophene / furan/ selenophene in the core of the macrocycle. Some of the possible 38π octaphyrins that can be envisaged are shown in Figure IIIB.2.

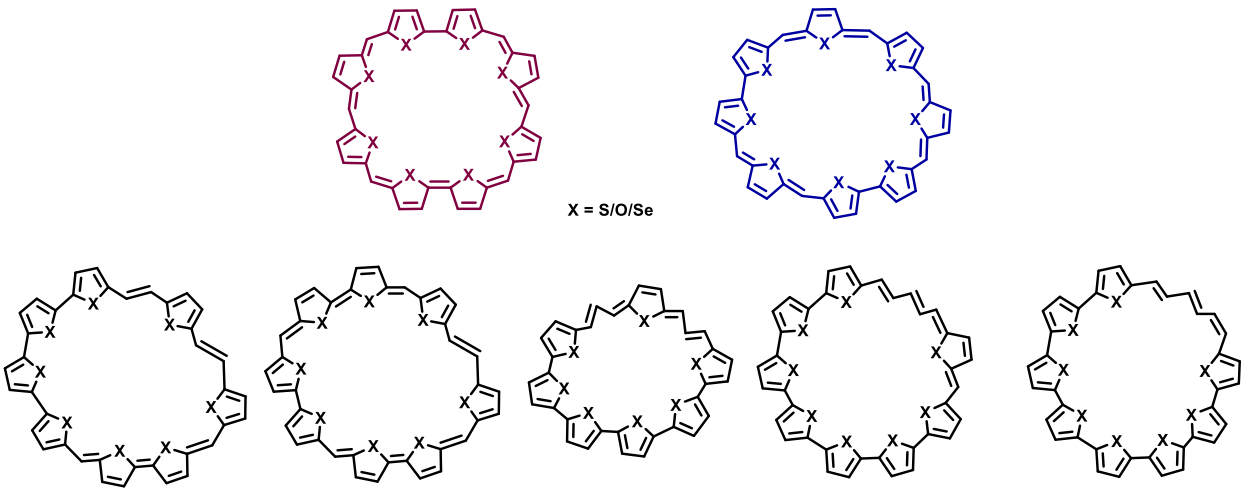

Figure IIIB.2: *Possible 38π octaphyrins with six bridging units*

However, a quick analysis reveals that, it is easier to obtain either of the first two octaphyrins shown in purple and blue due to the easy-to-make precursors for these macrocycles. Relatively, the other macrocycles demand multiple synthetic steps for monomeric units required for their synthesis. Therefore, the first two octaphyrins were chosen as the synthetic targets as they require an asymmetric tristhiophene synthesized previously with thiophene/ furan diol.

Till date, a variety of isomeric porphyrins and isophlorins have been synthesized, but all vary in synthetic route. No two isomeric porphyrinoids have been isolated from the same reaction mixture. In this section an unique attempt, to synthesize two different isomers of the 38π octaphyrins in the same reaction will be described. Also, the serendipitous discovery of a novel 38π octaphyrin in the reaction will be highlighted.

IIIB.2 Synthesis of 38π expanded isophlorin

The 38π expanded isophlorin synthesis was attempted by condensing the asymmetric tristhiophene **IIIB.3** with either thiophene[15] or furan diol[16] **IIIB.4** in equimolar concentration in the presence of $BF_3.OEt_2$ followed by DDQ oxidation (Scheme-IIIB.1). After stirring the reaction mixture for two hours it was passed through basic alumina. MALDI TOF/TOF

spectrometric analysis revealed a [2+2] condensation was favored over the [1+1] condensation to yield an eight membered octaphyrin as the major product. As tristhiophene **IIIB.3** being asymmetrical in nature, there are multiple possibilities of macrocyclization, which can be understood well only by purifying the products obtained from the reaction.

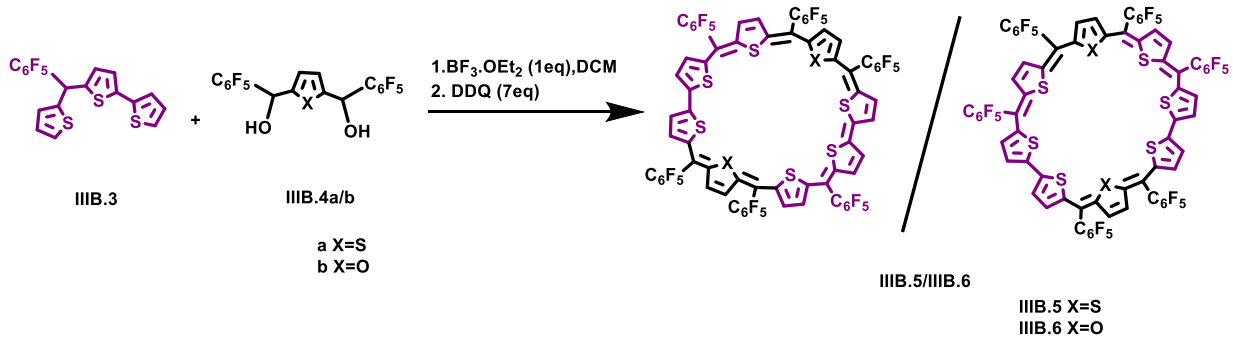

Scheme IIIB.1: *Synthesis of 38π octaphyrins*

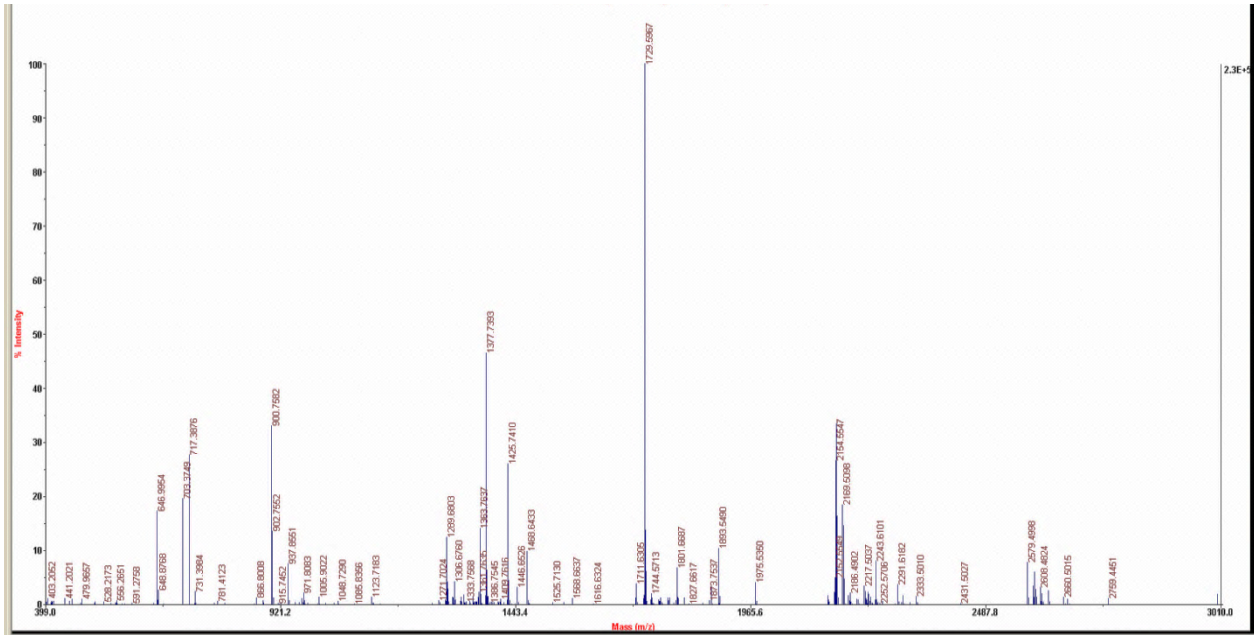

Figure IIIB.3: *MALDI TOF/TOF mass spectrum of the reaction mixture with thiophene diol and tristhiophene*

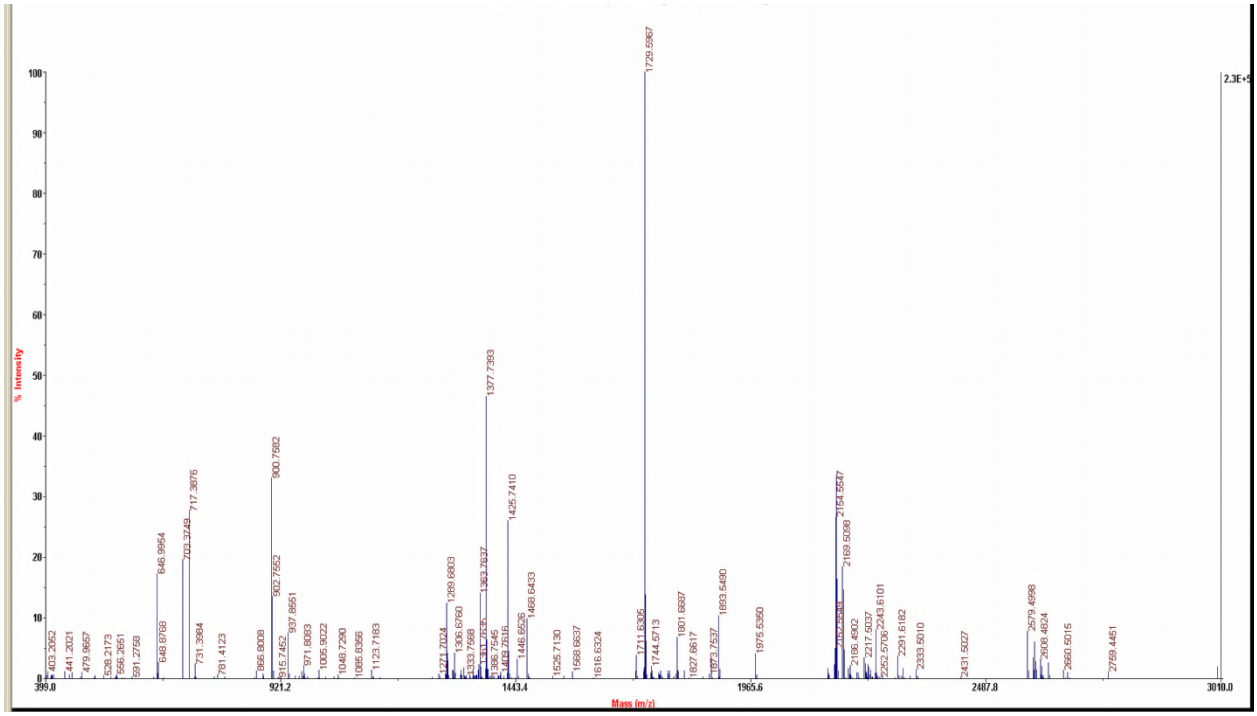

Figure IIIB.4: *MALDI TOF/TOF mass spectrum of the reaction mixture with furan diol and tristhiophene*

IIIB.3 Isolation and characterization of 38π Octaphyrins

IIIB.3.1 Isolation of octaphyrin having all thiophene units (IIIB.5)

After the reaction mixture was filtered through basic alumina column, it was purified using alumina packed glass column with DCM/Hexane as eluent. An intense blue colored band was isolated, which displayed an intense band at 585 nm (256000 ε, $Lmol^{-1}cm^{-1}$) along with another absorption at 428 nm (94500) in its electronic absorption spectrum (Figure IIIB.6). It displayed molecular ion peak at 1729.8518 in its HR-MS spectrum corresponding to $C_{74}H_{16}F_{30}S_8$ compared to the calculated M^+ value for $C_{74}H_{16}F_{30}S_8$ (Figure IIIB.5). No other major product was isolated from the reaction mixture, suggesting the exclusive formation of a single octaphyrin **IIIB.5** in the reaction.

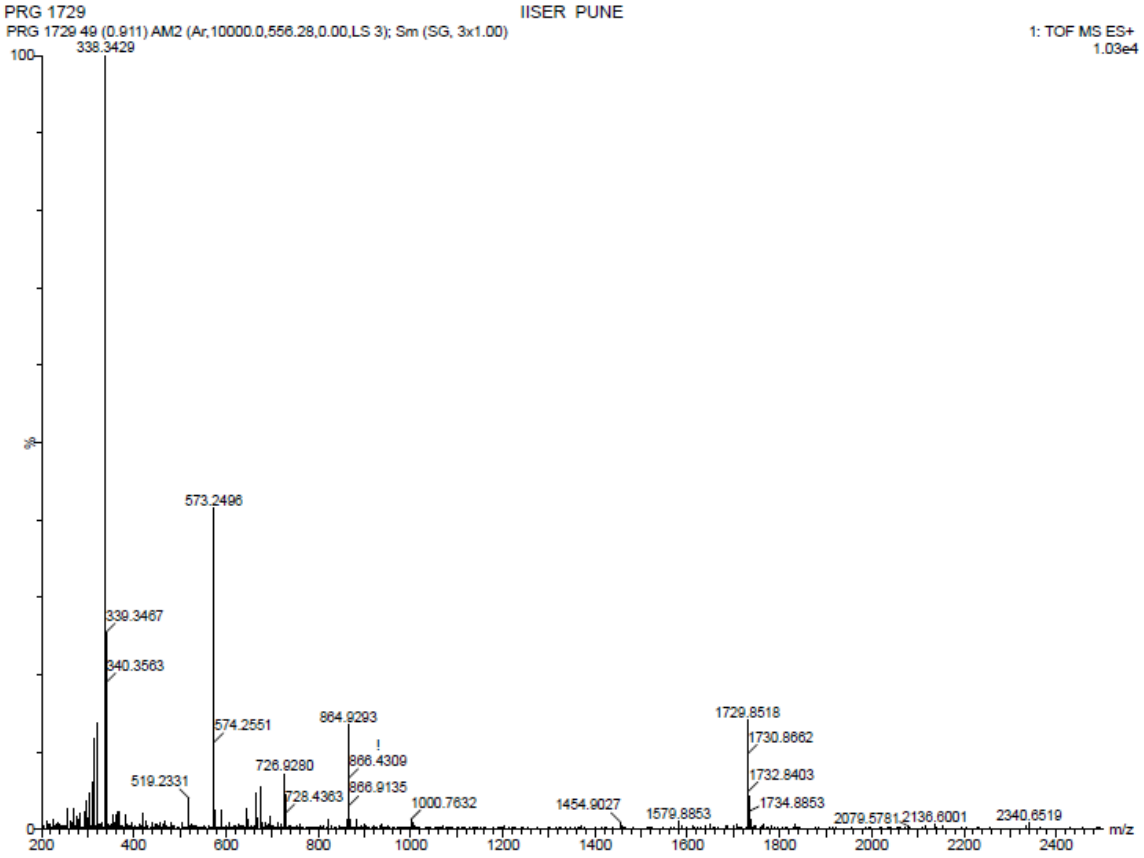

Figure IIIB.5: *HR-MS of* ***IIIB.5***

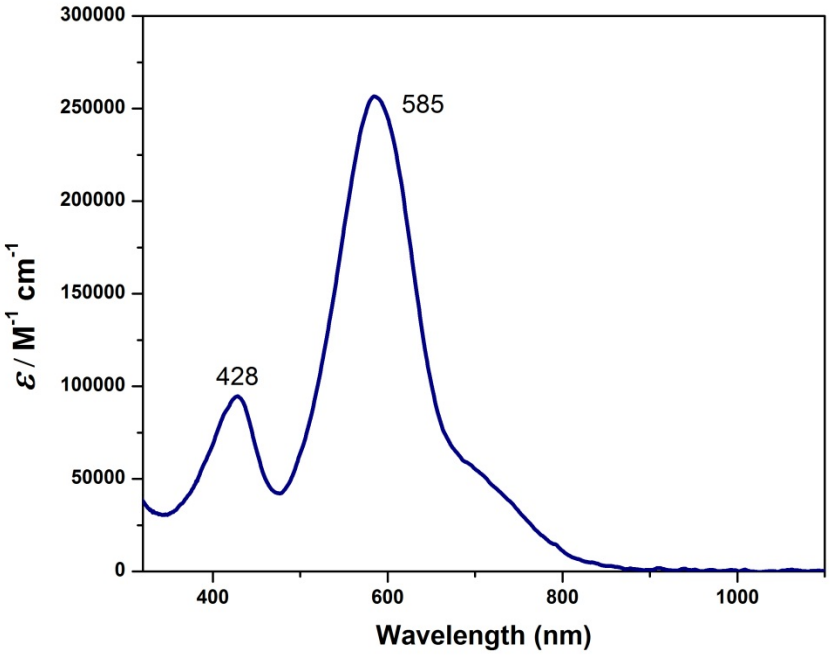

Figure IIIB.6: *Electronic absorption spectrum of* ***IIIB.5*** *recorded in dichloromethane at ~10^{-5}M concentration*

The isolated octaphyrin **IIIB.5** displayed a well resolved ^{1}H NMR spectrum at room temperature. It displayed six signals corresponding to a total of sixteen protons resonating between δ 6.30 and 8.42 ppm. Three doublets with coupling constant of 4 Hz were observed at δ 6.30, 6.44 and 7.40 ppm corresponding to two protons each. Another two doublets with a coupling constant of 8 Hz were observed at δ 7.51 and 7.61 ppm corresponding to four protons and two protons respectively. A doublet of doublet with a coupling constant of 4 Hz resonated at δ 8.38 ppm corresponding to a total of four protons (Figure IIIB.7). The ^{1}H-^{1}H COSY spectrum displayed clear four correlations between the four doublets (Figure IIIB.8).

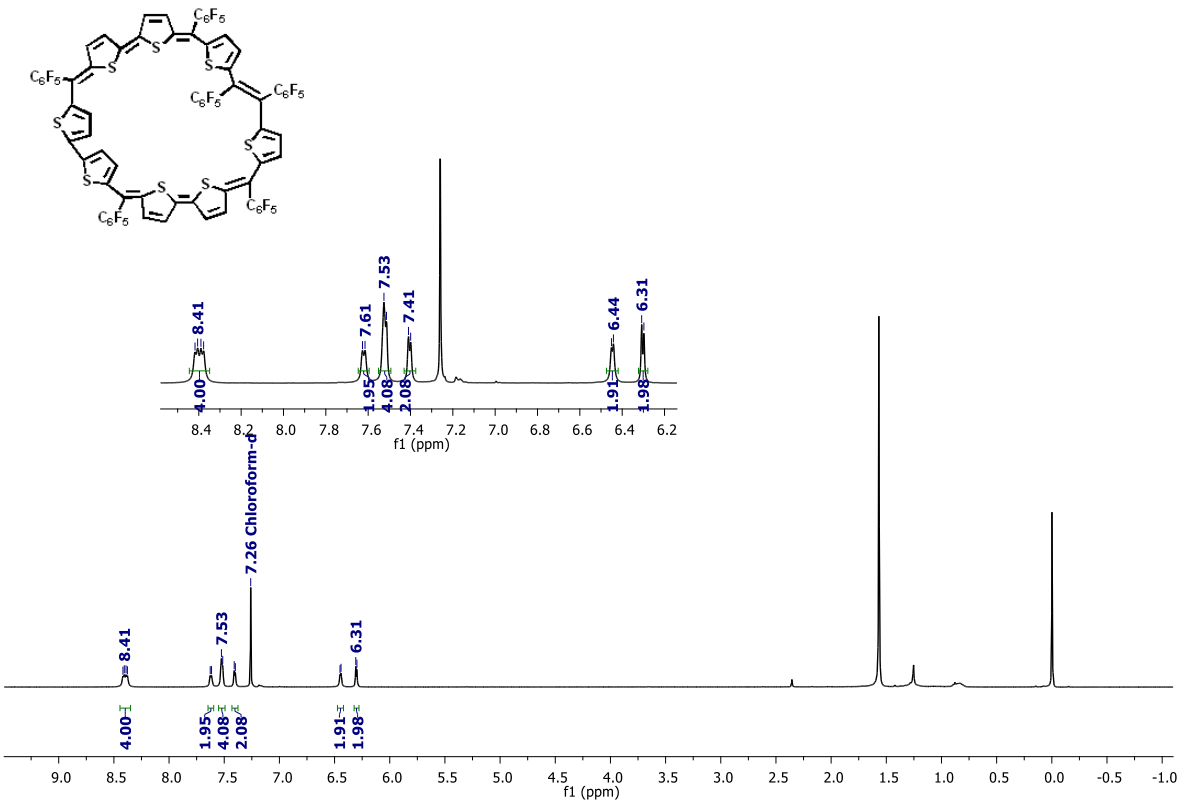

Figure IIIB.7: *Proton NMR spectrum of* ***IIIB.5*** *in $CDCl_3$ at room temperature*

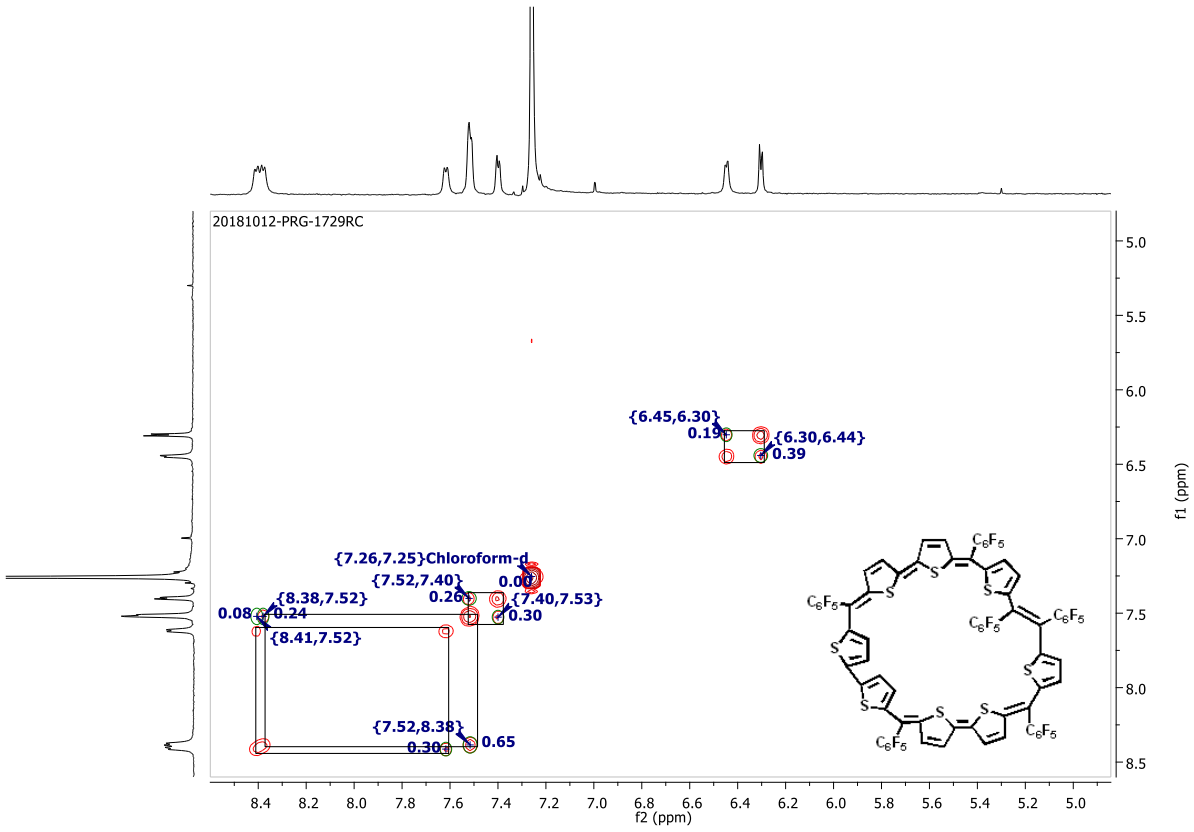

Figure IIIB.8: *^{1}H-^{1}H COSY spectrum of* ***IIIB.5*** *in $CDCl_3$ at room temperature*

Due to the possibility of more than one isomer, the structure of the octaphyrin could not be exactly deduced by spectroscopic results. Hence attempts were made to obtain good quality crystals for the 38π octaphyrin by vapor diffusion of hexane into a solution of **IIIB.5** in dichloromethane.

However X-ray diffraction analysis surprisingly, did not reveal either of the predicted octaphyrin. Instead, the macrocycle identified by (Figure IIIB.9) crystal structure revealed that alike to previously obtained heptaphyrin, two asymmetric tristhiophene underwent α-α coupling at their Head-to-Head position and a simultaneous condensation with thiophene diols on the other end. This serendipitous discovery displayed that the two terminal thiophene diols condensed together probably by elimination of H_2O_2. The structure of the macrocyle was nearly planar with an ethylene bridge formation. Ethylene bridge adopted a *Z* conformation with one

pentafluorophenyl group inside the macrocyclic ring and the other towards outside. Interestingly, this structure also corresponds to the same *m/z* value as of **IIIB.5**.

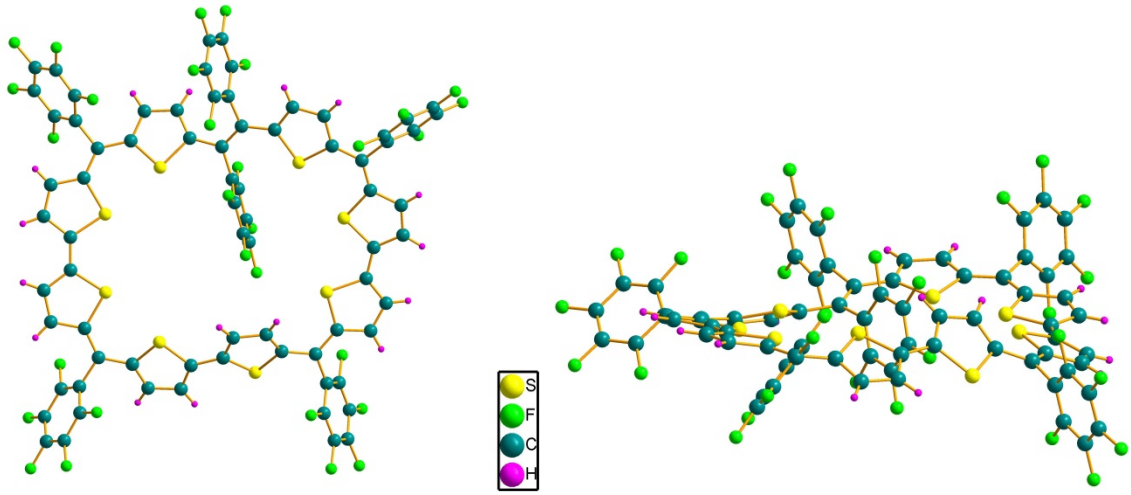

Figure IIIB.9: *Single Crystal X-ray structure [top view(left) and lateral view (right)] of* ***IIIB.5***

IIIB.3.2 Isolation of octaphyrin having two furan units (IIIB.6)

Based on the synthesis of the 38π octathiophene, a similar protocol was followed to with furan diol to obtain a difuran derivative of octaphyrin **IIIB.5**. The asymmetric tristhiophene **IIIB.3** was condensed with furan diol **IIIB.4b** under identical reaction conditions employed for the synthesis of **IIIB.5**. After the reaction mixture was passed through basic alumina column, the resulting solution was concentrated under vacuum. It was further purified over a neutral alumina packed over glass column using DCM/Hexane as the eluent. Surprisingly, two different bands having different R_f values (Figure IIIB.10), were found to display the same molecular *m/z* in MALDI TOF/TOF mass spectrum. This result was further confirmed by HR-MS studies, wherein both the isolated products displayed similar molecular ion peak corresponding to the desired octaphyrin. An intense blue colored band with higher R_f value **IIIB.6a** was isolated in less than one percent yields, displaying an intense absorption at 616 nm (10300 ε, $Lmol^{-1}cm^{-1}$) along with peaks at 379 nm (7100), 499 nm (5390) and 858 nm (3000) in its electronic absorption spectrum (Figure IIIB.11). The octaphyrin displayed

molecular ion peak at 1697.9347 in its HR-MS spectrum corresponding to $C_{74}H_{16}F_{30}S_6O_2$ having a molecular mass of 1697.8995 (Figure IIIB.12).

Figure IIIB.10: *TLC displaying different R_f values of* ***IIIB.6a*** *and* ***IIIB.6b***

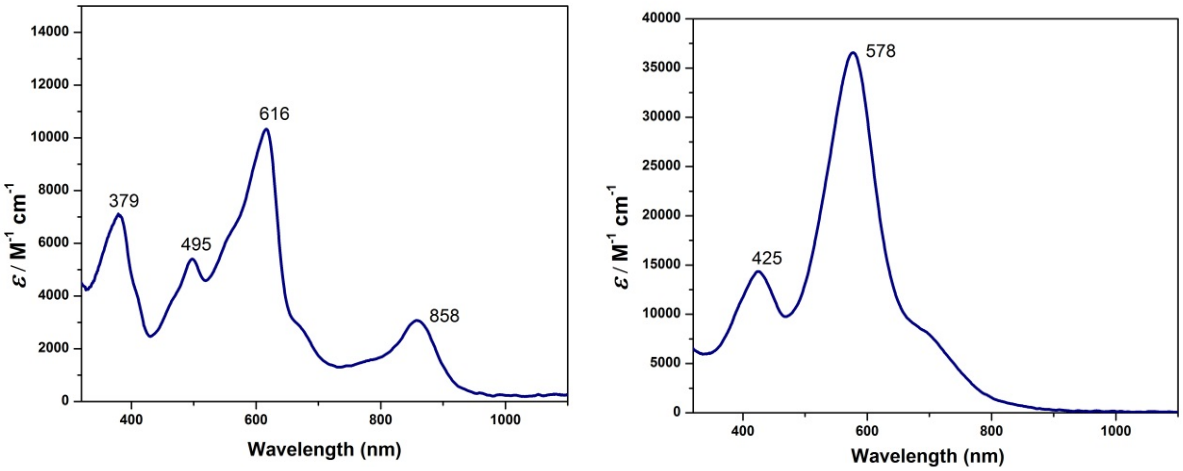

A **B**

Figure IIIB.11: *Electronic absorption spectrum of (A)* ***IIIB.6a*** *and (B)* ***IIIB.6b*** *recorded in dichloromethane at ~10^{-5}M concentration*

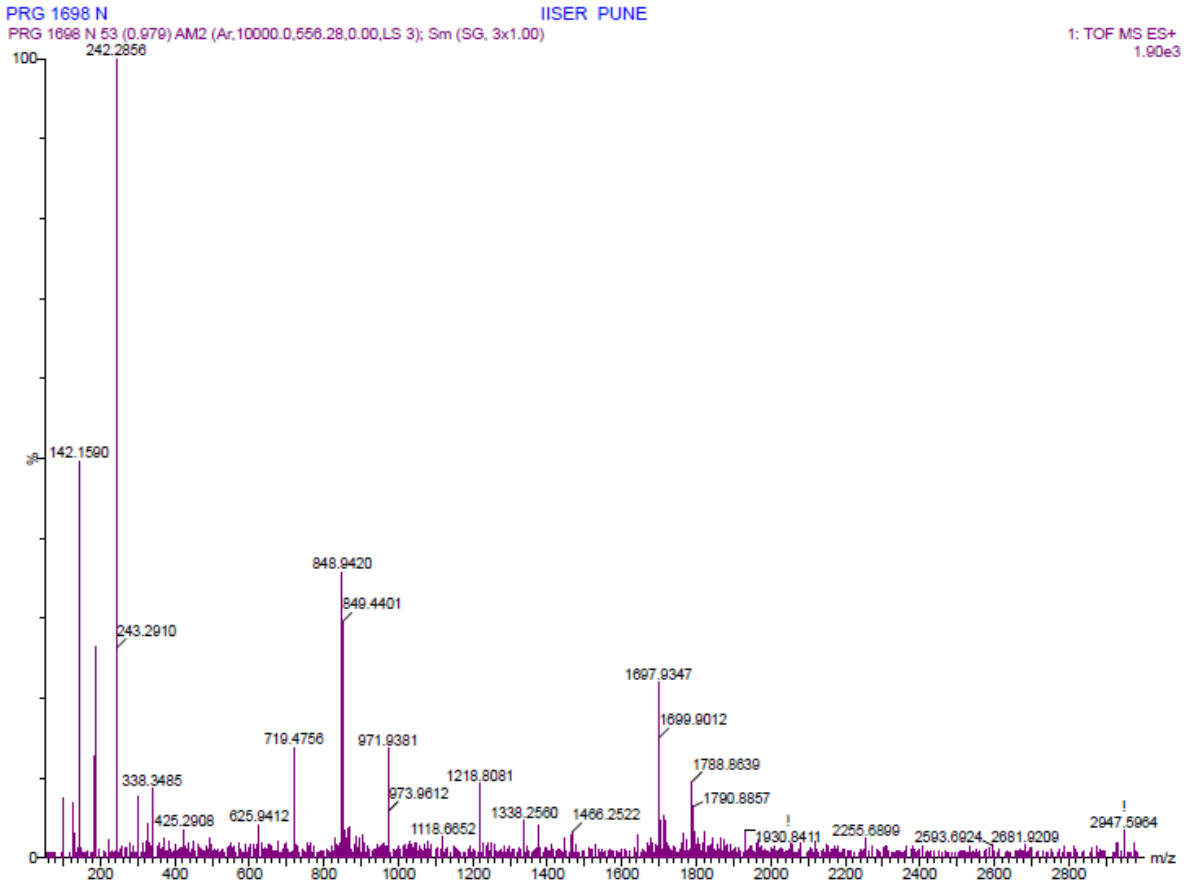

Figure IIIB.12: *HR-MS spectrum of* ***IIIB.6a***

However, the octaphyrin **IIIB.6a** did not display a well resolved proton NMR suggestive of solution state dynamics at room temperature. Well resolved signals were observed upon lowering the temperature to 213 K (Figure IIIB.13).

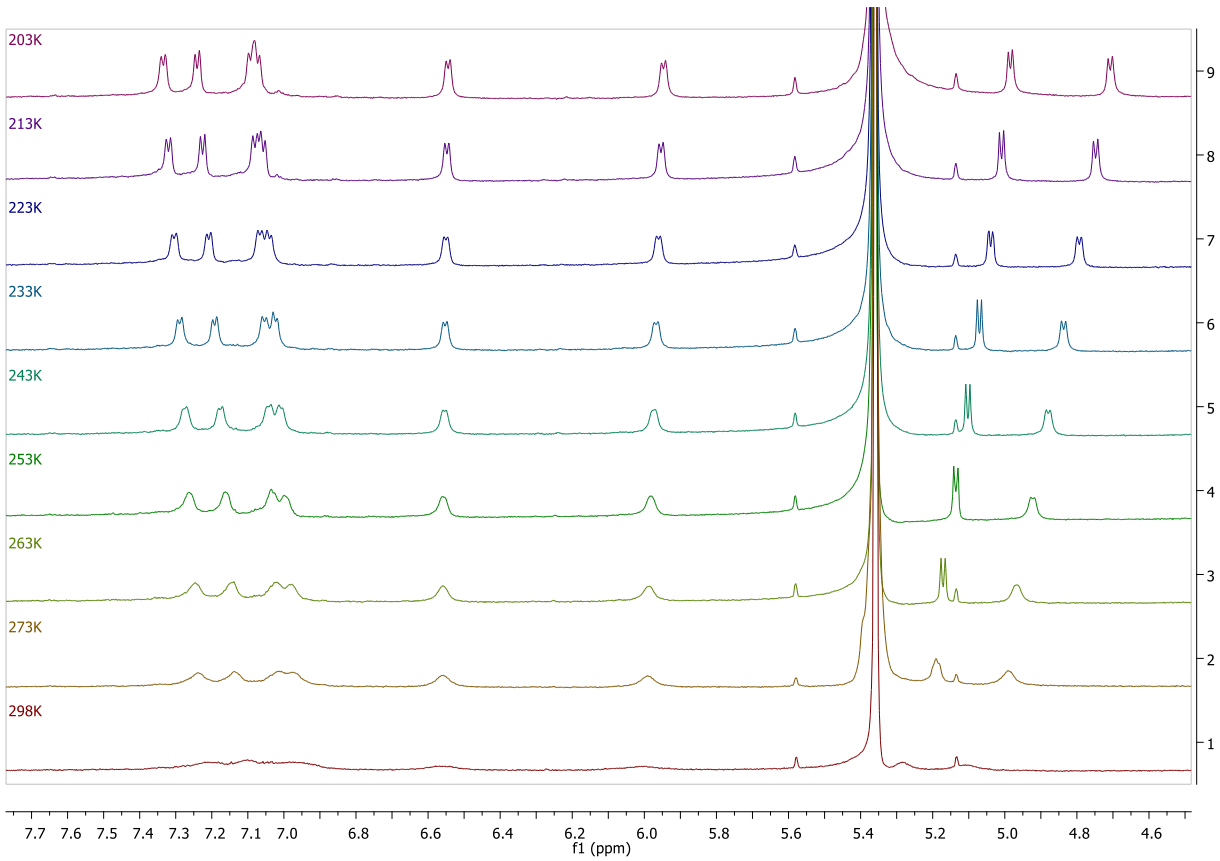

Figure IIIB.13: *Variable temperature proton NMR spectra of* ***IIIB.6a*** *in CD_2Cl_2 from 298K to 203K*

The proton NMR at 213 K displayed seven signals resonating between δ 4.70 and 7.27 ppm. Six doublets corresponding to two protons each resonated with a coupling constant of 4 Hz at δ 4.70, 4.96, 5.91, 6.50, 7.18 and 7.27 ppm. While a doublet of doublet corresponding to four protons with a coupling constant of 4 Hz was observed at δ 7.01 ppm (Figure IIIB.14). This proton NMR suggested the formation of a symmetric octaphyrin. Its ^{1}H-^{1}H COSY spectrum at 213 K displayed three correlations among the doublets (figure IIIB.15). Many attempts were made to elucidate the molecular structure by single crystal X-ray diffraction. However, all attempts went futile to obtain good quality single crystals.

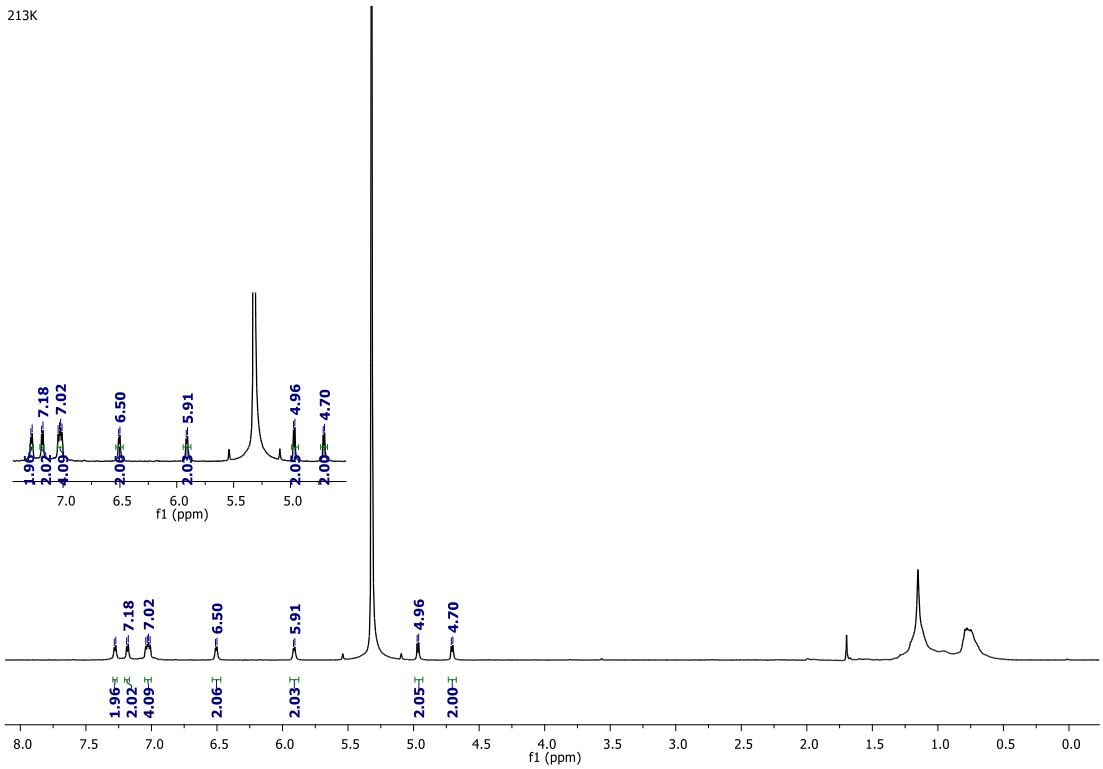

Figure IIIB.14: *Proton NMR spectrum of* ***IIIB.6a*** *in CD_2Cl_2 at 213 K*

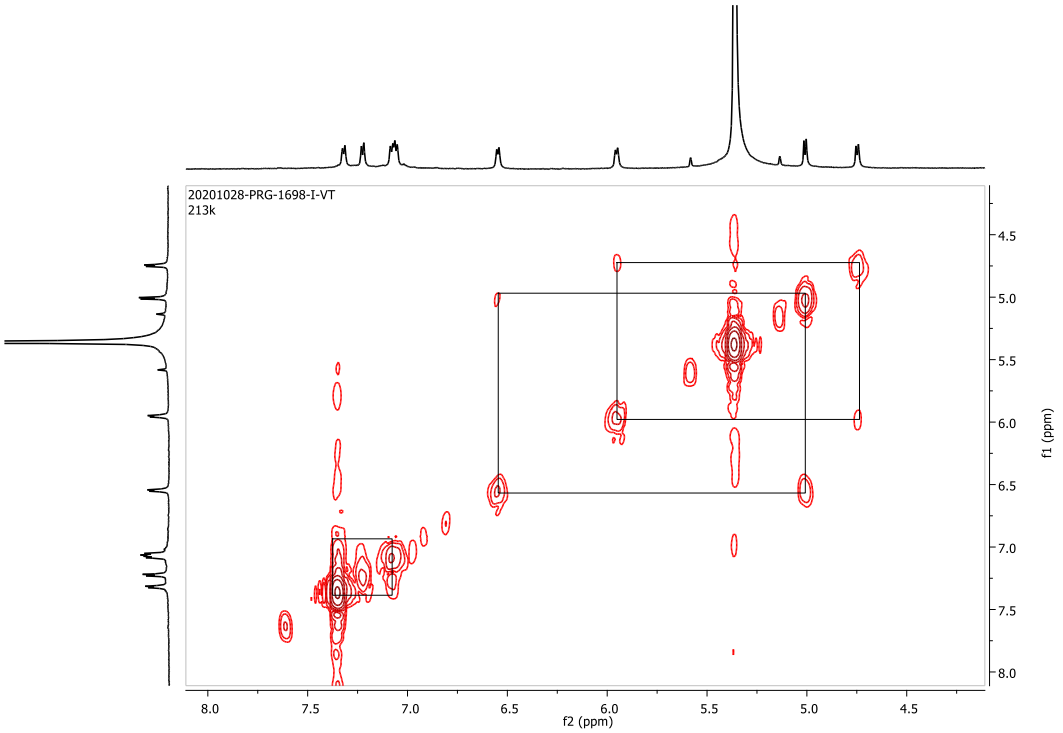

Figure IIIB.15: *^{1}H-^{1}H COSY NMR spectrum of* ***IIIB.6a*** *in CD_2Cl_2 at 213 K*

The second fraction dark violet in color, **IIIB.6b**, was isolated in eight percent yields. It displayed an intense absorption at 578 nm (36500 ε, $Lmol^{-1}cm^{-1}$) along with a peak at 425 nm (14300) in its electronic absorption spectrum (Figure IIIB.11). The macrocycle displayed *m/z* at 1697.9042 in its HR-MS spectrum corresponding to $C_{74}H_{16}F_{30}S_6O_2$ having a molecular mass of 1697.8995 (Figure IIIB.16).

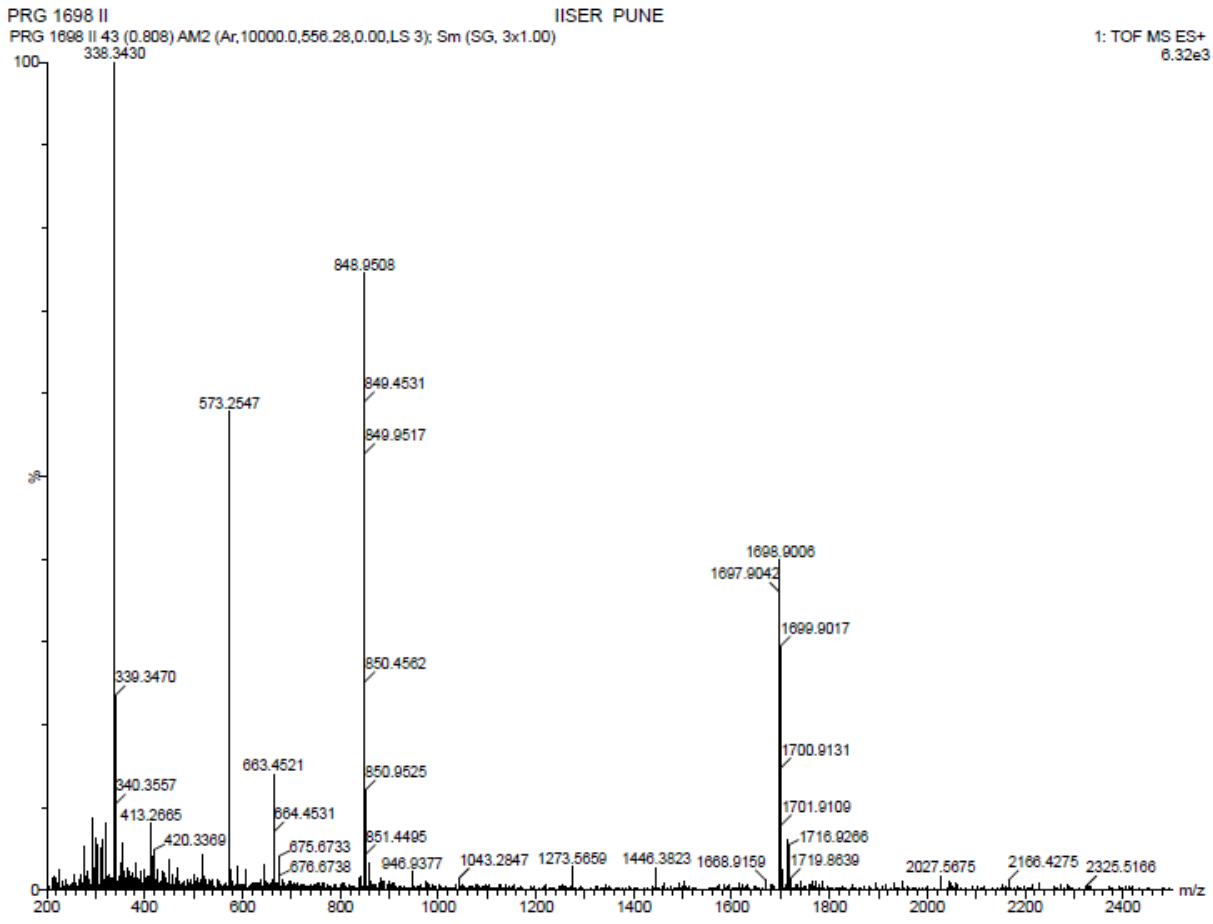

Figure IIIB.16: *HR-MS of* ***IIIB.6b***

Similar to **IIIB.6a**, even this octaphyrin did not display a well resolved proton NMR spectrum at room temperature suggestive of solution state dynamics. Variable temperature NMR studies were performed to obtain a resolved proton NMR spectrum at 233 K (Figure IIIB.18). There were multiple peaks resonating between δ 3.66 and 8.31 ppm corresponding to a total of sixteen protons. An increased number of signals indicated the formation of an unsymmetrical

octaphyrin. Many attempts were made to determine the molecular structure by X-ray diffraction. However, all attempts to grow good quality single crystals went futile and hence the absolute structure of the macrocycle could not be confirmed.

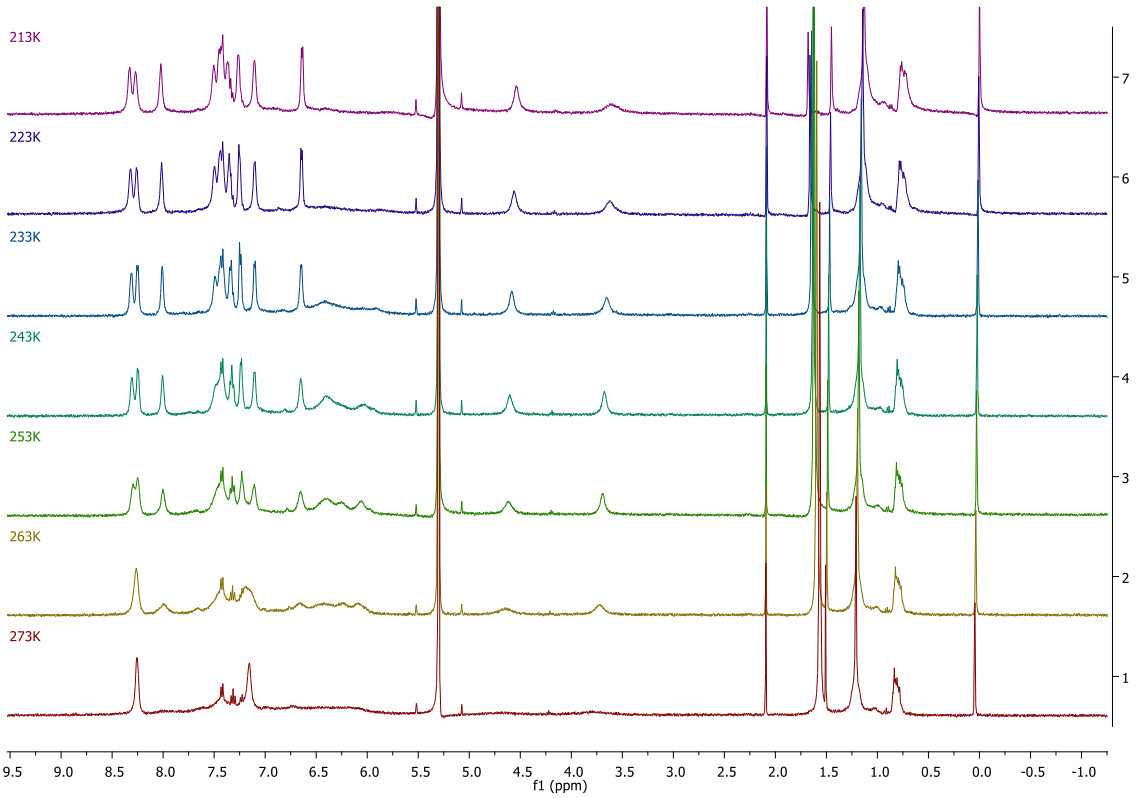

Figure IIIB.17: *Variable temperature proton NMR spectra of* ***IIIB.6b*** *in* CD_2Cl_2 *from 273K to 213K*

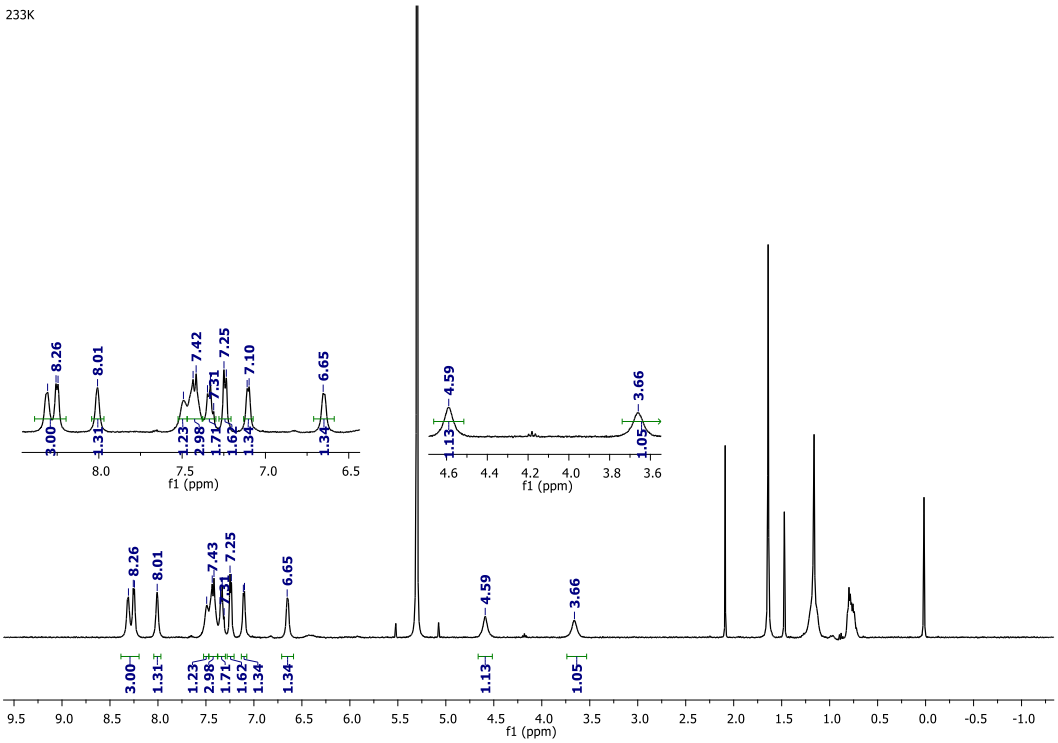

Figure IIIB.18: *^{1}H NMR spectrum of* ***IIIB.6b*** *in CD_2Cl_2 at 233K*

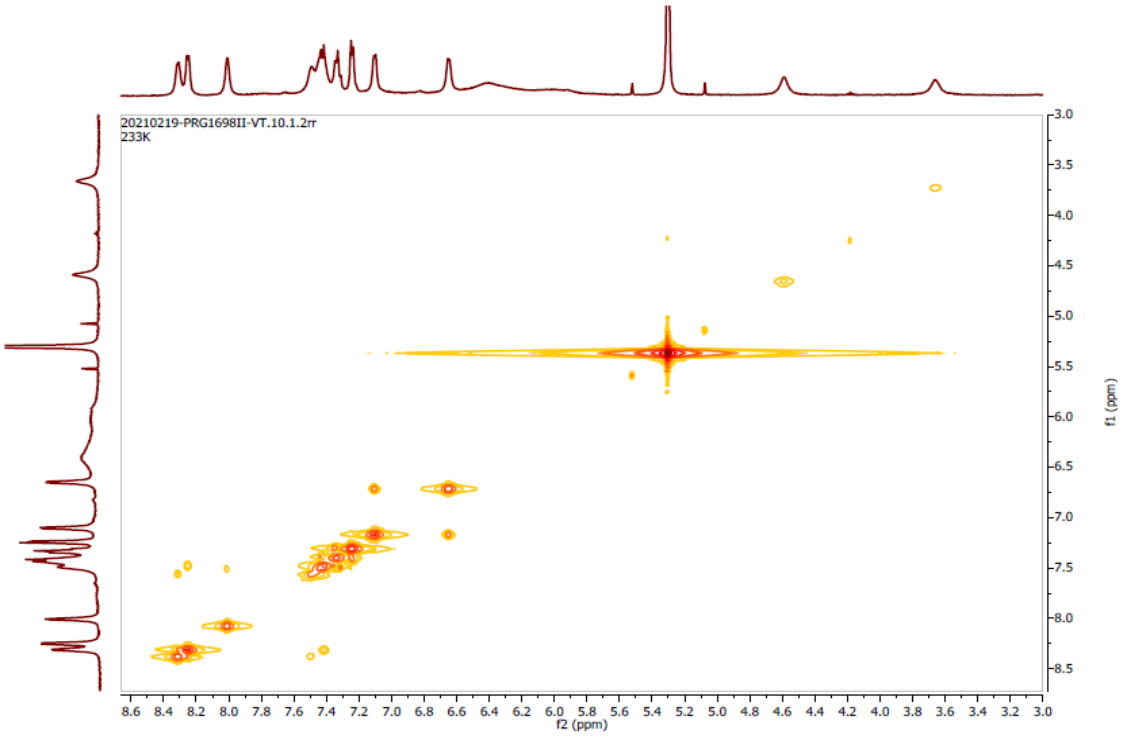

Figure IIIB.19: *^{1}H-^{1}H COSY spectrum of* ***IIIB.6b*** *in CD_2Cl_2 at 233 K*

Nevertheless, a probable structure of **IIIB.6a** and **IIIB.6b** can be proposed based on their respective ^{1}H NMR spectrum. Figure **IIIB.20** displays all the probable structures possible for the macrocycle **IIIB.6**. **IIIB.6a** displayed seven signals in its ^{1}H NMR (Figure IIIB.14) corresponding to a total of sixteen protons suggestive of having a C_2 axis of symmetry present in the macrocycle. Further only three correlations were observed in its ^{1}H-^{1}H COSY spectrum again suggesting the formation of a symmetric macrocycle. The only possible structure of **IIIB.6** which possessed C_2 axis of symmetry is **IIIB.6A** (Figure IIIB.20) indicating the possibility for the formation of **IIIB.6A**. While the ^{1}H NMR for **IIIB.6b** displayed eleven signals suggesting a totally asymmetric octaphyrin formation. Further five correlations could be seen in its ^{1}H-^{1}H COSY spectrum suggesting the formation of an asymmetric macrocycle. This is indicative for the construction of either asymmetric MacDonald condensation product **IIIB.6B** or a novel condensation product with H_2O_2 elimination **IIIB.6C** as observed in the previous case of condensation with thiophene diol leading to formation of **IIIB.5**. However, the proton NMR for **IIIB.6b** displayed two signals corresponding to one proton each at δ 3.66 and 4.59 ppm which were upfield shifted in comparison to the rest of the signals resonating between δ 6.5 and 8.5 ppm suggesting one ring inversion present in the macrocycle. The possible structure for **IIIB.6b** with one ring inversion could be either **IIIB.6D** or **IIIB.6E**. However, it was not possible to decisively conclude the exact structure for the octaphyrin **IIIB.6b** based on the available spectroscopic data.

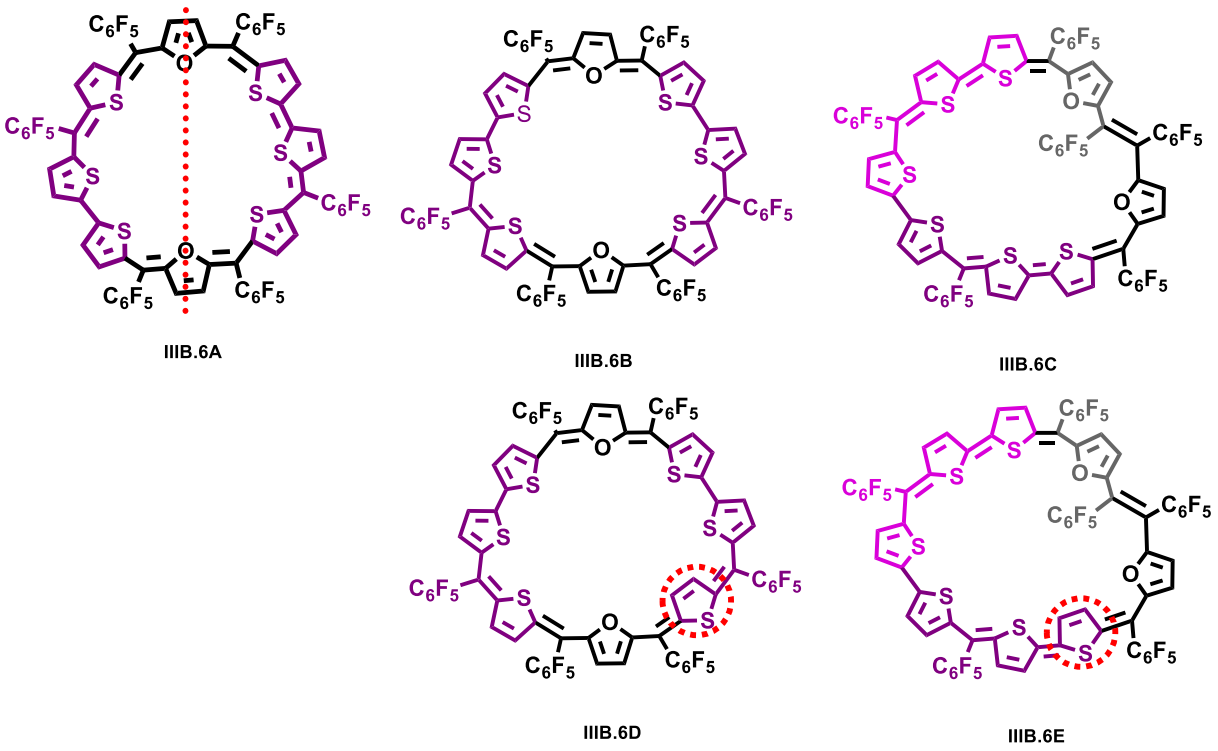

Figure IIIB.20: *Possible structures for the octaphyrin* ***IIIB.6***

Since it was difficult to conclusively deduce the structure of **IIIB.6b**, an attempt was made to modify the macrocycle **IIIB.6** by introducing mesityl group at four of the *meso* positions and explore the possibility of obtaining the crystal structure. Mesityl derivative of furan diol[16] **IIIB.4c** was condensed with asymmetric tristhiophene **IIIB.3** using $BF_3.OEt_2$ followed by DDQ oxidation under similar reaction conditions (Scheme IIIB.2). As the scheme depicts, there still exists the possibility of obtaining three different octaphyrins **IIIB.7a - IIIB.7c** from the same reaction mixture. MALDI TOF/TOF mass spectrum of the reaction mixture confirmed the formation of octaphyrin **IIIB.7** (Figure IIIB.21).

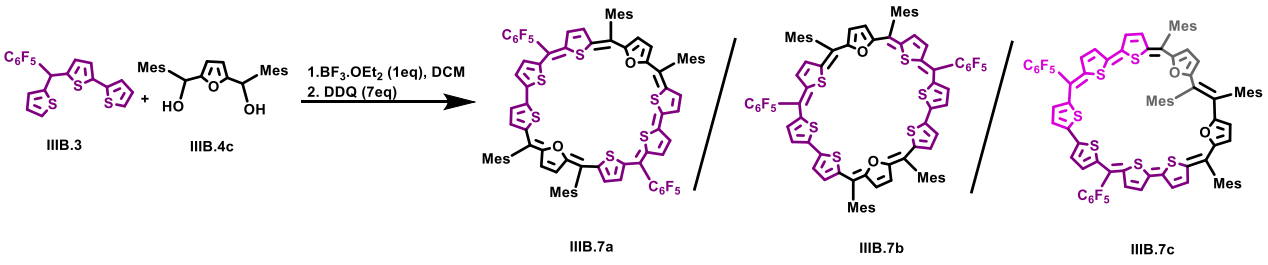

Scheme IIIB.2: *Synthesis of 38π octaphyrins* ***IIIB.7*** *with mesityl group at four meso positions*

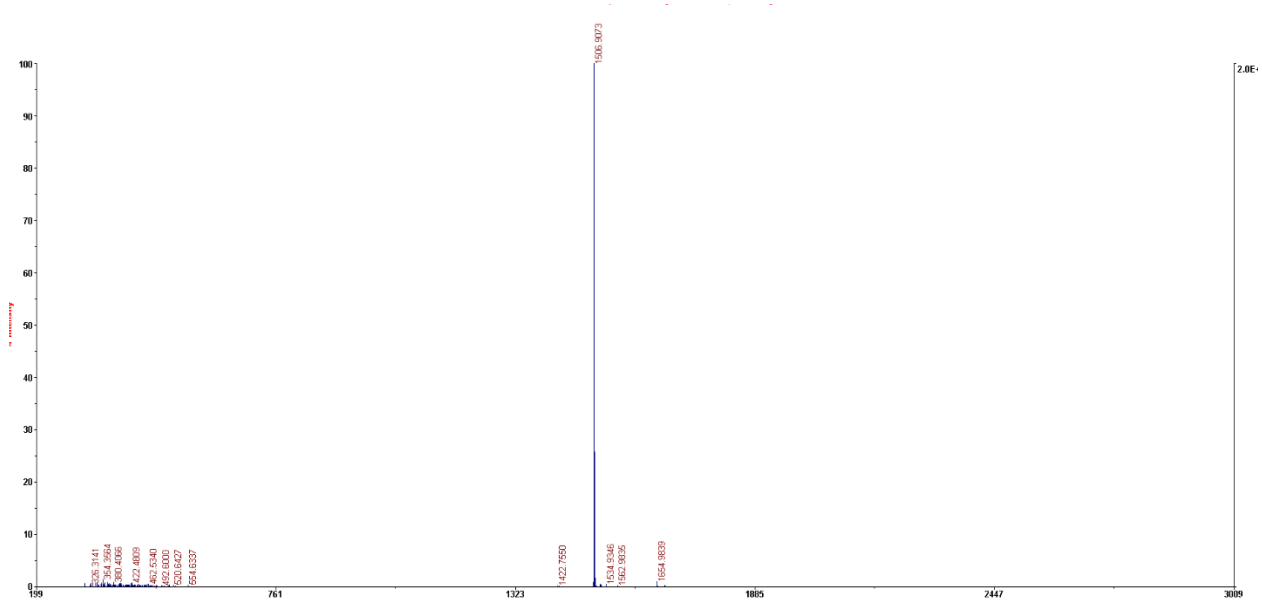

Figure IIIB.21: *MALDI TOF/TOF mass spectrum of the reaction mixture containing* ***IIIB.7***

A similar protocol was followed to isolate the octaphyrin **IIIB.7** using glass column chromatography with DCM/Hexane as eluent. A dark blue band was isolated in eight percent yields which displayed intense band at 611 nm (10300 ε, $Lmol^{-1}cm^{-1}$) along with peaks at 387 nm (3500) and 850 nm (2390) in its electronic absorption spectrum (Figure IIIB.23). The molecule displayed [M+H$^+$] peak at 1507.2810 corresponding to [M+H$^+$] peak for $C_{86}H_{60}F_{10}O_2S_6$ with mass of 1507.2831(Figure IIIB.22). No other band with a similar mass was isolated from this reaction indicating the formation of a single octaphyrin **IIIB.7**.

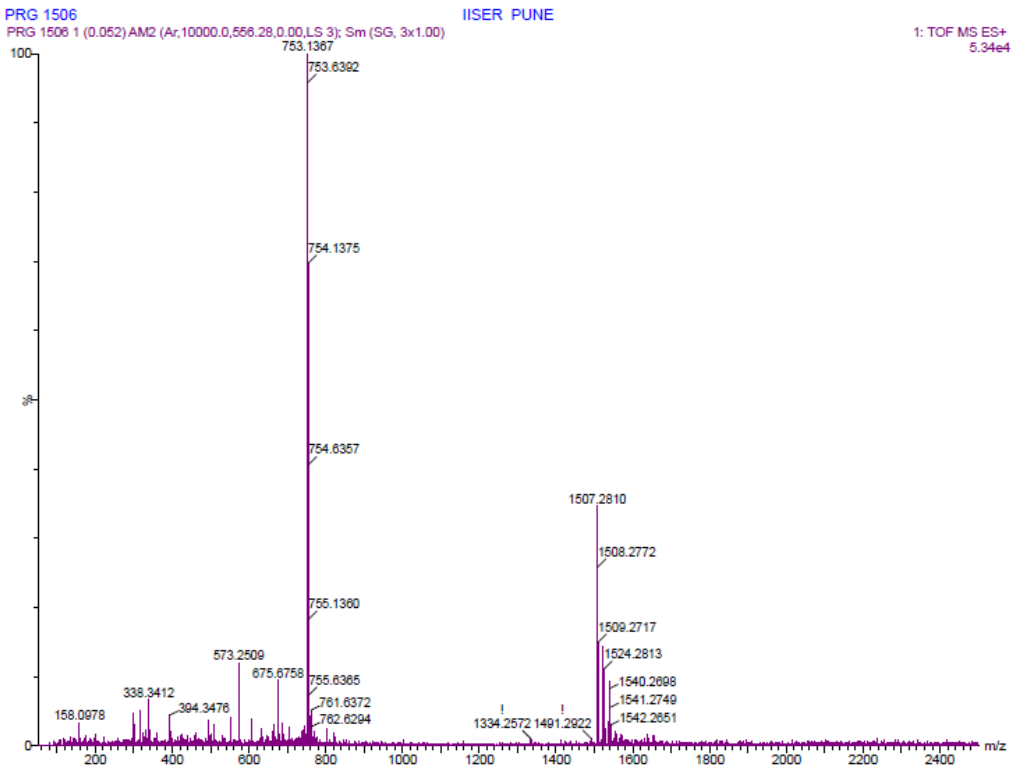

Figure IIIB.22: *HR-MS of* ***IIIB.7***

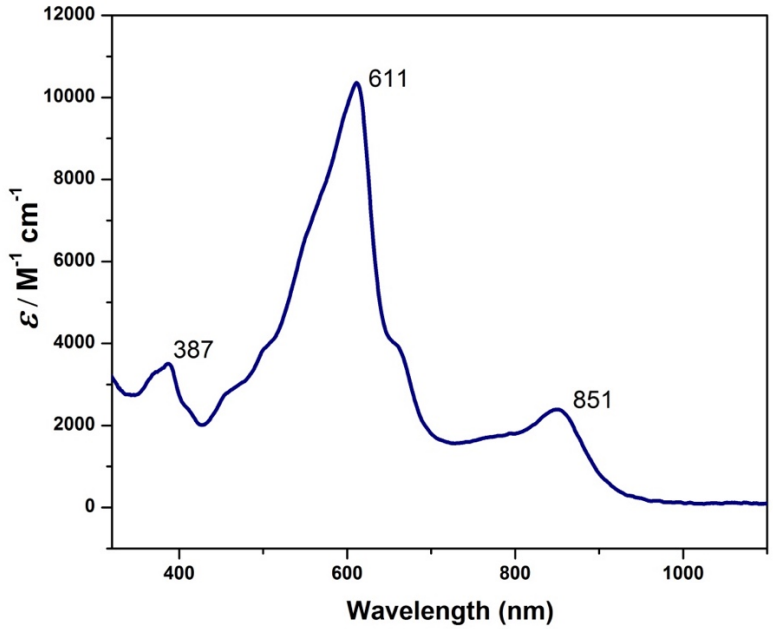

Figure IIIB.23: *Electronic absorption spectrum of* ***IIIB.7*** *in dichloromethane at ~10^{-5}M concentration*

As the macrocycle **IIIB.7** did not display a clear ^{1}H NMR spectrum at room temperature, variable temperature proton NMR spectra was recorded, and a relatively resolved spectrum

was observed at 233 K (Figure IIIB.24). Even at this temperature, the resonances were relatively broad suggesting the poor solubility of the macrocycle at lower temperatures. A total of twenty-four protons were found to resonate between δ 5.0 - 7.5 ppm (Figure IIIB.25). The thirty-six methyl protons of mesityl group resonated between δ 1.5- 2.3 ppm. The ^{1}H-^{1}H COSY spectrum displayed four correlations (Figure IIIB.26).

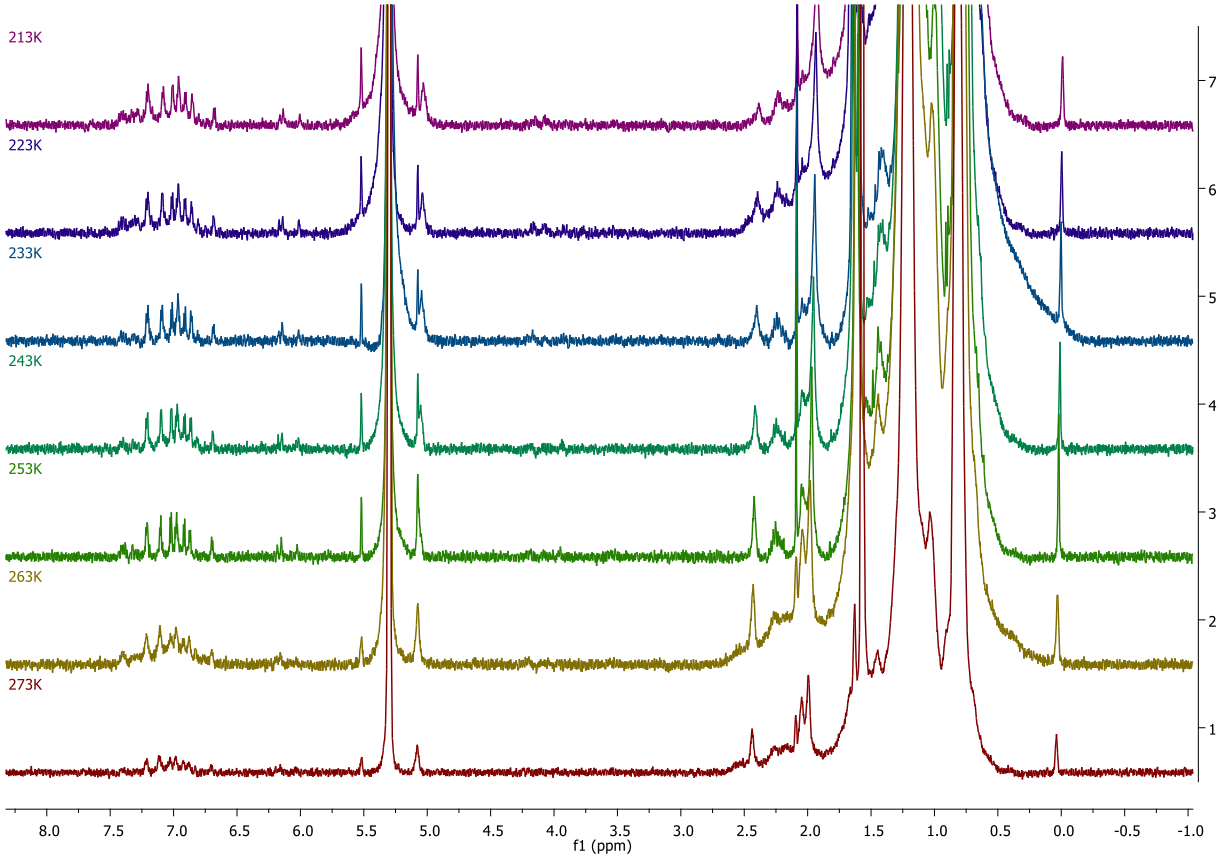

Figure IIIB.24: *Variable temperature proton NMR spectra of* ***IIIB.7*** *in CD_2Cl_2 from 273 K to 213 K*

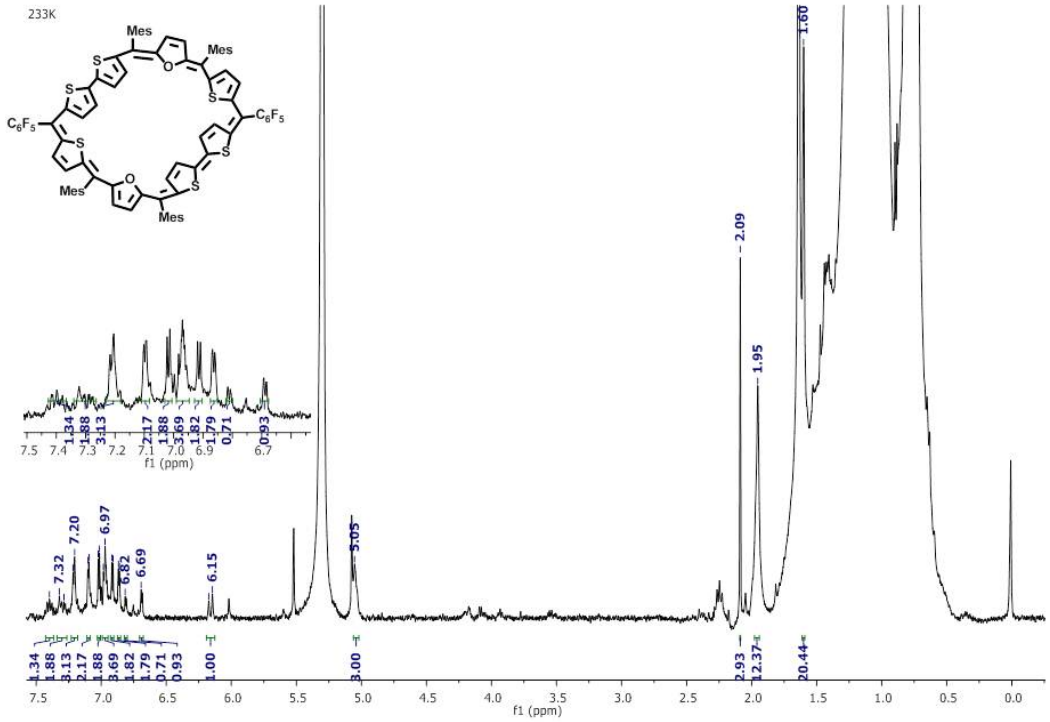

Figure IIIB.25: *^{1}H NMR spectrum of **IIIB.7** in CD_2Cl_2 at 233 K*

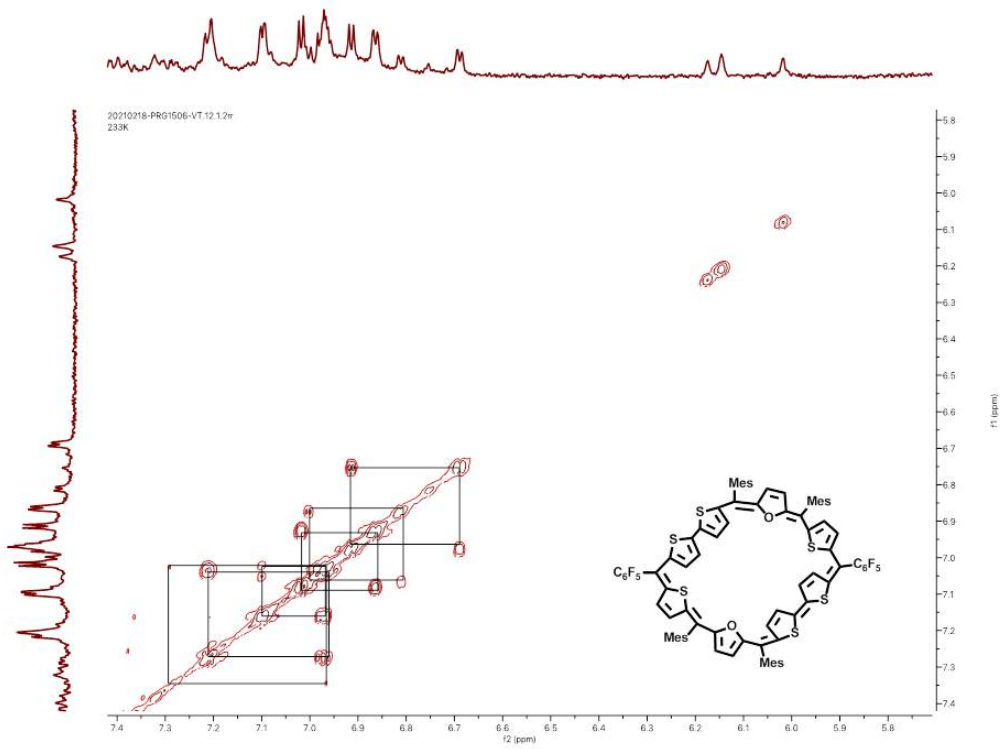

Figure IIIB.26: *^{1}H-^{1}H COSY NMR spectrum of **IIIB.7** in CD_2Cl_2 at 233 K*

However, the main objective to grow good quality crystals for the octaphyrin was achieved by vapor diffusion of hexane into a solution of the **IIIB.7** in chloroform. Unexpectedly, the crystal structure revealed four thiophene ring inversions in **IIIB.7a** (Figure IIIB.27).

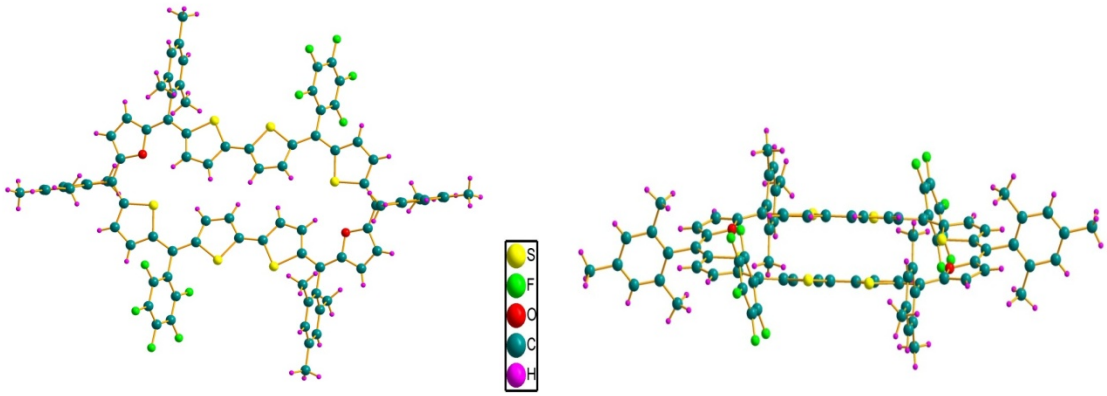

Figure IIIB.27: *Single Crystal X-ray structure [top view(left) and lateral view (right)] of* ***IIIB.7***

Based on the obtained molecular structure and other spectroscopic data, an attempt was made to correlate all the results for the three octaphyrin **IIIB.6a** and **IIIB.6b** with **IIIB.7a**. The electronic absorption spectrum for **IIIB.6a** was similar to that observed for **IIIB.7a**, whereas **IIIB.6a** displayed λ_{max} at 616 nm along with a peak at 858 nm. **IIIB.7a** displayed λ_{max} at 611 nm along with a peak at 851 nm. This result also supports previous assumption for the structure of **IIIB.6a**.

A quick comparison of the electronic absorption spectrum of **IIIB.6b** with that of **IIIB.5**, revealed similar characteristic features. **IIIB.5** displayed λ_{max} at 585 nm along with a peak at 428 nm while **IIIB.6b** displayed λ_{max} at 578 nm along with a peak at 425 nm suggesting a possibility for the formation of rearrangement product **IIIB.6C**.

IIIB.4 Quantum chemical calculations

To measure the aromaticity in all the octaphyrins, quantum chemical calculations were employed using Gaussian09 rev D programme. The structures were optimized using Density

Functional Theory (DFT) with Beckes's three-parameter hybrid exchange function and the lee-Yang-Parr correlation function (B3LYP)[11] and 6-31G(d,p) basis set for all the atoms in the molecule. Then the "Nucleus Independent Chemical Shift" (NICS)[12] value was calculated for these energy optimized structures (Table IIIB.1).

Molecule	NICS(0)	AICD	λ_{max} (nm)	Hückel Aromaticity
IIIB.5	-7.27	Clockwise	500	Aromatic
IIIB.6a	-17.53	Clockwise	616	Aromatic
IIIB.6b	-6.48	Clockwise	498	Aromatic
IIIB.7	-16.57	Clockwise	633	Aromatic

Table IIIB.1: *Quantum chemical calculations of* ***III.5-III.7***

The NICS value was obtained using gauge independent atomic orbital (GIAO)[13] method. NICS(0)[14] was calculated by denoting the global ring center at the non-weighed mean center of the macrocycle. A negative NICS(0) value justified the diatropic ring current effect observed in their respective proton NMR spectrum.

Anisotropy of Induced-Current Density (AICD) provided additional support for the aromatic characteristic features of these macrocycles.[18] It visualizes the ring currents present due to the delocalization of πelectrons. These plots help in viewing the magnitude and direction of the induced ring current when an external magnetic field is applied orthogonal to the plane of the molecule. Continuous set of gauge transformation (CGST) method is employed on the macrocycle which is than visualized using POV-ray 3.7 software. The clockwise direction of arrow suggests the aromatic nature of the molecule, while the anticlockwise direction of arrow suggests the anti-aromatic nature of the macrocycle.

All the octaphyrins **IIIB.5**-**IIIB.7** displayed clockwise direction of arrows in their AICD plot suggesting the aromatic nature of the molecule (Figure IIIB.28).

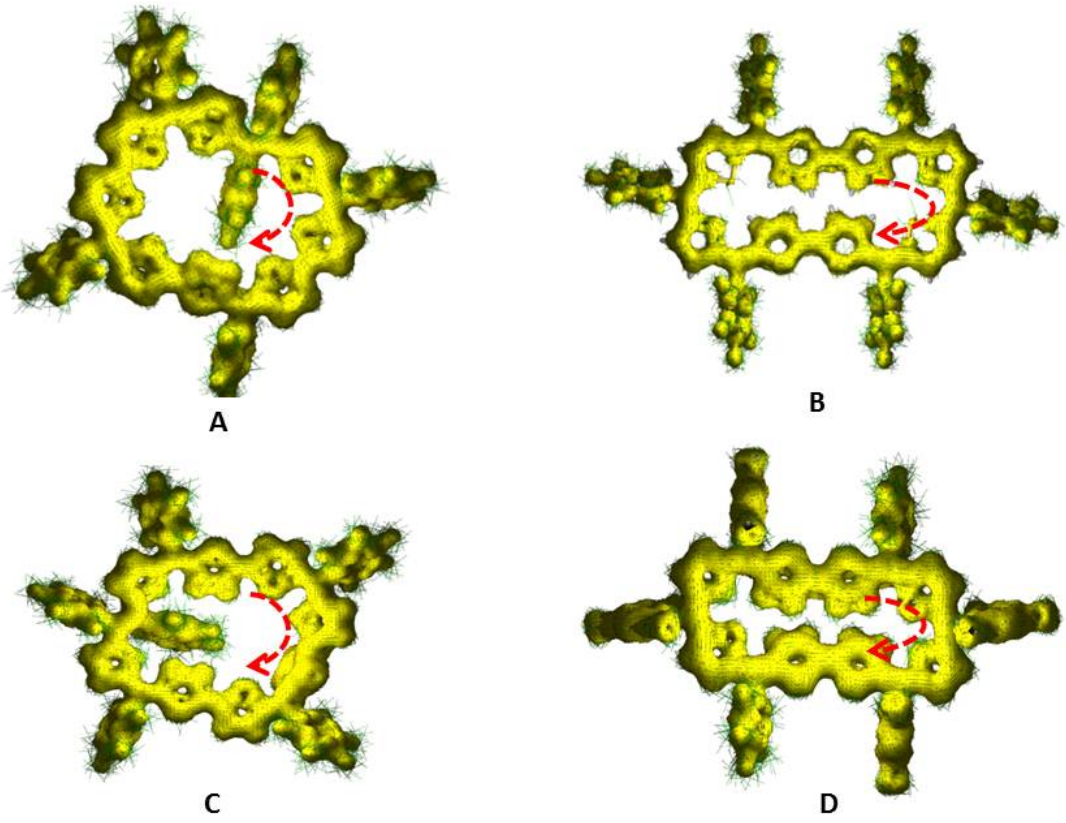

Figure IIIB.28: *AICD plot of A)* ***IIIB.5****, B)* ***IIIB.6a****, C)* ***IIIB.6b****, D)* ***IIIB.7***

Further, steady-state absorption spectra were studied using Time Dependent TD-DFT calculations. The calculated TD-DFT spectrum for the possible structures of **IIIB.6a** and **IIIB.6b** were similar to the observed experimental electronic absorption spectrum further in support of the proposed structures for **IIIB.6a** and **IIIB.6b** (Figure IIIB.29).

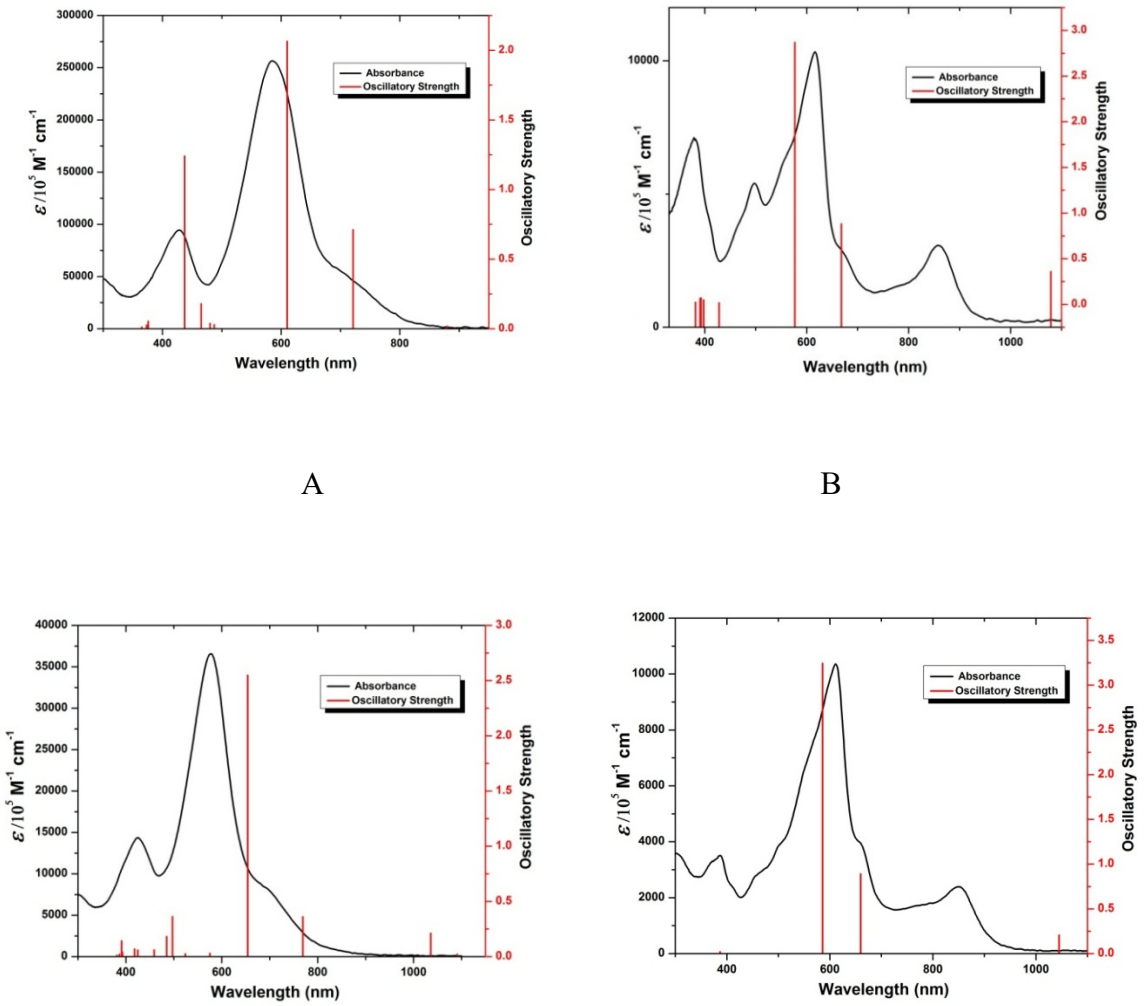

Figure IIIB.29: *TD-DFT plot of A)* ***III.5****, B)* ***III.6a****, C)* ***III.6b*** *and D)* ***III.7***

IIIB.5 Conclusions

In this section of Chapter 3, different 38π octaphyrins were synthesized successfully. Serendipitously, a novel condensation product of asymmetric tristhiophene **IIIB.3** with thiophene diol **IIIB.4a** was identified. Two asymmetric tristhiophene **IIIB.3** units underwent α-α coupling at its Head-to-Head position along with an ethylene bridge formation by an unusual condensation of two thiophene diols together with a possibility of H_2O_2 elimination. In addition, for the very first time two different structural isomers of the same 38π octaphyrin

containing two furan units in the macrocylic core having all the pentafluoro substituents at its bridging position were successfully isolated. It was also observed that the meso substituent was crucial to the nature of the cyclisation product. Changing the bridging unit from pentafluorophenyl to mesityl group, exclusively yielded only one isomer of the 38π octaphyrin. Though the structure for two of the octaphyrins could not be deduced, the possible structures were predicted using proton NMR and the studies were by justified by quantum chemical and TD-DFT calculations.

IIIB.6 Experimental section

Asymmetric tristhiophene **IIIB.3** and corresponding diol **IIIB.4** was dissolved in one is to one ratio in 180 mL of dry dichloromethane and degassed with nitrogen for five minutes. Then the round bottom flask containing the solution was covered with aluminum foil to maintain dark conditions. To this mixture, one equivalent of $BF_3.OEt_2$ was added and stirred the solution for two hours maintaining the dark and inert conditions. After two hours the reaction mixture was subjected to five equivalents of dichlorodicyanoquinone (DDQ) and stirred for four hours. Finally, the reaction mixture was passed through basic alumina column and purified using alumina column.

Synthetic procedure of IIIB.5

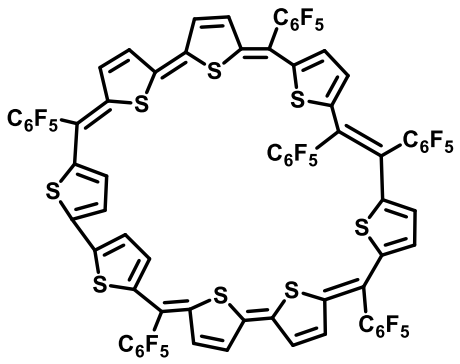

A clean dried 250 mL round bottom flask was charged with compound **IIIB.3** (107 mg, 249.74 μmol). To this compound **IIIB.4a**[15] (118.95 mg, 249.74 μmol) was added and 180 mL of dry dichloromethane was added. The solution was nicely stirred and maintained under dark and inert condition. To this reaction mixture, $BF_3.OEt_2$ (249.74 μmol, 0.03 mL) was added slowly and stirred further for two hours. Subsequently after two hours, dichlorodicyanoquinone (340 mg, 1.5 mmol) was added to the reaction mixture and stirred further for four hours. The reaction mixture was filtered through basic alumina column and purified on a neutral alumina glass column. The major fraction obtained was an eight membered, 40π octaphyrin isolated in 9% yield. The molecule was completely characterized using the HR-MS and spectroscopic techniques.

HR-MS (ESI) m/z: $[M+H]^+$Calcd. for $C_{88}H_{36}F_{20}O_4S_4$-1665.1255; Found -1665.1107

UV-Vis (CH_2Cl_2): λ_{max} nm (ε, $Lmol^{-1}cm^{-1}$): 587 nm (9.3×10^4), 406 nm (1.3×10^5)

^1H NMR (400 MHz, $CDCl_3$) δ: 8.40 (dd, *J* = 4 Hz, 4H), 7.62 (d, *J* = 8 Hz, 2H), 7.52 (d, *J* = 8 Hz, 4H), 7.40 (d, *J* = 4 Hz, 2H), 6.45 (d, *J* = 4 Hz, 2H), 6.30 (d, *J*= 4 Hz, 2H).

Selected Crystal data: triclinic, space group P -1, a = 12.874, b = 23.833, c = 24.769 Å, α = 90.004, β = 90.00, γ = 101.658, V= 7443Å^3, T= 120 K, D_{cal} = 1.930 gcm^{-3}, R_1 = 0.1148, wR_2 = 0.4088, GOF = 0.872

Synthetic procedure of IIIB.6a- IIIB.6b

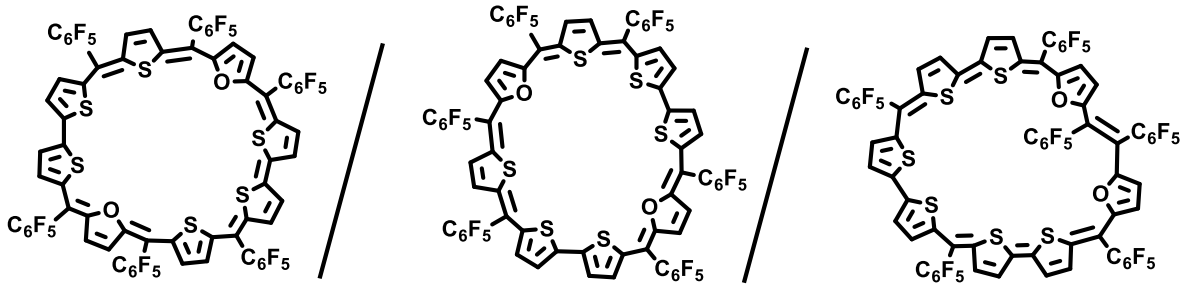

In a clean and dried 250 mL round bottom flask, **IIIB.3** (107 mg, 249.74 μmol) and **IIIB.4b**[15] (114.94 mg, 249.74 μmol) were dissolved in 180 mL of dry dichloromethane. The solution was stirred under dark and inert atmosphere. To this solution $BF_3.OEt_2$ (249.74 μmol, 0.03 mL) was added slowly and stirred under dark and inert conditions for two hours. Later, the reaction was oxidized using dichlorodicyanoquinone (500 mg, 3 mmol) and stirred further for additional four hours. The reaction mixture was filtered through basic alumina column and purified on a neutral alumina glass column. **III.6a** was isolated as an intense blue colored band in 1% yields and **III.6b** was isolated as an intense purple colored band in 8% yields. Both the molecules were fully characterized using HR-MS and spectroscopic techniques

Spectral data for IIIB.6a

HR-MS (ESI) m/z: $[M]^+$Calcd. for $C_{74}H_{16}F_{30}S_6O_2$-1697.8995; Found -1697.9347

UV-Vis (CH_2Cl_2): λ_{max} nm (ε, $Lmol^{-1}cm^{-1}$): 616 nm (10300 ε, $Lmol^{-1}cm^{-1}$), 379 nm (7100), 499 nm (5390) and 858 nm (3000)

^1H NMR (400 MHz, CD_2Cl_2) δ: 7.28 (d, J = 4 Hz, 2H), 7.18 (d, J = 4 Hz, 2H), 7.03 (dd, J = 4 Hz, 4H), 6.51 (d, J = 4 Hz, 2H), 5.91 (d, J = 4 Hz, 2H), 4.97 (d, J = 4 Hz, 2H), 4.71 (d, J = 4 Hz, 2H).

Spectral data for IIIB.6b

HR-MS (ESI) m/z: $[M]^+$Calcd for $C_{74}H_{16}F_{30}S_6O_2$ -1697.8995; Found -1697.9042

UV-Vis (CH_2Cl_2): λ_{max} nm (ε, $Lmol^{-1}cm^{-1}$): 578 nm (36500ε, $Lmol^{-1}cm^{-1}$), 425 nm (14300)

^1H NMR (400 MHz, CD_2Cl_2) δ: 8.39-8.20 (m, 3H), 8.01 (s, 1H), 7.49 (s, 1H), 7.43 (d, J = 4 Hz, 3H), 7.33 (t, J = 8 Hz, 2H), 7.24 (d, J = 8 Hz, 2H), 7.10 (d, J = 4 Hz, 1H), 6.65 (s, 1H), 4.59 (s, 1H), 3.66 (s, 1H).

Synthetic procedure of IIIB.7

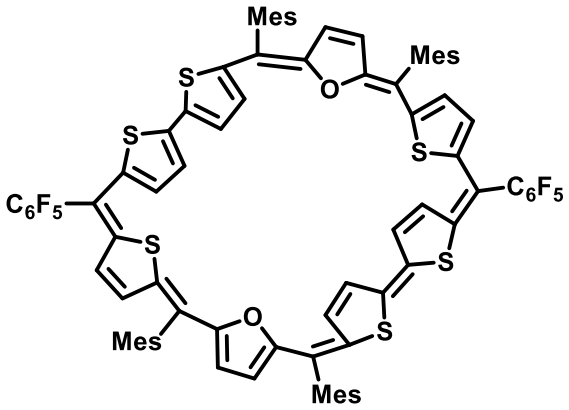

In a clean and dried 250 mL round bottom flask, **IIIB.3** (107 mg, 249.74 μmol) and **IIIB.4c**[16] (91.02 mg, 249.74 μmol) were dissolved in 180 mL of dry dichloromethane. The solution was stirred under dark and inert atmosphere. To this solution $BF_3.OEt_2$ (249.74 μmol, 0.03 mL) was added slowly and stirred under dark and inert conditions for two hours. Later, the reaction was oxidized using $FeCl_3$ (243.04 mg, 1.5 mmol) and stirred further for additional two hours. The reaction mixture was filtered through basic alumina column and purified on a neutral alumina glass column. **IIIB.7** was isolated as an intense blue colored band in 6% yield.

HR-MS (ESI) m/z: $[M+H]^+$Calcd. for $C_{86}H_{60}F_{10}O_2S_6$ -1507.2831; Found -.1507.2810

UV-Vis (CH_2Cl_2): λ_{max} nm (ε, $Lmol^{-1}cm^{-1}$): 611 nm (10300 ε, $Lmol^{-1}cm^{-1}$), 387 nm (3500) and 850 nm (2390)

^1H NMR (400 MHz, CD_2Cl_2) δ: 7.21 (d, J = 4.0 Hz, 3H), 7.10 (d, J = 4.0 Hz, 3H), 7.02 (d, J = 4.0 Hz, 2H), 6.98 (d, J = 4.0 Hz, 4H), 6.91 (d, J = 4.0 Hz, 2H), 6.86 (d, J = 4.0 Hz, 2H), 6.82 (d, J = 4.0 Hz, 1H), 6.69 (s, 1H), 6.16 (d, J = 8.0 Hz, 1H), 5.05 (s, 3H), 2.09 (s, 3H), 1.95 (s, 13H), 1.60 (s, 20H).

Selected Crystal data: triclinic, space group P-1, a = 12.502, b = 15.225, c = 24.893 Å, α = 104.999, β = 98.237, γ = 96.839, V= 4467.5 $Å^3$, T= 120 K, D_{cal} = 1.437 gcm^{-3}, R_1 = 0.3658 , wR_2 = 0.7750 , GOF = 3.341

Crystal Parameters	**IIIB.5**	**IIIB.7**
Crystal System	Triclinic	Triclinic
Space group	P-1	P-1
a (Å)	12.874 Å	12.502 Å
b (Å)	23.833 Å	15.225 Å
c (Å)	24.769 Å	24.893 Å
α	90.004	104.999
β	90.00	98.237
γ	101.658	96.839
Volume ($Å^3$)	7443 $Å^3$	4467.5 $Å^3$
T	120 K	120 K
Z	2	2
Density calculated (gcm^{-3})	1.930 gcm^{-3}	1.437 gcm^{-3}
F(000)	4320.0	1964.0
Absorption coefficient	1.080 mm^{-1}	0.579 mm^{-1}
Reflections reported	36293	22510
Theta (max)	28.403	28.577
Goodness-of-fit on F^2	0.872	3.341
R_1	0.1148	0.3658
wR_2	0.4088	0.7750

Table IIIB.2*: Selected Crystal data for* ***IIIB.5*** *and* ***IIIB.7***

IIIB.7 References

(1) Shivran, N.; Gadekar, S. C.; Anand, V. G., *Asian Journal of Organic Chemistry* **2017**, *12* , 6-20.

(2) Seidel, D.; Lynch, V.; Sessler, J. L *Angew. Chem., Int. Ed.***2002**, *41*, 1422-1425.

(3) Bröring, M.; Jendrny, J.; Zander, L.; Schmickler, H.; Lex, J.; Wu, Y. D.; Nendel, M.; Chen, J.; Plattner, D. A.; Houk, K. N.; Vogel, E. *Angew. Chem., Int. Ed. Engl*. **1995**, *34*, 2515−251.

(4) Taniguchi, R.; Shimizu, S.; Suzuki, M.; Shin, J. Y.; Furuta, H.; Osuka, A. *Tetrahedron Lett*. **2003**, *44*, 2505−2507.

(5) Reddy, J. S.; Mandal, S.; Anand, V. G. *Org. Lett.* **2006**, *8*, 5541-5543.

(6) Sprutta, N.; Latos-Grazynski, L. *Chem. Eur. J.* **2001**, *7*, 5099-5112.

(7) Arsenault, G. P.; Bullock, E.; MacDonald, S. F. *J. Am. Chem. SOC.* **1960**, *82*, 4384-4389.

(8) Won-Seob, C.; Chang-Hee, L. *Bull Korean Chem Soc.***1998**, *19*, 314-318

(9) Singh, K.; Sharma, S.; Sharma, A. *J. Mol. Catal. A: Chem*. **2011**, *347*, 34-37.

(10) Rathore, R.; Kumar, A. S.; Lindeman, S. V.; Kochi, J. K. *J. Org. Chem.* **1998**, *63*, 5847-5856.

(11) Gaussian 09; Revision A.2; Frisch, M. J.; Trucks, G. W.; Schlegel, H. B.; Scuseria, G. E.; Robb, M. A.; Cheeseman, J. R.; Scalmani, G.; Barone, V.; Mennucci, B.; Petersson, G. A.; Nakatsuji, H.; Caricato, M.; Li, X.; Hratchian, H. P.; Izmaylov, A. F.; Bloino, J.; Zheng, G.; Sonnenberg, J. L.; Hada, M.; Ehara, M.; Toyota, K.; Fukuda, R.; Hasegawa, J.; Ishida, M.; Nakajima, T.; Honda, Y.; Kitao, O.; Nakai, H.; Vreven, T.; Montgomery, J., J. A.; Peralta, J. E.; Ogliaro, F.; Bearpark, M.; Heyd, J. J.; Brothers, E.; Kudin, K. N.; Staroverov, V. N.; Kobayashi, R.; Normand, J.; Raghavachari, K.; Rendell, A.; Burant, J. C.; Iyengar, S. S.; Tomasi, J.; Cossi, M.; Rega, N.; Millam, N. J.; Klene, M.; Knox, J. E.; Cross, J. B.; Bakken, V.; Adamo, C.; Jaramillo, J.; Gomperts, R.; Stratmann, R. E.;

Yazyev, O.; Austin, A. J.; Cammi, R.; Pomelli, C.; Ochterski, J. W.; Martin, R. L.; Morokuma, K.; Zakrzewski, V. G.; Voth, G. A.; Salvador, P.; Dannenberg, J. J.; Dapprich, S.; Daniels, A. D.; Farkas, Ö.; Foresman, J. B.; Ortiz, J. V.; Cioslowski, J.; Fox, D. J.; *Gaussian, Inc., Wallingford CT*, **2009**.

(12) (a) Becke, A. D. *J. Chem. Phys.***1993,** *98*, 5648-5652. (b) Lee, C.; Yang, W.; Parr, R. G. *Phys. Rev. B* **1988,** *37*, 785-789. (c) Yanai, T.; Tew, D. P.; Handy, N. C. *Chem. Phys. Lett.* **2004,** *393*, 51-57. (d) Ditchfield, R.; Hehre, W. J.; Pople, J. A. *J. Chem. Phys.* **1971,** *54*, 724-728. (e) Hehre, W. J.; Lathan, W. A. *J. Chem. Phys.***1972,** *56*, 5255-5257. (f) Hariharan, P. C.; Pople, J. A. *Theor chim acta.* **1973,** *28*, 213-222.

(13) Schleyer, P. V. R.; Maerker, C.; Dransfeld, A.; Jiao, H.; van Eikema Hommes, N. J. R. *J. Am. Chem. Soc.***1996**, *118*, 6317-6318.

(14) Karthik, G.; Lim, J. M.; Srinivasan, A.; Suresh, C. H.; Kim, D.; Chandrashekar, T. K. *Chem. Eur. J.* **2013**, *19,* 17011-17020.

(15) Reddy, J. S.; Anand, V. G. *J. Am. Chem. Soc.* **2008**, *130*, 3718-3719.LLL

(16) Gopalakrishna, T. Y.; Anand, V. G. *Angew. Chem., Int. Ed.* **2014**, *53*, 6678-6682.

(17) Reddy, J. S.; Anand, V. G. *J. Am. Chem. Soc.* **2009**, *131*, 15433-15439

(18) Geuenich, D.; Hess, K.; Köhler, F.; Herges, R. *Chem. Rev.* **2005**, *105*, 3758-3772.

Chapter 4

Synthesis and Characterization of 46π Decaphyrins

IV.1 Introduction

Decaphyrins are a class of expanded porphyrnoids with ten heterocyclic units present in the core of the macrocycle. The first decaphyrin[1] **IV.1** (Figure IV.1) was reported by Sessler and co-workers in 1994 with only pyrrole rings in the core of the macrocycle. It was identified as a 40π tetracation with four chloride counter anions and characterized as a non-planar figure-of-eight conformation. Despite being a Hückel 4nπ system, it did not display characteristic paratropic ring current effects in its ^{1}H NMR spectrum. Later, X-ray diffraction analysis confirmed a non-planar topology structure which attributed to the structure induced loss of antiaromaticity. Since the molecule displayed a range of colors varying from intense purple to blue and green in organic solvents, which was accorded to the different degrees of protonation and hence was termed as Turcasarin. Later, the same group synthesized another 40π decaphyrin in order to achieve a planar system. In 2001[2] they reported a similar system, but with two of the pyrrole rings replaced by furan units **IV.2** (Figure IV.1). Even, in this case the neutral macrocycle was characterized as a figure of eight conformation.

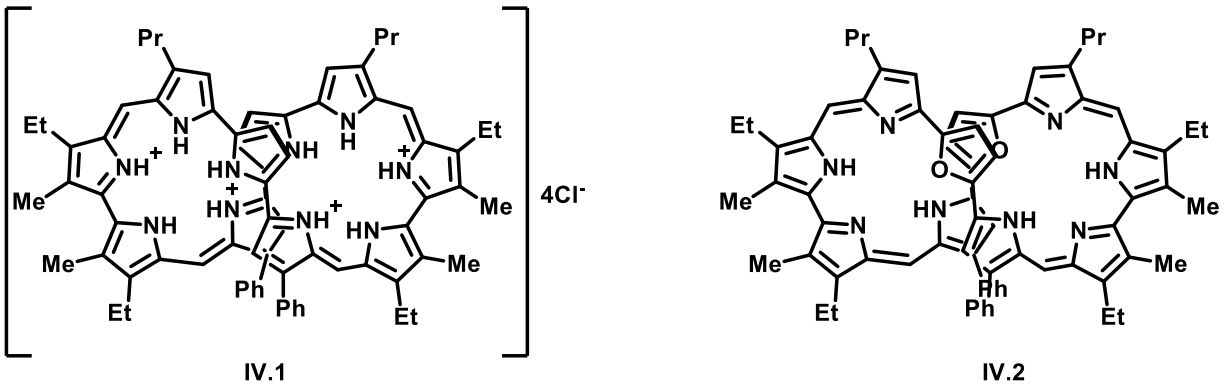

***Figure IV.1**: 40π Non-planar decaphyrins*

Later, in 2006 Chandrashekhar and coworkers reported another decaphyrin[3] with a combination of six thiophene and four pyrrole units bearing six bridging carbons **IV.3** (Figure IV.2). It was also identified as a non-planar 42π system, which displayed aromatic behavior in solution state.

In 2016, Kobayashi and co-workers reported a *meso* free 38π decapyrrolic decaphyrin[4] **IV.4** (Figure IV.2). However, they reported poor solubility in organic solvents and hence was stabilized as a diaction. However, synthesis of planar decaphyrins has remained a challenge except in few cases wherein additional support such as benzene ring in the center of the macrocycle provides sufficient strength to sustain a planar topology. Therefore, varying the ratio of bridging carbons and heterocyclic units is still an underexplored option to synthesize planar decaphyrins. In an effort to access planar decaphyrin, a novel synthetic approach was designed by employing easy to make precursors. In pursuit of a planar decaphyrin, this chapter describes a rational synthesis of a decaphyrin with six bridging carbons.

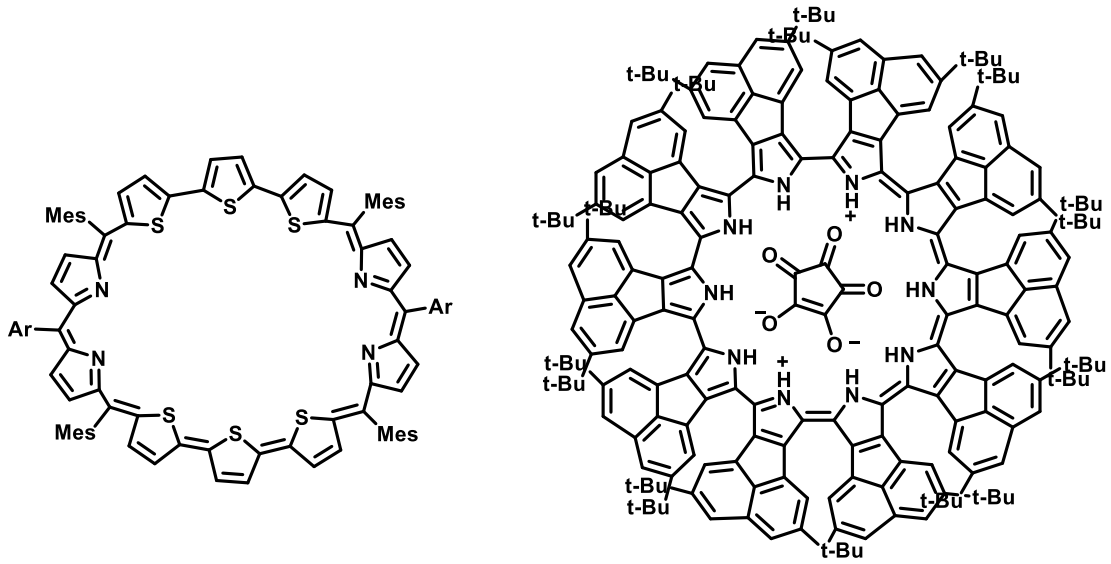

***Figure IV.2**: 42π and 38π decaphyrins*

IV.2 Synthesis of 46π expanded decaphyrins

The targeted synthesis of 46π decaphyrin required the condensation of a quaterthiophene with a suitable diol to yield the desired decaphyrin. However, the poor solubility of this unit demanded an alternative synthetic strategy to insert the quaterthiophene unit in the macrocycle. Therefore, a tetrathiophene unit **IV.6** with a pentafluoro substituent was synthesized for the first time via two steps, (Scheme IV.1). Initially pentafluorobenzaldehyde was condensed with

excess of 2-Bromothiophene using $BF_3.OEt_2$ to yield the dibromo derivative **IV.5**. Further, it was coupled with Grignard of 2-bromothiophene under Kumada coupling conditions to obtain **IV.6** in 54% yields.

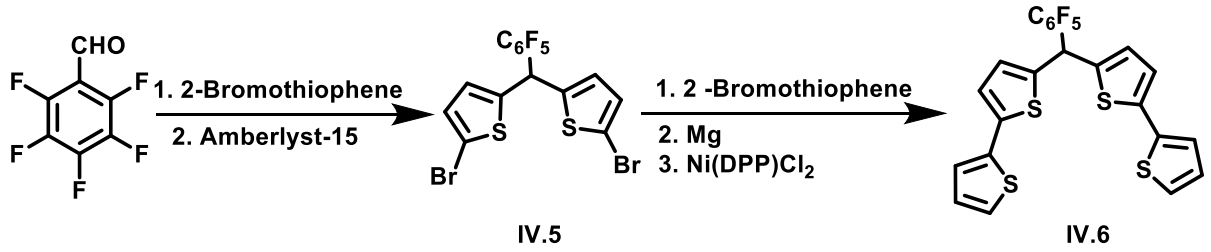

Scheme IV.1*: Synthesis of terthiophene with pentafluoro substituent at meso position*

The synthesis of 46π decaphyrin was now attempted by condensing tetrathiophene **IV.6** with thiophene/ furan diol **IV.7a-b**[5-6] using $BF_3.OEt_2$ and stirring for two hours under dark and inert conditions. It was followed by oxidation using dichlorodicyanoquinone and further the reaction mixture was stirred for two hours (Scheme IV.2). After two hours, the reaction mixture was neutralized by adding one drop of triethyl amine and then filtered it through basic alumina column. The reaction mixture was concentrated under reduced pressure and then purified over alumina column using ethyl acetate/ hexane as eluent. In both the cases MALDI TOF/TOF spectrum (Figure IV.3- IV.4) displayed the formation of partially oxidized nine-member macrocycle (**IV.8a-b**) along with completely oxidized 46π decaphyrin (**IV.9a-b**) (Scheme IV.2).

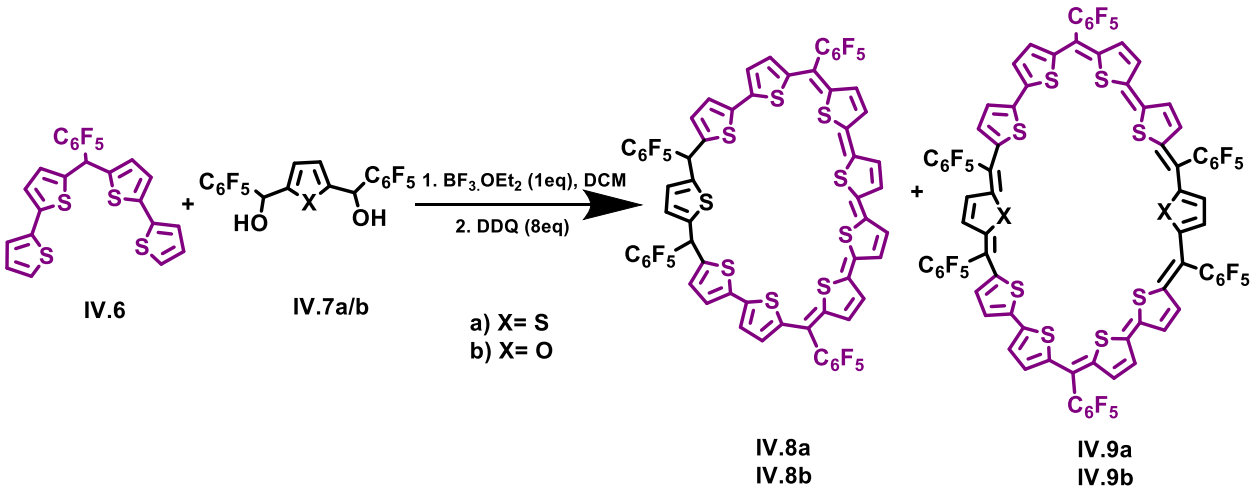

***Scheme IV.2**: Synthesis of 46π decaphyrin and the unconjugated nonaphyrin*

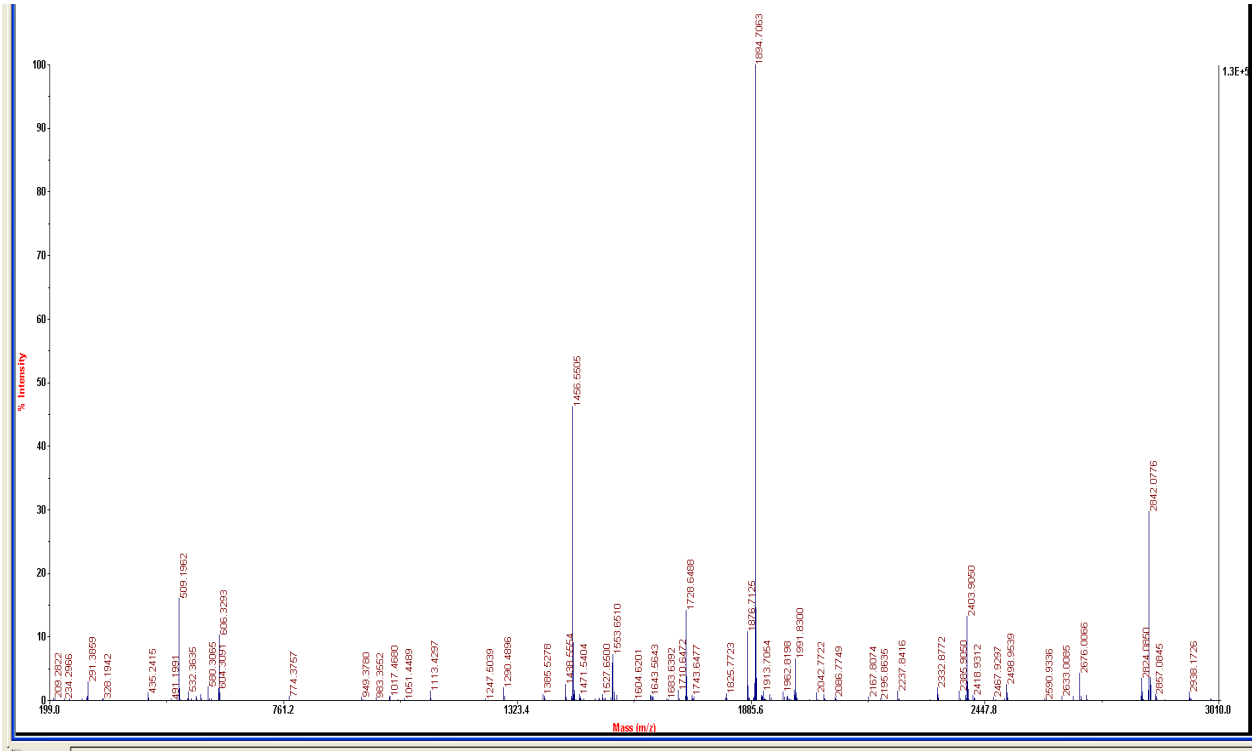

Figure IV.3**: MALDI TOF/TOF spectrum of reaction mixture containing **IV.8a** and **IV.9a

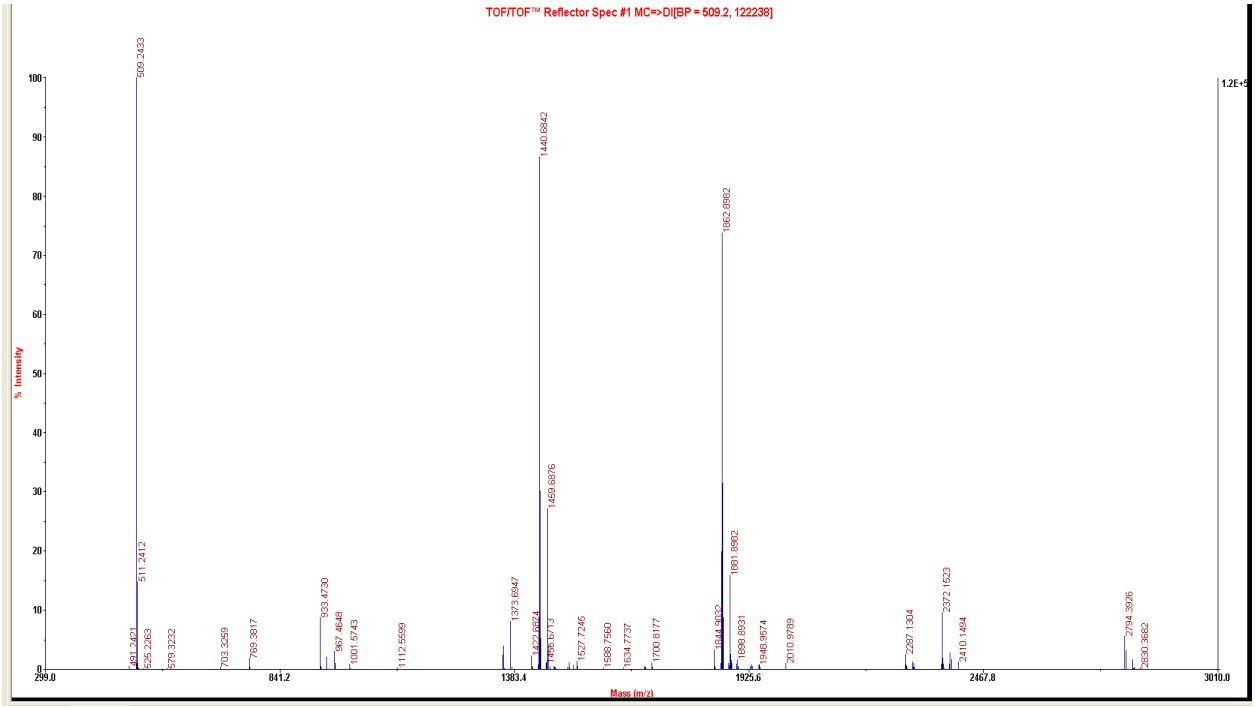

Figure IV.4**: MALDI TOF/TOF spectrum for reaction mixture containing **IV.8b** and **IV.9b

IV.3 Isolation and characterization of 46π decaphyrins

IV.3.1 Isolation of decaphyrin having all thiophene units (IV.9a)

After the reaction mixture was filtered through basic alumina and concentrated under reduced pressure, it was subjected to purification via column chromatography. The decaphyrin **IV.9a** was purified over basic alumina column using ethyl acetate/ hexane as eluent in 3.5% yields. After repeated column chromatographic separation, decaphyrin was purified and isolated as a pink band which displayed an intense absorption at 559 nm (1743 ε, $Lmol^{-1}cm^{-1}$) along with a band at 512 nm (1683) in its electronic absorption spectra (Figure IV.6). It displayed molecular ion peak at 1893.8396 corresponding to $C_{82}H_{20}F_{30}S_{10}$ for the calculated M^+ value of 1893.8293 in its HR-MS spectrum (Figure IV.5).

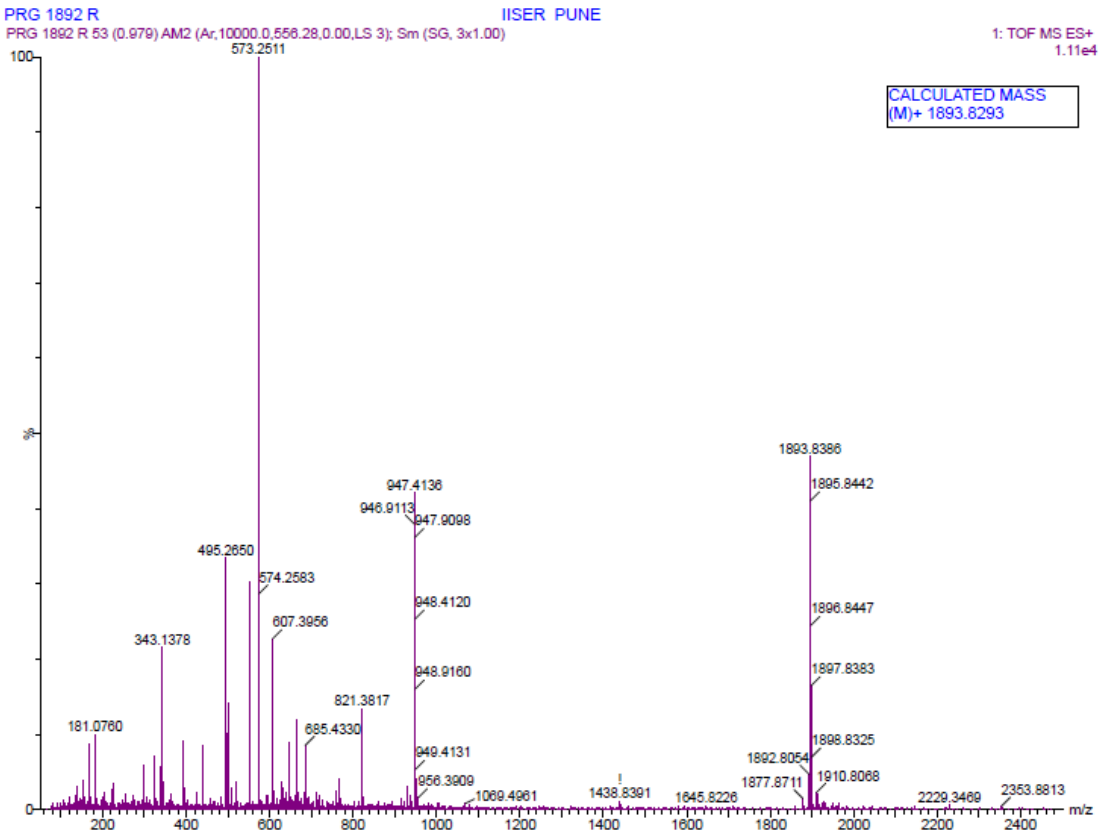

Figure IV.5**: HR-MS spectrum for **IV.9a

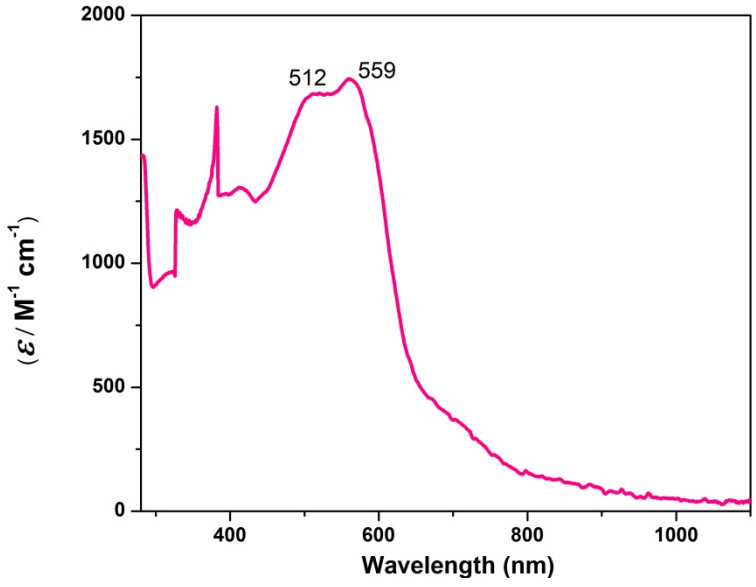

***Figure IV.6**: Electronic absorption spectrum of **IV.9a** in dichloromethane at ~10^{-5}M concentration*

A well resolved proton NMR was completely integrated at room temperature and no significant change was observed on lowering the temperature (Figure IV.7). A total of twenty protons

resonated between δ 7.20 to 7.50 ppm (Figure IV.8). There was no significant ring current effect being observed in its proton NMR spectrum. This result was further supported by NICS (0) calculation performed over energy optimized structure shown in Figure 1V.10, where a low value of δ -1.68 ppm suggested non-aromatic nature of the macrocycle. The ^{1}H-^{1}H COSY spectrum displayed clear correlations between the signals (Figure IV.9). Observation of only a few peaks suggested the formation of a symmetrical macrocycle.

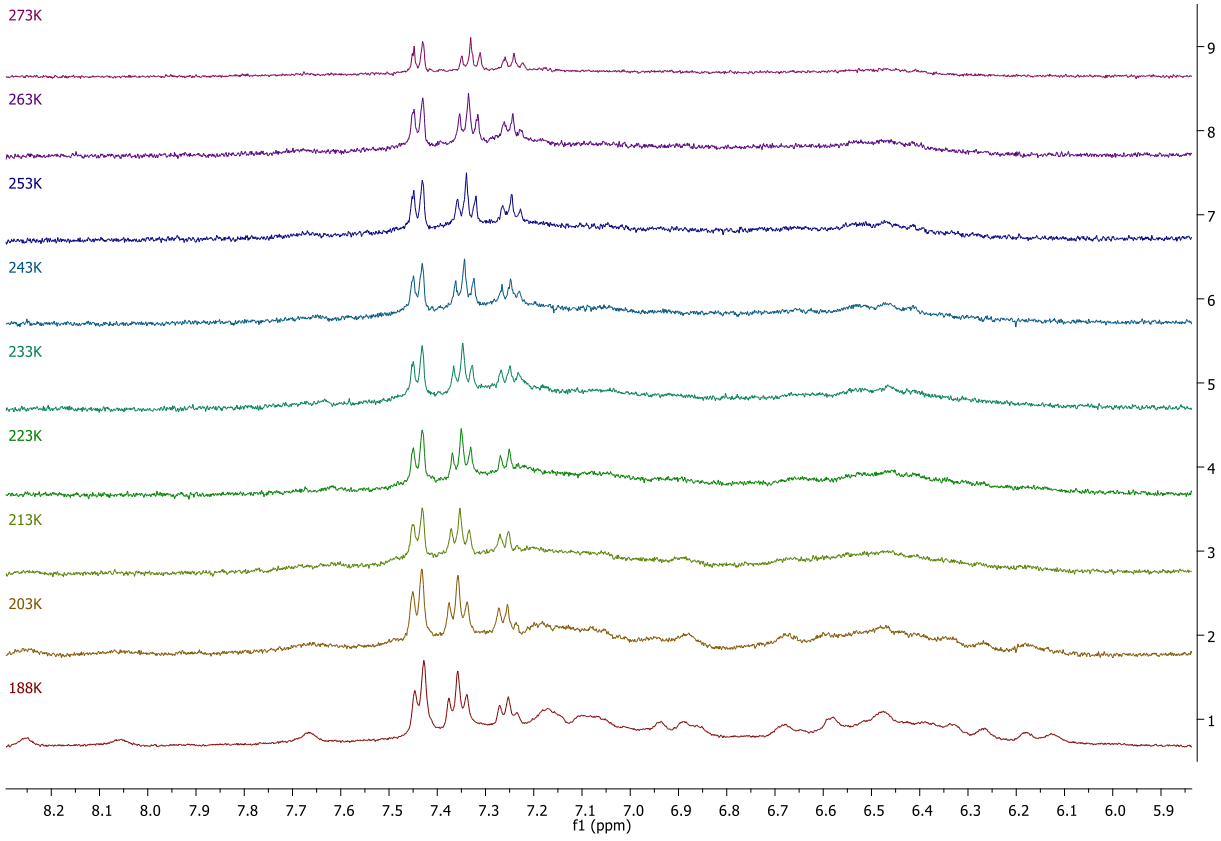

Figure IV.7*: Variable temperature proton NMR spectra for* ***IV.9a*** *in CD_2Cl_2 from 273 K to 188 K*

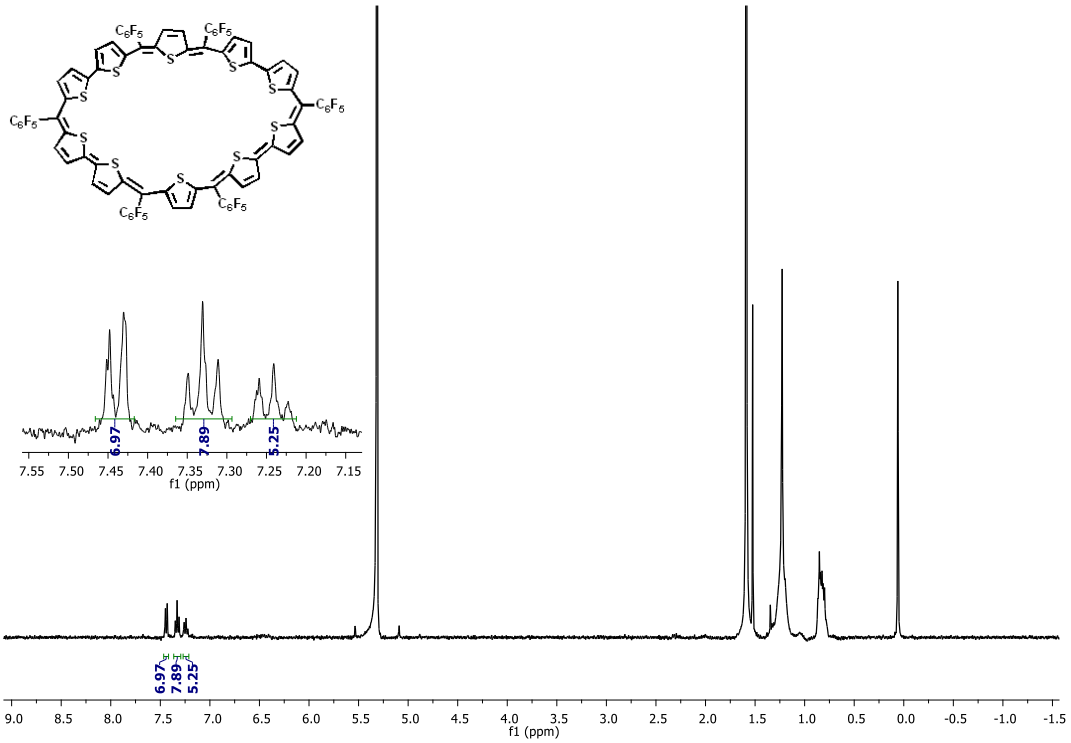

***Figure IV.8**: Proton NMR spectrum for **IV.9a** recorded in CD_2Cl_2 at room temperature*

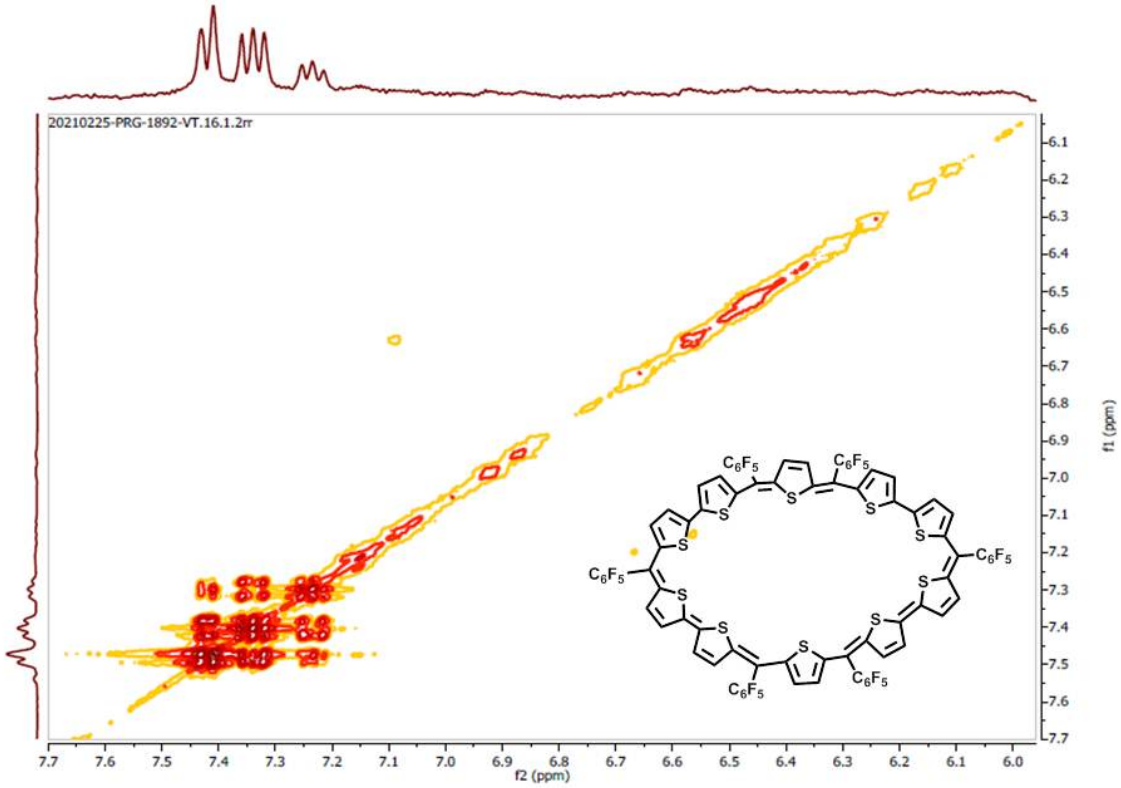

***Figure IV.9**: ^1H-^1H COSY spectrum for **IV.9a** recorded in CD_2Cl_2 at room temperature*

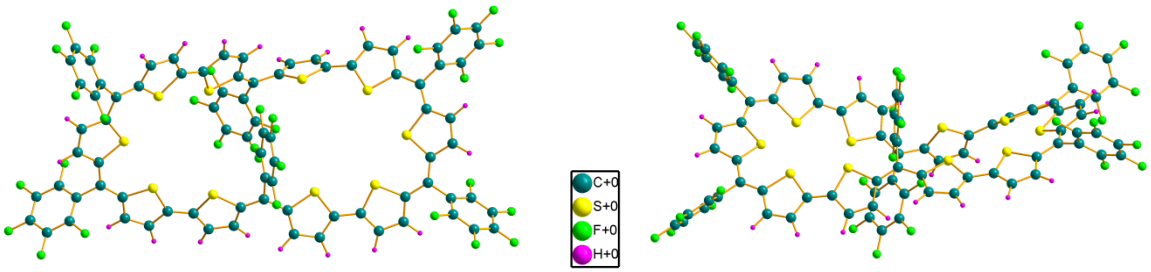

Figure IV.10**: Frontal (left) and lateral (Right) energy optimized structure for **IV.9a

However, the absolute structure could not be determined by X-ray diffraction analysis. Despite multiple attempts, good quality crystals could not be isolated for the decaphyrin **IV.9a** due its poor solubility in many organic solvents. The poor solubility of the molecule is attributed to large number of heterocylic units and fewer *meso* carbons in the macrocycle.

IV.3.2 Isolation of decaphyrin having two furan units (IV.9b)

After the reaction mixture was filtered through basic alumina and concentrated under reduced pressure, it was subjected to purification via column chromatography. The decaphyrin **IV.9b** was purified over basic alumina column using ethyl acetate/ hexane as eluent in 3% yields. After repeated column chromatographic separations, decaphyrin could be completely purified and isolated as a blue band which displayed an intense absorption at 669 nm (2161 ε, $Lmol^{-1}cm^{-1}$) along with a band at 525 nm (1377) and 416nm (2036) in its electronic absorption spectra (Figure IV.12). It displayed molecular ion peak at 1861.8848 corresponding to $C_{82}H_{20}F_{30}O_2S_8$ calculated M^+ value of 1861.8750 in its HR-MS spectrum (Figure IV.11).

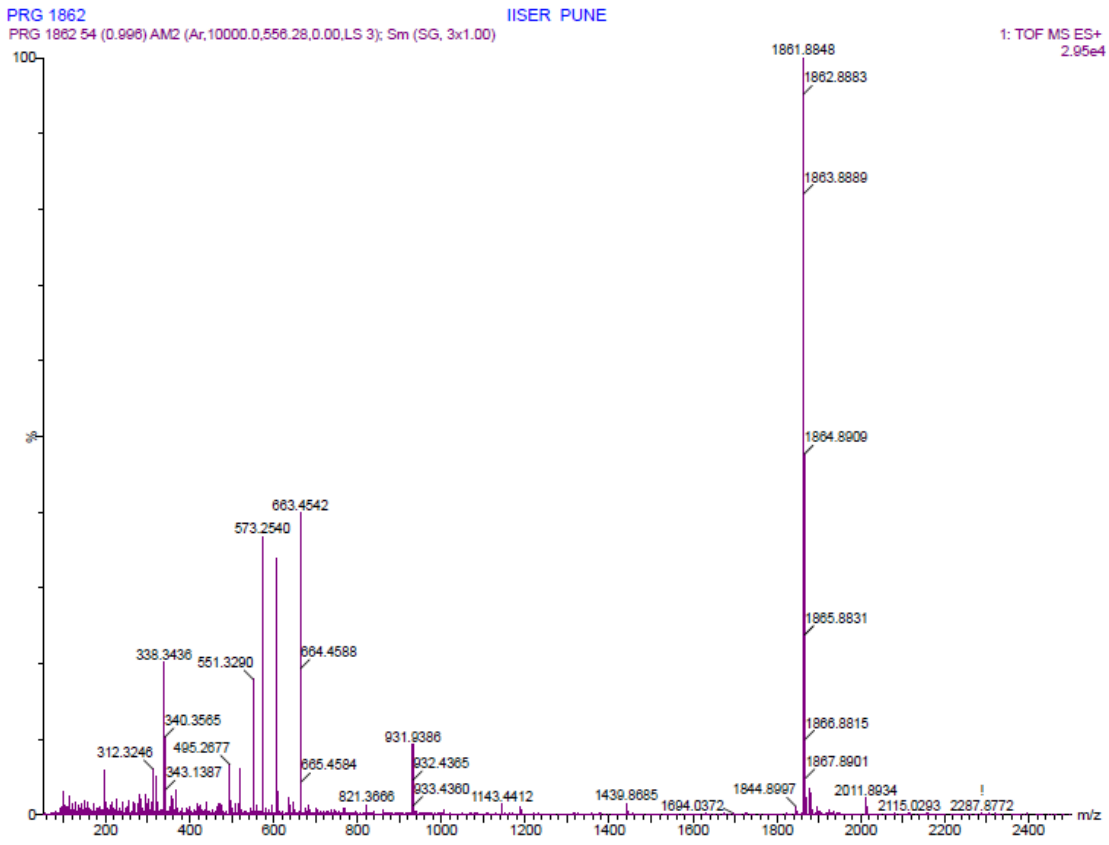

Figure IV.11**: HR-MS spectrum for **IV.9b

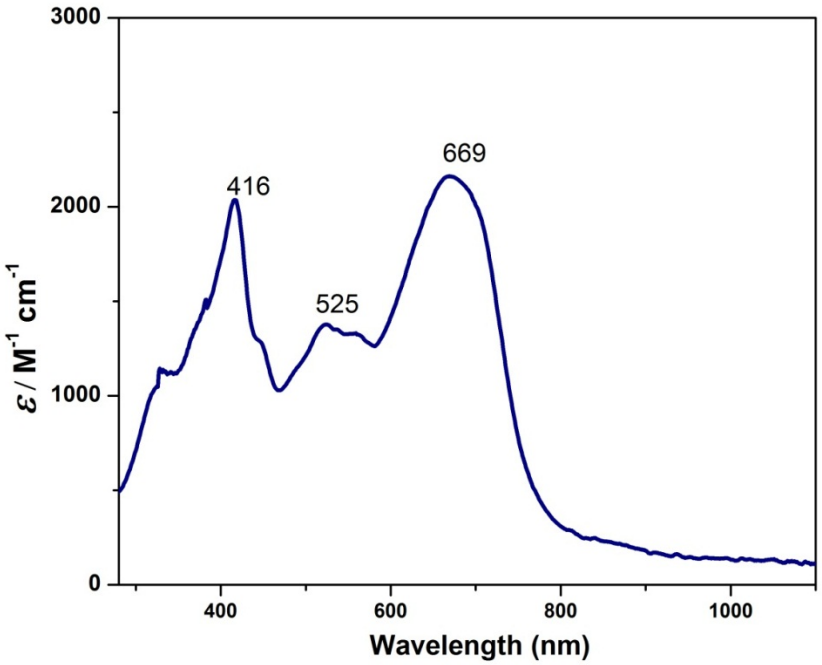

***Figure IV.12**: Electronic absorption spectrum of **IV.9b** in dichloromethane at ~10^{-5}M concentration*

Its proton NMR was well resolved at room temperature. There were a total of twenty protons being resonated between δ 6.70 to 7.30 ppm (Figure IV.12). No significant diatropic ring current effect was observed for the 46π decaphyrin. This can be attributed to the possible non-planar or a twisted topology for the macrocycle. Further support for this hypothesis was supported by NICS(0) calculation performed over energy optimized structure shown in Figure 1V.14. A poor value of δ +1.61 ppm suggested non-aromatic nature of the macrocycle.

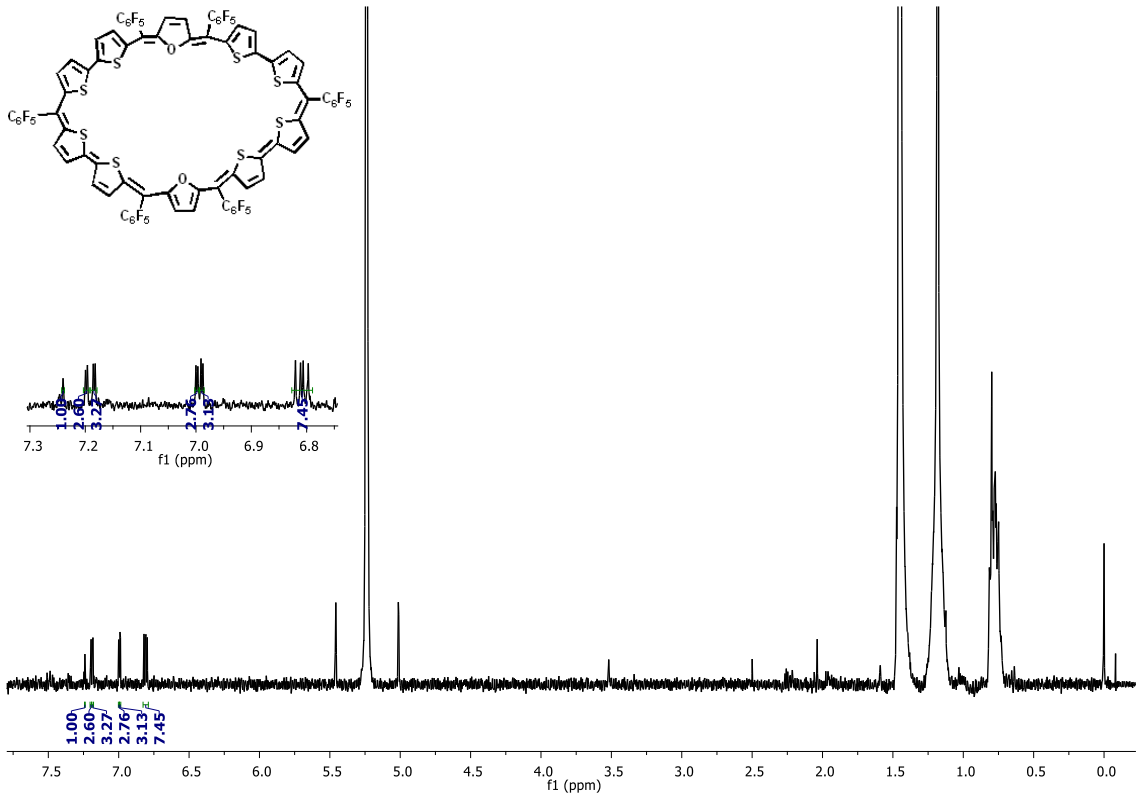

***Figure IV.13**: Proton NMR spectrum for **IV.9b** in CD_2Cl_2 at room temperature*

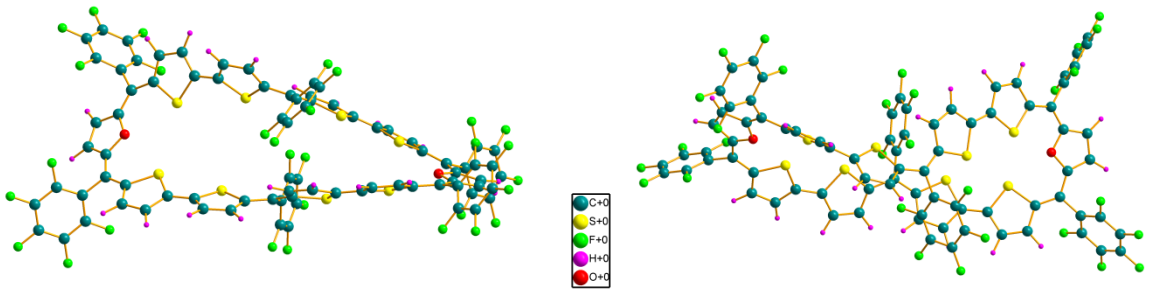

Figure IV.14**: Frontal (left) and lateral (Right) energy optimized structure for **IV.9b

However, all efforts to support the spectroscopic investigations could not be justified in the solid state. Despite multiple attempts, decaphyrin did not yield good quality crystals. A crucial reason for this drawback can be attributed to the poor solubility of the macrocyle **IV.9b** in a variety of organic solvents.

IV.4 Quantum chemical calculations

Since both the decaphyrins could not be characterized in solid state, (**IV.9a-b**), Quantum Chemical Calculations were performed on energy optimized structure. These structures were optimized using Density Functional Theory (DFT) with Beckes's three-parameter hybrid exchange function and the lee-Yang-Parr correlation function (B3LYP)[7] and 6-31G(d,p) basis set for all the atoms in the molecule. Then the negative of the calculated magnetic shielding at the center of the ring, first introduced by Schleyer, commonly referred as "Nucleus Independent Chemical Shift" (NICS)[8] value was calculated. Decaphyrin **IV.9a** displayed NICS(0) value at δ -1.68 ppm while the decaphyrin **IV.9b** displayed NICS(0) value at δ +1.61 ppm. Both these values are very close to zero suggesting the non-aromatic nature of the decaphyrins.

Further, steady-state absorption spectra were studied using Time Dependent TD-DFT calculations. The experimentally recorded absorption spectra for **IV.9a** and **IV.9b** matched the calculated TD-DFT values.

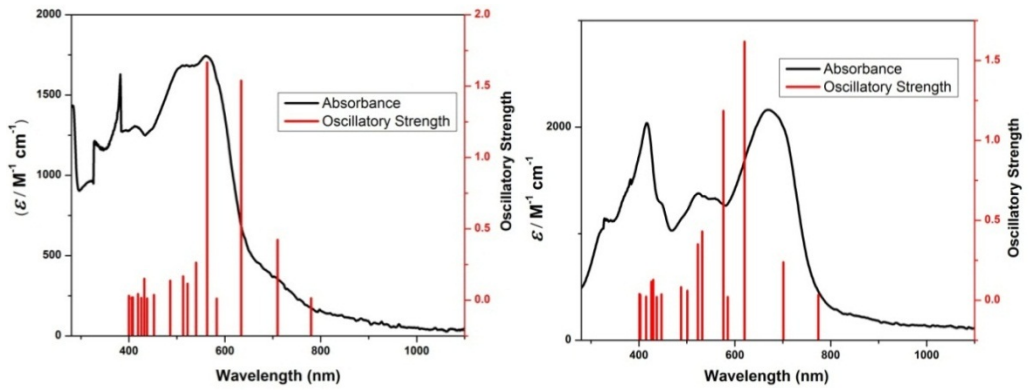

Figure IV.13*: Time dependent functional theory (TDFT) calculation overlaid on experimental UV-VIS absorption spectra of* ***IV.9a*** *(left) and* ***IV.9b*** *(right)*

IV.5 Conclusion

This chapter describes the successful synthesis of 46π core modified decaphyrin containing both thiophene and furan units. Both the decaphyrins had poor solubility in many organic solvents. None of the decaphyrins exhibited any significant ring current effects and this was supported by computational studies performed on energy optimized structures suggesting the non-aromatic nature of both of the decaphyrins.

IV.6 Experimental section

5,5''-((perfluorophenyl)methylene)di-2,2'-bithiophene **IV.6** and the corresponding diol **IV.7a/b** were dissolved in dry DCM in an equimolar ratio in a round bottom flask and stirred under dark and dry conditions. One equivalent of $BF_3.OEt_2$ was added to the reaction mixture and stirred for two hours under dark and inert conditions. Further after two hours eight equivalents of DDQ was added to the reaction mixture and stirring was continued for further three hours. Finally the reaction mixture was passed through basic alumina column and reaction mixture was concentrated and further purified.

Synthetic procedure of 5,5''-((perfluorophenyl)methylene)di-2,2'-bithiophene (IV.6):

IV.6 was synthesized in two steps

Step 1: Synthesis of 5,5'-((perfluorophenyl)methylene)bis(2-bromothiophene) (IV.5):

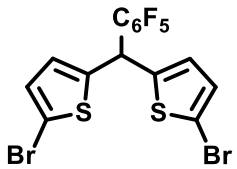

Pentafluorobenzaldehyde (30.60 mmol, 3.8 mL) was added to a stirred solution of 2-bromothiophene (612.01 mmol, 60 mL) in a round bottom flask, under nitrogen atmosphere and dark conditions. $BF_3.OEt_2$ (15.30 mmol, 1.89 mL) was added to the reaction mixture and

stirred for 45 minutes. The reaction was quenched with saturated NaOH solution and extracted using diethyl ether. The compound was purified using silica gel glass column using hexane as eluent. The compound was isolated as yellowish oily liquid in 60% yield.

^{1}H NMR (400 MHz, $CDCl_3$) δ 6.92 (d, *J* = 4 Hz, 1H), 6.72 (d, *J* = 4 Hz, 2H), 6.02 (s, 2H).

Step 2: Synthesis of 5-((perfluorophenyl)(thiophen-2-yl)methyl)-2,2'-bithiophene (IV.6):

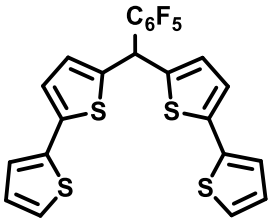

To a stirred solution of above compound **IV.5** (5.95 mmol, 3 g) in 30 mL of dry diethyl ether at 0 ˚C, 0.04 equivalent of $Ni(dpp)_2Cl_2$ catalyst was added under argon atmosphere.To this solution, freshly prepared Grignard reagent ($C_{15}H_6F_5S_2MgBr$) (23.80 mmol) was added slowly maintaining the temperature at 0 ˚C. The solution was slowly brought to room temperature and further refluxed for 40 hours to obtain the desired product. The reaction was cooled to room temperature and as being exothermic in nature, was carefully quenched using ice cold ammonium chloride solution. The compound **IV.6** was extracted using diethyl ether and purified using silica gel mesh 100-200 glass column using hexane as eluent. The compound was purified in 54 % yield and was yellowish oily liquid.

^{1}H NMR (400 MHz, $CDCl_3$) δ 7.21 (dd, *J* = 5.1, 4 Hz, 2H), 7.13 (dd, *J* = 3.6, 4 Hz, 2H), 7.03 (d, *J* = 4 Hz, 2H), 7.00 (dd, *J* = 4, 3.6 Hz, 2H), 6.90 (d, *J*= 4 Hz, 2H), 6.15 (s, 1H).

Synthetic procedure of IV.9a

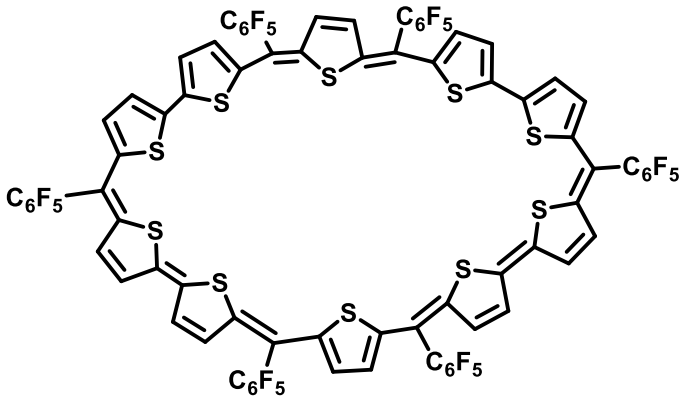

A clean dried 250 mL round bottom flask was charged with compound **IV.6** (125 mg, 244.82 μmol). To this compound **IV.7a**[5] (116.61 mg, 244.82 μmol) was added and 150 mL of dry dichloromethane was added. The solution was nicely stirred and maintained under dark and inert condition. To this reaction mixture, $BF_3.OEt_2$ (244.82 μmol, 0.03 mL) was added slowly and stirred further for two hours. Subsequently after two hours, dichlorodicyanoquinone (444 mg, 1.96 mmol) was added to the reaction mixture and stirred further for 2.5 hours. The reaction mixture was filtered through basic alumina column and purified on a neutral alumina glass column. The major fraction obtained was a ten membered 46π decaphyrin isolated in 3.5% yield. The molecule was completely characterized using the HR-MS and spectroscopic techniques.

HR-MS (ESI) m/z: $[M]^+$Calcd. for $C_{82}H_{20}F_{30}S_{10}$1893.8293; Found 1893.8396.

UV-Vis (CH_2Cl_2): λ_{max} nm (ε, $Lmol^{-1}cm^{-1}$): 559 (1743), 512 (1683).

^1H NMR (400 MHz, CD_2Cl_2) δ: 7.44 (d, J = 8 Hz, 7H), 7.33 (t, J = 8 Hz, 8H), 7.25 (d, J = 8 Hz, 5H).

Synthetic procedure of IV.9b

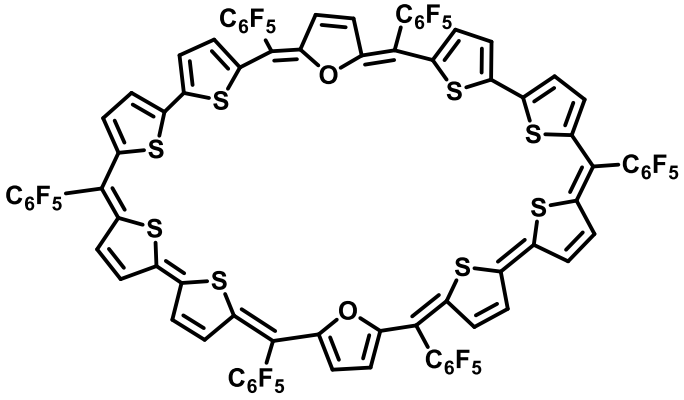

A clean dried 250mL round bottom flask was charged with compound **IV.6** (125 mg, 244.82 μmol). To this compound **IV.7b**[6] (112.67 mg, 244.82 μmol) was added and 150 mL of dry dichloromethane was added. The solution was nicely stirred and maintained under dark and inert condition. To this reaction mixture, $BF_3.OEt_2$ (244.82 μmol, 0.03 mL) was added slowly and stirred further for two hours. Subsequently after two hours, dichlorodicyanoquinone (444 mg, 1.96mmol) was added to the reaction mixture and stirred further for 2.5 hours. The reaction mixture was filtered through basic alumina column and purified on a neutral alumina glass column. The major fraction obtained was asten membered, 46π decaphyrin isolated in 3% yield. The molecule was completely characterized using the HR-MS and spectroscopic techniques.

HR-MS (ESI) m/z: $[M]^+$Calcd. for $C_{82}H_{20}F_{30}O_2S_8$1861.8750; Found 1861.8848.

UV-Vis (CH_2Cl_2): λ_{max} nm (ε, $Lmol^{-1}cm^{-1}$): 669 (2161), 525 (1377) and 416 (2036).

^1H NMR (400 MHz, CD_2Cl_2) δ 7.24 (s, 1H), 7.20 (d, J = 4 Hz, 3H), 7.18 (d, J = 4 Hz, 3H), 7.00 (d, J = 4 Hz, 3H), 6.99 (d, J = 4 Hz, 3H), 6.81 (dd, J = 4, 3.7 Hz, 7H).

IV.7 References

(1) Sessler, J. L.; Weghorn, S. J.; Lynch, V.; Johnson, M. R. *Angew. Chem., Int. Ed. Engl.* **1994**, ***33***, 1509-1512.

(2) Sessler, J. L.; Seidel, D.; Gebauer, A.; Lynch. V.; Abboud, K. A. *J. Heterocycl. Chem.* **2001**, *38*, 1419-1424.

(3) Rath, H.; Prabhuraja, V.; Chandrashekar, T. K.; Nag, A.; Goswami, D.; Joshi, B. S. *Org. Lett.* **2006**, *8*, 2325-2328.

(4) Okujima*et, T.;* Ando. C.; Agrawal, S.; Matsumoto, H.; Mori, S.; Ohara, K.; Hisaki, I.; Nakae, T.; Uno, H.; Kobayashi, N. *J. Am. Chem. Soc.* **2016**, *138*, 7540-7543.

(5) Reddy, J. S.; Anand, V. G. *J. Am. Chem. Soc.* **2008**, *130*, 3718-3719.

(6) Gopalakrishna, T. Y.; Anand, V. G. *Angew. Chem., Int. Ed.* **2014**, *53*, 6678-6682.

(7) (a) Becke, A. D. *J. Chem. Phys.***1993,** *98*, 5648-5652. (b) Lee, C.; Yang, W.; Parr, R. G. *Phys. Rev. B* **1988,** *37*, 785-789. (c) Yanai, T.; Tew, D. P.; Handy, N. C. *Chem. Phys. Lett.* **2004,** *393*, 51-57. (d) Ditchfield, R.; Hehre, W. J.; Pople, J. A. *J. Chem. Phys.* **1971,** *54*, 724-728. (e) Hehre, W. J.; Lathan, W. A. *J. Chem. Phys.***1972,** *56*, 5255-5257. (f) Hariharan, P. C.; Pople, J. A. *Theor chim acta.* **1973,** *28*, 213-222.

(8) Schleyer, P. V. R.; Maerker, C.; Dransfeld, A.; SJiao, H.; van Eikema Hommes, N. J. R.*J. Am. Chem. Soc.* **1996**, *118*, 6317-6318.

Chapter 5

Synthesis and Characterization of 32π and 48π Porphyrnoids Containing Ethylene Bridge

V.1 Introduction

Porphycenes are structural isomers of porphyrins with bipyrrolic units connected via ethylene bridges. Vogel and coworkers reported the first example of an 18π porphycene in 1986.[1] Akin to porphyrin, the porphycene exhibited aromaticity albeit in a lesser degree. Further, it also displayed versatile metal complexing ability similar to porphyrins.[2] In a parallel to expanded porphyrins, modifications in the core, ring expansion or replacing pyrrolic units with other heterocyclic units results in range of porphycene molecules.[3] These molecules are mostly synthesized through McMurry coupling. Particularly, a range of thiophene containing porphycenes[3] have been studied till date (Figure V.1; **V.1-V.4**).

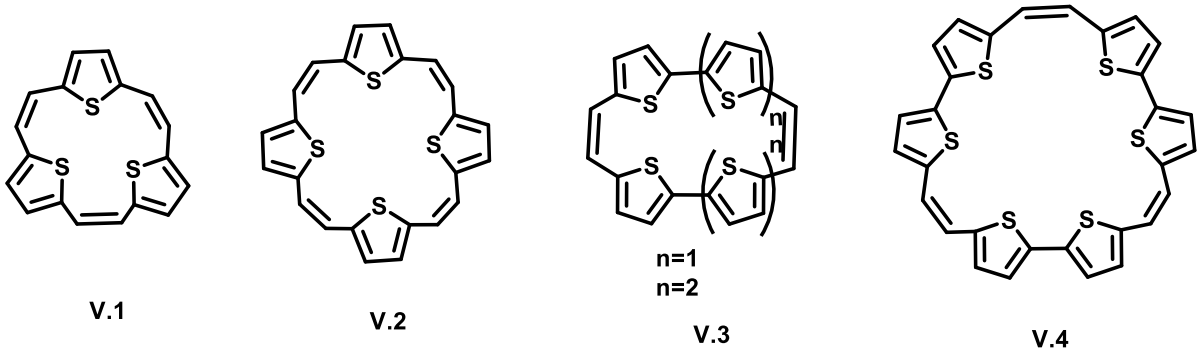

Figure V.1*: Core-modified porphycenes*

In an alternate synthetic method ethylene unit can be incorporated in between the heterocyclic oligomeric precursor units. Some examples known in literature[4] report *E* conformer of ethylene unit in the monomer to yield macrocycle without changing the conformation of the ethylene (Figure V.2; **V.5-V.7**). Therefore, a predetermined precursor with an ethylene bridge can be employed as a basis for a specific conformation. However, larger annulenes are usually fluxional in nature and can thermodynamically interchange between the *E* and *Z* conformations.[5]

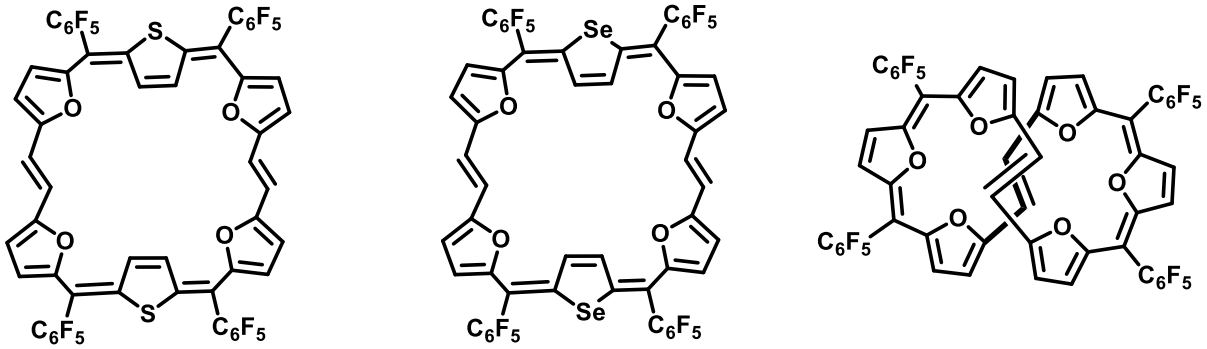

Figure V.2*: Macrocycles containing ethylene bridge in E conformer*

There are very few examples with *Z* conformer of ethylene bridged in the macrocycle synthesized via MacDonald condensation. Therefore, this chapter describes the efforts to synthesize such *Z* ethylene bridged macrocycles with suitable substituents on the carbon atoms.

V.2 Synthesis of 32π hexaphyrin and 48π nonaphyrin

Tetrasubstituted ethylene[6] are valuable precursors for the synthesis of desired macrocycles. These substituents can be either *Z* or *E* conformations and the choice of precursors can be pre-decided in the precursor. By adopting this strategy, an attempt was made to synthesize 32π and 48π ethylene bridge antiaromatic macrocycles. Initially (*Z*)-1,2-diphenyl-1,2-bis(4,4,5,5-tetramethyl-1,3,2-dioxaborolan-2-yl)ethane[7] **V.8** was synthesized using platinum catalyzed reaction and it was further coupled with 2-bromothiophene to yield Suzuki coupled product (*Z*)-1,2-diphenyl-1,2-di(thiophen-2-yl)ethane[6] **V.9** (Scheme V.1).

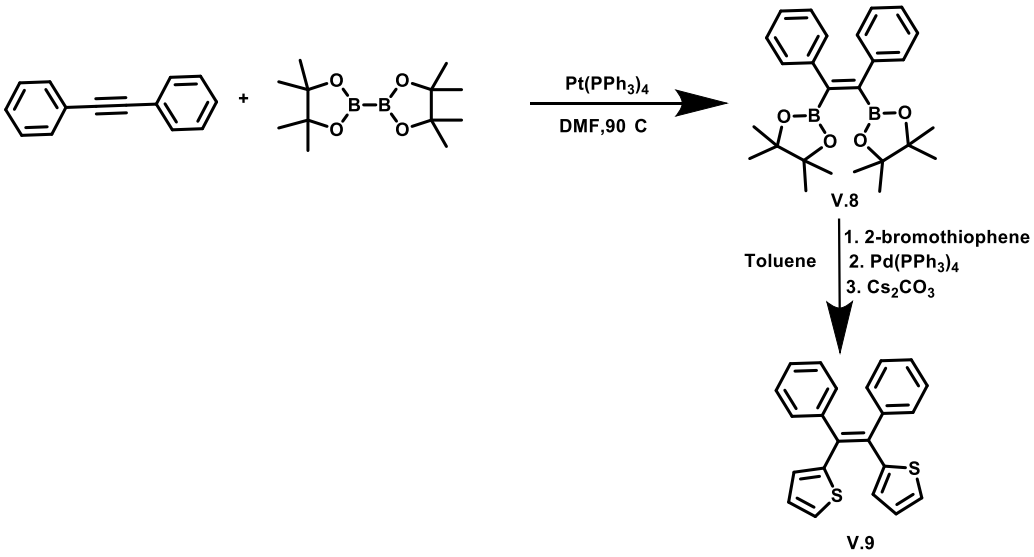

Scheme V.1*: Synthesis of (Z)-1,2-diphenyl-1,2-di(thiophen-2-yl)ethane*

(*Z*)-1,2-diphenyl-1,2-di(thiophen-2-yl)ethane **V.9** and thiophene diol[8] **V.10** were condensed in an equimolar ratio in high dilution of DCM using one equivalent of $BF_3.OEt_2$ under dark and inert conditions (Scheme V.2). The reaction was stirred for two hours and then oxidized using six equivalents of dichlorodicyanoquinone (DDQ) and further stirring was continued for two hours.

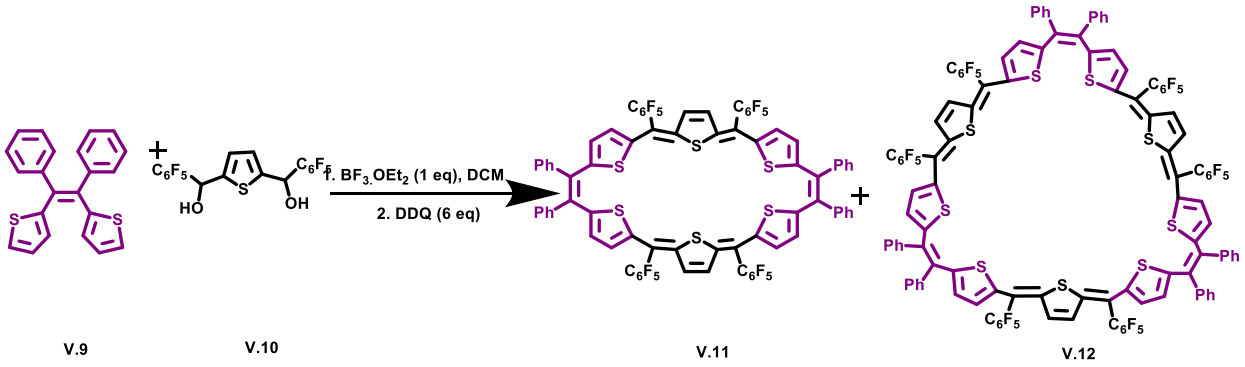

Scheme V.1*: Synthesis of ethylene bridged macrocycles*

The reaction mixture analyzed by MALDI TOF/TOF mass spectrometry (Figure V.3) confirmed the formation of both, the six membered **V.11** and the nine membered **V.12** (Scheme V.1) macrocycles. The reaction mixture was filtered through basic alumina column and concentrated under reduced pressure. Further it was subjected to column chromatography to purify and isolate each macrocycle.

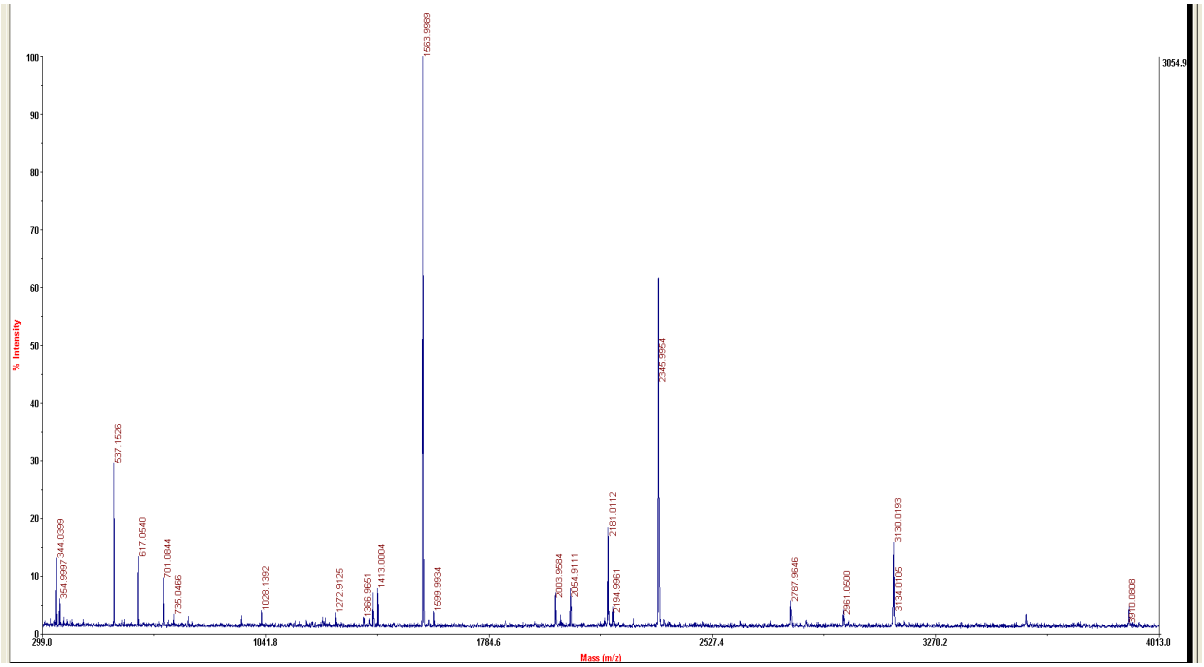

***Figure V.3**: MALDI TOF/TOF mass spectrum of reaction mixture*

V.3 Isolation and characterization of 32π hexaphyrin V.11

Once the reaction mixture was concentrated under reduced pressure, it was purified using silica gel column with DCM/ hexane as eluent. A brown colored band was identified as 32π hexaphyrin **V.11** and eluted after repeated column chromatographic separations. The brown colored band displayed $(M+H)^+$ peak at 1565.0524 corresponding to $C_{80}H_{32}F_{20}S_6$ with an exact mass of 1564.0509 (Figure V.4). The brown band displayed an intense absorption band at 498 nm (13180 ε, $Lmol^{-1}cm^{-1}$) in its electronic absorption spectra (Figure V.5).

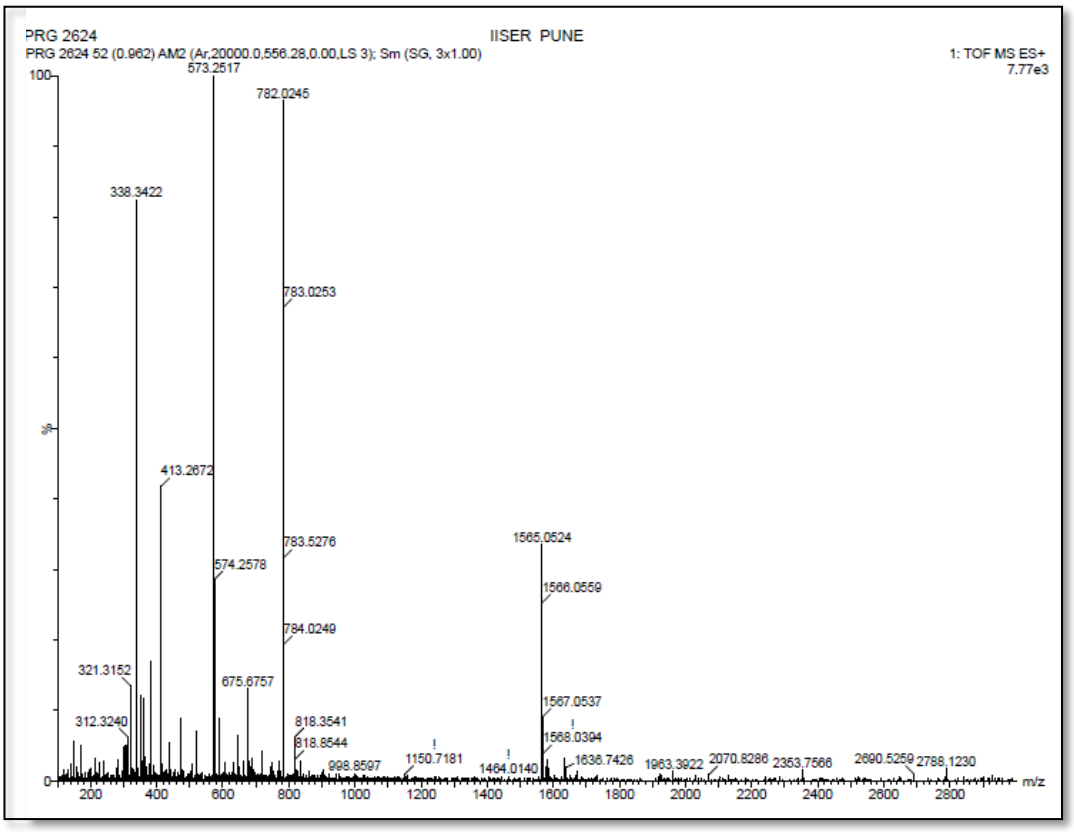

Figure V.4**: HR-MS spectrum of **V.11

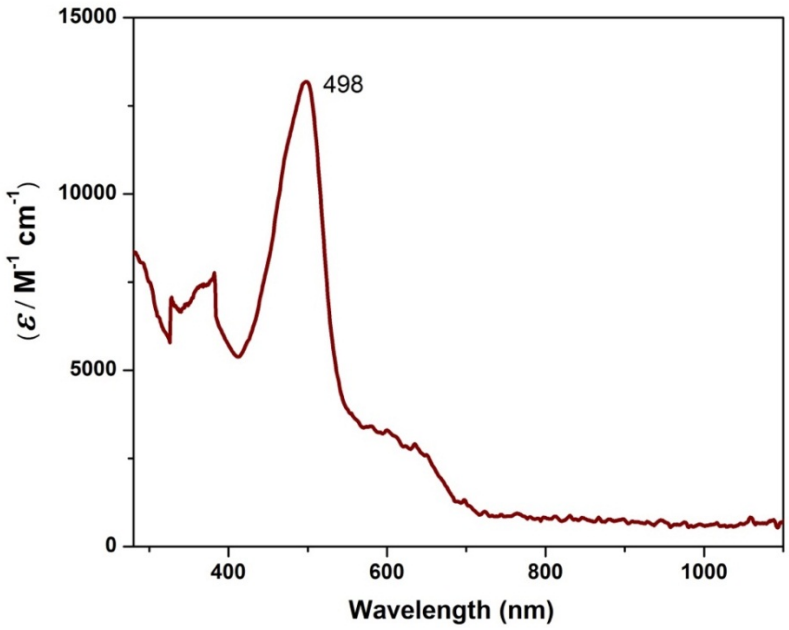

***Figure V.5**: Electronic absorption spectrum of **V.11** in DCM at ~10^{-5}M concentration*

The proton NMR was well resolved at room temperature and displayed two doublets and a singlet resonating between δ 6.4 and 6.6 ppm corresponding to the thiophene protons. However, all the phenyl protons resonated as a multiplet at δ 7.4 ppm (Figure V.6). Unlike the 32π macrocycles **V.5** or **V.6** ^{1}H NMR spectrum of **V.11** suggested that the macrocycle was devoid of any paratropic ring current effects expected of an antiaromatic system. Since the chemical shift value of thiophene protons did not suggest any ring current effect and all the phenyl protons appeared to resonate together as a multiplet at δ 7.4 ppm, lead to the understanding that the macrocycle might be non-antiaromatic in the solution state. The ^{1}H-^{1}H COSY spectrum also showed single correlation between the thiophene protons (Figure V.7).

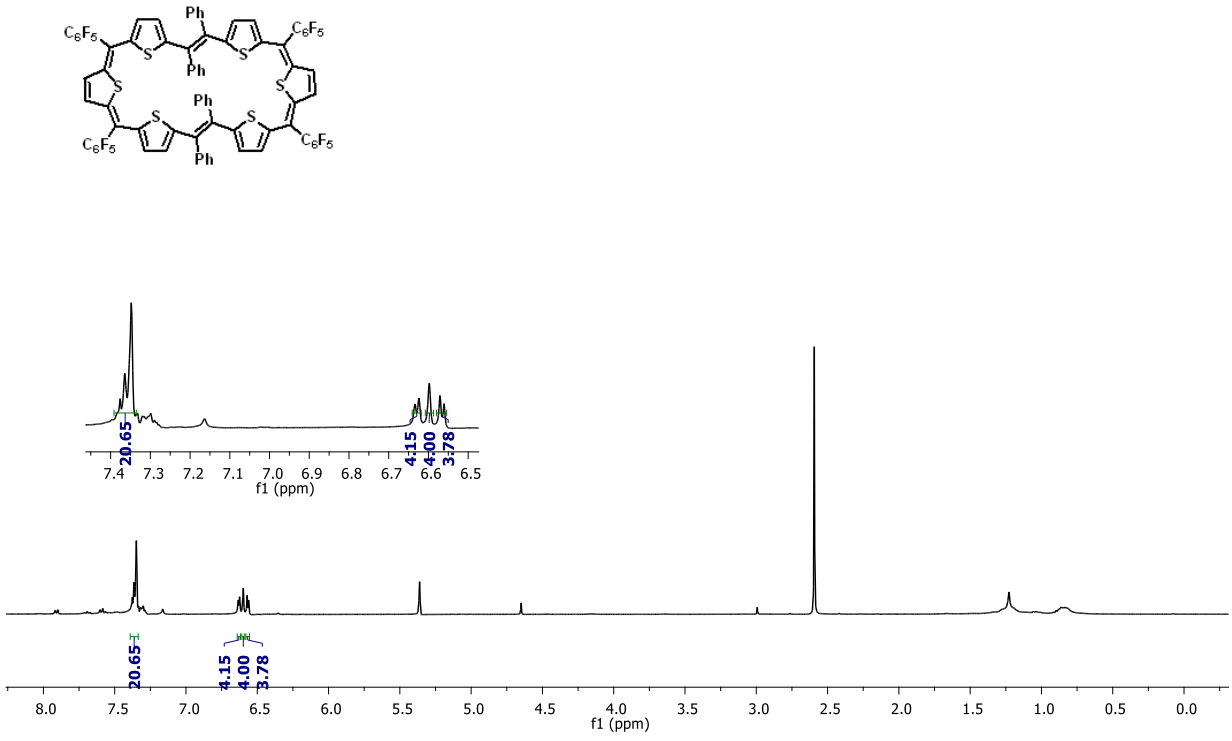

***Figure V.6**: Proton NMR spectrum of **V.11** in $CDCl_3$ at room temperature*

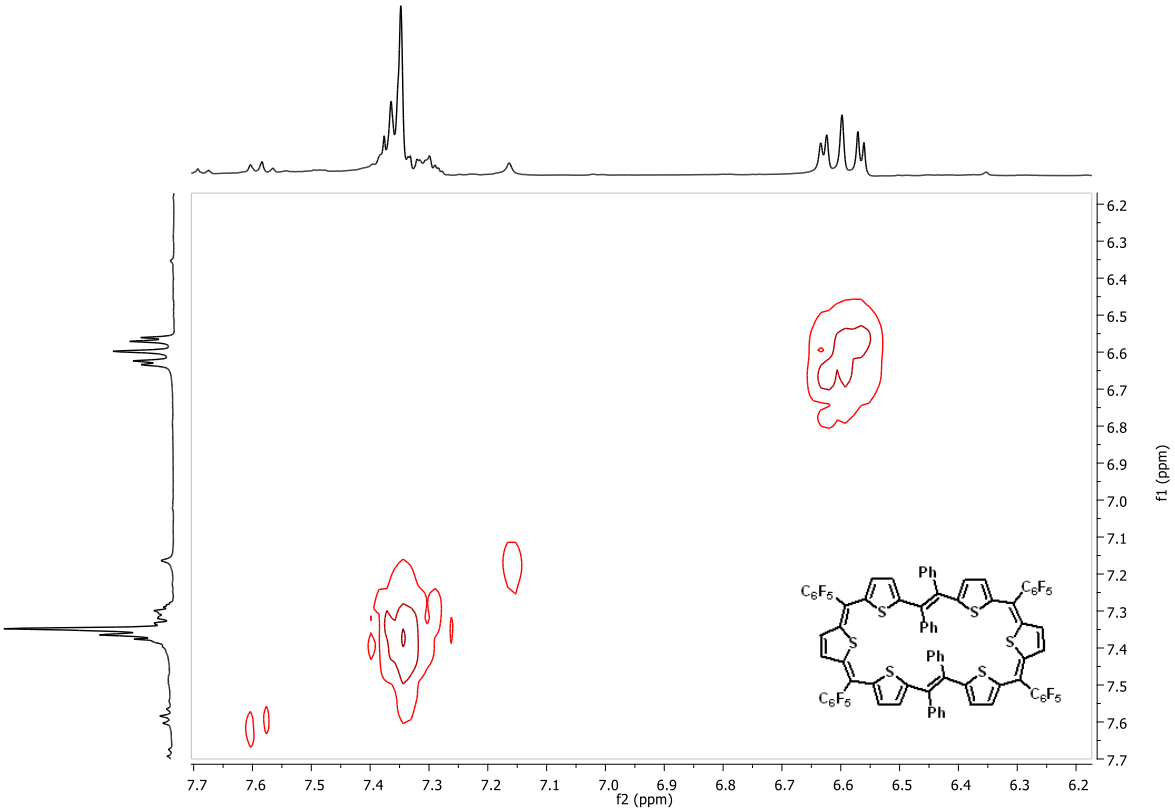

***Figure V.7**: ^{1}H-^{1}H COSY spectrum of **V.11** in $CDCl_3$ at room temperature*

However, the single crystal X-ray analysis revealed that the molecule had adopted *E* configuration over the *Z* form of the ethylene bridge (Figure V.8). Quantum chemical calculations further supported the non-antiaromatic character of the macrocycle. Interestingly, the estimated NICS(0)[9] value of δ +5.0 ppm did not support strong paratropic ring current effects, which is in tune with the observed NMR spectrum. There are a few examples of cyclic conjugated systems which are characterized to be more benzenoid than annulenoid in character due to the poor overlap of the orbitals for the effective π-electrons delocalization.[10]

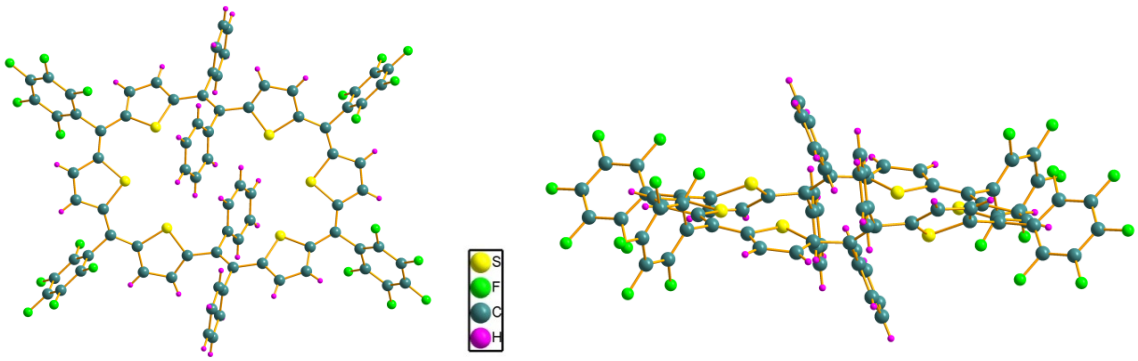

Figure V.8**: Single Crystal X-ray structure [top view(left) and lateral view (right)] of **V.11

Further, Anisotropy of Induced-Current Density (AICD)[11] calculation was performed on the hexaphyrin **V.11** and it displayed anti-clockwise direction of arrows in its AICD plot suggesting the antiaromatic nature of the macrocycle (Figure V.9). Subsequently, steady-state absorption spectrum was evaluated using Time dependent TD-DFT calculations. The absorption spectrum for **V.11** matched the calculated TD-DFT values (Figure V.10).

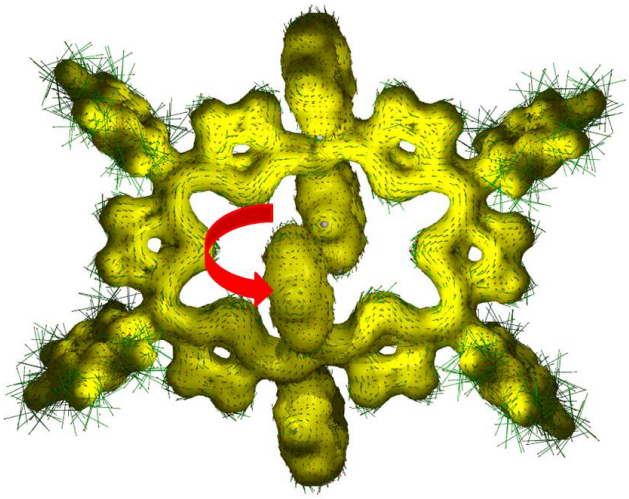

Figure V.9**: AICD plot for **V.11

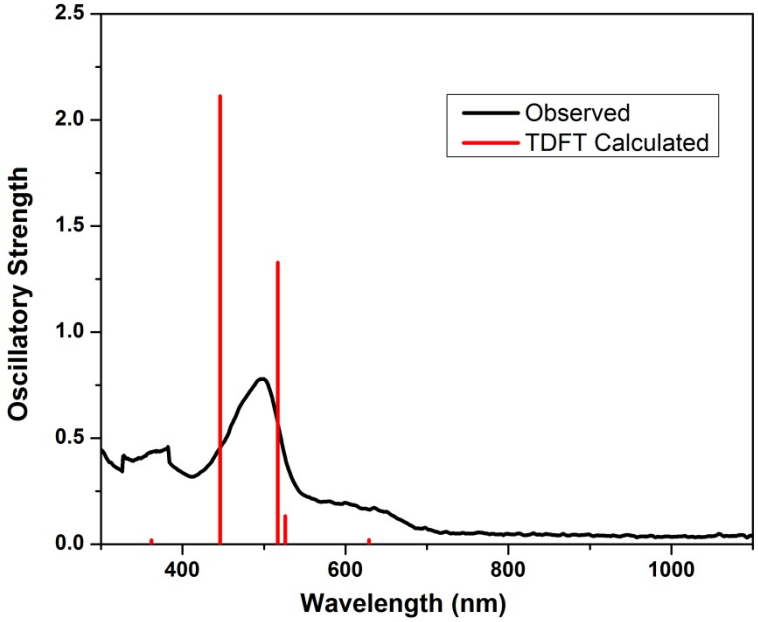

Figure V.10**: Time dependent functional theory (TD-DFT) calculation overlaid on experimental UV-Vis absorption spectrum of **V.11

V.4 Isolation and characterization of 48π nonaphyrins (V.12)

Since 48π macrocycle was also identified in the reaction mixture, attempts were made to isolate the same through column chromatographic separation. Once the reaction mixture was concentrated under reduced pressure, it was purified using silica gel column. A pink colored band of 48π nonaphyrin **V.12** was identified and purified after repeated column chromatographic separation. The pink colored band displayed M^+ peak at 2346.0784 corresponding to $C_{120}H_{48}F_{30}S_9$ with exact mass of 2346.0763 (Figure V.11). It displayed intense absorption at 577 nm (20318 ε, $Lmol^{-1}cm^{-1}$) along with a weak absorption band at 539 nm (13149) in its electronic absorption spectra (Figure V.12).

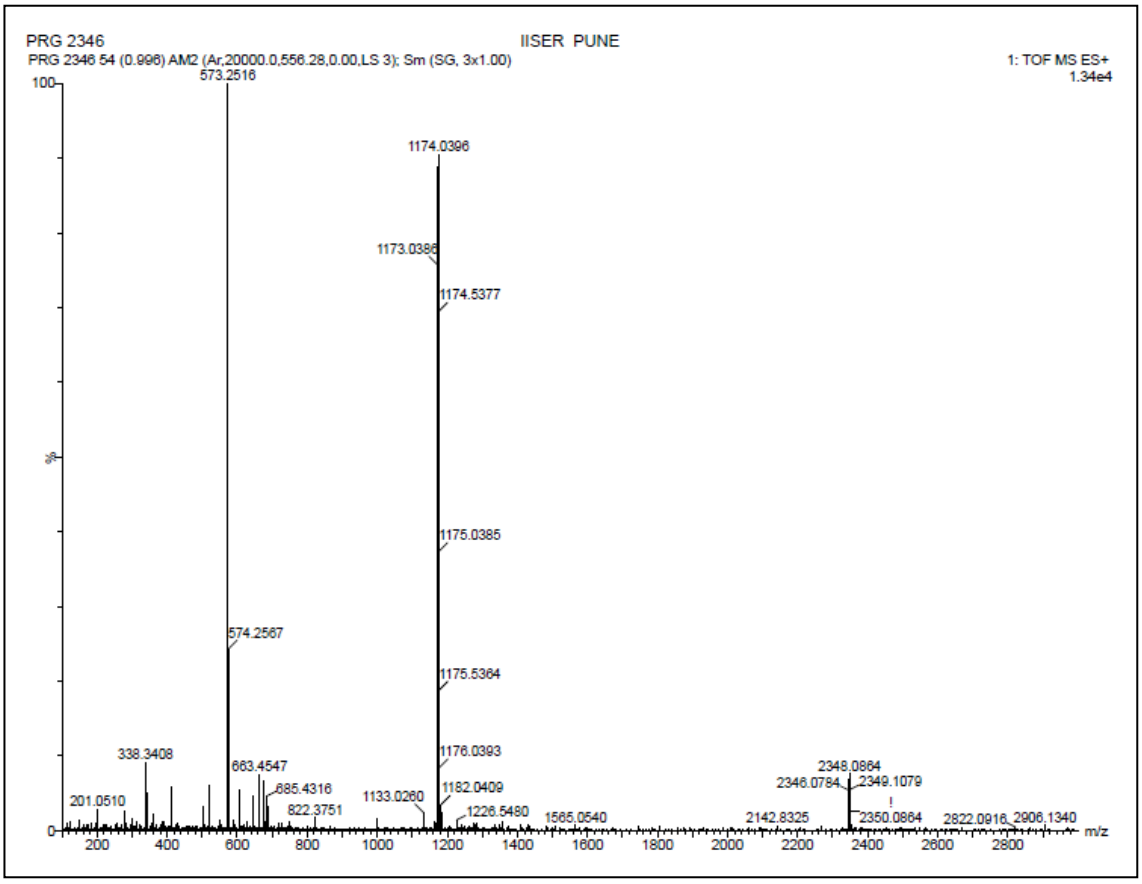

Figure V.11**: HR-MS of **V.12

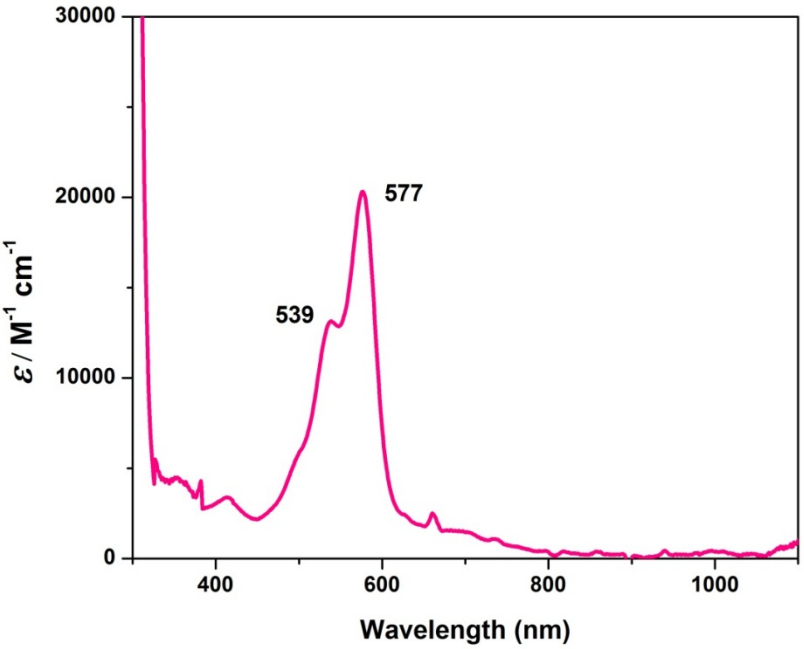

***Figure V.12**: Electronic absorption spectrum of **V.12** in DCM at ~10^{-5}M concentration*

The proton NMR of **V.II** was not so well resolved at room temperature probably due to the solution state dynamics at room temperature. However a well resolved NMR spectrum was obtained upon lowering the temperature to 203 K (Figure V.13). Multiple signals resonated between δ 4.4 and 10.0 ppm corresponding to a total of forty-eight protons (Figure V.14). The proton NMR suggested the formation of a completely asymmetric macrocycle. The upfield signals between δ 4.5 to 6.0 ppm can be attributed either to the phenyl rings directed towards cavity of the macrocycle or for the inverted thiophene units present in the macrocycle. The ^{1}H-^{1}H COSY spectrum also could not give a definite idea for the absolute structure of **V.12** (Figure V.15). A conclusive structure could not be justified for the nonaphyrin **V.12** based on the proton NMR.

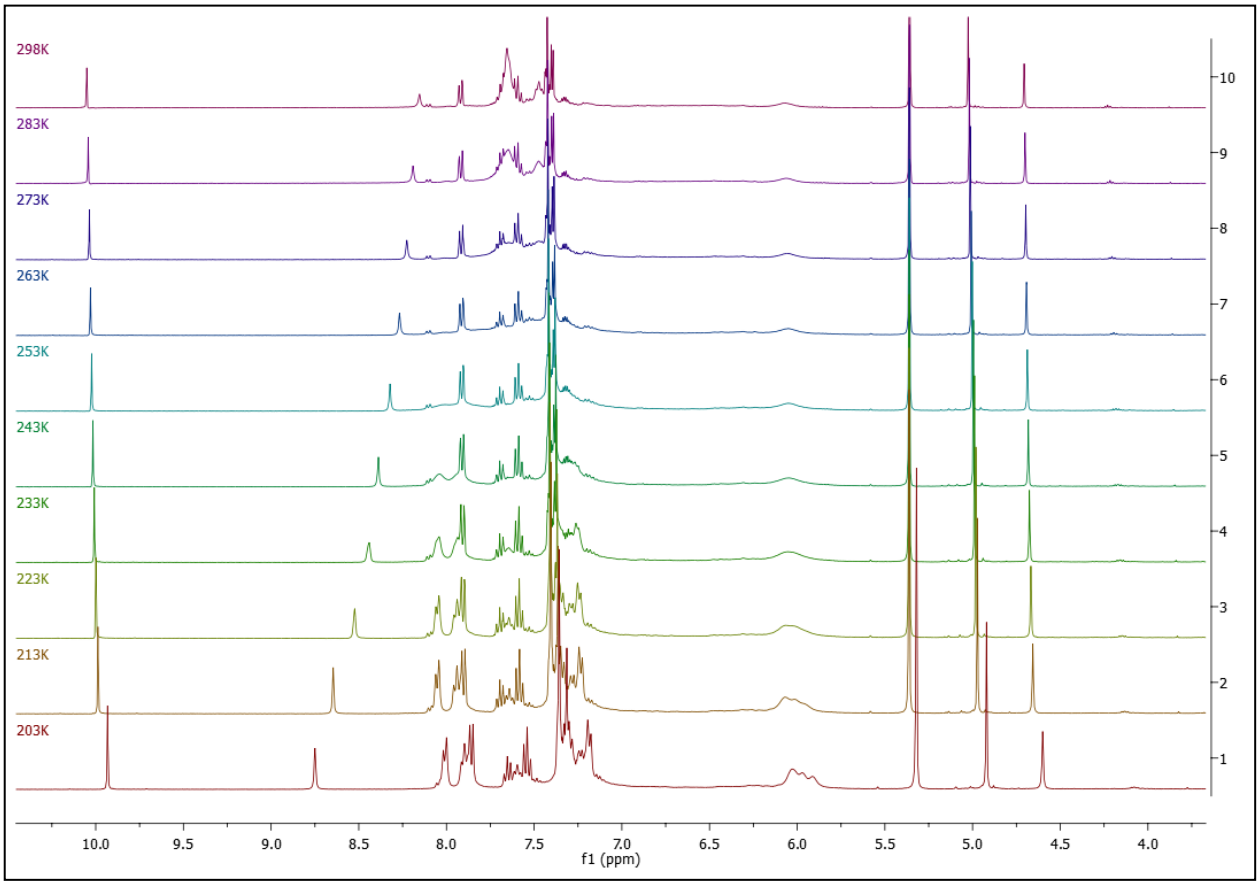

Figure V.13*: Variable temperature proton NMR spectra of* ***V.12*** *in CD_2Cl_2 from 298K to 203K*

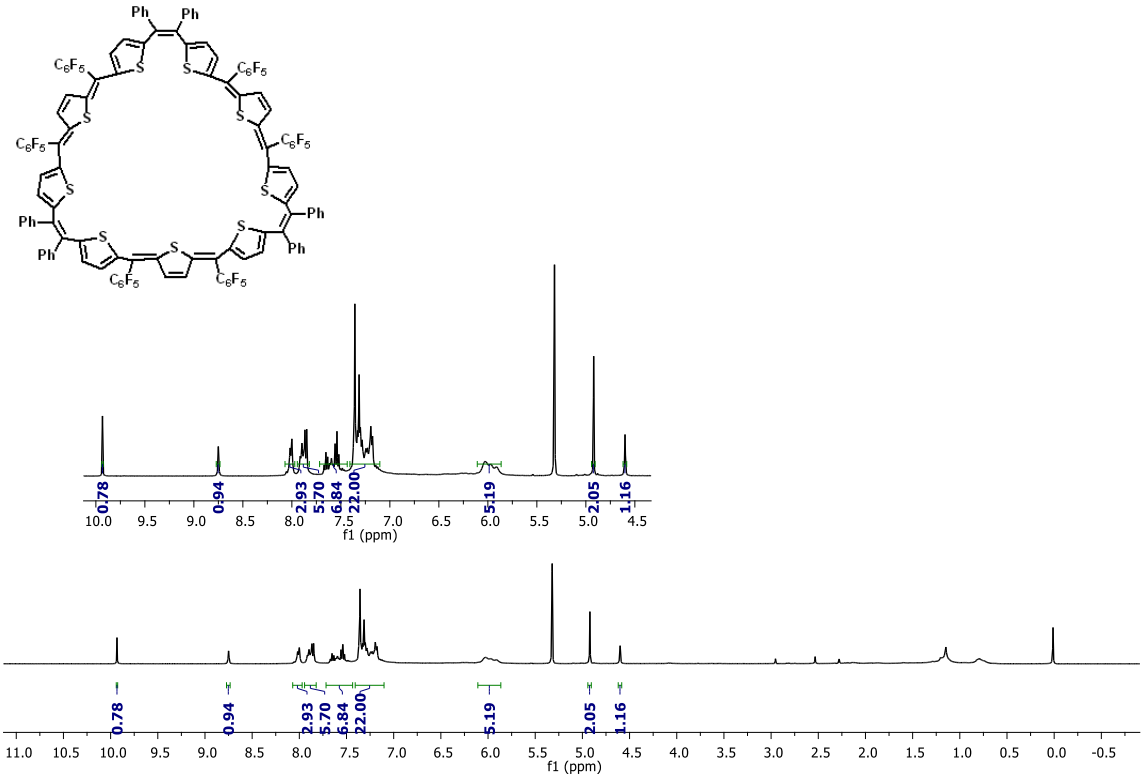

***Figure V.14**: Proton NMR spectrum of **V.12** in CD_2Cl_2 at 203K*

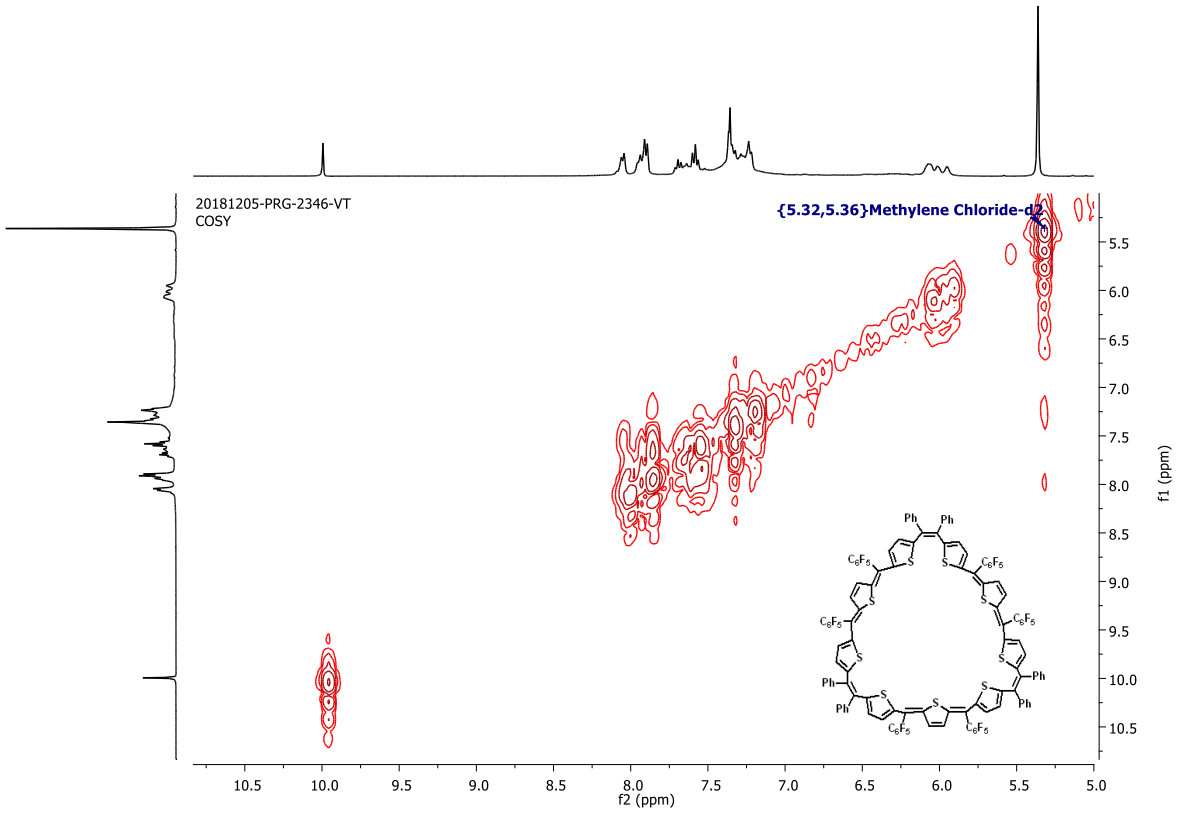

***Figure V.15**: ^1H-^1H COSY spectrum of **V.12** in CD_2Cl_2 at 203K*

Various attempts to grow single crystals of the macrocycle went futile, and hence its absolute structure still remains ambiguous and needs further studies.

V.5 Conclusion

In conclusion, ethylene bridge macrocycles, 32π hexaphyrin and 48π nonaphyrin were synthesized with phenyl substituents on the ethylene carbon atoms. Though the synthesis was initiated with an oligomeric unit encompassing ethylene bridge in *Z* conformer, the resulting macrocycle **V.11** was found to adopt the ethylene bridge in *E* conformer as confirmed by single crystal X-ray structure. This suggests the relative stability of *E* confirmer of ethylene bridge in hexaphyrin over the *Z* conformer. Though the structure for hexaphyrin was revealed by single crystal X-ray analysis, all the attempts to obtain the crystal structure for nonaphyrin went futile and hence it still remains ambiguous.

V.6 Experimental section

(*Z*)-1,2-diphenyl-1,2-di(thiophen-2-yl)ethane (**V.9**) and thiophene diol (**V.10**) was dissolved in equimolar ratio in 150 mL of dry dichloromethane and degassed with nitrogen for five minutes. Then the round bottom flask containing the solution was covered with aluminum foil to maintain dark conditions. To this mixture, one equivalent of $BF_3.OEt_2$ was added and stirred the solution for two hours maintaining the dark and inert conditions. After two hours the reaction mixture was subjected to six equivalents of dichlorodicyanoquinone (DDQ) and stirred for two hours. Finally the reaction mixture was passed through basic alumina column and purified using alumina column.

Synthetic procedure of (*Z*)-1,2-diphenyl-1,2-di(thiophen-2-yl)ethane V.9

Step 1: Synthesis of V.8[7]

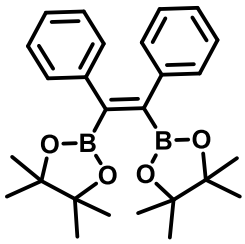

To a 250 mL round bottom flask, tetrakis(triphenylphosphine)platinum ($Pt(PPh_3)_4$) (1 mol%) and bis(pinacolato)diboron (7.20 g, 27.77 mmol) was added and then flushed with nitrogen. To this 75 mL of DMF and 1,4-Diphenylethyne (2.47 g, 13.89 mmol) were successively added. The reaction was refluxed at 90° C for 24 hours, and then the reaction mixture was concentrated under reduced pressure. 5.1 g of product (*Z*)-1,2-diphenyl-1,2-bis(4,4,5,5-tetramethyl-1,3,2- was obtained in 85% yield after drying.

^1H NMR (400 MHz, $CDCl_3$) δ: 7.06-7.02 (m, 6H), 6.96-6.93 (m, 4H), 1.32 (s, 24H)

Step 2: Synthesis of V.9[6]

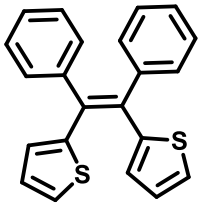

To a 250 mL round bottom flask, $Pd(PPh_3)_4$ (17.33 mg, 0.015 mmol) and compound **V.12** (4.32 g, 10 mmol) was added and flushed with nitrogen.2-bromothiophene (20 mmol), toluene (100 mL), and 2 mol/L K_2CO_3 aq. (10 mL) was further added to the reaction mixture. The reaction was stirred at room temperature and monitored via TLC continuously until the complete conversion of the starting material. After the completion of reaction, it was extracted using dichloromethane and concentrated. Finally the residue was purified by using silica gel column chromatography using petroleum ether/ dichloromethane as eluent to obtain the desired product

in 92% yield (3.27 g). The *Z* conformation of the molecule was confirmed using single crystal X-ray analysis.

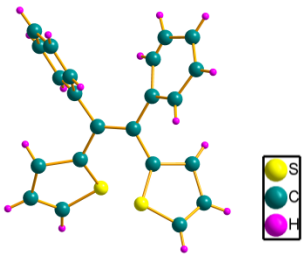

^{1}H NMR (400 MHz, $CDCl_3$) δ: 7.12 (dd, *J* = 4.0 Hz, 2H), 6.96 (s, 10 H), 6.77 – 6.72 (m, 2H), 6.66 (dd, *J* = 4.0 Hz, 2H).

Selected Crystal data: triclinic, space group P 1, a = 9.708, b = 13.672, c = 21.068 Å, α = 104.495, β = 97.368, γ 101.403, V= 2607Å^3, T= 100 K, D_{cal} = 1.665 gcm^{-3}, R_1 = 0.1375, wR_2 = 0.3492, GOF = 1.704

Synthetic procedure of V.11 and V.12

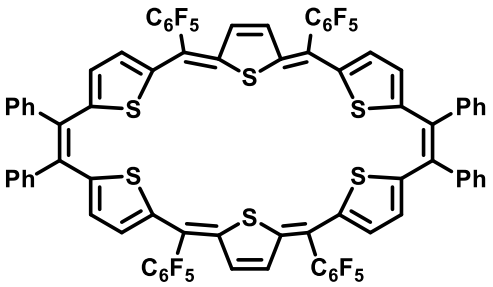

V.11

+

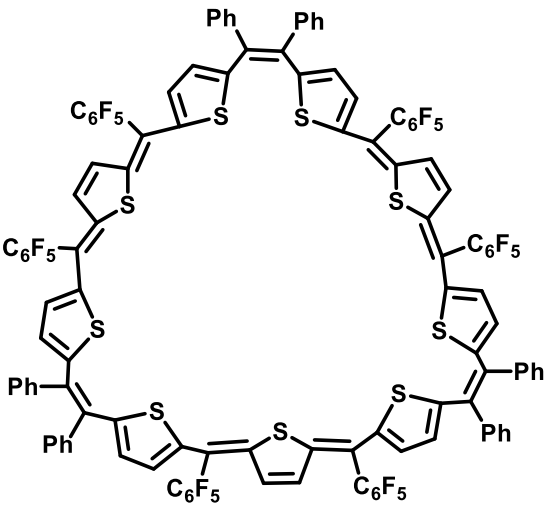

V.12

A clean dried 250 mL round bottom flask was charged with compound **V.9** (172 mg, 499.29 µmol). To this compound **V.10** (237.81 mg, 499.29 µmol) was added and 150 mL of dry dichloromethane was added. The solution was nicely stirred and maintained under dark and inert condition. To this reaction mixture, $BF_3.OEt_2$ (499.29 µmol, 0.06 mL) was added slowly and stirred further for two hours. Subsequently after two hours, dichlorodicyanoquinone (680

mg, 3 mmol) was added to the reaction mixture and stirred further for two hours. The reaction mixture was filtered through basic alumina column and purified on a neutral alumina glass column. The major fraction obtained was a six membered, 32π hexaphyrin **V.11** isolated in 9% yield along with nine membered 48π nonaphyrin **V.12** isolated in 5% yields. Both the molecules were completely characterized using the HR-MS and spectroscopic techniques.

Spectroscopic characterization of V.11

HR-MS (ESI) m/z: $[M]^+$ Calcd. for $C_{80}H_{32}F_{20}S_6$: 1564.0509 Observed: 1565.0524

UV-Vis (CH_2Cl_2): λ_{max} nm (ε, $Lmol^{-1}cm^{-1}$): 498 nm (13180)

^1H NMR (400 MHz, CD_2Cl_2) δ: 7.36 (d, *J* = 4.0 Hz, 20H), 6.63 (d, *J* = 4.0 Hz, 4H), 6.60 (s, 4H), 6.57 (d, *J* = 4.0 Hz, 4H).

Selected Crystal data: triclinic, space group P -1, a = 10.080, b = 14.037, c = 15.294 Å, α = 73.64, β = 71.17, γ = 69.579, V= 1884.4 $Å^3$, T= 100 K, D_{cal} = 1.914 gcm^{-3}, R_1 = 0.0829, wR_2 = 0.2119, GOF = 1.131

Crystal Parameters	V.11
Crystal System	Triclinic
Space group	P-1
a (Å)	10.080 Å
b (Å)	14.037 Å
c (Å)	15.294 Å
α	73.64
β	71.17
γ	69.579
Volume ($Å^3$)	1884.4 $Å^3$
T	100 K
Z	2
Density calculated (gcm^{-3})	1.914 gcm^{-3}
F(000)	1088.0
Absorption coefficient	1.072 mm^{-1}
Reflections reported	9298
Theta (max)	28.905
Goodness-of-fit on F^2	1.131
R_1	0.0829
wR_2	0.2119

Table V.1: Selected crystal parameters for 32π hexaphyrin **V.11**

Spectroscopic characterization of V.12

HR-MS (ESI) m/z: $[M]^+$ Calcd. for $C_{120}H_{48}F_{30}S_9$: 2346.0763 Observed: 2346.0784

UV-Vis (CH_2Cl_2): λ_{max} nm (ε, $Lmol^{-1}cm^{-1}$): 577 nm (20318), 539 nm (13149)

^1H NMR (400 MHz, CD_2Cl_2) δ: 9.93 (s, 1H), 8.75 (s, 1H), 8.01 (d, *J* = 8.0 Hz, 3H), 7.86 (m, 6H), 7.59 (m, 7H), 7.34 (m, 22H), 6.16-5.74 (m, 5H), 4.92 (s, 2H), 4.60 (s, 1H).

V.7 References

(1) Vogel, E.; Köcher, M.; Schmickler, H.; Lex, J. *Angew. Chem., Int. Ed. Engl.* **1986**, *25*, 257-259.

(2) Vogel, E.; Bröring, M.; Erben, C.; Demuth, R.; Lex, J.; Nendel, M.; Houk, K. N. *Angew. Chem. Int. Ed. Engl.* **1997**, *36*, 353-357.

(3) Hu, Z.Y.; Atwood, J.L.; Cava, M.P. *J. Org. Chem.* **1994**, *59*, 8071-8075.

(4) Gopalakrishna, T.Y.; Anand, V.G. *Angew. Chem., Int. Ed.* **2014**, *53*, 6796-6800.

(5) Kennedy, R. D.; Lloyd, D.; McNab, H. *J. Chem. Soc., Perkin Trans. 1*, **2002**, 1601-1621.

(6) Yang, J.; Chen, M.; Ma, J.; Huang, W.; Zhu, H.; Huang, Y.; Wang, W. *J. Mater. Chem. C*. **2015**, *3*, 10074-10078.

(7) Ishiyama, T.; Matsuda, N.; Miyaura. N.; Suzuki, A. *J. Am. Chem. Soc.* **1993**, *115*,11018-11019.

(8) Reddy, J. S.; Anand, V. G. *J. Am. Chem. Soc.* **2008**, *130*, 3718-3719.

(9) Schleyer, P. V. R.; Maerker, C.; Dransfeld, A.; Jiao, H.; Van Eikema Hommes, N. J. R. *J. Am. Chem. Soc.***1996**, *118*, 6317-6318.

(10) (a) Kromer, J.;Rios-Carreras, I.; Fuhrmann, G.; Musch, C.; Wunderlin, M.; Debaerdemaeker, T.; Mena-Osteritz, E.; Bauerle, P. *Angew. Chem., Int. Ed.*, **2000**, *39*, 3481-3486. (b) Iyoda, M.; Yamakawa, J.; Rahman, M. J. *Angew. Chem. Int. Ed. Engl.* **2011**, *50*, 10522-10553.

(11) Geuenich, D.; Hess, K.; Köhler, F.; Herges, R. *Chem. Rev.* **2005**, *105*, 3758-3772.

Summary of the thesis

This thesis describes the synthesis, characterization and redox properties of completely core modified expanded isophlorinoids. It delves into a range of expanded isophlorins with varying number of heterocyclic units ranging from six to ten. As the thesis describes from 32π heptaphyrins to 46π decaphyrins, it is observed the aromatic properties of all the expanded porphyrins differed drastically depending on their π electron count and planarity of the system. On increasing the heterocyclic units and the bridging positions in the macrocyclic core, the flexibility of the macrocycle was enhanced, and it tends to deviate from the planar geometry. The synthesis of expanded isophlorins was carried via MacDonald condensation of various oligomeric units with corresponding diol under acidic conditions followed by oxidation. A completely core modified 32π antiaromatic heptaphyrin was obtained for the first time and it was further explored for its reversible two-electron oxidation. After the successful attempt of studying the 32π heptaphyrin, a range of 40π and 38π octaphyrins were synthesized and explored for their electronic and redox properties. The 40π octaphyrin with eight bridging carbons deviated from planarity and achieved a figure-of-eight conformation. The 40π octaphyrin was redox active and was chemically oxidized to yield the 38π dication. In the process to obtain neutral 38π octaphyrins, a novel condensation product was identified wherein two diols condensed together possibly via H_2O_2 elimination. On exploring the chemistry of 38π octaphyrins further, two different isomers of 38π octaphyrins were formed in the same reaction. This was observed for the very first time that two different structural isomers of an expanded isophlorin were obtained from the same reaction. After successfully studying the core modified heptaphyrins and octaphyrins, the study was further extended to 46π decaphyrins with eight bridging positions. The large number of heterocyclic units lead to the poor solubility of the 46π decaphyrin and hence it could not be characterized by single crystal X-ray

diffraction. Finally, expanded isophlorins with ethylene bridges were also explored. The synthesis was attempted by condensing an oligomeric unit containing ethylene unit in *Z* conformer. It was interesting to find the stability of *E* conformer of ethylene bridge in the 32π hexaphyrin over *Z* conformer as confirmed by single crystal X-ray analysis. Though an array of expanded isophlorins were synthesized and studied in this thesis, still a vast range of expanded porphyrins with interesting properties remains unexplored and keeps the scope open for further studies. It is expected that the synthetic methodologies employed in this thesis can be useful to identify possible structural isomers for a variety of expanded antiaromatic isophlorins.